

e-ISSN : 2320-0847

p-ISSN : 2320-0936



AJER

American Journal of Engineering Research

Volume-2 Issue-4



AJER

American Journal of Engineering Research

**American Journal of
Engineering Research**

Editorial Board

American Journal of Engineering Research (AJER)

Dr. Jonathan Okeke Chimakonam

Qualification: PHD
Affiliation: University of Calabar
Specialization: Logic, Philosophy of
Maths and African Science,
Country: Nigeria

Dr. ABDUL KAREEM

Qualification: MBBS, DMRD, FCIP, FAGE
Affiliation: UNIVERSITI SAINS Malaysia
Country: Malaysia

Dr. sukhmander singh

Qualification: Phd
Affiliation: Indian Institute Of
Technology, Delhi
Specialization : PLASMA PHYSICS
Country: India

Dr. Nwachukwu Eugene Nnamdi

Qualification: Phd
Affiliation: Michael Okpara University of
Agriculture, Umudike, Nigeria
Specialization: Animal Genetics and
Breeding
Country: Nigeria

Dr. June II A. Kiblasan

Qualification : Phd
Specialization: Management, applied
sciences
Country: PHILIPPINES

Dr. Narendra Kumar Sharma

Qualification: PHD
Affiliation: Defence Institute of Physiology
and Allied Science, DRDO
Specialization: Proteomics, Molecular
biology, hypoxia
Country: India

Prof. Dr. Shafique Ahmed Arain

Qualification: Postdoc fellow, Phd
Affiliation: Shah Abdul Latif University
Khairpur (Mirs),
Specialization: Polymer science
Country: Pakistan

Dr. Alcides Chaux

Qualification: MD
Affiliation: Norte University, Paraguay,
South America
Specialization: Genitourinary Tumors
Country: Paraguay, South America

Dr. Md. Nazrul Islam Mondal

Qualification: Phd
Affiliation: Rajshahi University, Bangladesh
Specialization: Health and Epidemiology
Country: Bangladesh

CONTENTS

Volume-2 Issue-4

S.No.	Title Name	Page No.
01.	Exploring operational Characteristics of Battery operated AutoRickshaws in Urban Transportation System Md. Sohel Rana, Fahim Hossain, Shuvangk Shusmoy Roy, Mr. Suman Kumar Mitra	01-11
02.	The Effects of Groundnut Shell Addition on The Insulating Properties of Clay Samples From Kogi State Nigeria Manukaji John U.	12-15
03.	Study of Noise Pollution Due To Railway and Vehicular Traffic at Level Crossing and Its Remedial Measures Anurag V. Tiwari, Prashant A. Kadu, Ashish R.Mishra	16-19
04.	Determination operation Time Risk of Box Spinning Components-oe Spinning Machine Slobodan Stefanovic	20-32
05.	Industrial Potential of Some Clay Deposits In Kogi State North Central Nigeria Manukaji John U.	33-38
06.	A COMPARATIVE STUDY OF BYG SEARCH ENGINES Kailash Kumar, Vinod Bhađu	39-43
07.	Transient Pressure Analysis of Horizontal Wells in a Multi Boundary System S. Al Rbeawi and D.Tiab	44-66
08.	Evaluation of Relationship Between Mechanical Properties of High Strength Self Compacting Concrete S.SeshaPhani, Dr.Seshadri Sekhar T , Dr.Srinivasa Rao, Dr Sravana	67-71
09	Carbon Emissions from air-Conditioning Rajesh Kumar, RK Aggarwal, Dhirender Gupta, Jyoti Dhar Sharma	72-74
10.	Design and Analysis of an Efficient Primary Synchronization Signal Detector Mathana.J.M, Ashvanth.R, Bhavanam Jagadish, Ashok Robert.J	75-85
11.	Data Warehousing Concept Using ETL Process for SCD Type-2 K.Srikanth, N.V.E.S.Murthy, J.Anitha	86-91
12.	Influence of the Type of Measuring Device in Determining the Static Modulus of Elasticity of Concrete Suélio da Silva Araújo, Gilson Natal Guimarães, e André Luiz Bortolacci Geyer	92-101
13.	Inspection of Buildings in Rio de Janeiro-Brazil: Proving the greater tendency of corrosion at the base of reinforced concrete columns using potential corrosion technique Marcelo Henrique Farias de Medeiros; Mikko Knuutila, Eduardo Pereira; Paulo Helene	102-112
14.	Analyzing of urban green spaces development process with emphasis on sustainable principles (Case study: Mashhad metropolitan) Maryam Ebrahimpour, Hamid Reza Saremi, Baratali Khakpour	113-119

15.	Context of qos In Web Service Selection Nabil Keskes	120-126
16.	Treatment of Municipal Wastewater by using Rotating Biological Contractors (Rbc's) Prashant A.Kadu, Amruta A.Badge, Dr.Y.R.M.Rao	127-132
17.	Strength of Ternary Blended Cement Sandcrete Containing Afikpo Rice Husk Ash and Saw Dust Ash L. O. Ettu, O. M. Ibearugbulem, K. O. Njoku, L. Anyaogu, and S. I. Agbo	133-137
18.	Traffic and Transportation Problems of Metro Cities: Case of Meerut, Uttar Pradesh Vijay kumar, Dr R.K.Pandit	138-151
19.	The Effect of Temperature on Mechanical Properties of M100 Concrete A. Sreenivasulu, Dr. K. Srinivasa Rao	152-157
20.	Properties of Reactive Compatibilized Dika Nutshell Powder filled Recycled Polypropylene (PP)/Polyethylene Terephthalate (PET) Biocomposites using Maleated Polypropylene and Epoxy Resin Dual Compatibilizers. G. N. Onyeagoro, C. M. Ewulonu, M. D. Ayo	158-169

Exploring operational Characteristics of Battery operated Auto-Rickshaws in Urban Transportation System

Md. Sohel Rana¹, Fahim Hossain², Shuvangk Shusmoy Roy³,
Mr. Suman Kumar Mitra⁴

¹Graduate, Department of Urban & Regional Planning, Bangladesh University of Engineering & Technology, Bangladesh

²Graduate, Department of Urban & Regional Planning, Bangladesh University of Engineering & Technology, Bangladesh

³Graduate, Department of Urban & Regional Planning, Bangladesh University of Engineering & Technology, Bangladesh

⁴Assistant Professor, Department of Urban & Regional Planning, Bangladesh University of Engineering & Technology, Bangladesh

Abstract: The paper contains primary data based analysis on the role played by Battery Operated Auto-rickshaw in urban transportation system. As a transport mode, different aspects of battery operated auto-rickshaw like trip characteristics, travel speed, travel fare, type of use, problems associated etc have been explored with a view to providing a generalized idea on the mode. The paper would provide guidelines to the policy makers of a country regarding whether and how to incorporate the mode in the local town's transportation system. Moreover, the paper with scientific outcomes might assist transport planners in modeling for efficient transportation in the mixed traffic condition where battery operated auto-rickshaw co-exists as well.

Keywords: Battery operated auto-rickshaw, Trip characteristics, Frequency of trips, Home-bus/tempo stand-work place network, Travel distance, Traffic safety, Performance index.

I. INTRODUCTION

Battery operated auto-rickshaw (locally called 'Easy-bike') is a newly added para-transit mode in urban transportation system of Bangladesh. The mode, being introduced in 2008 in Bangladesh attains much popularity among urban passengers since it involves lower travel cost than other locally available transport modes as well as provides reasonable safety and comfort to the users during travel [1]. This popularity, in turn results rapid growth of the mode in urban areas of Bangladesh. Now, the mode has become inseparable part of urban people's mobility network, especially in small-compact towns [2]. Therefore, it requires careful attention in incorporating the mode in local urban traffic-mix. To serve the purpose, the study is made to explore and analyze different attributes associated with the mode both from operators' and users' point of view.

II. OBJECTIVE OF THE STUDY

The objective of the research is to explore operational characteristics of battery operated auto-rickshaws in local urban transportation system.

III. METHODOLOGY OF THE STUDY

3.1 Study Area Selection

Two study areas are selected for carrying out the study on the basis of two major criteria as following-

- i. Number of battery operated auto-rickshaws running within the town.
- ii. Proximity of the area (town) to Dhaka.

Initially several urban areas of Bangladesh are considered on the basis of availability of data regarding the number of battery operated auto-rickshaws running within the town. Among them, two are selected as study areas finally based upon the aforementioned criteria. Numbers of battery operated auto-rickshaws running within the urban centers as well as physical distances (road/travel distances) of these areas from Dhaka are presented in Table-1.

Table-1: Number of battery operated auto-rickshaws and physical distances of towns from Dhaka

From	To	Number of Battery Operated Auto-rickshaws Running within the Town*	Distance (km) of the Town from Dhaka**
Dhaka	Comilla	8,687	97
Dhaka	Kushtia	2,521	277
Dhaka	Jessore	1,800	274
Dhaka	Faridpur	1,200	145
Dhaka	Meherpur	1,250	286

*Source: Easy-bike⁴ Owner's Association, Kushtia & Faridpur, 2011 [3]; District Traffic Police, Comilla, 2011 [4]; The Daily Prothom Alo, January 3, 2011 [5]

** Source: Discovery Bangladesh, Travel Info: Distance City to City, 2011 [6]

According to the stated criteria and imposing priority on the first one to ensure data quality, Comilla City Corporation Area and Kushtia Municipal Town are selected as study areas.

3.2 Variable Selection and Data Collection

Variables selected to fulfill the objective are presented in Table-2.

Table-2: List of variables

Objective	Parameters	Variables
To explore operational characteristics of battery operated auto-rickshaw in local urban transportation system	Travel/trip related issues	Travel speed, Travel cost, Travel length, Travel time, Types of trips, Trip frequency, Trip length
	Modal issues/ attributes	Costs/benefits over other modes, Type of use, Change in mode choice, Travel safety, Fare Rate, Travel Time, Travel Comfort, Travel Speed, Crowd, Operator's Behavior, Quality of Service

Operator opinion and user opinion surveys are conducted extensively to collect data on selected variables. The sample size for each type of survey is calculated 384 at 95% confidence level and confidence interval of 5.

IV. RESULTS AND DISCUSSION

4.1 Trip Characteristics

General characteristics of trips made by battery operated auto-rickshaws in urban areas of Bangladesh are discussed in following segments.

4.1.1 Type and Length of Trips

The trip of length less than 5 kilometers is characterized as 'short' trip, between 5 and 10 kilometers as 'medium' and greater than 10 kilometers as 'long' trips. The study shows that most of the operators of battery operated auto-rickshaw tend to make short trips within the town as presented in Table-3.

Table-3: Type of trips made by battery operated auto-rickshaws

Types of trips	Percentage
Short (< 5 km)	85.15
Medium (>= 5 km and <= 10 km)	11.46
Long (> 10 km)	3.38

Source: Operator Opinion Survey, 2011

Short and medium trips generally serve passengers' travel demand within the town while long trips serve their inter-town travel demand as found from the study. Around 85% of battery operated auto-rickshaws make short trips as shown in Table-3. The mode generates medium trips at considerable percentage. Very few operators go for long trips to meet inter-town travel demand of passengers. However, average length of trips made by the mode is 3.29 km as shown in Table-4.

Table-4: Length of trips made by battery operated auto-rickshaws

Types of Trips		Trip Length (km)
Short (< 5 km)	Maximum	4
	Minimum	1
	Average	2.51
Medium (≥ 5 km and ≤ 10 km)	Maximum	10
	Minimum	5
	Average	6.52
Long (> 10 km)	Maximum	13
	Minimum	11
	Average	11.65
Average		3.29

Source: Operator Opinion Survey, 2011

4.1.2 Frequency of Trips

Number of trips made by the mode per day is presented in Table-5 in accordance to types of trip.

Table-5: Frequency of trips made by battery operated auto-rickshaws

Types of Trips		Trip Frequency per Day
Short (< 5 km)	Maximum	32
	Minimum	8
	Average	19
Medium (≥ 5 km and ≤ 10 km)	Maximum	20
	Minimum	6
	Average	10
Long (> 10 km)	Maximum	8
	Minimum	4
	Average	6
Average		16

Source: Operator Opinion Survey, 2011

Table-5 shows that battery operated auto-rickshaw can make average 16 trips of 3.29 km average length per day in local urban areas of Bangladesh.

4.1.3 Fare Rate

The average income generated by battery operated auto-rickshaw per day is BDT 532.32 as found from operator opinion survey. This indicates that the mode with average 16 trip frequencies per day is capable to generate income of BDT 33.27 per trip. Since the average length of trip made by the mode is 3.29 km as mentioned before, it generates income of BDT 10.11 at per kilometer operation. Therefore, the mode with average occupancy of 4 passengers [7] should require BDT 2.53 as fare per head at per kilometer travel. However, the actual fare rate moves between BDT 2.00 to BDT 5.00 as found from user opinion survey.

4.2 Characteristics of Battery Operated Auto-rickshaws from Users' Point of View

Characteristics of battery operated auto-rickshaws are also identified and analyzed from user's point of view as following.

4.2.1 Users of Battery Operated Auto-rickshaws

Around 88% of total population living in a town where battery operated auto-rickshaw is available, use the mode now-a-days to meet their travel demand as presented in Table-6.

Table-6: User of battery operated auto-rickshaws

Users	Percentage to the Total Population
Use Battery Operated Auto-rickshaw	88.02
Do Not Use Battery Operated Auto-rickshaw	11.98

Source: User Opinion Survey, 2011

4.2.2 Information on Users of Battery Operated Auto-rickshaws

The information regarding age group, sex, educational qualification and occupation of urban passengers who avail battery operated auto-rickshaw to meet travel demand are presented in Table-7.

Table-7: Information on users of battery operated auto-rickshaws

Information on		Percentage to the Users
Age Group (years)	0-14	3.85
	15-29	58.88
	30-44	14.50
	45-60	22.19
	60+	0.59
Sex	Male	72.78
	Female	27.22
Educational Qualification	Illiterate	15.09
	Primary	4.73
	Secondary	34.91
	Higher Secondary	37.57
	Degree/Pass course	2.66
	Technical/ Vocational	1.77
	Honors/ University	3.25
Occupation	Govt. Service	9.76
	Private service	27.22
	Business	21.30
	Student	30.77
	Laborer	4.14
	Unemployed	3.85
	Housewife	4.14
	Others	0.00

Source: User Opinion Survey, 2011

Table-7 shows that most of the users of battery operated auto-rickshaws are aged between 15 and 29 years. This mode is popular especially to students as found from the study. In addition, the people doing small scaled business and low paid private job avail the mode considerably.

However, around 12% of the populations living in towns are found not using the mode at all. Information on those non-users is presented in Table-8.

Table-8: Information on people not using battery operated auto-rickshaw

Information on		Percentage to the Non-users
Age Group (years)	0-14	0.00
	15-29	30.43
	30-44	43.48
	45-60	26.09
	60+	0.00
Sex	Male	82.61
	Female	17.39
Educational level	Illiterate	0.00
	Primary	8.70
	Secondary	6.52
	Higher secondary	19.57
	Degree/ Pass course	15.22
	Technical	0.00
	Honors/ University	50.00
Occupation	Govt. Service	21.74
	Private service	26.09
	Business	26.09
	Student	19.57
	Laborer	0.00
	Unemployed	0.00
	Housewife	8.70
	Others	0.00

Source: User Opinion Survey, 2011

Table-8 shows that mostly the people aged between 30 and 44 years, having higher educational qualification and doing well paid private job, government job and medium or large scaled business do not use the mode. In addition, most of them own a private transport like bi-cycle, motor-cycle or private car as found from the study.

4.2.3 Reasons for Using Battery Operated Auto-rickshaw

Battery operated auto-rickshaw offers series of benefits over other locally available transport modes, which attract urban passengers to avail it. Study shows that around 94% of total users of the mode avail it inclusively for lower travel cost the mode involves as illustrated in Figure-1.

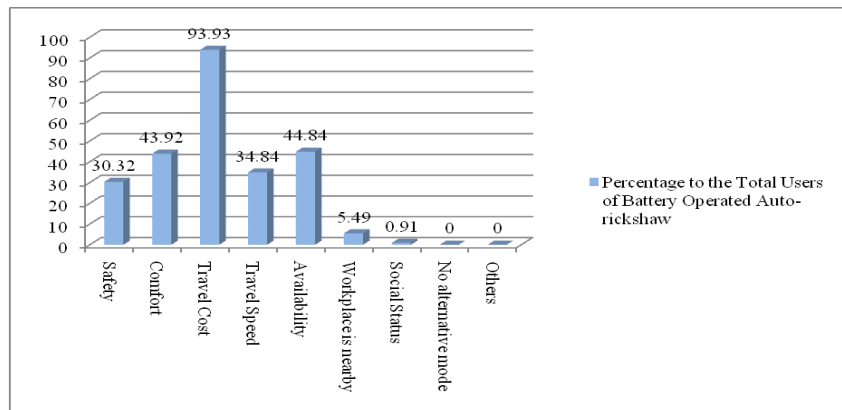


Figure-1: Graphical representation of reasons for availing battery operated auto-rickshaws

In addition, it offers greater travel comfort than others which affect urban dweller’s choice for the mode considerably. Furthermore, large number of battery operated auto-rickshaws in local towns of Bangladesh makes the mode easily available throughout the town. This aspect associated with the mode plays important role as well to make it a popular transport mode among passengers since availability of the mode reduces their waiting time. Because of limited speed and light weight the mode does not create any fatal accidents as users opined. Due to this safety issue, also a considerable percentage of users avail the mode as found from the study.

4.2.4 Reasons for Not Using Battery Operated Auto-rickshaw

Around 91% of people who do not avail battery operated auto-rickshaw accuse the lack of safety issues that the mode involves, for not using the mode. The mode doesn’t cause fatal traffic accident though. However, light weight of the mode, driver’s lack of skill and training, and indiscriminate plying of the mode on the heavy traffic carrying urban roads make it vulnerable sometimes to small scaled traffic accidents. Considerable percentages of non-users do not go for the mode since they have access to private transport like bicycle, motor-cycle or car, and/or for the crowding passengers associated with battery operated auto-rickshaw as presented in Figure-2.

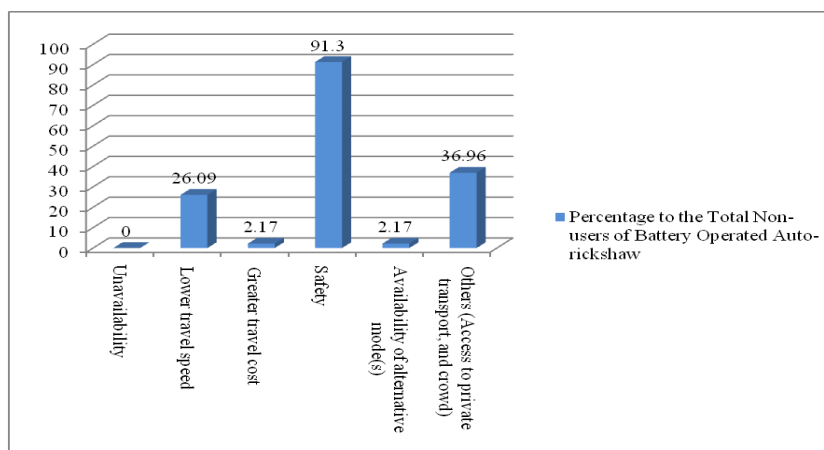


Figure-2: Graphical representation of reasons for not using battery operated auto-rickshaws From the above discussions it can be concluded that battery operated auto-rickshaw plays important role to meet the travel demand of low income urban dwellers seeking for low cost travel mode in local urban areas of Bangladesh. The mode provides comfort during travel along with reasonable safety and travel speed to low income people while higher income people do not use the mode for the lack of safety and comfort, and lower travel speed the mode associates. This is because definition of comfort and travel speed varies with people’s income level. From

neutral point of view, battery operated auto-rickshaw involves lower travel cost and hence it is easily accessible to all income group people. The mode provides service to majority of people of a city with considerable comfort and travel speed. In case of safety, it is drivers/operators with lack of skills and training who are responsible more for causing traffic accidents than the mode.

4.3 Type of Use

Around 86% of users of battery operated auto-rickshaws use it as primary mode in local urban areas as showed in Table-9.

Table-9: Type of use of battery operated auto-rickshaws

Type of Use	Percentage to the Total Users of Battery Operated Auto-rickshaw
As primary mode	86.09
As secondary mode	13.91

Source: User Opinion Survey, 2011

Users who avail local minibus or auto-tempo as primary mode generally avail battery operated auto-rickshaw as secondary mode within the ‘home- bus/tempo stand- work place’ network as illustrated in Figure-3.

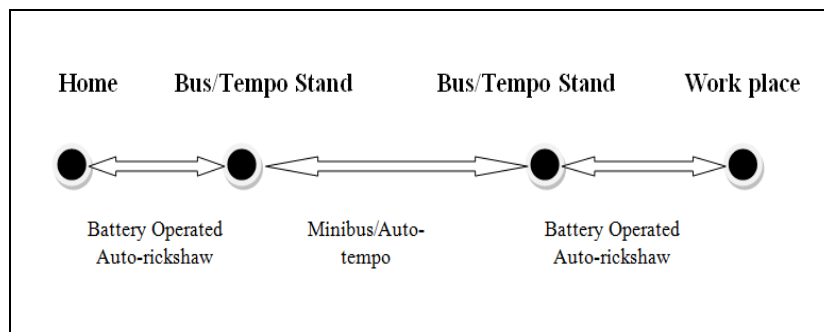


Figure-3: The ‘home- bus/tempo stand- work place’ network

Average length of a trip made by battery operated auto-rickshaws in local towns is 3.29 km as mentioned above. In transposition, average travel distance of users is found 1.31 km as calculated from the survey data presented in Table-10.

Table-10: User’s travel distance

Travel Distance	Percentage to the Total Users of Battery Operated Auto-rickshaw
< 1/2 km	4.44
1/2 to 1 km	11.24
1 to 1.5 km	60.65
1.5 to 2 km	20.71
2 to 3 km	1.78
3 to 4 km	0.00
4 to 5 km	1.18
> 5 km	0.00

Source: User Opinion Survey, 2011

Since battery operated auto-rickshaw makes trip of 3.29 km length on average and users of the mode in towns demand for travel for average 1.31 km distance, the mode can serve user’s travel demand as primary mode substantially. Therefore, most of the users of battery operated auto-rickshaws tend to use it as primary mode in local towns of Bangladesh.

Prior to the advent of battery operated auto-ricksaws in local urban areas of Bangladesh, passengers used to avail rickshaw, minibus, auto-tempo and nosimon (a locally developed, 8-12 hp diesel engine operated and three-wheeled para-transit mode) as primary mode as found from the study. After battery operated auto-ricksaw becomes available it mostly replaces rickshaw as primary mode as presented in Figure-4.

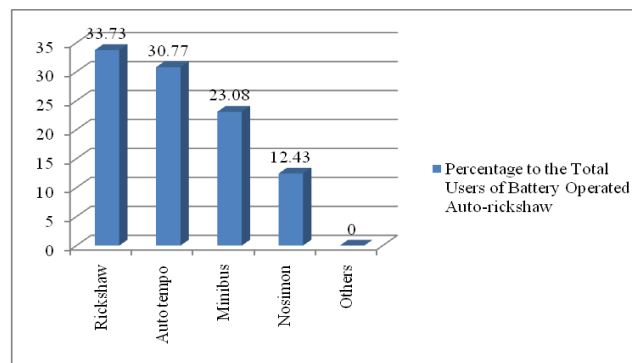


Figure-4: Graphical representation of primary mode choice of users in previous.

Figure-4 also shows that battery operated auto-rickshaw as primary mode replaces auto tempo and minibus considerably as well. As secondary mode, battery operated auto-rickshaw mostly replaces rickshaws and vangari (flat-bed rickshaw) as illustrated in Figure-5.

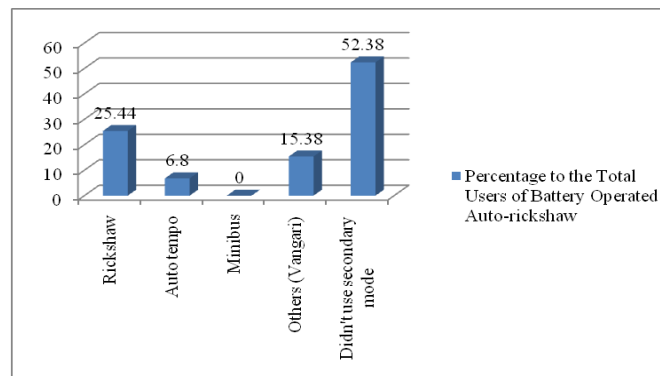


Figure-5: Graphical representation of secondary mode choice of users of battery operated auto-rickshaw in previous

4.4 Travel Speed

During user opinion survey, users of battery operated auto-rickshaws are asked to mention how much time the mode takes to serve up to their travel distance. Accordingly, it is calculated that the average travel speed at which battery operated auto-rickshaws serve urban passenger's travel demand in local towns of Bangladesh is 9.95 kilometer/hour.

4.5 Changes in Mode Choice

Battery operated auto-rickshaw attracts urban passengers from other transport modes for series of reasons discussed above. Around 59% of users of the mode inclusively used rickshaw before battery operated auto-rickshaw get introduced in their town. Accordingly, 40% of the users shift from auto-tempo, 28% from nosimon and 24% from minibus in inclusive manner as shown in Figure-6.

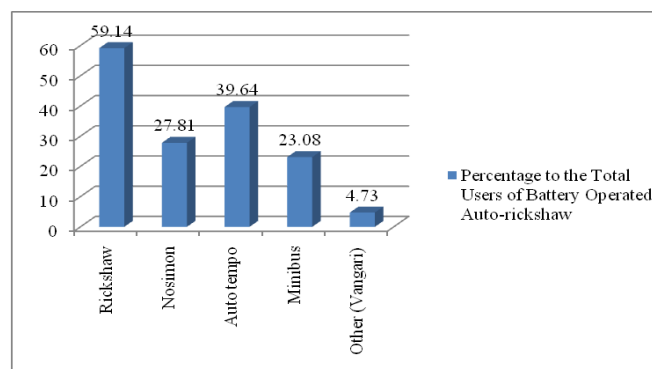


Figure-6: Graphical representation of user's mode choice in previous

Figure-6 shows that most of the users of battery operated auto-rickshaw shifts from rickshaws. In addition to this, the mode attracts passengers from auto-tempo, nosimon and minibus considerably. Study reveals that lower travel cost and better travel speed that battery operated auto-rickshaw involves have played vital role to attract passengers from rickshaw. Most of the passengers who availed auto-tempo, minibus and nosimon previously change their mode choice to battery operated auto-rickshaw for the sake of comfort mainly.

4.6 Frequency of Using Battery Operated Auto-rickshaws in A Week

During user opinion survey, users of battery operated auto-rickshaw are asked to mention how frequently they avail the mode in a week. Around 86% of the users of battery operated auto-rickshaws avail the mode daily as presented in Figure-7.

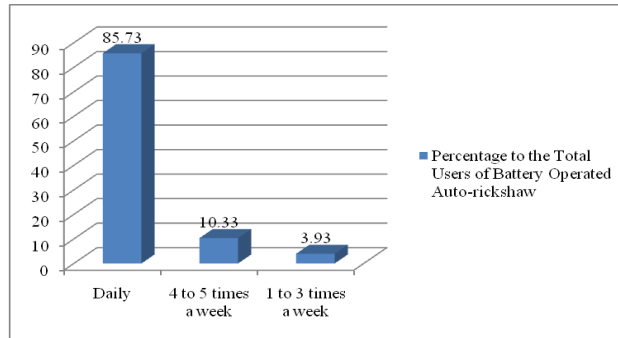


Figure-7: Graphical representation of frequency of using battery operated auto-rickshaw throughout a week

Figure-7 illustrates that most of the users of battery operated auto-rickshaws in local towns of Bangladesh use the mode on daily basis. Some of the users avail the mode irregularly and mostly of them use it as instant alternative to other modes like auto-tempo or rickshaws. Large scale availability of battery operated auto-rickshaws affects user’s instant mode choice decision. From the study it is found that passengers who are not regular user of battery operated auto-rickshaw generally use the mode as an alternative to their regular mode in case of its unavailability.

4.7 Problems Associated with Battery Operated Auto-rickshaws

Most of the users of battery operated auto-rickshaw identify its vulnerability to traffic accident as a major problem. In addition to this, frequent stopping of the mode to load and unload passengers is another problem as found from the study. A considerable percentage of users also accuse low travel speed that the mode involves as a problem as shown in Figure-8.

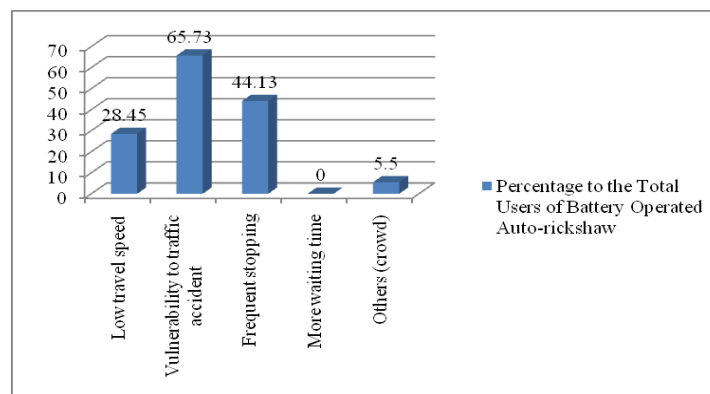


Figure-8: Graphical representation of problems associated with battery operated auto-rickshaws

4.8 Performance Index (PI) of Battery Operated Auto-rickshaws on Its Attributes

During user opinion survey respondents are asked to give their opinion on different attributes of battery operated auto-rickshaw over a 5 point scale (0-5), where 0 indicates the worst performance and 5 the excellent. The scale is constructed as shown in Figure-9. The higher the scale value the better is the performance. For instance, the scale value between 4 and 5 indicates nearly excellent performance.

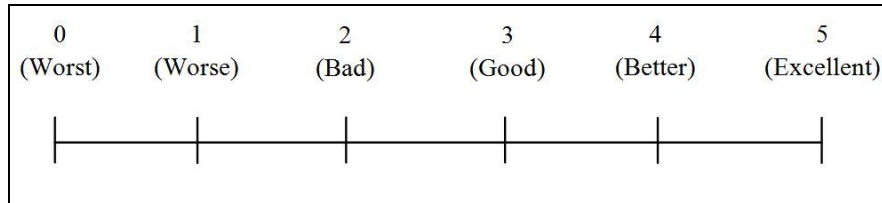


Figure-9: Performance Index scales

Respondent’s opinions are taken on the attributes- ‘fare rate’, ‘travel time’, ‘travel comfort’, ‘safety’, ‘travel speed’, ‘crowd’, ‘operator’s behavior’ and ‘quality of service’ associated with battery operated auto-rickshaws. Performance Index of the mode is calculated both from user of the mode and non-user of the mode’s point of view. The study results obtained from opinions of users of battery operated auto-rickshaw on attributes of the mode are presented in Table-11.

Table-11: Performance of battery operated auto-rickshaw based on opinion of users of the mode

Attributes	Scales					
	0	1	2	3	4	5
Fare Rate	0	0	3	23	104	208
Travel Time	0	0	27	115	172	24
Travel Comfort	0	0	30	21	136	151
Safety	15	27	109	92	77	18
Travel Speed	0	3	42	136	136	21
Crowd	0	9	17	208	104	0
Operator's Behavior	0	3	54	222	59	0
Quality of Service	0	0	27	103	172	36

Source: User Opinion Survey, 2011

Note: Figures presented in the table are frequencies of responses

Out of 384 sampled respondents, 338 respondents (88.02% of the total) use battery operated auto-rickshaw to meet their travel demand as found from the study. According to opinions of these users, calculation of performance index for battery operated auto-rickshaw for a single attribute (e.g. Fare rate) is demonstrated hereafter.

$$\text{Performance Index of Battery Operated Auto-rickshaw on Its Fare rate} = \frac{(0 \times 0 + 1 \times 0 + 2 \times 3 + 3 \times 23 + 4 \times 104 + 5 \times 208)}{338}$$

$$= 4.53$$

Accordingly, performance index of other attributes of the mode based on opinion of users are calculated and presented in Table-12.

Table-12: Performance index of battery operated auto-rickshaw on its attributes

Attributes	Performance Index
Fare Rate	4.53
Travel Time	3.57
Travel Comfort	4.21
Safety	2.72
Travel Speed	3.38
Crowd	3.20
Operator's Behavior	3.00
Quality of Service	3.64

Average fare that battery operated auto-rickshaw requires per head at per kilometer operation is BDT 2.53 as mentioned above. From Table-12, it is seen that the fare rate of the mode is nearly excellent to the users. In addition, the mode includes satisfactory performance on travel comfort issue. Regarding quality of service, travel time, travel speed, crowd and operator’s behavior with passengers, the mode holds good performance in meeting travel demand of users. However, regarding safety, the mode associates bad performance.

Respondents who are found not using the mode are asked also to give their opinions on attributes of battery operated auto-rickshaws. Performance index of the mode on its different attributes according to those non-users are presented in Table-13.

Table-13: Performance index of battery operated auto-rickshaws based on opinions of non-users of the mode

Attributes	Scales						Performance Index
	0	1	2	3	4	5	
Fare Rate	0	0	0	11	35	0	3.76
Travel Time	0	4	15	23	4	0	2.59
Travel Comfort	8	23	15	0	0	0	1.15
Safety	27	19	0	0	0	0	0.41
Travel Speed	0	11	12	23	0	0	2.26
Crowd	0	0	27	19	0	0	2.41
Operator's Behavior	0	0	35	11	0	0	2.24
Quality of Service	0	0	4	42	0	0	2.91

Source: User Opinion Survey, 2011

Note: Figures presented in the table are frequencies of responses

Table-13 shows that safety issue associated with battery operated auto-rickshaw has a performance index value of 0.41. This indicates that the mode cannot ensure safety to its users at all. In addition, travel comfort offered by the mode is hardly satisfactory. However, fare rate is satisfactory even to the non-users of the mode. Now, performance index of battery operated auto-rickshaws calculated from total respondent's opinion is presented in Table-14.

Table-14: Performance index of battery operated auto-rickshaws according to the opinions of total respondents

Attributes	Scales						Performance Index
	0	1	2	3	4	5	
Fare Rate	0	0	3	34	134	213	4.45
Travel Time	0	3	40	137	180	24	3.47
Travel Comfort	6	18	43	21	140	156	3.92
Safety	37	43	113	94	79	18	2.49
Travel Speed	0	12	52	159	140	21	3.28
Crowd	0	9	40	228	107	0	3.13
Operator's Behavior	0	3	82	238	61	0	2.93
Quality of Service	0	0	30	140	177	37	3.58

Source: User Opinion Survey, 2011

Note: Figures presented in the table are frequencies of responses

Table-14 presents that battery operated auto-rickshaws with nearly excellent fare structures involves highly satisfactory travel comfort, travel time, and overall quality of service. Crowd and travel speed that the mode associates with are satisfactory as well. However, operator's behavior, and safety associated with the mode are not satisfactory to urban passengers.

V. CONCLUSION

Battery operated auto-rickshaw with average trip length of 3.29 km compatible to urban passenger's average travel distance of 1.31 km, have become popular mode of travel to them. Around 88% of urban passengers are availing this mode now to meet their travel demand. The mode attracts urban passengers mostly from rickshaw and also considerably from nosimon, auto-tempo and minibus through offering a set of benefits over those modes, such as, lower travel cost than rickshaw, greater comfort than minibus, nosimon or auto-tempo, limited but acceptable travel speed and satisfactory quality of service.

Battery operated auto-rickshaws are mostly used as primary mode in urban areas since people living in local towns tend to generate short trips frequently, which can be better served by this mode. However, the mode involves lack of travel safety as operators/drivers of the mode are not well trained, the mode is light weighted and it plies on heavy traffic carrying urban road frequently, which increase its vulnerability to traffic accident.

VI. RECOMMENDATIONS TO IMPROVE SERVICES OFFERED BY BATTERY OPERATED AUTO-RICKSHAWS

Route Fixation:

The indiscriminate plying of the mode on national or regional highways which carry heavy traffics should be controlled by direct intervention of town's authority. This might minimize the mode's chance of getting engaged to traffic accidents.

Driving License:

Mostly the operators of battery operated auto-rickshaws are unknown of traffic rules. This issue has increased the mode's vulnerability to traffic accidents at great extent. Therefore, operators should be required with driving license to ensure all of them are well trained. They should be provided with training on town authority's own accord in this regard as most of them are from poor section of the town and hence reluctant to spend money on training or driving license purposes.

REFERENCES

- [1]. The Daily Star, "Electric Rickshaws Run out of Steam", Published on May 30, 2011.
- [2]. The New Age, "Unregistered Easy-bikes Still Plying City Streets", Published on January 06, 2011.
- [3]. Easy-bike Owner's Association, Kushtia and Faridpur, Unpublished Office Documents Keeping Records of the Number of Battery Operated Auto-rickshaws in Town, 2011.
- [4]. District Traffic Police, "Traffic and Registration, Comilla District", An Unpublished Office Document Keeping Records of the Number of Different Types of Vehicles in the District Area, 2011.
- [5]. The Daily Prothom Alo, "Easy Biker Busy Shohor" (in Bangla), "Busy City with Easy-bike", Published on January 03, 2011.
- [6]. Discovery Bangladesh, "Travel Info: Distance City to City", 2011, Available: http://www.discoverybangladesh.com/travel_info_distance_chart.html, [Accessed: November 04, 2011].
- [7]. UTIDP, "Upazilla Town Infrastructure Development Project: Transport Survey Report", An Unpublished Document, Local Government Engineering Department (LGED), Level-8, RDEC Building, Dhaka, Bangladesh, 2011.

The Effects of Groundnut Shell Addition on The Insulating Properties of Clay Samples From Kogi State Nigeria

Manukaji John U.

Federal Polytechnic, Bida Niger State Nigeria

Abstract: Clay samples from three towns in Kogi state were examined with the aim of determining their chemical composition as well as testing for their suitability as refractory insulating materials for local furnaces. Refractories are required for many other industries in Nigeria like in chemical, ceramic, petrochemical, oil, foundry and iron and steel industries. The presence of air in these pores reduces the conductive capacity of the refractories and therefore increasing their insulating characteristics. Apart from the natural occurring fire clays which has been adjudged an insulating refractories, other clays can have their insulating characteristics improved by the addition of materials like saw dust, rice husks and other farm wastes. Experiments were carried out to determine how the addition of groundnut shell could improve the refractory properties of clay samples from Kogi State. The experiments were carried out on the four mechanical properties that enhance the insulating properties of clay which are linear shrinkage, thermal conductivity, apparent porosity and solid density. The results showed significant improvement in these properties.

Keywords: Effects, groundnut shell on insulating properties, clay, Kogi State Nigeria

I. INTRODUCTION

Nigeria as a developing economy houses a lot of industries that utilize refractory material in abundance. Nigeria also has abundant mineral resources including clay. Despite the large deposits of clay in many parts of the country, local manufacturing of refractory materials for local use had been very low. Refractories are used in metal melting and heat treatment industries because of their high temperature operating conditions. It is also used in industries both as lagging and insulating material. They degenerate with time and therefore need replacement Abifarin (1999). If the industries that use them are to remain in business, replacement must not only be produced but also must be locally sourced. clay minerals are of secondary geologic origin i.e. they were formed as alteration products of alumino-silicate rocks in an environment in which water is present Olusola (1998). Clay minerals are produced mainly from the weathering of feldspars and micas. They form part of a group of complex alumino-silicates of potassium, magnesium and iron, known as layer-lattice minerals. They are very small in size and very flaky in shape, and so have considerable surface area Thring (1962).

MATERIALS AND METHODS

The clay samples to be used for the manufacturing of the base plates were mined from ten different locations on a particular sight in order to have a good representation of the sight. Three sights were used for the state in order to further give a wider sample spread for the state. The sights are

KOGI STATE : Uhodo, Oguma, Odogi

The mined clay samples from the ten locations on a sight were mixed properly and a representative specimen for test from that sight was produced using the cone and quartering system as recommended by the American Society of Testing Materials (ASTM).

The resultant specimen for each sight were kept in a P.V.C. bags and labeled as follows.

LOCATION SPECIMEN LABEL

Uhudo	G
Oguma	H
Odogi	I

The raw materials for the production of various refractory products include kaolinite ($Al_2O_3 \cdot 2SiO_2 \cdot 2H_2O$), chromite ($FeOCr_2O_3$), magnesite ($MgCO_3$) and various other types of clays. Agha (1998) Therefore in determining the suitability of the clay samples from Kogi state, as refractory material the chemical constituents of the specimens, were first determined using The Atomic Absorption Spectroscopy method. The results obtained are as shown in the table below

TABLE 2: CHEMICAL ANALYSIS

Oxides in Specimen	SiO ₂	Al ₂ O ₃	Fe ₂ O ₃	TiO ₂	CaO	MgO	K ₂ O	Na ₂ O	L.O.I
G in %	44	35	1.3	2.4	0.5	0.6	1.5	0.7	14
H in %	45	34	1.5	1.5	0.4	0.1	1.4	0.1	16
I in %	46	34	0.9	3.0	0.2	0.4	1.2	0.3	14

Manukaji(2004)

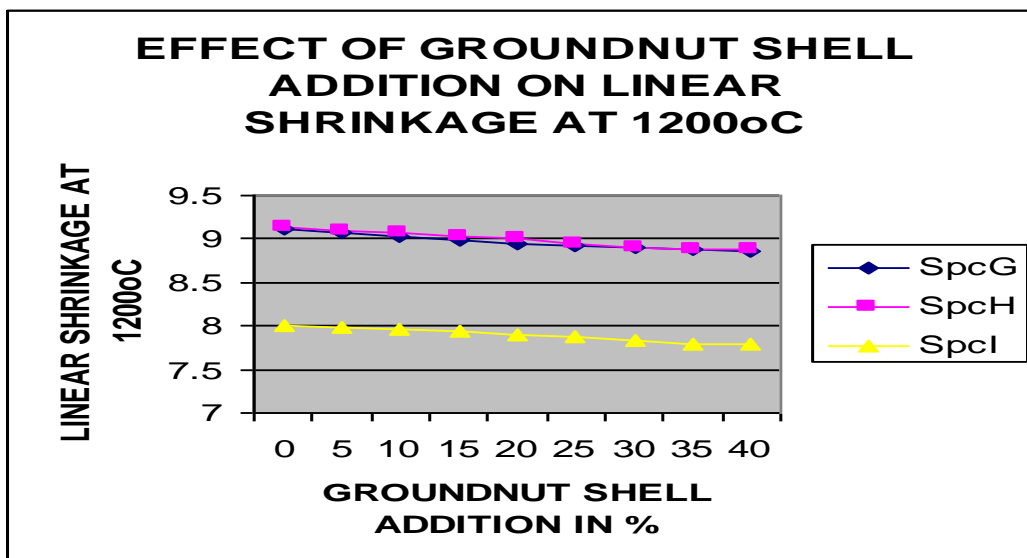
opined that for a refractory clay to have good insulating characteristics, it must have amongst others the following characteristics

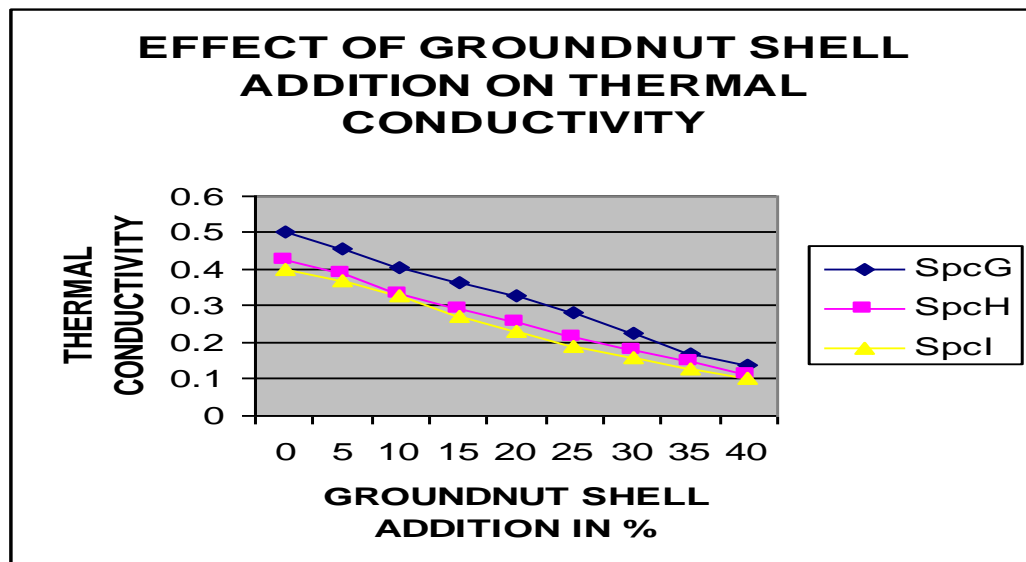
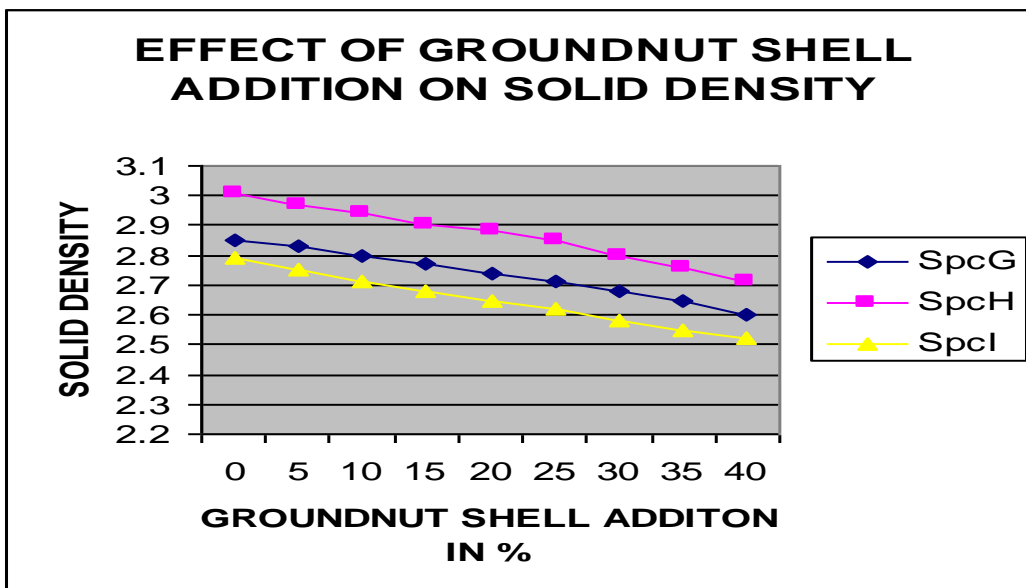
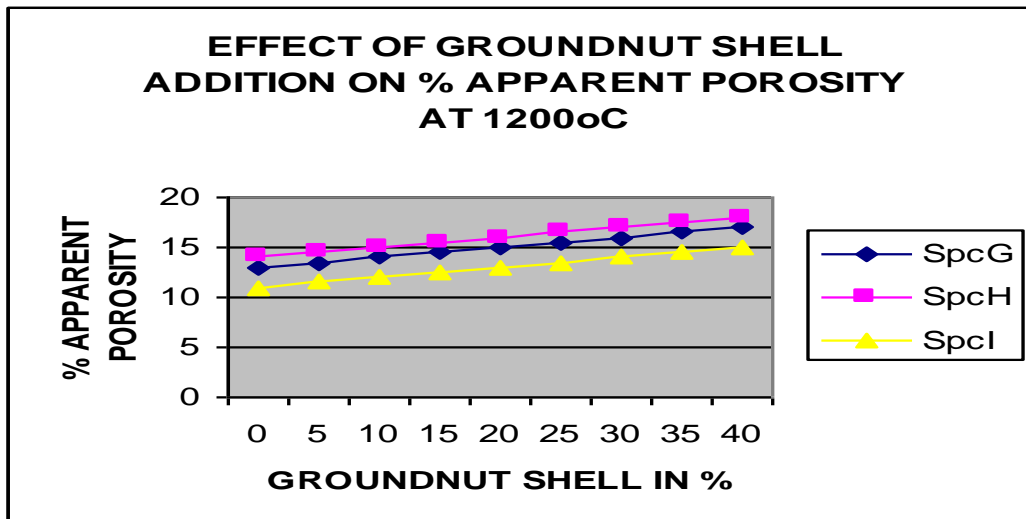
- (1) It must be highly porous
- (2) It must have low thermal conductivity
- (3) It must have low solid density
- (4) It must have a reasonably low linear shrinkage.

II. RESULTS AND DISCUSSION

The effects of groundnut shell addition on the above properties of the clay specimens were studied and the results are shown and discussed as follows.

1. The linear shrinkage showed a steady reduction in value as the quantity of groundnut shell addition increased thereby bringing the values closer to the lower values of the acceptable range of 7-10% IEE(1992).
2. The apparent porosity increased in value from 12% to 18% in most of the samples thereby bringing them closer to the international range of 20-80% Theraja et al(1999), Oaikhinan (1988).
3. The solid density of the samples reduced steadily as the groundnut shell addition increased moving them closer to the lower acceptable range of 2.3-3.5g/cm³ Ijagbemi (2002)
4. The thermal conductivity of the samples decreased steadily as more groundnut shell was added making the samples better insulators Manukaji(2004)





III. CONCLUSION AND RECOMMENDATION

From the tests carried out on the addition of groundnut shell to the clay samples, it could be concluded that properties like porosity, thermal conductivity, linear shrinkage and solid density of the clays from these locations improved significantly and can be varied to suit the particular insulating property desired.

RECOMMENDATIONS FOR FURTHER WORK

Based on the tests carried out on clay samples from Kogi State, further improvements on the insulating properties could be achieved by the addition of materials like rice husks, sawdust, bentonite, graphitic asbestos, coal and other farm wastes. Further improvement could also be carried out by passing the clay samples through a magnetic sieve to reduce the content of Fe_2O_3 present in the clay.

REFERENCES

- [1]. Agha O A (1998) Testing of local refractory clay for producing furnace lining bricks. M. Eng. Thesis: Mech. Eng. Dept. F.U.T. Minna
- [2]. Abifarin M. S. (1999) Investigation on local refractory materials for high temperature applications, PhD Thesis mech. eng. dept. Federal University Of Technology, Minna
- [3]. IEE (1992) Wiring regulation requirement for electrical installation BS7671 , 15th Edition , A Mclay and co. Ltd Cardiff
- [4]. Ijagbemi C.O.(2002) Development and performance evaluation of a biomass clay lined cookstove. Meng thesis , Department of mechanical Federal University of Technology Akure, Nigeria.
- [5]. Manukaji J.U.(2004) An investigation into the use of local clays as a high temperature insulator for electric cookers. PhD Thesis mech. eng. dept. Federal University Of Technology, Minna
- [6]. Oaikhinan E.P (1988) Rheological properties of certain Nigerian clay. Proceedings of the international ceramic conference Australia.
- [7]. Olusola E O (1998) Investigation of Zungeru clay as refractory material for high temperature applications M. Eng. Thesis, Dept. of mech. engrg. F. U. T. Minna
- [8]. Theraja B. L. and Theraja A. K , (1999) Electrical technology, S. Chand and co. Ltd, New Delhi

Study of Noise Pollution Due To Railway and Vehicular Traffic at Level Crossing and Its Remedial Measures

Anurag V. Tiwari¹, Prashant A. Kadu², Ashish R. Mishra³

¹Lecturer, Department of Civil Engineering, G H Raison Polytechnic, Amravati

²Associate Professor, Department of Civil Engineering, PRMITR, Badnera

³Lecturer, Department of Civil Engineering, Jagdamba college of engineering and technology, Yavatmal

Abstract: Amravati is second largest and very important city in Vidarbha region. As Amravati is developing area and a good education centre there is a rapid urbanization and alarming growth of population is causing serious environmental problems. Noise is one of the environmental problem that uncomferts in daily life. Noise pollution has become major concern for communities living within the city. Considering the sudden increase in the number of trains from Amravati railway station, rapid growth and illness effect due to noise pollution, there is need to study noise pollution in Amravati. In this study an attempt is made to monitor the noise pollution due to railway and vehicular traffic at one of the major intersection Rajapeth using digital sound meter along with the collection of traffic volume data and train frequency. The variation in the noise level due to railway crossing, traffic flow and traffic volume data in the peak hours are studied and presented in the graphical form for the selected location. The study also includes the remedies which can be provided for minimizing the noise pollution.

Keywords: Noise Pollution, Railways, Traffic noise

I. INTRODUCTION

Amravati is the seventh most populated metropolitan city in Maharashtra located at 20° 56' North latitude 77° 47' East longitude. The total area of the Municipal Corporation is about 121.56 Sq. Km. and the population as per 2011 census record is 899,579 souls. Amravati has good road, rail connectivity with almost all important cities like Nagpur, Mumbai, Kolkata, and Chennai. Noise is an inevitable part of everyday life. Mild noise can be annoying, excessive noise can destroy a person's hearing. The slightest unwanted sound can become very annoying if it continues for any length of time. The vehicular traffic and railways are the major sources of noise. Railways are noisy, it contributes a high concentration of noise in a very less time period, which is very dangerous for human health. The major factors influencing the generation of noise due to railways are Frequency of Trains, Speed of Trains, Nature of Railway Track, Intensity of Horn and many more.

Rajapeth is one of the important intersection in Amravati. From this intersection one of the major road goes towards Badnera and another one go towards Ambadevi, Rajkamal and Dasturnagar. Also a railway route from Amravati railway station to Badnera railway station passes through this intersection. The various Educational institutes, vegetable market, religious places, temples, commercial market, marriage hall, bus stop, auto stop etc., are connected by this intersection. Recently due to sudden increase in the number of train from Amravati railway station the railway gate at Rajapeth railway crossing is closed for almost 2:30 hours a day which causes traffic conjunction, which causes great inconvenience to the road users and nearby locality. Roadway noise is the collective sound energy emanating from motor vehicles. It contributes more to environmental noise exposure than any other noise source, and is constituted chiefly of engine, tire, aerodynamic and braking elements. According to C.C. Bhattacharya, et al. (2001), the major factors which influence the generation of road traffic noise are Traffic flow, Traffic speed, Proportion of heavy vehicles, Gradient of the road, Nature of the road surface, Obstruction due to noise barriers, etc.

II. AMBIENT AIR QUALITY NOISE STANDARDS (AAQNS)

Most of the countries, keeping in view the alarming increase in environmental noise pollution, have given the permissible noise standards. These are depending on the location and period of day. Industrial areas obviously have somewhat higher acceptable sound levels than those prescribed for residential areas. The collected night standards are stringent than the daytime standards.

2.1 Standards by Law in India

Noise has been recognized as ambient air pollutant. Standards in this regard are laid down under Environment (Protection) Rules, 1986 and under the Model Rules of the Factories Act, 1948. The Central Pollution Control Board constituted a Committee on Noise Pollution Control. The Committee recommended noise standards for ambient air and for automobiles, domestic appliances and construction equipment, which were later notified in Environment (Protection) Rules, 1986 as given below in Table.

Table 1: Noise Standards for Different Category of Area

Area Code	Category of Area	Limits in dB	
		Day time	Night time
A	Industrial area	75	70
B	Commercial area	65	55
C	Residential area	55	45
D	Silence Zone	50	40

2.2 Recommended noise levels by the Bureau of Indian Standards (BIS)

Bureau of Indian Standards has recommended acceptable noise levels in residential areas, injury range and safe range are as given in Table below.

Table2: Acceptable noise levels in Residential Areas

Sr. No.	Location	Acceptable Noise Level in Residential Areas, dB
1	Rural	25-35
2	Suburban	30-40
3	Residential (urban)	35-45
4	Urban (Residential and Business)	40-45
5	City	45-50
6	Industrial Areas	50-60

III. MATERIALS AND METHODS

Studies have mentioned that periodical noise study is most appropriate and less expensive of course continuous noise study is desirable but not necessary and is more expensive. The study was carried out using the Digital sound level meter (TES-1350A). In the present study, a noise sample size of 5 minute in each hour was taken at the selected location. Noise sample were collected in dB (A) scale at every 30 second interval (i.e. 2 counts per minute) or total 10 reading in one sample size. The observations were taken at a distance 1.2 meter from the edge of road and at right angle to the centerline of road and the railway track. The continuous monitoring of noise level was observed from morning 8:00 am to 08:00 pm daily for the span of 3 months generally when the train used to pass from the route.

IV. RESULTS

All the days the recorded values are very-very high than the permissible levels. The maximum noise pollution is recorded is during the passage of train through level crossing which is notable. The effects of noise pollution are auditory and non-auditory. Deafness, heart attack, increase in cholesterol, high blood pressure, hyper tension, causes emotional disturbance, constriction of blood vessels such sever adverse effects are recorded due to the noise pollution.

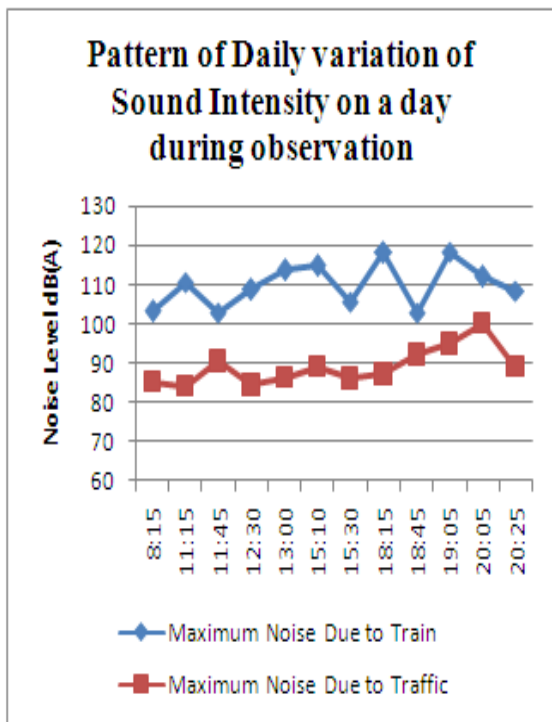


Fig 1: Pattern of variation of sound Intensity on a day during observation

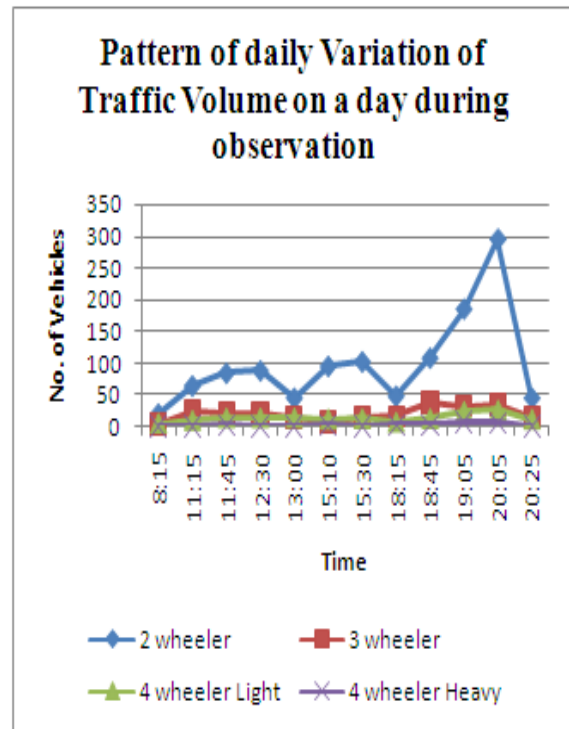


Fig 2: Pattern of variation of Traffic volume on a day during observation

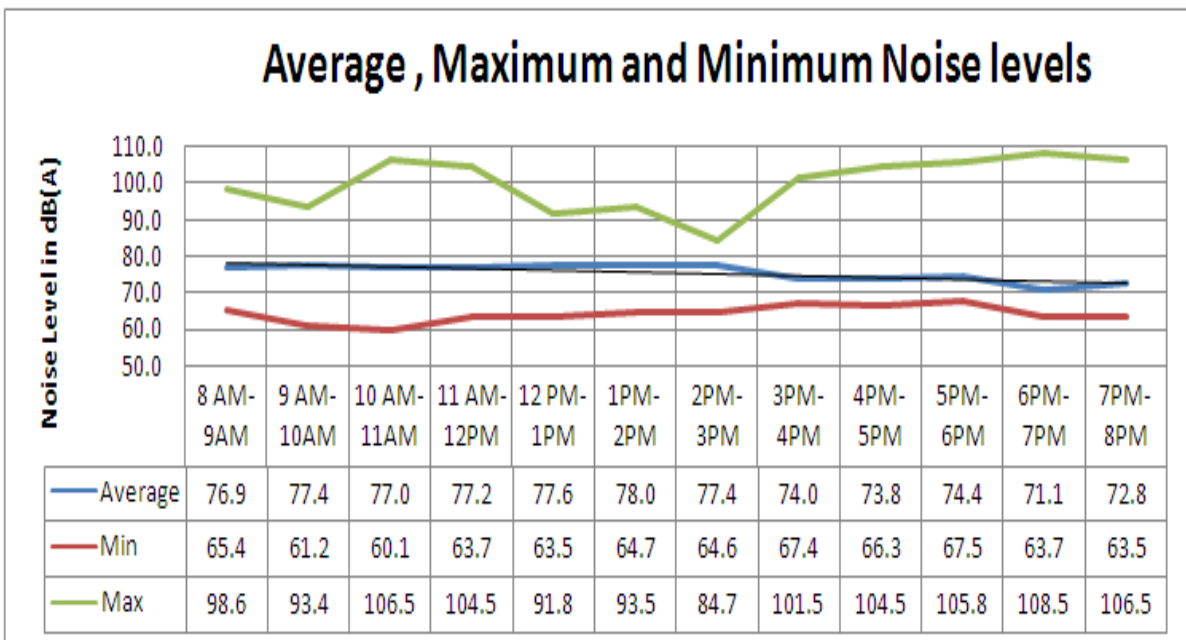


Fig 3: Average, Minimum and Maximum Noise Levels during the observation period

V. REMEDIAL MEASURES

Since the fact that public health has been matter of great concern for us control of noise pollution is necessary. The remedial measure for noise pollution can be broadly classified as control at source, control in the transmission path, using protective equipment. The noise pollution can be controlled at the source of generation itself by reducing the noise levels from domestic sectors, Maintenance of automobiles, Control over vibrations, Low voice speaking, Prohibition on usage of loud speakers and optimum selection of machinery, tools or equipment reduces excess noise levels. The change in the transmission path will increase the length of travel for the wave and get absorbed/refracted/radiated in the surrounding environment. The noise pollution can be

reduced during transmission path by Vegetation, Installation of barriers and design of the building incorporating the use of suitable noise absorbing material for wall/door/window/ceiling will reduce the noise levels. Protective equipment usage is the ultimate step in noise control technology i.e., after noise reduction at source and after diversion or engineer control of transmission path of road. The usage of protective equipment and the worker's exposure to the high noise levels can be minimized by Job rotation, Exposure reduction, Hearing protection, use of Equipment like earmuffs, ear plugs etc. are the commonly used devices for hearing protection. Attenuation provided by ear-muffs varies widely in respect to their size, shape, seal material etc. Literature survey shows that, average noise attenuation up to 32 dB can be achieved using earmuffs. Also Strict enforcement of existing law to prohibit air horns inside the town, Proper maintenance of the vehicles, Laying good roads and their maintenance, Strict enforcement of the existing law to remove the encroachments on road sides, Plantation of trees like Neem and Coconut and other vegetation inside the town on road sides and around the silence zone, Highly noise producing machines can be kept in isolated buildings and glass cabin can be provided, Educating people about the hazards of loud sound and restriction on the use of pressure horns, loud speakers and fire crackers shall play an important role in mitigating sound will reduce the noise levels.

VI. CONCLUSION

From the observations taken at the selected station, it was found that the sound exceeds permissible limit of 55 dB for residential and 65dB for commercial area. On all study at the selected location the maximum noise limits were ranging between 70 dB to 110 dB which was almost 1.5 times the permissible limits for commercial zone. This variation of sound from 70dB to 120dB may have moderate to very severe effects on human health such as, poor concentrations, stress, cardiovascular illness and many more. It is very essential to control noise at source, along the transmission path and at receivers end by using the remedial measures.

REFERENCES

- [1] R. K. Mishra, M. Parida, S. Rangnekar. "Evaluation and analysis of traffic volume noise along has rapid transit system corridor" Int. Journal of Environ. Science Tech., 1 September 2010. pp 737-750.
- [2] Prof. S. M. Patil, "Law on Environment – Some Reflections", pp 177-1185, 2005.
- [3] Anisa B. Khan "Impact of noise pollution on community health – A study at Pondicherry ", Indian Association of Biomedical Scientists , Vol. 18, No. 3, 1998, pp 183-190.
- [4] N. Tandon and H. Pandey, "Noise levels of some vehicles and Traffic Noise at some Major Road Crossing in south Delhi", Indian J.Environmental Protection, Vol. 18, No. 6, June 1998, pp 454-458.
- [5] T. VidyaSagar and G. NageswaraRao. "Noise Pollution Levels in Visakhapatnum City (India)" Journal of Environ. Science and Engg. Vol. 48, No. 2, pp 139-142, April 2006.
- [6] C. C. Bhattacharya, Dr. S. S. Jain, S. P. Sing, Dr. M. Parida, Ms. Namita Mittal, "Development of Comprehensive Highway Noise Model for India Condition" Indian Road Congress Journal, Paper No. 481, 2001, pp 453-488.
- [7] Digvijay Sing, B. D. Joshi "Study of noise pollution for three consecutive years during Deepawali festival in Meerut City", Utter Pradesh. New York Science Journal.
- [8] P M Raut. A thesis on " Study of Noise Pollution in Akola City"
- [9] M.N. Rao, H.V.N. Rao, Air Pollution Control, Tata McGrawHill. 5. Peavy2008.
- [10] <http://m.indiarailinfo.com/faq/post/756>

Determination operation Time Risk of Box Spinning Components-oe Spinning Machine

Slobodan Stefanovic

Graduate School of Applied Professional Studies, Vranje, Serbia

Abstract: Based on the constructed dependency diagram reliability of the exploitation operation time of each constituent components of the analyzed frame in the case of selected statistical distributions, areas of the operation exploitation and repair intervals are determined. This is done by determining the first inflection points. Based on these points analysis to determine the time of safety operation of frame components with allowable risk to the segmental linear function of the intensity of failure from empirical data components. Mathematical dependence dependability is determined on the basis of universal quadratic equation based on will determine the allowable risk time in operating the components of the analyzed frame.

Keywords: reliability, depending diagrams, inflection points, universal quadratic equations.

I. INTRODUCTION

BASIC PRINCIPLE OE - spinning

Basic Principles of the rotor - bezvretenskog spinning procedure consists in the formation of individual fibers, yarns, which were previously isolated from the output tape (tape carded). Display labels R1 OE spinning machines whose circuits are analyzed in this dissertation was carried out on **picture 1**.

Phases of this type of spinning (spinning classic bezvretenski way) consists of the following operations:

- bed (I and II), the operation of discretization of fibers (separation of individual fibers) from the output carded strip,
- transport of individual fibers with the air stream,
- stacking of individual fibers (group) at the entrance to the report,
- spinning fibers in the report and
- finished winding the yarn at the exit of the rotor.



Picture (1) Showing OE - spinning label R1 (Rieter)

Table 1: Comparison of phase spinning

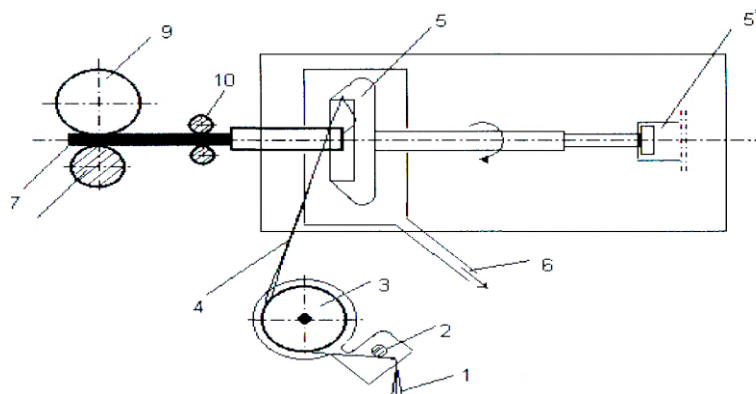
CLASSIC without spindles PROCEDURE	CURRENT PROCEDURE without spindles
1. CLEANING Second carding Third bed and Stretch II without spindles SPINNING	1. Automatic line Interrelated: • OPENING • Mixing • CLEANING • carding • REGULATORY 2. Stretch Second without spindles SPINNING

One of the main advantages without spindles spinning procedure for the processing of cotton and chemical fibers, cotton is a type in the number of phases. In the classical process of spinning the ring spinning machine, spinning process occurs in seven stages of work, while in modern without spindles spinning process occurs in two stages of spinning, which are shown in Table 1.

According without spindles spinning process, the material in the form of strips (1) with the other passages stretch over the opening roller (2) into the zone of action devices bed (3). Bed roller whose speed of 7000-8000 rpm (r / min) was coated with special serrated set so that the pull tapes from a single fiber (4), which is followed by electricity in the air transport for the spinning rotor (5). Individual fibers extracted with the help of air flow entering tangentially to the wall of the rotor. The high-speed rotor (rotor with a diameter ϕ 32 and the rotor 115 000 (o / min)) fibers are packed into the groove of the rotor in the form of wedge-beam parallel. Rotating rotor due to the effects of centrifugal force and effect Koriolisovog acceleration ie. force, formed by some form of the yarn balloon. Yarn spun from the rotor through the outlet rollers (10) wound on the spool (9). Cross drainage Speed ranges from 25-220 (m / min), the capacity of the coil to 5 (kg) with yarn wound on it (usually a coil capacity up to 2 (kg) with a wound yarn). Scheme without spindles ways of spinning the OE spinning type R1, manufacturer of Swiss company Rieterr is shown in **picture 2**.

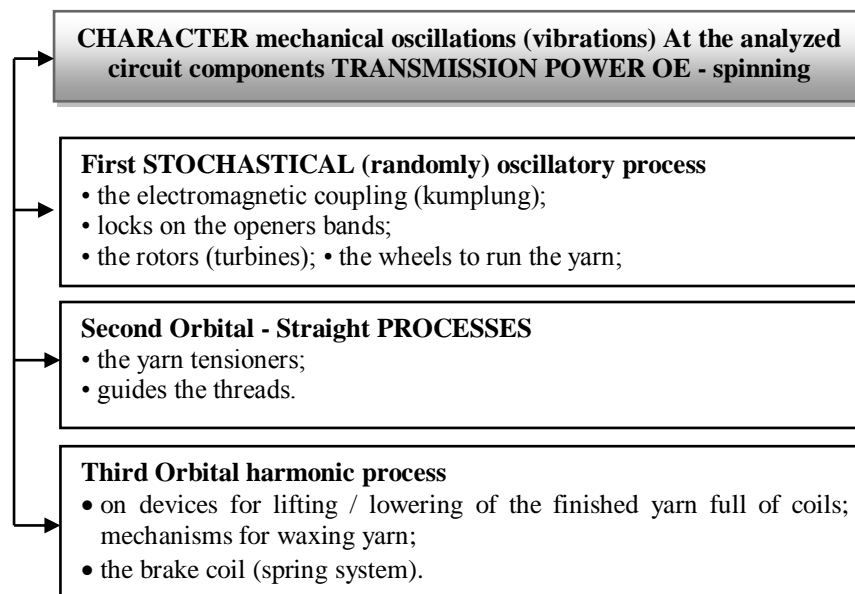
II. CHARACTER MECHANICAL OSCILLATIONS (VIBRATIONS) IN THE ANALYZED OE - SPINNING

The analysis of mechanical oscillations, given the importance of character formation that these phenomena. types of events that cause failures of component parts and components analyzed OE - spinning machine. The character (s) of the mechanical oscillations of the control points on the power transmission assemblies for spinning boxes and assembly of the finished yarn winding coils appear in three forms, namely as (**picture 2**).



1.First Ribbon fiber, 2. The opening roller, 3. Roller bed fiber, 4. Oriented fibers, 5. Rotor, 5'. Aerobed, 6. Dust extraction nozzle out of the box, 7. Yarn, 8. Guide or, 9 Coil. , 1.0 Rollers for tensioning the yarn before winding the bobbin **Picture (2)** A simplified view of how to obtain yarn spinning method without spindles

1. First Stochastic (random) oscillatory processes;
2. Second Oscillation of the oscillatory processes - pan;
3. Third Oscillation of the oscillatory processes - harmonic motion.



Picture (3) Diagram of classification character of mechanical oscillations of the analyzed components, fluid power components OE – spinning

III. INTRODUCTION TECHNICAL DESCRIPTION OF SPINNING BOX

The basic components are:

INTRODUCTORY CHANNEL(A6)

serves to introduce carded strips in spinning box. Introductory channel or sprayer for removal carded strip is made of sintered ceramic which has high resistance to abrasion and wear. The sprayer is universal for all types of removal carded strip (Fig. 2).

LOCKS BAND OPENER (A7)

a steel cylinder in which a larger diameter is pulled a assembly for combing (comb carding strips) which performs parallelization of the fiber bundle. On the one hand this roller is over bearing and it is supported. Roller diameter is \varnothing 80 mm. This construction of roller allows properly opening (combing) with full preservation of their own carded fibers from the strips. Gear profile is optimal for smooth and complete opening of strip locks. Set with gear is resistant to the occurrence of friction for improved performance when working circuit and a longer duration. When mixed fiber yarn which themselves have anti-static (usually titanium dioxide is added to the yarn to shine) comb set is much faster wore out, respectively the gear set is quickly wore out, and 3-5 times faster than without antistatic yarn processing (Figure 6.).

ELECTROMAGNETIC COUPLING (KUMPLUNG) (E1)

its design provides security retraction of carded strip into the comb roller. If comes to a withdrawal of the carded strip mass it responds and stops the spinning process. Coupling rotational speed range is from $v_{ob} = 0,2 \div 0,8$ (m/min). Carded strip that introduces by electromagnetic coupling, is in range: for cotton 5,88 tex, for mixture 5,0 tex. These values are constant for all carded strip (Fig. 3.).

NOZZLE (Dekle) (A3)

perform material feed (individual fibers in the rotor - turbine) and is called the rotor lid.

SYSTEM OUTLET PIPE FOR VACUUM DIRT (A4)

constructively through compressed air outlet pipe increases separation of impurities utilization by 15-25% and avoiding an increase in waste good fiber compared to other manufacturers of these spinning machines. This aims to reduce the the ability to break of yarn during the spinning because a total separation of impurities affect the reduction of the ability to break yarn to 55%. Through the outlet pipe stand out all the dirt from carded strip, and it is constantly during operation of OE – spinning machine (Figure 6.).

ROTOR (TURBINES) (A1)

rotor diameter of the analyzed transmission system is \varnothing 32 mm, and is used for quality yarns 10-120 tex (8 - 100 Nm). The material of the rotor is specially alloyed titanium steel with high resistance to abrasion and high hardness up to 70 HRC. Rotor speed is 115 000 (r/min). The construction of this type of rotor has the following advantages: less rotor weight compared to conventional systems non spindle spinning, the lower consumption of this solution rotor, use is universal for all types of yarn, high resistance against the appearance of friction when reclining operation strip.

AIRCRAK (A2)

constructively is a combination of bearing with protective plates and consists of AERO static bearing in air. This is the first construction so far this kind of bearings. Constructive solutions of aircranks so far were performed with conventional plates where the bearing for axially moving is permanently lubricated, and in this way of performing all processes take place over an air, over a layer of air. This layer of air is compressed air and brings it to the rotor and the ends of the rotor. Such constructive aircrank performance not allow any effect of mechanical friction. This layer of air is intended to keep leading to the ends of the rotor, so that at the highest rotor speed can prevent vibrations. Because of this structural solution, aircrank and the rotor have quiet operation with virtually no noise. Because of all the above mentioned advantages this type of construction ensures the self future as a constructive solution to the largest number of spinning rotor speed (to 130 000 r/min). Also, cleaning of aircranka and the rotor during operation is performed with compressed air, which is carried out safely remove the tiniest bit of dirt. It should be noted that in the rotor is forming yarn with a number of turns.

- The previously explained, reliance of rotor and centricity in the radial direction on the pads - friction wheels, while in the axial direction his reliance and centricity is on air-cushion which is forcing air construction.
- **INTAKE BOX (A5)** - perform removal of dirt which is in carded stripe at its entrance to the roller for combing.
- **ELECTRONIC READERS (E2)** - controls the quality of yarn per cycle spinning in box spinning. Certainly, at any time signalize quality of the yarn by the party, and automatically provides information if there is ability to break or to inadequate or yarn characteristics. Also controls measurement of the yarn length which is made in spinning box. The main types of errors that it finds and registers are: N-nope, S-short thick places, L-long thick places, T -thin places, Mo-moire, C-number of yarn.
- **WHEEL RUNNING YARN (A8)** – is made of special type of Ebonite (hard rubber), which crafted the pressure evenly to tensioner could function properly. When the wheel is taken for such material coating which is resistant to mechanical damages (cutting and lining) due to cross the yarn, and it is also resistant to the occurrence of friction.
- **TENSIONER YARN (A9)** - is structurally designed as a simple spring system that tightens the yarn evenly with any numerous yarn. Tensioner movement is oscillatory harmonic, with its deflection angle $\alpha = 8-12^\circ$.
- **WAXING YARN MECHANISM (A10)** - at the individual plant in each spinning box. The mechanism causing the paraffin yarn stops at each break yarn. The mechanism has a closed housing with a large block of paraffin in it, which is good thing from the standpoint with the smooth operation of making large quantities of yarn with one battery housing. Installation and removal so as replacement of paraffin is very simple. Waxing the yarn is necessary due to a decrease in the influence of electrostatic friction yarn.

IV. Diagrams Of Reliability Of Operation Of Spinning Box Components On Which Are Not Implemented Preventive Maintenance Technologies Procedures In Case Of Lognormal Statistical Distribution

Shown diagrams of reliability give an accurate determination of the proper operation dependency of each constituent component and the reliability of inflection points in the transition state of repair (views in Figures 4. – 12.).

Based on the constructed diagram dependency of the reliability of the constituent components of the analyzed frame $f(R_e(t), t)$ (views in Figures 3. – 21.) are determined the area of the operation exploitation and interval repairs. This was necessary in order to implement the timing analysis of the constituent components of the mean interval to failure.

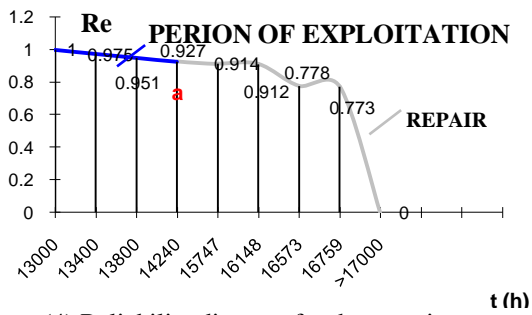


Figure (4) Reliability diagram for the constituent component rotor (turbine) - A1

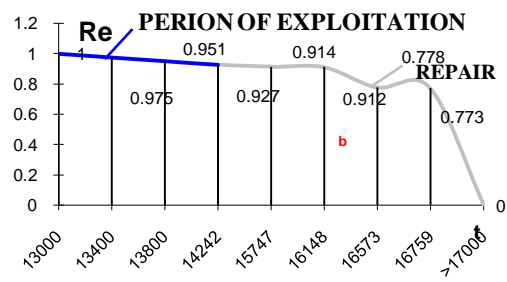


Figure (5) Diagram of reliability for component aircrank - A2

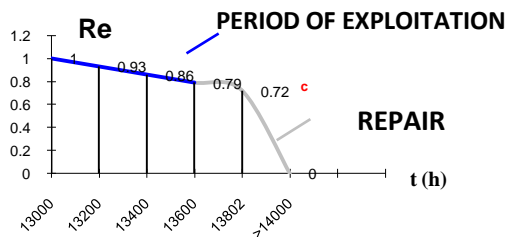


Figure (6) Diagram of reliability for constituent component dekla (rotor lid) - A3

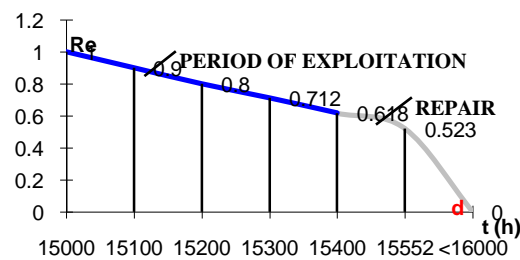


Figure (7) Diagram of reliability for constituent component outlet pipe spout - A4

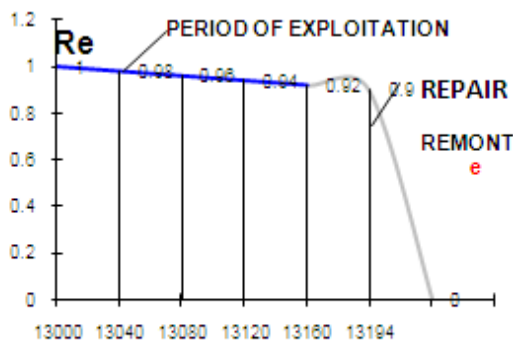


Figure (8) Diagram of reliability for constituent Component intake box - A5

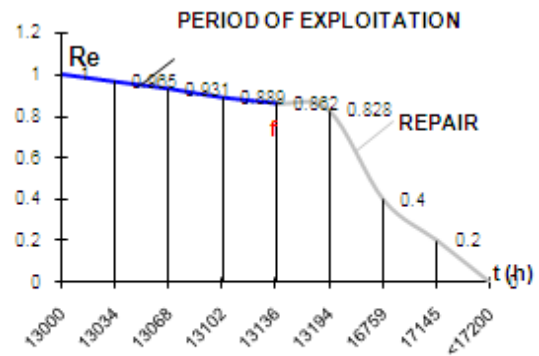


Figure (9) Diagram of reliability for constituent component introductory channel - A6

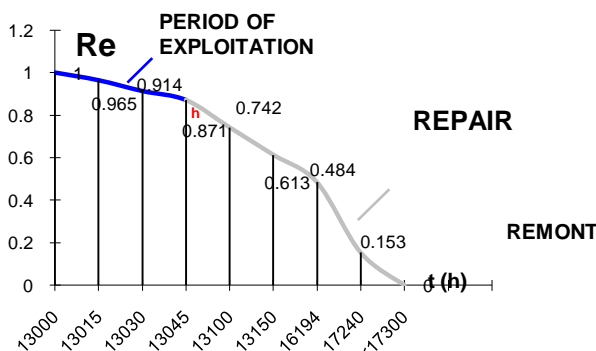


Figure (10) Diagram of reliability for constituent component locks band opener - A7

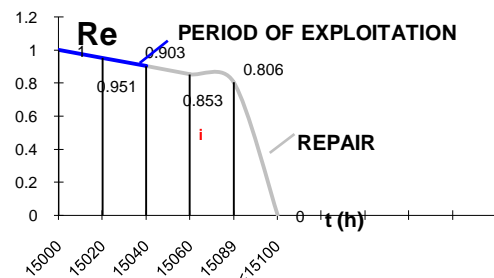


Figure (11) Reliability diagram for the constituent component electromagnetic coupling - E1

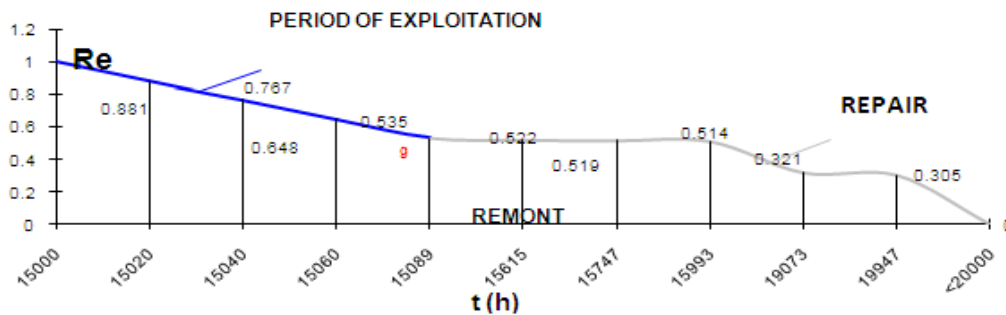


Figure (12) Reliability diagram for electronic reader – E2

Based on shown reliability diagrams crossing points are visible, and basis of them a table dependency of boundary intervals to analyze the reliability of each constituent component (Table 2.) is formed. Also in these intervals to monitor the value of the amplitude of oscillation at selected measuring points. Based on these intervals in its boundaries, we come to the field of monitoring of each constituent component. Further analysis of the security of function of the constituent components of the analyzed frame is committed within the limits of these intervals, respectively to border monitoring their work to repair.

Table 2: Depending on the limit of the interval to analyze the reliability of each constituent component of analyzed frame where are not implemented preventive maintenance technology procedures

Components mark	Mark inflection points in the diagram reliability p_t	The marginal value of the exploitation time of the components of Δt_{ξ_i}	The marginal reliability value of the exploitation time of the components of Δp_{ξ_i}
A6	f	13136	0,862
A5	e	13160	0,92
A7	g	15089	0,535
E1	h	13045	0,871
A3	c	13600	0,79
A4	d	15400	0,618
A1	a	14240	0,927
A2	b	14240	0,927
E2	i	15040	0,903
A8, A9, A10		> 20000	1,0

V. Correction Value Of Operation Reliability Of Components Spinning Box Frame In Case Lognormal Statistical Distribution Where Preventive Maintenance Technology Procedures Are Applied

1. Introductory channel

The procedure for determining the reliability of this constituent component will be detail processed. Procedures for obtaining reliable values for the time intervals of the constituent components to failure, where preventive maintenance technology procedures are implemented. The basic parameters are taken:

- The time interval $t = 15\ 750$ (h) operation component to failure,
- The breakdown frequency $f_{e(A6\ 1)}(t) = 1,33 \cdot 10^{-6}$,
- Correction value of reliability obtained from empirical patterns $P_{eA6}(t) \cong \varphi(z)$.

Correction standard deviation obtained from the form:

$$\sigma \approx \frac{\varphi(z)}{t \cdot f_z(t)} \approx \frac{0,8}{15750 \cdot 1,33 \cdot 10^{-6}} \approx 3,819(h);$$

Admitted: $|\sigma = 3,8(h) \Rightarrow \varphi(z) = 0,796 \Rightarrow R_{A6-0}(t) = \varphi(z) = 0,796$.

From the table of values for the area under the standard normal statistical distribution of reliability is adopted:
 $z = 0,84 \Rightarrow \mu = \ln t - z \cdot \sigma = \ln 15750 - 0,84 \cdot 3,8 = 6,47(h)$

Note: Further should not be analyzed reliability values $R(t) = P_z(t) \leq 0,5$ because the surfaces are covered in the confidence interval had no significant value by default Lognormal standard distribution. The values of the parameters that deal with the reliability of the constituent components spinning box frame (introductory channel) in the case lognormal reliability distribution (Table. 3.).

Table 3: Includes all the parameters that determine the operation reliability of the constituent components spinning box frame (introductory channel) in the case of Lognormal reliability distribution

Name system constituent component	Component mark	Time operation interval of component to failure $\Delta t, (h)$	$f_{A6-0}(t)$	z	μ	σ	$R_{A6-0}(t) = \varphi(z)$
Introductory channel	A6	14 001	-	-	-	-	1,0
		14 300	$1,33 \cdot 10^{-6}$	2,32	-2,495	5,128	0,989
		14 600	$1,33 \cdot 10^{-6}$	1,17	1,17	5,0	0,9563
		14 900	$1,33 \cdot 10^{-6}$	1,38	3,23	4,79	0,916
		15 200	$1,33 \cdot 10^{-6}$	1,16	4,6	4,595	0,877
		15 500	$1,33 \cdot 10^{-6}$	0,98	4,05	4,394	0,836
		15 750	$1,33 \cdot 10^{-6}$	0,84	3,8	-	0,796
		16 850	$1,33 \cdot 10^{-6}$	0,25	2,7	-	0,5987

Table 4: Includes all the parameters that determine the operation reliability of the constituent components spinning box frame (intake box) in the case of Lognormal reliability distribution

Name system constituent component	Component mark	Time operation interval of component to failure $\Delta t, (h)$	$f_{A5-0}(t)$	z	μ	σ	$R_{A5-0}(t) = \varphi(z)$
Intake box	A5	14 001	-	-	-	-	1,0
		15 850	$7,14 \cdot 10^{-6}$	1,22	0,094	7,85	0,888
		16 902	$7,14 \cdot 10^{-6}$	0,77	7,43	3,11	0,7794

2. Locks band opener

Table 5: Includes all the parameters that determine the operation reliability of the constituent components spinning box frame (locks band opener) in the case of Lognormal reliability distribution

Name system constituent component	Component mark	Time operation interval of component to failure $\Delta t, (h)$	$f_{A7-0}(t)$	z	μ	σ	$R_{A7-0}(t) = \varphi(z)$
Lock band opener	A7	15 630	-	-	-	-	1,0
		15 730	$3,64 \cdot 10^{-3}$	1,31	7,595	1,579	0,904
		15 830	$3,64 \cdot 10^{-3}$	0,85	8,186	1,392	0,8023
		15 930	$3,64 \cdot 10^{-3}$	0,53	9,034	1,21	0,7019
		16 030	$3,64 \cdot 10^{-3}$	0,26	9,413	1,0327	0,6026
		16 330	$3,64 \cdot 10^{-3}$	0	9,7	0,841	0,5
		16 820	$3,64 \cdot 10^{-3}$	0	9,73	0,651	0,3989

3. Electromagnetic coupling

Table 6: Includes all the parameters that determine the operation reliability of the constituent components spinning box frame (electromagnetic coupling) in the case of Lognormal reliability distribution

Name system constituent component	Component mark	Time operation interval of component to failure $\Delta t, (h)$	$f_{E1-0}(t)$	z	μ	σ	$R_{E1-0}(t) = \varphi(z)$
Electromagnetic coupling	E1	14 001	-	-	-	-	1,0
		14 151	$5,12 \cdot 10^{-5}$	1,36	-7,8	12,6	0,913
		14 251	$5,12 \cdot 10^{-5}$	0,94	-1,07	11,32	0,826
		14 351	$5,12 \cdot 10^{-5}$	0,64	3,17	10	0,738
		14 451	$5,12 \cdot 10^{-5}$	0,38	6,25	8,75	0,648
		14 501	$5,12 \cdot 10^{-5}$	0,16	8,38	7,55	0,563
		14 751	$5,12 \cdot 10^{-5}$	-	-	-	0,472
		15 001	$5,12 \cdot 10^{-5}$	-	-	-	0,384
		15 501	$5,12 \cdot 10^{-5}$	-	-	-	0,296
		15 751	$5,12 \cdot 10^{-5}$	-	-	-	0,2107
16 001	$5,12 \cdot 10^{-5}$	1,13	6,67	2,57	0,21		

4. Dekla (Nozzle) - rotor lid

Table 7: Includes all the parameters that determine the operation reliability of the constituent components spinning box frame (dekla - rotor lid) in the case of lognormal reliability distribution

Name system constituent component	Component mark	Time operation interval of component to failure $\Delta t, (h)$	$f_{A3-0}(t)$	z	μ	σ	$R_{A3-0}(t) = \varphi(z)$
Dizna - Dekla	A3	14 128	-	-	-	-	1,0
		14 300	$6,66 \cdot 10^{-5}$	1,59	7,992	0,991	0,944
		14 600	$6,66 \cdot 10^{-5}$	1,21	8,486	0,911	0,886
		14 900	$6,66 \cdot 10^{-5}$	0,96	8,80	0,837	0,831
		15 200	$6,66 \cdot 10^{-5}$	0,75	9,056	0,764	0,773
		15 500	$6,66 \cdot 10^{-5}$	0,43	9,371	0,645	0,666
		15902	$6,66 \cdot 10^{-5}$	0,42	9,41	0,625	0,6628
		16 830	$6,66 \cdot 10^{-5}$	0	9,7	0,356	0,3989

5. Outlet pipe

Table 8: Includes all the parameters that determine the operation reliability of the constituent components spinning box frame (outlet pipe) in the case of Lognormal reliability distribution

Name system constituent component	Component mark	Time operation interval of component to failure $\Delta t, (h)$	$f_{A4-0}(t)$	z	μ	σ	$R_{A4-0}(t) = \varphi(z)$
Odvodna cev	A4	15 995	-	-	-	-	1,0
		16 150	$4,16 \cdot 10^{-5}$	1,59	7,455	1,405	0,944
		16 300	$4,16 \cdot 10^{-5}$	1,22	8,10	1,309	0,888
		16 450	$4,16 \cdot 10^{-5}$	0,97	8,525	1,219	0,834
		16 600	$4,16 \cdot 10^{-5}$	0,74	8,892	1,115	0,7703
		16 750	$4,16 \cdot 10^{-5}$	0,43	9,31	0,961	0,67
		16 900	$4,16 \cdot 10^{-5}$	0	9,735	0,948	0,6664

6. Rotor (turbine)

Table 9: Includes all the parameters that determine the operation reliability of the constituent components spinning box frame (rotor- turbine) in the case of Lognormal reliability distribution

Name system constituent component	Component mark	Time operation interval of component to failure $\Delta t, (h)$	$f_{A1-0}(t)$	z	μ	σ	$R_{A1-0}(t) = \varphi(z)$
Rotor	A1	13 983	-	-	-	-	1,0
		14 100	$4,52 \cdot 10^{-5}$	1,41	7,518	1,44	0,9207
		14 200	$4,52 \cdot 10^{-5}$	1,0	8,56	1,312	0,8423
		14 300	$4,52 \cdot 10^{-5}$	0,71	9,0014	1,177	0,7611
		14 400	$4,52 \cdot 10^{-5}$	0,47	9,08	1,046	0,6808
		14 500	$4,52 \cdot 10^{-5}$	0,26	9,34	0,919	0,6026
		14 600	$4,52 \cdot 10^{-5}$	0,06	9,54	0,794	0,5239
		14 700	$4,52 \cdot 10^{-5}$	0	9,6	0,662	0,44
14 830	$4,52 \cdot 10^{-5}$	0	9,605	0,547	0,3668		

7. Aircrank

Table 10: Includes all the parameters that determine the operation reliability of the constituent components spinning box frame (aircrank) in the case of lognormal reliability distribution

Name system constituent component	Component mark	Time operation interval of component to failure $\Delta t, (h)$	$f_{A2-0}(t)$	z	μ	σ	$R_{A2-0}(t) = \varphi(z)$
Aeroleaj	A2	13 983	-	-	-	-	1,0
		14 100	$4,11 \cdot 10^{-5}$	2,58	5,436	1,596	0,925
		14 200	$4,11 \cdot 10^{-5}$	1,04	7,95	1,548	0,8508
		14 300	$4,11 \cdot 10^{-5}$	0,76	8,56	1,321	0,7764
		14 400	$4,11 \cdot 10^{-5}$	0,53	8,946	1,186	0,7019
		14 500	$4,11 \cdot 10^{-5}$	0,32	9,246	1,049	0,625
		14 600	$4,11 \cdot 10^{-5}$	0,13	9,47	0,919	0,5517
		14 830	$4,11 \cdot 10^{-5}$	0	9,6	-	-

8. Reader

Table 11: Includes all the parameters that determine the operation reliability of the constituent components spinning box frame (electronic reader) in the case of lognormal reliability distribution

Name system constituent component	Component mark	Time operation interval of component to failure $\Delta t, (h)$	$f_{E2-0}(t)$	z	μ	σ	$R_{E2-0}(t) = \varphi(z)$
ita	E2	15 905	-	-	-	-	1,0
		17 230	$5 \cdot 10^{-5}$	0,85	8,96	0,93	0,8023

For other frame components of spinning box reliability is $R_{A8}(t) = R_{A9}(t) = R_{A10}(t) = 1,0$ and at the same did not show any cancellations during the period of their work.

VI. Operation Reliability Diagrams Of Frame Component Spinning Box Where Preventive Maintenance Technologies Procedures Are Implemented In Case Of Lognormal Statistical Distribution

Certain reliability diagrams are shown in Figures 13. – 21.

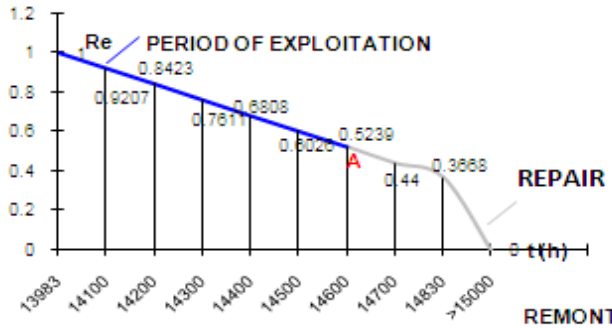


Figure (13) Reliability diagram for the component rotor (turbine) - A1

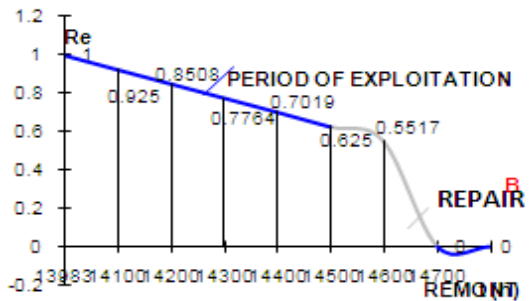


Figure (14) Diagram of reliability for component aircrank - A2

Note: Low limit value for the reliability of the components of the rotor (A1) and aircrank (A2) spinning box frame are because it does not make any substitution of these components with new ones, but they carried out the repair that included grinding the rotor shaft and cleaning the openings (holes) on aircranks. This was done because of the high price of these components on the market.

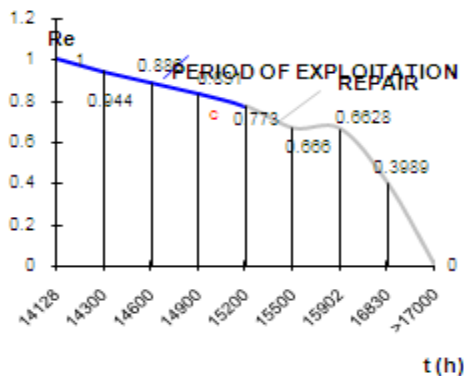


Figure (15) Reliability diagram for the component nozzle (dekla - rotor li) - A3

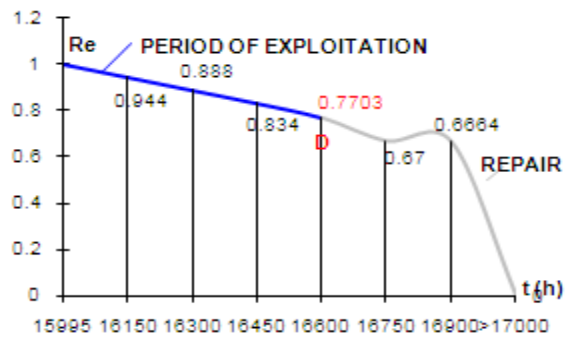


Figure (16) Diagram of reliability for outlet pipe - A4

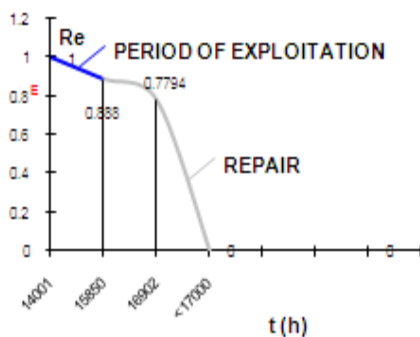


Figure (17) Diagram of reliability for intake box-A5

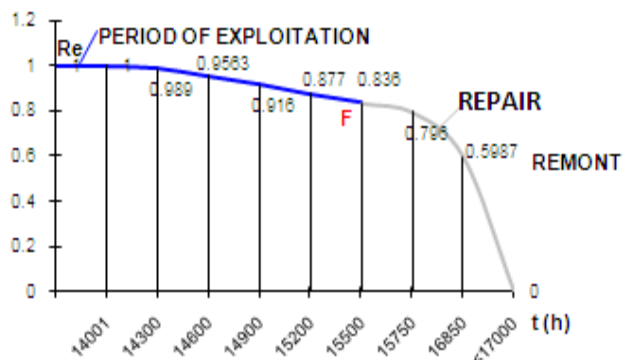


Figure (18) Diagram of reliability for component introductory channel - A6

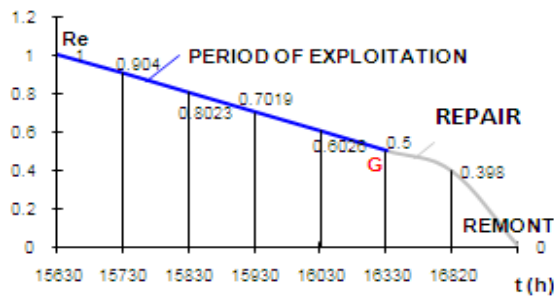


Figure (19) Diagram of reliability for component Locks band opener-A7

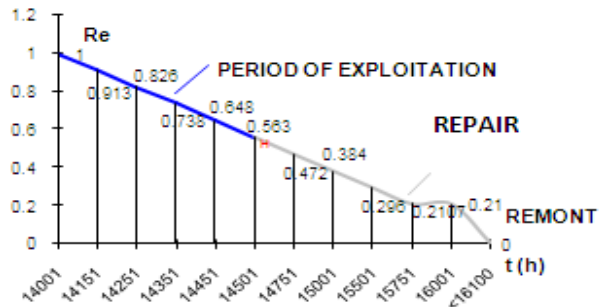


Figure (20) Reliability diagram for the component electromagnetic coupling-E1

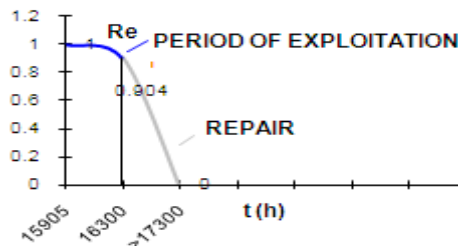


Figure (21) Reliability diagram for component electronic reader - E2

On the basis of the diagrams is completed tabulation (Table 12.) limits the state of exploitation of the constituent components of the analyzed frame where preventive maintenance technology procedures are applied.

Based on the values in Table 12. clearly are defined limits dependency on the reliability of exploitation operation for each component of analyzed frame. These values are authoritative and will be used in determining the correlation dependence.

Table 12: Dependency on the limit interval to analyze the reliability of each constituent component of analyzed frame where preventive maintenance technology procedures are implemented

Component frame mark	Mark inflection points in the reliability diagram p_{t_i}	The marginal value of the exploitation operation time of the constituent components Δt_{g_i}	The marginal value of the reliability for exploitation operation time of the constituent components Δp_{g_i}
A6	F	15500	0,868
A5	E	15850	0,888
A7	G	16330	0,5
E1	H	14501	0,563
A3	C	15200	0,773
A4	D	16600	0,7703
A1	A	14600	0,5239
A2	B	14500	0,625
E2	I	17230	0,904
AS, A9, A10		>20000	1,0

VII. TIME SEQUENCE OF SAFETY COMPONENTS CIRCUITS ANALYZED WITH ALLOWED RISK

Time sequence of the components of security frame with allowable risk is determined at intervals of components including: a safe time to failure of the frame components (t_2) and time of when the first cancellation of frame components (t'_2).

The author has chosen for this analysis because it can be determined and allowed risk of components frame to the planned time for the repair and continued productivity regardless of the risk of falling under allowed.

Analysis of the timing of safety frame components to the allowable risk being carried by segmental linear function of the intensity of failures from empirical data to time interval $t_2 \leq t_R \leq t'_2$, in which the t_R -components of allowable time (during the allowed risk).

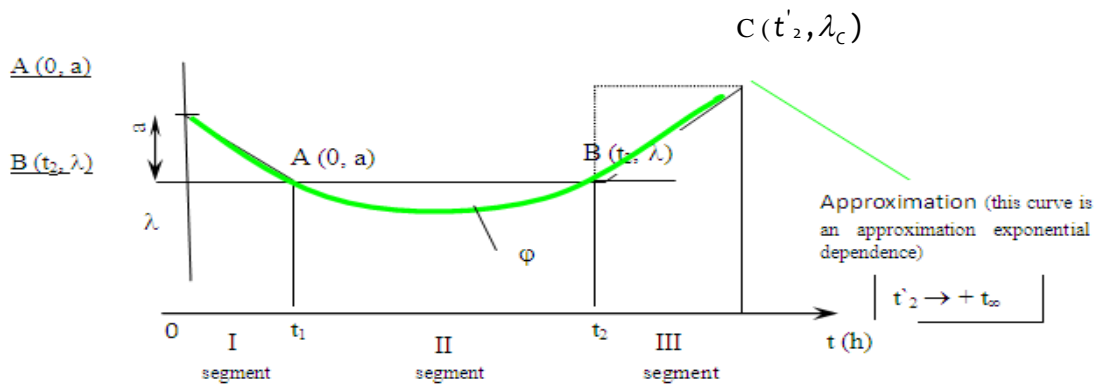
Any failure intensity function can be approximated in a way that its graph divided into a number of segments (shown in Figure 19.).

In this analysis we have taken three segments:

Part I: The component frame operation during his run-in period (the time t_1). Running assemblies is also running OE – spinning machine, and it lasted 500 (h).

Part II: Operation of the frame components (time interval $t_1 < t \leq t_2$).

Part III: Operation of component assemblies with allowed risk (time interval $t_2 < t \leq t'_2$).



A and B are the coefficients of the line direction
 Figure (19) Sectional divisions failure intensity function

Failure intensity function is shown in segments:

1. $\lambda_{(t)} = a - A \cdot t, 0 \leq t \leq t_1 = const.$ during this period did not cause any failure of any component parts assemblies, and this period is called the initial period.
2. $a = \lambda(t), t_1 < t \leq t_2 = const.$ This is the period of safe operation of the frame components.
3. $\lambda'_{(t)} = \lambda_{C(t_2)} + B(t' - t_2), t_2 < t' < t'_2$ The period of occurrence of the first failure (risk period).

Analysis of the timing of safety components assemblies with allowed risk is related to the analysis of period created of first failures (segment III in Figure 19.), and for this period the reliability function is expressed by the formula:

$$R_i(t') = e^{-\left[at_1 - \frac{At_1^2}{2} + \lambda_{C(t_2)}(t' - t_2) + \frac{B}{2}(t' - t_2)^2 \right]}$$

where as $a, A = 0$, because in the initial period components did not cause failures of the analyzed constituent components.

Rearranging equation reliability to time, we get the final expression of the universal quadratic equation that characterizes the allowed time travel:

$$\frac{B}{2}t'^2 + (\lambda_{C(t_2)} - B \cdot t_2) \cdot t' + \left(\ln R_i(t')_{sr} - \lambda_{C(t_2)} \cdot t_1 + \frac{B}{2}t_1^2 \right) = 0,$$

whose solutions are: $t_{I,II}$, where are the allowable travel time (t_R) is calculated as the sum of the time to the first failure t_2 , and the time $t_{I,II}$ (one of the solutions to the time value of universal quadratic equations)

$$t_R = t_2 + t_{I,II}.$$

The universal values which the quadratic equation in figuring it (make it) are as follows: $\frac{B}{2} \leftarrow$ the coefficient of the quadratic term, and direction of the line coefficient is determined by the expression

$$B = tg\varphi = \frac{\lambda_{C(t_2)} - \lambda_{C(t_1)}}{t_2 - t_1}, \text{ of which was } \lambda_{C(t_2)} = \frac{f_C(t)}{R_i(t)}, \text{ until the value of reliability } R_i(t_2) \text{ is taken}$$

from Lognormal statistical reliability distribution for the period of risk (time t_2) and is expressed as the mean value for the reliability $R_i(t_2)_{sr}$. for time interval of risk time t_2 , in other words

$$R_i(t_2)_{sr} = \frac{\sum_{i=1}^n R_i(t_2)}{n}. \lambda_{C(t_2)} - B \cdot t_2 \leftarrow \text{coefficient that goes along with the linear member;}$$

$$\left(\ln R_i(t)_{sr} - \lambda_{C(t_2)} \cdot t_1 + \frac{B}{2} \cdot t_2^2 \right) - \text{Constant coefficient.}$$

VIII. CONCLUSION

On the basis of universal quadratic equation can be formed tabulation of the values of its solutions, which leads to the determination of the allowable operation time of components of the analyzed frames (Table 13.). Tabular presentation included the value of the two methods of analyzing safety work time of components to the allowable risk as follows:

1. Without implementing the preventive maintenance technology procedures in operation of the components analyzed frame and
2. With implementing the preventive maintenance technology procedures in operation of the components analyzed frame.

Table 13: Safety operation time of components of analyzed frame with allowable risk where the preventive maintenance technology procedures are not implemented

Values	A ₆	A ₅	A ₇	E ₁	A ₃	A ₄	A ₁	A ₂	E ₂
$\lambda_{C(t_2)}$	1,428 · 10 ⁻³	7,93 · 10 ⁻³	4,16 · 10 ⁻³	5,49 · 10 ⁻⁴	2,38 · 10 ⁻³	4,166 · 10 ⁻³	5 · 10 ⁻³	4,54 · 10 ⁻³	1,428 · 10 ⁻³
t ₁ (h)	500	500	500	500	500	500	500	500	500
t ₂ (h)	13 000	13 000	15 000	13 000	13 000	15 000	13 000	13 000	15 000
t' ₂ (h)	13136	13160	15089	13045	13600	15400	14240	14240	15060
R _i (t' ₂) _{sr}	0,931	0,971	0,767	0,9335	0,895	0,809	0,963	0,963	0,903
Quadratic equation solutions t _{i,jl}	68	80	40	23	300	190	600	600	300
Time allowed risk limits t _R	13068	13080	15040	13023	13300	15190	13600	13600	15040

REFERENCES

- [1]. Application of Reliability – centered maintenance to naval aircraft, weapon systems and support equipment, MIL-HDBK-266, DoD, USA, 1
- [2]. Arnold D., Auf dem Weg zum Autonomen Materialfluss, Logistik im Unternehmen, Nov./Dez., 1989.
- [3]. Barlow, G., Proshan, F., Statistical Theory of Reliability and Life Testing Probability Models, Holt, Richard and Winston Inc., New York, 1975.
- [4]. Callick, E.B., Teretechnology – principles and practice, teretechnology Handbook, HMSO, London, 1978.
- [5]. Stefanovic S., Effect of mechanical vibration on the occurrence of functional safety circuits in the power transmission system of textile machines, Ph.D. Thesis, Technical Faculty "Mihajlo Pupin", Zrenjanin, 2006.
- [6]. Stefanović S., DETERMINATION OF THE VALUE OF SELECTED OSCILLATION FREQUENCY MEASUREMENT POINT ANALYZED PARTS OE SPINNING - On theboxspinning, International Journal Of Mechanical Engineering Research and Development, India, 2012.

Industrial Potential of Some Clay Deposits In Kogi State North Central Nigeria

Manukaji John U.

Federal Polytechnic, Bida Niger State Nigeria

Abstract: The samples collected from ten sites each from Uhodo, Oguma and Odogi were pulverized, dried, sieved and quantitatively analyzed. Physical, chemical and mechanical properties of the samples were determined. Results of the chemical analysis carried on the raw samples showed that it contained substantial amount of silicon oxides (44-46%) and aluminum oxides (34-35%), which qualifies it as Alumino-silicates. Physical and mechanical properties also determined are particle size distribution, specific gravity, bulk density, solid density, water absorption, apparent porosity, permeability to air, refractoriness, thermal shock resistance, modulus of rupture, linear shrinkage and thermal conductivity. The sieve test showed that most of the clay were retained within 300 μm . The values for specific gravity, bulk density, solid density and apparent porosity averaged 2.82, 2.88 g/cm^3 , 2.88 g/cm^3 , and 12.67% respectively and they were within the internationally accepted range. The values for linear shrinkage, permeability to air and thermal shock averaged 8.75%, 77.3, and 29+ respectively and these also were within the accepted limits. The values for modulus of rupture and thermal conductivity averaged 90.67 MN/m^2 and 0.443 $\text{W/m}^2\text{K}$. The refractoriness of all the samples were $>1300^\circ\text{C}$ and this showed that they could be used as insulating materials.

Keywords: Industrial, Potential, Clay Deposits, Kogi State Nigeria

I. INTRODUCTION

Clay is a common name for a number of fine-grained, earthy materials that become plastic when wet. Chemically, clays are hydrous aluminum silicates, ordinarily containing impurities, e.g., potassium, sodium, calcium, magnesium, or iron, in small amounts Grimshaw (1959). They are divided into two classes: residual clay, found in the place of origin, and transported clay, also known as sedimentary clay, removed from the place of origin by an agent of erosion and deposited in a new and possibly distant position. Residual clays are most commonly formed by surface weathering, which gives rise to clay in three ways—by the chemical decomposition of rocks, such as granite, containing silica and alumina; by the solution of rocks, such as limestone, containing clayey impurities, which, being insoluble, are deposited as clay; and by the disintegration and solution of shale Manukaji (2004). One of the commonest processes of clay formation is the chemical decomposition of feldspar. Clay minerals are typically formed over long periods of time by the gradual chemical weathering of rocks, usually silicate-bearing, by low concentrations of carbonic acid and other diluted solvents. These solvents, usually acidic, migrate through the weathering rock after leaching through upper weathered layers. In addition to the weathering process, some clay minerals are formed by hydrothermal activity Guggenheim et al (1995). Clay deposits may be formed in place as residual deposits in soil, but thick deposits usually are formed as the result of a secondary sedimentary deposition process after they have been eroded and transported from their original location of formation. Clay deposits are typically associated with very low energy depositional environments such as large lakes and marine basins. Primary clays, also known as kaolins, are located at the site of formation. Secondary clay deposits have been moved by erosion and water from their primary location. Depending on the academic source, there are three or four main groups of clays: kaolinite, montmorillonite-smectite, illite, and chlorite. Chlorites are not always considered a clay, sometimes being classified as a separate group within the phyllosilicates. There are approximately 30 different types of "pure" clays in these categories, but most "natural" clays are mixtures of these different types, along with other weathered minerals. Ehlers et al(1982)

Clays exhibit plasticity when mixed with water in certain proportions. When dry, clay becomes firm and when fired in a kiln, permanent physical and chemical changes occur. These reactions, among other changes, cause the clay to be converted into a ceramic material. Because of these properties, clay is used for making pottery items, both utilitarian and decorative. Different types of clay, when used with different minerals and firing conditions, are used to produce earthenware, stoneware, and porcelain. Clay, being relatively impermeable to water, is also used where natural seals are needed, such as in the cores of dams, or as a barrier in landfills against toxic seepage (lining the landfill, preferably in combination with geotextiles). Hillier (2003) Clay is one of the oldest building materials on Earth, among other ancient, naturally-occurring geologic materials such as stone and organic materials like wood. Between one-half and two-thirds of the world's population, in traditional societies as well as developed countries, still live or work in a building made with clay as an essential part of its load-bearing structure.

Properties of the clays include plasticity, shrinkage under firing and under air drying, fineness of grain, color after firing, hardness, cohesion, and capacity of the surface to take decoration. On the basis of such qualities clays are variously divided into classes or groups; products are generally made from mixtures of clays and other substances. The purest clays are the china clays. A refractory material is one that retains its strength at high temperatures. ASTM C71 defines refractories as "non-metallic materials having those chemical and physical properties that make them applicable for structures, or as components of systems, that are exposed to environments above 1,000 °F (811 K; 538 °C)". Guggenheim et al (1995)

Refractory materials are used in linings for furnaces, kilns, incinerators and reactors. They are also used to make crucibles. Refractory materials must be chemically and physically stable at high temperatures. Depending on the operating environment, they need to be resistant to thermal shock, be chemically inert, and/or have specific ranges of thermal conductivity and of the coefficient of thermal expansion. The oxides of aluminium (alumina), silicon (silica) and magnesium (magnesia) are the most important materials used in the manufacturing of refractories. Another oxide usually found in refractories is the oxide of calcium (lime). Fire clays are also widely used in the manufacture of refractories. Refractories must be chosen according to the conditions they will face. Some applications require special refractory materials. Zirconia is used when the material must withstand extremely high temperatures. Silicon carbide and carbon (graphite) are two other refractory materials used in some very severe temperature conditions, but they cannot be used in contact with oxygen, as they will oxidize and burn.

Binary compounds such as tungsten carbide or boron nitride can be very refractory. Hafnium carbide is the most refractory binary compound known, with a melting point of 3890 °C. Hugh(1992) The ternary compound tantalum hafnium carbide has one of the highest melting points of all known compounds (4215 °C). McGraw-Hill (1977)

MATERIALS AND METHODS

The clay samples to be used for the manufacturing of the base plates were mined from ten different locations on a particular sight in order to have a good representation of the sight. Three sights were used for the state in order to further give a wider sample spread for the state. The sights are

KOGI STATE NIGERIA: Uhodo, Oguma, Odogi

The mined clay samples from the ten locations on a sight were mixed properly and a representative specimen for test from that sight was produced using the cone and quartering system as recommended by the American Society of Testing Materials (ASTM). The resultant specimen for each sight were kept in a P.V.C. bags and labeled as follows.

LOCATION	SPECIMEN LABEL
Uhudo	G
Oguma	H
Odogi	I

COLOUR INSPECTION

The specimen were physically inspected for colour appearance and the following results as shown below were observed.

SPECIMEN	COLOUR
G	Grayish
H	Whitish ash
I	Creamy Yellow

II. SIEVE TESTING

Each specimen was milled down using a ball or hammer mill. It was soaked in water for 48 hours after which, it was dried by spreading it on a tray and placing it in the sun to dry. It was milled to powdery form using a ball or hammer mill after which 600g of the specimen were sieved using 700 μ m, 500 μ m, 300 μ m, 100 μ m, 50 μ m. The sieve were placed on a mechanical vibrator operated for 30 minutes after which the content of each sieve was weighed. The mass of the specimen left at each compartment of the sieve, the percentage retained and the percentage passed were calculated.

TABLE 1: SIEVE ANALYSIS

CLAY SPECIMEN	Sieve no in μ m	Mo	M1	%R	%P
SPECIMEN G	700	600	27.20	4.53	95.47
	500	600	125.42	20.90	79.10
	300	600	230.07	38.35	61.65
	100	600	140.47	23.41	76.59
	50	600	60.47	10.08	89.92
SPECIMEN H	700	600	32.21	5.37	94.63
	500	600	152.51	25.42	74.58
	300	600	230.17	38.36	61.64
	100	600	112.47	18.75	81.25
	50	600	61.30	10.22	89.78
SPECIMEN I	700	600	38.19	6.37	93.63
	500	600	143.02	23.84	76.16
	300	600	220.09	36.68	63.32
	100	600	128.08	21.35	78.65
	50	600	43.31	7.22	92.78

CHEMICAL ANALYSIS

In determining the chemical constituents of the specimens, The Atomic Absorption Spectroscopy method was used and the results were as follow

TABLE 2: CHEMICAL ANALYSIS

Oxides in Specimen	SiO ₂	Al ₂ O ₃	Fe ₂ O ₃	TiO ₂	CaO	MgO	K ₂ O	Na ₂ O	L.O.I
G in %	44	35	1.3	2.4	0.5	0.6	1.5	0.7	14
H in %	45	34	1.5	1.5	0.4	0.1	1.4	0.1	16
I in %	46	34	0.9	3.0	0.2	0.4	1.2	0.3	14

FURTHER TESTS

The specimen were subjected to further standard refractory test and the result obtained are tabulated below.

TABLE 3: SPECIFIC GRAVITY

Clay specimen	G	H	I
Specific Gravity	2.92	2.78	2.77

TABLE 4: BULK DENSITY

Clay specimen	G	H	I
Bulk density g/cm ³	1.91	2.08	2.01
Solid densityg/cm ³	2.85	3.01	2.79

TABLE 5: LINEAR SHRINKAGE

Clay specimen	G	H	I
% average drying shrinkage	2.32	2.16	2.27
% average firing shrinkage at 1200°C	9.11	9.13	8.01

TABLE 6: PERCENTAGE WATER ASORPTION

Clay Specimen	G	H	I
% water absorption at 110°C	29.2	28.7	30.1
% water absorption at 1200°C	3.1	3.0	3.1

TABLE 7: APPARENT POROSITY

Clay specimen	G	H	I
% apparent porosity at 110°C	23	25	20
% apparent porosity at 1200°C	13	14	11

TABLE 8: PERMEABILITY

Clay Specimen	G	H	I
Permeability	78.3	74.5	79.1

III. REFRACTORINESS

Test cones were prepared from each clay specimen, dried and placed in a furnace along with pyrametric cones designed to deform at 1000, 1300, and 1500°C respectively in accordance with the American society of testing materials (ASTM). The temperatures were then raised at 10°C per min. and was determined by the means of an optical pyrometer. The maximum temperature available in the furnace was 1300°C and the test cones did not show any sign of failure or deformation, meaning that all the clay samples have a > 1300°C refractoriness.

IV. THERMAL SHOCK RESISTANCE

Test cubes 50mm square were also produced from each clay specimen and put in an electric furnace that already attained a temperature of 900°C. They were soaked there for 20 minutes after which they were brought out and cooled in stream of air. The cubes were tested by using hand to pull them apart. If they do not fracture or crack, they were returned to the furnace for the process to be repeated. This process must continue repeatedly until fracture or crack occurs. The results showed that non of the cubes cracked under 29 cycles.

TABLE 9: MODULUS OF RUPTURE

Clay specimen	G	H	I
M.O.R at 110°C KN/m ²	6283	7172	6983
M.O.R at 1200°C MN/m ²	88	94	90

TABLE 10 : THERMAL CONDUCTIVITY

CLAY SPECIMEN	G	H	I
THERMAL CONDUCT W/mK	0.502	0.427	0.401

V. RESULTS AND DISCUSSION

FIRING COLOUR CHANGE.

The samples showed some darkened colour changes at temperatures of 1200°C from their original colour to ashy black. This was however attributed to the fact that the firewood smoke had serious effect on the colour change.

SIEVE ANALYSIS

Tables 1 showed the particle distribution of the clay samples. It was however observed that most of the particles were retained within the sieve mesh of 300µm

CHEMICAL ANALYSIS

TABLE 2 showed the chemical analysis of the clay samples. The results showed that most of the clays were siliceous in nature, having the highest number of silica present. Also the presence of Aluminum oxide of the order of between 25—45% makes them to fall under the class of Alumino-Silicate refractories. **Hassan et al (1993)**

SPECIFIC GRAVITY

The specific gravity values of the samples in table 3 fell between 2.7 – 3 and this fell within the ranges for Nigerian clays as reported by **Akinbode (1996)**, **Hussaini (1997)**. It is pertinent to note that the values compared favourably with international range of 2.0 and 2.9. Sample **I** had the lowest value of 2.77 while sample **G** had the highest value of 2.92. **Obi(1995)**

BULK DENSITY AND SOLID DENSITY

The bulk densities of the samples were shown in table 4 and the values fell within the internationally accepted range of 1.7—2.1g/cm³ for fire clays .Thring (1962)

The solid density of the samples also fell within the internationally accepted range of 2.3—3.5g/cm³. Ryan (1978). The highest solid density value was recorded by sample H while the least was by sample I

LINEAR SHRINKAGE

Table 5 showed the linear shrinkage of the samples at 110°C and 1200°C. The linear shrinkage values obtained at 1200°C varied from 8.01 in sample I, 9.11 in sample G to 9.13 in sample H. Although this gives an indication of the efficiency of firing, it fell within the internationally accepted value of 7—10% value for Alumino-silicates, Kaolin and fireclays.Zubeiru(1997)

WATER ABSORPTION

Table 6 showed the percentage water absorption at 110°C and 1200°C. From the table, sample I showed the highest percentage of water absorbed while sample H showed the least at 110°C. At 1200°C, sample G and I showed the highest value while sample H showed the least Hassan(1990).

APPARENT POROSITY.

Table 7 showed the apparent porosity of the samples at 110°C and 1200°C respectively. Sample I had the least value while samples H had the highest at 110°C. Meanwhile all the samples fell within the internationally accepted value of 20% and 80% Thring (1962) for fired bricks. At 1200°C, samples I had the least value of 11% while samples H had the highest of 14%. This shows that as the temperature increases, the percentage apparent porosity decreases, indicating more closure of the pores. This can be increased for insulation purposes by adding saw dust, corn or rice husks. Olusola(1998)

PERMEABILITY TO AIR

The permeability of the samples were presented in table 8. It is important however to state that all the samples had their permeability to air within the internationally accepted value of 25—90, following the observations of Hassan (1990). Sample I recorded the highest permeability to air while sample H recorded the least. High permeability is highly recommended for insulating refractories. The permeability can also be improved by incorporating saw dust and rice husks in the clay, while molding. Manukaji(2004)

REFRACTORINESS

For the fact that all the samples did not show any sign of failure at temperatures of 1200°C and above, it means that their sintering level is very high and will fall within the internationally accepted range of 1580°C – 1750°C. This eventually showed that the samples have high and good refractoriness qualities and can withstand the high temperatures the clay will be subjected to in operation. Abifarin(1999)

THERMAL SHOCK RESISTANCE

All the samples showed a thermal shock resistance of 29+ cycle. The thermal shock resistance values for the samples are acceptable for siliceous fire clays. This property is vital for materials used in places where heating and cooling operation is carried out repetitively Agha(1998)

MODULUS OF RUPTURE.

Table 9 showed the values of modulus of rupture for all the samples. At 110°C sample G showed the least value while sample H showed the highest value. At 1200°C, all the samples showed an improvement in their modulus of rupture but sample G still recorded the least while sample H recorded the highest values Ijagbemi(2002).

THERMAL CONDUCTIVITY

Table 10 showed the values of the thermal conductivity test for all the samples. The values showed that specimen I had the least thermal conductivity value, while the highest value was specimen G. Ijagbemi(2002)

VI. CONCLUSION

With a critical look on the properties of the clay samples surveyed, tested and analyzed during this investigation, the following conclusions can be deduced.

- (1) From the chemical analysis, all the clay samples had silica and alumina as the predominant substances and it could be concluded that they are siliceous in nature and are of the Alumino-Silicate refractories.

- (2) The water content of the clay samples made handling of the clay (mouldability) very possible. The fire shrinkage values which hovered between 8 and 10% were found to be within the internationally accepted range for clays. The clays from sites showed a permeability range of 68-82% which also falls within the range of 24-92% for typical fire clays bricks. The apparent porosity of the clays, compared favourably with the normal acceptable standards as they fell between 20 to 25%. The samples had a thermal shock range of 29 cycles, which closely coincided with the acceptable values internationally. The internationally acceptable range for bulk density is between 1.7 to 2.2 g/cm³ and the samples fell within the range thereby conforming to the approved values. The refractoriness of the clays showed that the clays could withstand temperatures between 1200 to 1600°C which is good for industrial use.

REFERENCES

- [1]. Agha O A (1998) Testing of local refractory clay for producing furnace lining bricks. M. Eng. Thesis: Mech. Eng. Dept. F.U.T. Minna
- [2]. Akinbode F O. (1996). An investigation on the properties of termite hill as refractory material for furnace lining: Indian Foundry Journal. Pp 11-13
- [3]. Ehlers, Ernest G. and Blatt, Harvey (1982). 'Petrology, Igneous, Sedimentary, and Metamorphic' San Francisco: W.H. Freeman and Company. ISBN 0-7167-1279-2
- [4]. Grimshaw R. W (1959) The chemistry and physics of clay, 4th edition Ernest Benn Publishers, London.
- [5]. Guggenheim, Stephen; Martin, R. T. (1995), "Definition of clay and clay mineral: Journal report of the AIPEA nomenclature and CMS nomenclature committees", *Clays and Clay Minerals* 43 (2): 255–256, doi:10.1346/CCMN.1995.0430213, <http://www.clays.org/journal/archive/volume%2043/43-2-255.pdf>
- [6]. Hassan .S .B and Adewara J.O.T (1993) Refractory properties of some Nigerian clays. Nigerian society of engineers transaction vol. 28 No 3 pp 22-25
- [7]. Hassan S.B (1990)The study of the refractory properties of some clays . M. Sc. Thesis Dept. of mech. Engrg. A.B.U. Zaria
- [8]. Hillier S. (2003) Clay Mineralogy. pp 139–142 In: Middleton G.V., Church M.J., Coniglio M., Hardie L.A. and Longstaffe F.J.(Editors) Encyclopedia of sediments and sedimentary rocks. Kluwer Academic Publishers, Dordrecht.
- [9]. Hugh O. Pierson (1992). *Handbook of chemical vapor deposition (CVD): principles, technology, and applications*. William Andrew. pp. 206–. ISBN 978-0-8155-1300-1. <http://books.google.com/books?id=NF3W6zIN9WsC&pg=PA206>. Retrieved 22 April 2011.
- [10]. IEE (1992) Wiring regulation requirement for electrical installation BS7671 , 15th Edition , A Mclay and co. Ltd Cardiff
- [11]. Ijagbemi C.O.(2002) Development and performance evaluation of a biomass clay lined cookstove. Meng thesis , Department of mechanical Federal University of Technology Akure, Nigeria.
- [12]. Mac Graw-Hill(1977) Encyclopedia of science and technology .Vol 3 , McGraw-Hill book company N.Y U.S.A pp 172-179
- [13]. Oaikhinam E.P (1983) Refractories for high temperature industries in Nigeria, A paper delivered at the National workshop on raw materials ASCON Badagry, Lagos 4-6 July
- [14]. Olusola E O (1998) Investigation of Zungeru clay as refractory material for high temperature applications M. Eng. Thesis, Dept. of mech. engrg. F. U. T. Minna
- [15]. Obi V S (1995) Experimental analysis of clay for refractory purpose , B.Eng. Thesis, Dept. of mech. engrg. F. U. T. Minna pp 34-48
- [16]. Ryan W. (1978) Properties of ceramic raw materials 4th Edition, Pergamon Publishers LTD Oxford
- [17]. Thring M.W. (1962) The science of flames and furnaces, 2nd Edition, Chapman and Hall Ltd London
- [18]. Zubeiru S. E (1997) Investigation on refractory clays for application in Nigerian industries B. Eng. Thesis , Dept. of mech. engrg. F.U.T Minna pp 12-34

A COMPARATIVE STUDY OF BYG SEARCH ENGINES

Kailash Kumar¹, Vinod Bhadu²

Research Scholar, Suresh Gyan Vihar University, Jaipur Technology Lead, Infosys Limited, Chandigarh

Abstract: This paper compares the retrieval effectiveness of the Bing, Yahoo and Google (BYG) Search Engines. The precision and relative recall of each search engine was considered for evaluating the effectiveness of the search engines. General Queries were tested. Results of the study showed that the precision of Google was high as compared to other two search engines and Yahoo has better precision than Bing.

Keywords: Internet, Search engines, Google, Yahoo, Bing, Precision, Relative recall.

I. INTRODUCTION

The Web can be used as a quick and direct reference to get any type of information all over the world. However, information found on the Web needs to be filtered and may include voluminous misinformation or non-relevant information. The Internet surfer may not be aware of many search engines to get information on a topic quickly and may use different search strategies. Finding useful information quickly on the Internet poses a challenge to both the ordinary users and the information professionals. Though, the performance of currently available search engines has been improving continuously with powerful search capabilities of various types, the lack of comprehensive coverage, the inability to predict the quality of retrieved results, and the absence of controlled vocabularies make it difficult for users to use search engines effectively. The use of the Internet as an information resource needs to be carefully evaluated as no traditional quality standards or control have been applied to the Web. In this study, an attempt was made to assess the precision and recall three major search engines i.e., Bing, Yahoo and Google (BYG).

II. SEARCH ENGINES AND SEARCH QUERIES

Three search engines namely Bing, Yahoo and Google (BYG) were considered to examine the precision for some selected search queries during March 10, 2013 to March 17, 2013. In order to retrieve relevant data from each search engine, the advanced search features of the search engines were used. Since, more sites were retrieved from the search engines for each query; it was decided to select only the first 30 sites as user hardly goes beyond three to four pages of the search results. Results from India only were selected for evaluation. A total of 15 queries from various discipline were selected for the study. (See Appendix 1).

III. PRECISION OF SEARCH ENGINES

After a search, the user is sometimes able to retrieve relevant information and sometimes able to retrieve irrelevant information. The quality of searching the right information accurately would be the precision value of the search engine (Shafi & Rather, 2005). In this paper, the search results which were retrieved by the Google, Yahoo and Bing were categorized as 'more relevant', 'less relevant', 'irrelevant', 'links' and 'sites can't be accessed' on the basis of the following criteria (Chu & Rosenthal, 1996; Leighton, 1996; Ding & Marchionini, 1996; Clarke & Willett, 1997):

- If the web page is closely matched to the subject matter of the search query then it was categorized as 'more relevant' and given a score of 2.
- If the web page is not closely related to the subject matter but consists of some relevant concepts to the subject matter of the search query then it was categorized as 'less relevant' and given a score of 1.
- If the web page is not related to the subject matter of the search query then it was categorized as 'irrelevant' and given a score of 0.

- If a web page consists of a whole series of links, rather than the information required, then it was categorized as 'links' and given a score of 0.5 if inspection of one or two of the links proved to be useful.
- If a message appears "site can't be accessed" for a particular URL the page was checked again later. If the message occurs repeatedly the page was categorized as 'site can't be accessed' and given a score of 0.

These criteria enabled the calculation of the precision of the search engines for each of the search queries by using the formula:

$$\text{Precision} = \frac{\text{Sum of the scores of sites retrieved by a search engine}}{\text{Total number of sites selected for evaluation}}$$

Total number of sites selected for evaluation

Table 1: Precision of Google

S.No.	Total Results	Result Selected	More Relevant	Less Relevant	Irrelevant	Link	Site can't be accessed	Precision
1	1,550,000	30	15	8	4	1	2	1.283333
2	12,300,00	30	21	4	4	1	0	1.55
3	2,780,00	30	19	6	0	5	0	1.55
4	1,950,000	30	20	5	4	1	0	1.516667
5	6,260,000	30	20	8	1	1	0	1.616667
6	2,040,000	30	24	3	1	2	0	1.733333
7	534,000	30	23	2	2	3	0	1.65
8	93,100	30	15	10	4	1	0	1.35
9	163,000	30	25	3	0	2	0	1.8
10	652,000	30	20	2	3	5	0	1.483333
11	1,360,000	30	21	5	4	2	0	1.6
12	2,810,000	30	21	3	2	4	0	1.566667
13	2,220,000	30	24	0	5	1	0	1.616667
14	1,500,000	30	26	2	0	2	0	1.833333
15	136,000	30	25	1	1	3	0	1.75
Total	21,268,100	450	319	62	35	34	2	23.9
Percentage			70.88889	13.77778	7.77778	7.55556	0.44444	
Mean								1.5933333

3.1 Precision of Google

Google, being one of the most popular search engines on the Internet, was selected as one of the search engines for comparison. Google focuses on the link structure of the Web to determine relevant results and is representative of the variety of easy-to-use search engines. This study would measure the relevance of the web sites retrieved for each search query. Only English pages were searched for each search query since the web pages in other languages would be difficult to assess for relevancy. Since the number of search results retrieved was large, only the first 30 sites were selected for analysis.

Around 70% results are found to be more relevant, 13.77% results are less relevant and only 7.77% results are found to be irrelevant. 7.5% results are useful but do not contain any direct information but useful information is found only by clicking on links provided in the results and only 0.44% results were either shown but deleted or pages not available.

3.2 Precision of Yahoo

Yahoo is another popular and well-known Internet search engine. The same set of search queries and the same methodology were used in Yahoo. Yahoo is the second largest search directory on the web by query volume, at 6.42%, after its competitor Google at 85.35%.

Around 67% results are found to be more relevant, 16.88% results are less relevant and only 8.0% results are found to be irrelevant. 6.8% results are useful but do not contain any direct information but useful information is found only by clicking on links provided in the results and only 1.0% results were either shown but deleted or pages not available.

Table 2: Precision of Yahoo

S. No.	Total Results	Result Selected	More Relevant	Less Relevant	Irrelevant	Link	Site can't be accessed	Precision
1	89,400	30	16	9	3	1	1	1.383333
2	170,000	30	19	6	2	2	1	1.5
3	305,000	30	17	6	4	2	1	1.366667
4	138,000	30	20	7	1	2	0	1.6
5	31,800	30	19	6	3	2	0	1.5
6	75,000	30	27	1	0	1	1	1.85
7	37,100	30	24	5	1	0	0	1.766667
8	24,100	30	20	6	1	3	0	1.583333
9	6,710	30	26	3	0	1	0	1.85
10	16,200	30	24	4	0	2	0	1.766667
11	256,000	30	18	7	2	3	0	1.483333
12	34,000	30	17	4	5	3	1	1.316667
13	24,700	30	19	2	2	7	0	1.45
14	175,000	30	20	4	4	2	0	1.5
15	27,300	30	16	6	8	0	0	1.266667
Total	1,410,310	450	302	76	36	31	5	23.18333
Percentage			67.111111	16.88889	8	6.888889	1.111111	
Mean								1.5455556

3.3 Precision of Bing

Bing is yet another popular and well-known Internet search engine. The same set of search queries and the same methodology were used in Bing. Bing was unveiled by Microsoft CEO Steve Ballmer on May 28, 2009 at the *All Things Digital* conference in San Diego for release on June 1. Notable changes include the listing of search suggestions while queries are entered and a list of related searches (called "Explore pane") based on semantic technology from Powerset which Microsoft purchased in 2008.

Around 64% results are found to be more relevant, 15.77% results are less relevant and only 9.0% results are found to be irrelevant. 10.0% results are useful but do not contain any direct information but useful information is found only by clicking on links provided in the results and only 0.66% results were either shown but deleted or pages not available.

Table 3: Precision of Bing

S. No.	Total Results	Result Selected	More Relevant	Less Relevant	Irrelevant	Link	Site can't be accessed	Precision
1	89,300	30	17	6	4	2	1	1.366667
2	1,72,000	30	19	5	3	3	0	1.483333
3	3,11,000	30	16	5	5	3	1	1.283333
4	1,37,000	30	19	6	3	2	0	1.5
5	32,800	30	20	5	2	2	1	1.533333
6	77,900	30	21	4	3	2	0	1.566667
7	36,400	30	22	5	2	1	0	1.65
8	28,300	30	23	4	3	0	0	1.666667
9	6,720	30	20	6	2	2	0	1.566667
10	16,900	30	21	4	4	1	0	1.55
11	2,53,000	30	19	3	2	6	0	1.466667
12	35,000	30	15	2	3	10	0	1.233333
13	25,000	30	19	3	2	6	0	1.466667
14	1,75,000	30	18	6	2	4	0	1.466667
15	27,300	30	19	7	1	3	0	1.55
Total	375,620	450	288	71	41	47	3	22.35
Percentage			64	15.77778	9.111111	10.44444	0.666667	
Mean Precision								1.49

IV. RELATIVE RECALL OF BING, YAHOO AND GOOGLE

Recall is the ability of a system to retrieve all or most of the relevant documents in the collection (Shafi & Rather, 2005). The relative recall can be calculated using following the formula:

Total number of sites retrieved by a search engine

$$\text{Relative recall} = \frac{\text{Total number of sites retrieved by a search engine}}{\text{Sum of sites retrieved by all Search Engines (BYG)}}$$

The relative recall of the Bing, Yahoo and Google (BYG), for general queries was calculated and presented in Table 4. The overall relative recall of the Google was 0.922, for Yahoo was 0.061 and for Bing it was 0.016

Table4: Relative Recall of Google, Yahoo and Bing

S. No.	Google	Yahoo	Bing	Total	Relative Recall (Google)	Relative Recall (Yahoo)	Relative Recall (Bing)
1	1,550,000	89,400	89,300	1,728,700	0.896627524	0.051715162	0.051657315
2	1,230,000	170,000	172,000	1,572,000	0.782442748	0.108142494	0.109414758
3	278,000	305,000	311,000	894,000	0.310961969	0.341163311	0.34787472
4	1,950,000	138,000	137,000	2,225,000	0.876404494	0.062022472	0.061573034
5	6,260,000	31,800	32,800	6,324,600	0.989785915	0.005027986	0.005186099
6	2,040,000	75,000	77,900	2,192,900	0.930274978	0.034201286	0.035523736
7	534,000	37,100	36,400	607,500	0.879012346	0.061069959	0.059917695
8	93,100	24,100	28,300	145,500	0.639862543	0.165635739	0.194501718
9	163,000	6,710	6,720	176,430	0.923879159	0.038032081	0.03808876
10	652,000	16,200	16,900	685,100	0.951685885	0.023646183	0.024667932
11	1,360,000	256,000	253,000	1,869,000	0.727661851	0.136971643	0.135366506
12	2,810,000	34,000	35,000	2,879,000	0.976033345	0.011809656	0.012156999
13	2,220,000	24,700	25,000	2,269,700	0.978102833	0.010882495	0.011014672
14	1,500,000	175,000	175,000	1,850,000	0.810810811	0.094594595	0.094594595
15	136,000	27,300	27,300	190,600	0.713536201	0.143231899	0.143231899
Total	21,268,100	1,410,310	1,423,620	24,102,030			
Recall	0.882419448	0.058514158	0.059066394				

Figure 1 shows the relative recall of Bing, Yahoo and Google (BYG) for general queries. In case of Google, the search query 5 had the highest relative recall value of 0.98 and least relative recall for search query 3 of value 0.31. In case of Yahoo, the

highest relative recall was for search query 3 (0.34) with the least relative recall for search query 5 (0.005). Similarly, the highest relative recall value of 0.34 for search query 3 and lowest value of 0.005 for search query 5.

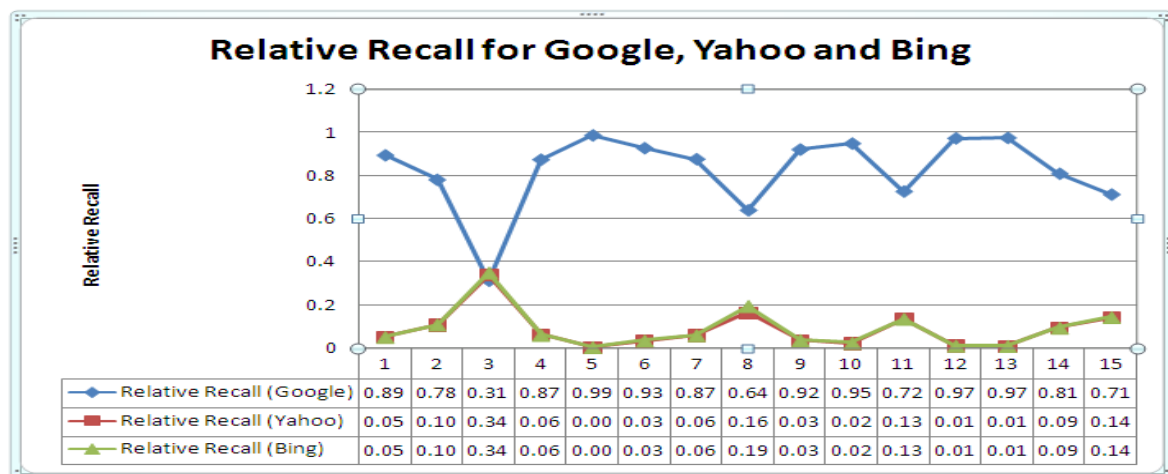


Fig 1: Relative Recall of Google, Yahoo and Bing Search Engines

V. CONCLUSION

The World Wide Web with its short history has experienced significant changes. While the earlier search engines were established based on the traditional database and information retrieval methods, many other algorithms and methods have since been added to them to improve their results. The precision value varies

among the search engines depending on the database size. The gigantic size of the Web and vast variety of the users' needs and interests as well as the potential of the Web as a commercial market have brought about many changes and a great demand for the development of better search engines. The present study estimated the precision of Google, Yahoo and Bing. The results of the study also showed that the precision of Google was high as compared to Yahoo and Bing and Yahoo has better precision than Bing. It was observed that Google, Yahoo and Bing showed diversity in their search capabilities, user interface and also in the quality of information. However these two search engines retrieved comparatively more relevant sites or links as compared to irrelevant sites. Google utilized the Web graph or link structure of the Web to become one of the most comprehensive and reliable search engines. This study provided evidence that the Google was able to give better search results with more precision and more relative recall as compared to Yahoo which would explain why it is the most widely used search engine for the Internet.

Appendix 1 List of Queries

S. No.	Query
1	Maruti car for sale in Rajasthan
2	Best price of Samsung galaxy
3	Land for sale in Jaipur
4	Fast food restaurants in Gurgaon
5	Features of LED TV
6	Price of Honda Bikes
7	Authorised Dealers of HP Computers in Delhi
8	Mineral Water Bottling Plants
9	Anti Hairfall Shampoo
10	Fairness Cream
11	Best Engineering Colleges in Rajasthan
12	Furniture shops in Ahemadabad
13	Second's Reymonds showroom in Hyderabad
14	Softwares for Android Mobiles
15	Solar Panel Manufactures in Rajasthan

REFERENCES

- Clarke, S., & Willett, P. (1997). Estimating the recall performance of search engines. *ASLIB Proceedings*, 49 (7), 184-189.
- Chu, H., & Rosenthal, M. (1996). Search engines for the World Wide Web: A comparative study and evaluation methodology. *Proceedings of the ASIS 1996 Annual Conference*, 33, 127-35.
- Ding, W., & Marchionini, G. (1996). A Comparative study of the Web search service performance. *Proceedings of the ASIS 1996 Annual Conference*, 33, 136-142
- Leighton, H. (1996). Performance of four WWW index services, Lycos, Infoseek, Webcrawler and WWW Worm. Retrieved from <http://www.winona.edu/library/webind.htm>
- Shafi, S. M., & Rather, R. A. (2005). Precision and recall of five search engines for retrieval of scholarly information in the field of biotechnology. *Webology*, 2 (2), Retrieved from <http://www.webology.ir/2005/v2n2/a12.html>
- Wu, G., & Li, J. (1999). Comparing Web search engine performance in searching consumer health information: Evaluation and recommendations. *Bulletin of the Medical Library Association*, 87 (4), 456-461.

Transient Pressure Analysis of Horizontal Wells in a Multi-Boundary System

S. Al Rbeawi and D. Tiab,
SPE, University of Oklahoma

Abstract: Horizontal wells can greatly increase the contact area of the wellbore and the pay zone; so they are commonly applied in oil reservoirs to enhance the production and ultimate recovery of oil and gas, especially, in low permeability formations. The purpose of this study is to develop a technique for the interpretation of transient pressure based on dimensionless pressure and pressure derivative. Type curve matching is one of the techniques that can be used to interpret the pressure data of horizontal wells in finite reservoirs. Starting from very short horizontal wells to extra-long wells, the pressure behavior of the wells has been analyzed for different conditions. The effect of the outer boundaries of the reservoir on the pressure behavior of the horizontal wells has been investigated for different configurations. Rectangular shape reservoirs with different dimensions have been used to study the pressure response in the well. Five flow regimes have been observed for regular length horizontal wells; early radial, early linear flow, pseudo radial flow, channel flow or late linear flow, and pseudo-steady state flow. Four flow regimes have been observed for the extra-long wells: linear flow, pseudo radial flow, channel flow, and pseudo-steady state or boundary-affected flow. Of course, those flow regimes do not always take place under all conditions. Pseudo-steady state flow is expected to occur after long production time. A pressure drawdown test was solved using the proposed type curve matching technique. The study has shown that the effect of the boundary on the pressure response of the horizontal wells and the type of flow regimes depend on the length of the horizontal wells and the distance to the nearest boundary.

I. INTRODUCTION

The use of horizontal wells for producing oil and gas from low-permeability and unconventional reservoirs is now very well established within the petroleum industry. The great increase of the surface area of the wellbore that allows fluids to freely flow from the reservoir to the wellbore is the main advantage of the horizontal well. Reducing the effects of the damaged zones and increasing the well deliverability are the direct impacts of this type of increment. Therefore, over the last two decades the number of horizontal wells that have been drilled worldwide has considerably increased due to the possibility of improving the well productivity and anticipating oil and gas recovery. Low-permeability and unconventional reservoirs are not the only common applications for horizontal wells. They also have been used successfully in fractured reservoirs: (a) to intersect natural fractures and effectively drain the reservoir; (b) in water and gas driven reservoirs to minimize water and gas coning; (c) in both low and high permeability gas reservoirs to reduce the number of producing wells; (d) in tertiary recovery application to enhance the contact between the well and the reservoir; and (e) finally, in offshore reservoirs, as well as in environmentally sensitive areas, to cut down the cost of drilling and the number of production facilities. Although, since the mid 1980s, horizontal well technology has provided the solutions for oil and gas production process where the conventional vertical technique either has failed or produced less than the desired rate, the rapid increase in the application of this technology during this period led to a sudden need for the development of analytical models that are capable of evaluating the performance of these horizontal wells. Giger, F. (1985) and Joshi, S. D. (1986) presented the applicability of horizontal wells in heterogeneous reservoirs and the impact of the well productivity using slanted or horizontal wells respectively. Spivak, D. (1988) explained that the advantages of horizontal wells, such as productivity increase, better sweep efficiency, and reduction of water and gas coning, have been reported by many researchers. At the same time, many researchers, such as Babu, D. K. and Odeh, A. S. (1989) and Goode, P. A. and Kuchuk, F. J. (1991), have attempted to develop practical models to study the performance and productivity of horizontal wells. Over time, transient pressure analysis techniques have been favorably applied for the evaluation of horizontal well performance and reservoir characterization. Daviau et al (1988) presented solutions using the Newman product

method for an infinite limited isotropic reservoir as well as for an isotropic reservoir with constant pressure at the outer boundaries. Clonts, M.D. and Ramey, H. J. (1986) developed one of the earliest analytical models for horizontal well test analysis based on the line source approximation of the partially penetrating vertical fracture solution. Ozkan et al (1989) have shown the effect of the producing length of horizontal wells on the pressure derivative response. Carvalho, R.S. and Rosa, A.J. (1989) introduced a mathematical model for pressure evaluation in infinite conductivity horizontal wells. Odeh, A.S. and Babu, D.K. (1990) studied the transient flow behavior for horizontal wells for both pressure drawdown and pressure build-up tests. Because of the increased complexity in the geometrical configuration of the wellbore as a result of the different horizontal well completion techniques, many concerns and limitations regarding the pressure behavior in the vicinity of the wellbore and outer no-flow boundaries have remained unanswered. These concerns are based on the fact that the ideal behavior is hardly ever seen in real production tests because the pressure derivative can exhibit very different trends depending on the geometrical configuration of the whole system, the petrophysical properties of the formation, and zonal damage. Therefore, the validity of the horizontal well models and the well test concepts adopted from vertical fracture analogues have been extensively investigated and new trends of horizontal well solutions were developed in the beginning of the 1990s. These solutions have been established under more realistic conditions to provide the answers for previous concern and limitations. Kuchuk et al (1991) studied the effect of the presence of the gas cap or aquifer on the pressure transient behavior of horizontal wells. Guo, G. and Evans, R. D. (1993) presented an analytical model for the pressure transient behavior and inflow performance of horizontal wells intersecting discrete fractures. Automatic type curve matching for horizontal wells has been introduced by Thompson, L.G. and Temng, K.O. (1993). Ozkan et al (1995) studied the effect of conductivity on transient pressure response of horizontal wells. Economides et al 1996 presented the effects of the well configurations on pressure behavior and well productivity for horizontal wells acting in anisotropic formation. They also introduced new methodology for horizontal plane shape factor determination. Verga et al (2001) investigated the transient dual-porosity pressure response of two horizontal wells and introduced numerical models to reproduce the reservoir internal geometry and simulate the pressure trend monitored at the wells. Khelifa and Taib (2002) proposed a technique for analyzing the variable rate tests in horizontal wells by using continuously changing flow rate test or by using a series of constant rate test. Hashemi et al (2004) demonstrated how the horizontal well flow regimes are affected by condensate accumulation and how this modifies the pressure derivative shapes. It is important to note that Escobar et al (2004) have used the TDS technique to analyze the pressure behavior of a horizontal well inside a channel system. A physically consistent model for describing transient pressure behavior of horizontal drainholes was established by Ogunsanya et al (2005) to overcome the basic limitations in previous models. The last ten years has seen a focus on using the convolution and deconvolution technique in well test analysis. Von Shorter et al (2001) showed that the use of deconvolution of well test data is a nonlinear total least squares problem. Gringarten et al (2003) proposed the use of downhole pressure gauges to diagnose production problems in North Sea horizontal wells. Ilk et al (2005) studied using B-spline deconvolution of variable rate reservoir performance data. Whittle et al (2009) introduced a technique for well production forecasting by extrapolation of the deconvolution of pressure transient data. Gringarten, A. C. (2010) explained the practical use of the well test convolution and the various usages of deconvolution in tests of short and long durations. Even though great attention has been focused on horizontal well technology either in the drilling and completion aspect or in the production and reservoir characterization aspect, more study is required to overcome the concerns and limitations of the models that are used to evaluate the performance of wells or to predict the pressure behavior around and in the wellbore. This fact is supported by the idea of the great complexity of the horizontal well system and the difficulties that are governing the recognitions of the flow dynamics and types of flow regimes especially in the area near the well where the geometrical configuration of flow becomes of great importance. In this paper a technique for the interpretation of transient pressure based on dimensionless pressure and pressure derivative is introduced. This technique depends on the results obtained from an analytical model for a horizontal well acting in finite reservoir having a rectangular shape. A set of type curve matching plots for the wells is established for very short horizontal wells and extra-long wells taking into account the change in either the distance to the outer boundaries in the two directions or the length of the producing horizontal section. The study includes the effect of the outer boundaries of the reservoir on the pressure behavior of the horizontal wells.

Horizontal well in an infinite reservoir

Consider a horizontal well, such as in Fig. (1), producing slightly compressible petroleum fluids from an infinite-acting reservoir at a constant rate. To simulate the transient pressure response of this well, an analytical model should be used for this purpose. The following assumptions are very important for the selection of this model:

- 1- The reservoir is homogenous and having constant and uniform thickness with two impermeable layers at the top and bottom of the formation.

- 2- Constant porosity and permeability in each direction, but the formation is anisotropic.
- 3- Gravitational and frictional effects are negligible.
- 4- No-flow boundaries.

The solution to the diffusivity equation based on the above conditions can be obtained using different techniques which are applicable for the transient flow of fluid in the porous media. Gringarten, A. C. and Ramey, H. J. (1973) were the first to introduce the use of the source and Green's function in solving unsteady state flow problems in the reservoirs. They stated that the infinite line source can be visualized as the intersection of two perpendicular infinite plane sources normal to two of the three principal axes of permeability while the point source can be visualized as the intersection of three perpendicular infinite plane sources normal to the principal axes of permeability. Ozkan, E. (1988) introduced new source solutions to the diffusivity equation using the Laplace space to overcome the difficulties that might result when we apply the Gringarten and Ramey's source solution in complex geometrical configurations such as dual-porosity and dual-permeability porous media. Spivak, D. (1988) presented the same solution considering the infinite line source as a result of the integrating process for any point from $(-\infty$ to $+\infty)$ and the pressure drop distribution created by a continuous source of any shape can be obtained by the principle of the superposition in time and space. Therefore a line or a plane source can be generated by superposing an infinite number of point source along the line or plane. The mathematical model can be used to simulate the pressure behavior created by the constant production of a horizontal well having a known length $(2L_w)$ and extending in the midpoint of an infinite formation having a known height (h) is (Daviau et al 1988):

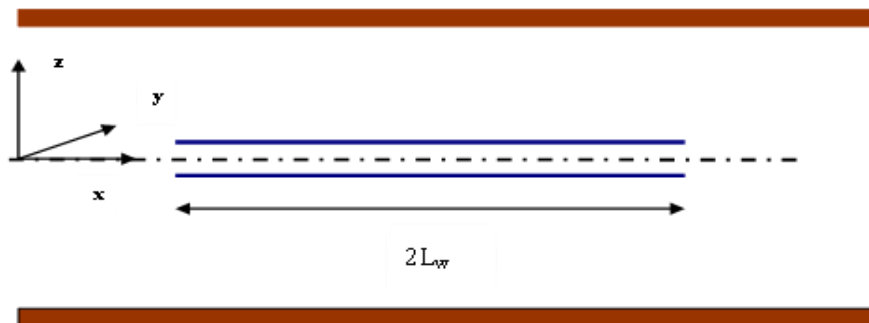


Figure 1: Horizontal well acting in an infinite reservoir.

$$P_D(x_D, y_D, z_D, z_{wD}, L_D, t_D) = \frac{\sqrt{\pi}}{4} \int_0^{t_D} \frac{e^{-\frac{y_D^2}{4\tau_D}}}{\sqrt{\tau_D}} \left[\operatorname{erf}\left(\frac{1+x_D}{2\sqrt{\tau_D}}\right) + \operatorname{erf}\left(\frac{1-x_D}{2\sqrt{\tau_D}}\right) \right] \times \left[1 + 2 \sum_{n=1}^{\infty} \exp(-n^2 \pi^2 L_D^2 \tau_D) \cos(n\pi z_{wD}) \cos(n\pi(\bar{z}_D + z_{wD})) \right] d\tau_D \tag{1}$$

where the dimensionless parameters in the above model are defined as follows:

$$x_D = \frac{x - x_w}{L_w} \tag{2}$$

$$y_D = \frac{y - y_w}{L_w} \sqrt{\frac{k_x}{k_y}} \tag{3}$$

$$z_D = \frac{z - z_w}{L_w} \sqrt{\frac{k_x}{k_z}} \tag{4}$$

$$z_{wD} = \frac{z_w}{h} \tag{5}$$

$$\bar{z}_D = \frac{z - z_w}{h} = z_D L_D \tag{6}$$

$$L_D = \frac{L_w}{h} \sqrt{\frac{k_z}{k_x}} \quad (7)$$

$$t_D = \frac{k_x t}{\phi \mu c_t L_w^2} = \frac{\eta_x t}{L_w^2}, \quad \text{where } \eta_x = \frac{k_x}{\phi \mu c_t} \quad (8)$$

$$P_D(x_D, y_D, z_D, z_{wD}, L_D, t_D) = \frac{2\pi \sqrt{k_x k_y} h \Delta P}{q \mu} \quad (9)$$

and:

$$Q = \frac{q}{2L_w} \quad (10)$$

It is clear that the above model consists of three instantaneous source functions which are $S(x, t)$, $S(y, t)$, and $S(z, t)$. $S(x, t)$ represents the infinite slab source in an infinite reservoir and $S(y, t)$ represents the infinite plane source in an infinite reservoir while $S(z, t)$ represents the infinite plane source in an infinite slab reservoir. To solve the above model, two approximations should be done for the three functions based on the fluid flow dynamic and flow regimes in early and late time.

Short-time approximation

At early time, it is known that there is no flow in the reservoir beyond the tips of the well. Therefore short-time approximation can be obtained by considering the asymptotic behavior of the three instantaneous source functions that are involved in the model. The first instantaneous function $S(x, t) = 1$ when the monitoring point is located inside the well as the time approaches zero (Spivak 1988):

$$S(x_D, t_D) = \frac{1}{2\sqrt{\pi \eta_x t}} e^{-\frac{(x-x_w)^2}{4\eta_x t}} = 1 \quad (11)$$

and the proper time limit for the above equation to be applied as determined by Gringarten and Ramey (1973) is:

$$t_D = \frac{(1-x_D)^2}{20} \quad (12)$$

The second instantaneous function $S(z, t)$ has the following formula:

$$S(z_D, t_D) = \frac{1}{2\sqrt{\pi \eta_z t}} e^{-\frac{(z-z_w)^2}{4\eta_z t}} = \frac{1}{2\sqrt{\pi \eta_z L_w}} \sqrt{\frac{k_x}{k_z}} e^{-\frac{z_D^2}{4t_D}} \quad (13)$$

Since this function deals with the infinite plane source in an infinite slab reservoir, there is a time at which the upper or lower boundary starts to affect the pressure behavior. This time can be estimated by:

$$t_D \leq \min \left[\frac{[(\bar{z}_D + 2z_{wD})/L_D]^2}{20}, \frac{[(\bar{z}_D + 2z_{wD} - 2)/L_D]^2}{20} \right] \quad (14)$$

while the third instantaneous function $S(y, t)$ has the following formula for the short time approximation:

$$S(y_D, t_D) = \frac{1}{2\sqrt{\pi \eta_y t}} e^{-\frac{(y-y_w)^2}{4\eta_y t}} = \frac{1}{2\sqrt{\pi \eta_y L_w}} \sqrt{\frac{\eta_x}{\eta_y}} e^{-\frac{y_D^2}{4t_D}} \quad (15)$$

and the proper time for this approximation to be applicable is:

$$t_D = \frac{y_D^2}{20} \quad (16)$$

Based on the short time approximations for the above three functions, the short time approximation for Eq. (1) can be written as the product of the three approximations:

$$P_D(x_D, y_D, z_D, z_{wD}, L_D, t_D) = \frac{1}{4L_D} \int_0^{t_D} \frac{1}{\tau_D} e^{-\frac{[y_D^2+z_D^2]}{4\tau_D}} d\tau_D = -\frac{1}{4L_D} Ei\left(-\frac{y_D^2+z_D^2}{4t_D}\right) \quad (17)$$

$$= \frac{1}{4L_D} \left(\ln\left(\frac{t_D}{y_D^2+z_D^2}\right) + 0.80907 \right) \text{ when } Ei\left(-\frac{y_D^2+z_D^2}{4t_D}\right) \leq 0.01$$

Long-time approximation

At late time, the pressure behavior of horizontal wells starts to be affected by the pseudo-steady state flow. Therefore the long time approximation of Eq. (1) takes into consideration this fact. The first instantaneous function which represents the infinite slab source in an infinite reservoir is approximated as follows (Spivak 1988):

$$S(x_D, t_D) = \frac{1}{2\sqrt{\pi\eta_x t}} e^{-\frac{(x-x_w)}{4\eta_x t}} = \frac{1}{\sqrt{\pi t_D}} \quad (18)$$

and the long limit of the time so that the pseudo steady state will take place is:

$$t_D = \frac{25}{3}(1-x_D)^2 \quad (19)$$

The approximation for the second source function and the time limit are:

$$S(y_D, t_D) = \frac{1}{2\sqrt{\pi t_D} L_w} \sqrt{\frac{\eta_x}{\eta_y}} \quad (20)$$

$$t_D = 25 y_D^2 \quad (21)$$

while the approximation and the time limit for the third function are:

$$S(z_D, t_D) = \frac{1}{h} \quad (22)$$

$$t_D = \frac{5}{\pi^2 L_D^2} \quad (23)$$

Therefore the long time approximation of Eq. (1) can be written as follows:

$$P_D(x_D, y_D, z_D, z_{wD}, L_D, t_D) = \frac{q}{2L_w \phi \mu} \int_0^{t_{D1}} S(x_D, \tau_D) \times S(y_D, \tau_D) \times S(z_D, \tau_D) d\tau_D + \frac{1}{2} \int_{t_{D1}}^{t_D} \frac{1}{\tau_D} d\tau_D \quad (24)$$

$$= P_D(x_D, y_D, z_D, z_{wD}, L_D, t_{D1}) + \frac{1}{2} \ln\left(\frac{t_D}{t_{D1}}\right)$$

where:

$$t_{D1} \geq \text{Max} \left[\begin{array}{l} \frac{25}{3}(1-x_D)^2 \\ 25 y_D^2 \\ \frac{5}{\pi^2 L_D^2} \end{array} \right] \quad (25)$$

In this study, the horizontal wells are classified as short horizontal wells in which $L_D < 20$ and long horizontal wells for $L_D > 20$ (Long horizontal wells, $L_D > 50$ Spivak 1988) (Long horizontal wells, $L_D > 10$ Joshi 1991). For long horizontal wells pressure behavior becomes exactly the same behavior as vertical fracture. This fact is related to the function of the infinite plane source in an infinite slab reservoir which is converging to:

$$S(z_D, t_D) = \left[1 + 2 \sum_{n=1}^{\infty} \exp(-n^2 \pi^2 L_D^2 \tau_D) \cos(n \pi z_{wD}) \cos(n \pi (\bar{z}_D + z_{wD})) \right] \times \frac{1}{h} = \frac{1}{h} \quad (26)$$

Therefore the model for long horizontal wells can be written as follows:

$$P_D(x_D, y_D, z_D, z_{wD}, L_D, t_D) = \frac{\sqrt{\pi}}{4} \int_0^{t_D} \frac{e^{-\frac{y_D^2}{4\tau_D}}}{\sqrt{\tau_D}} \left[\operatorname{erf}\left(\frac{1+x_D}{2\sqrt{\tau_D}}\right) + \operatorname{erf}\left(\frac{1-x_D}{2\sqrt{\tau_D}}\right) \right] d\tau_D \quad (27)$$

The short time approximation and the applicable time limit are:

$$P_D(x_D, y_D, z_D, z_{wD}, L_D, t_D) = \sqrt{\pi t_D} e^{-\frac{y_D^2}{4t_D}} - \frac{\pi y_D}{2} \operatorname{erfc}\left(\frac{y_D}{2\sqrt{t_D}}\right) \quad (28)$$

$$t_D = \frac{(1-x_D)^2}{20} \quad (29)$$

and for wellbore pressure:

$$P_{wD} = \sqrt{\pi t_D} \quad (30)$$

while the long time approximation and the time limit are the same as regular horizontal well presented in Eq. (24) and Eq. (25).

The pressure response of horizontal wells normally shows three flow regimes: the early radial flow, linear flow, and pseudo-radial flow as shown in Fig. (2). Long horizontal wells may develop two flow regimes only: the linear flow and the pseudo-radial flow as shown in Fig. (3).

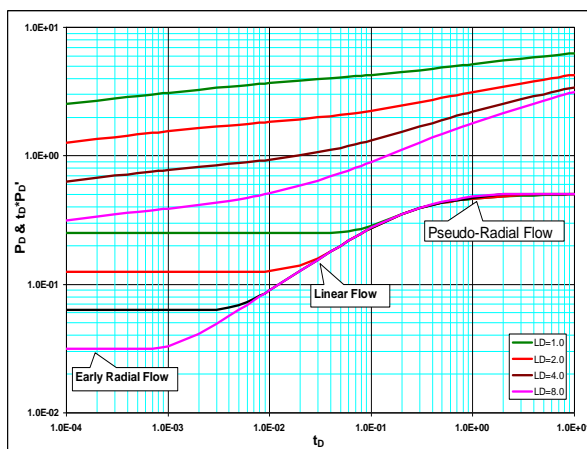


Figure 2: Pressure & pressure derivative long horizontal plot for horizontal wells ($L_D > 20$).

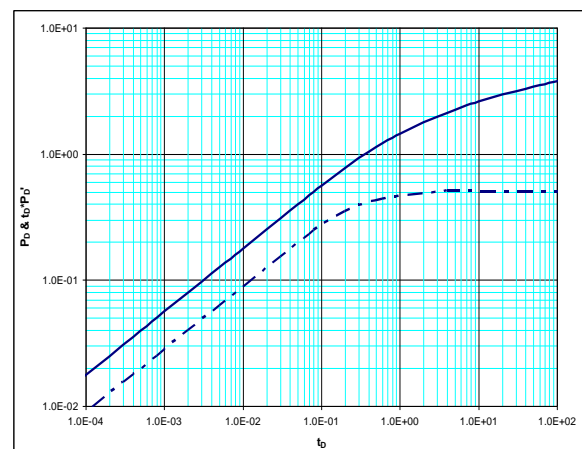


Figure 3: Pressure & pressure derivative plot for wells ($L_D < 20$).

Horizontal well in finite reservoir:

The mathematical model that can be used to simulate the pressure behavior created by the constant production of a horizontal well acting on finite or limited reservoir (impermeable boundary), as shown in **Fig. (4)**, also consists of the three instantaneous source solutions (Gringarten and Ramey 1973, Daviau 1988):

$$S(x,t) = \frac{L_w}{x_e} \left[1 + \frac{4x_e}{\pi L_w} \sum_{n=1}^{\infty} \frac{1}{n} \exp\left(-\frac{\pi^2 n^2 \eta_x^2 t}{4x_e^2}\right) \sin\left(n\pi \frac{L_w}{2x_e}\right) \cos\left(n\pi \frac{x_w}{2x_e}\right) \cos\left(n\pi \frac{x}{2x_e}\right) \right] \tag{31}$$

$$S(y,t) = \frac{1}{2y_e} \left[1 + 2 \sum_{n=1}^{\infty} \exp\left(-\frac{\pi^2 n^2 \eta_y^2 t}{4y_e^2}\right) \cos\left(n\pi \frac{y_w}{2y_e}\right) \cos\left(n\pi \frac{y}{2y_e}\right) \right] \tag{32}$$

$$S(z,t) = \frac{1}{h} \left[1 + 2 \sum_{n=1}^{\infty} \exp\left(-\frac{\pi^2 n^2 \eta_z^2 t}{h^2}\right) \cos\left(n\pi \frac{z_w}{h}\right) \cos\left(n\pi \frac{z}{h}\right) \right] \tag{33}$$

The pressure behavior model is developed by gathering the above source solutions together:

$$P_D(x_D, y_D, z_D, L_D, x_{eD}, y_{eD}, t_D) = \frac{\pi}{2} x_{eD} y_{eD} \int_0^{t_D} \left[1 + \frac{4}{\pi x_{eD}} \sum_{n=1}^{\infty} \frac{1}{n} \exp\left(-\frac{\pi^2 n^2 x_{eD}^2 \tau_D}{4}\right) \sin\left(n\pi \frac{x_{eD}}{2}\right) \cos\left(n\pi \frac{x_{wD}}{2}\right) \cos\left(\frac{n\pi}{2} (x_D x_{eD} + x_{wD})\right) \right] \times \left[1 + 2 \sum_{n=1}^{\infty} \exp\left(-\frac{\pi^2 n^2 y_{eD}^2 \tau_D}{4}\right) \cos\left(n\pi \frac{y_{wD}}{2}\right) \cos\left(\frac{n\pi}{2} (y_D y_{eD} + y_{wD})\right) \right] \times \left[1 + 2 \sum_{n=1}^{\infty} \exp\left(-n^2 \pi^2 L_D^2 \tau_D\right) \cos(n\pi z_{wD}) \cos(n\pi (z_D L_D + z_{wD})) \right] d\tau_D \tag{34}$$

where:

$$x_{wD} = \frac{x_w}{x_e} \tag{35}$$

$$y_{wD} = \frac{y_w}{y_e} \tag{36}$$

$$z_{wD} = \frac{z_w}{h} \tag{37}$$

$$x_{eD} = \frac{L_w}{x_e} \tag{38}$$

$$y_{eD} = \frac{L_w}{y_e} \sqrt{\frac{k_y}{k_x}} \tag{39}$$

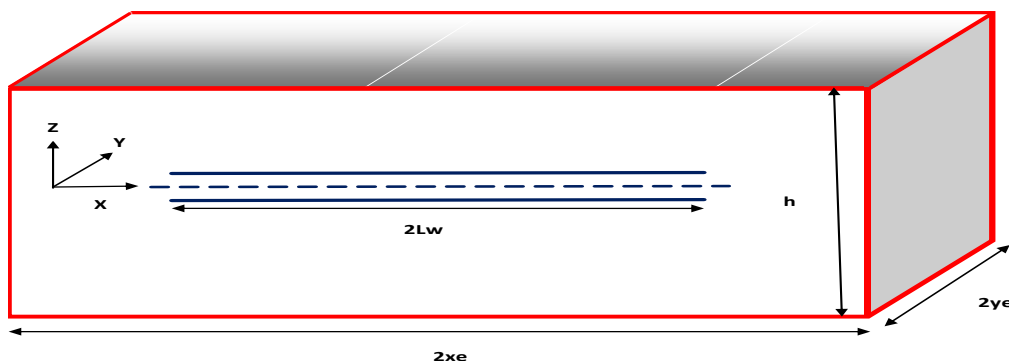


Figure 4: Horizontal well acting in finite reservoir.

Short-time approximation

Short-time approximation can be obtained using the same procedures that have been used for the horizontal well in infinite reservoirs. The first instantaneous function $S(x, t) = 1$ when the monitoring point is located inside the well as the time approaches zero.

$$S(x_D, t_D) = \frac{1}{2\sqrt{\pi\eta_x t}} e^{-\frac{(x-x_w)^2}{4\eta_x t}} = 1 \tag{40}$$

and the proper time limit for the above equation to be applied as determined by Gringarten and Ramey (1973) is:

$$t_D = \frac{(1-x_D)^2}{20} \tag{41}$$

The second instantaneous function $S(z, t)$ has the following formula:

$$S(z_D, t_D) = \frac{1}{2\sqrt{\pi\eta_z t}} e^{-\frac{(z-z_w)^2}{4\eta_z t}} = \frac{1}{2\sqrt{\pi\alpha_D L_w}} \sqrt{\frac{k_x}{k_z}} e^{-\frac{z_D^2}{4t_D}} \tag{42}$$

Since this function deals with the infinite plane source in an infinite slab reservoir, there is a time at which the upper or lower boundary starts to affect the pressure behavior. This time can be estimated by:

$$t_D \leq \min \left[\frac{\left[\frac{(\bar{z}_D + 2z_{wD})/L_D}{20} \right]^2}{\left[\frac{(\bar{z}_D + 2z_{wD} - 2)/L_D}{20} \right]^2} \right] \tag{43}$$

while the third instantaneous function $S(y, t)$ has the following formula for the short time approximation:

$$S(y_D, t_D) = \frac{1}{2\sqrt{\pi\eta_y t}} e^{-\frac{(y-y_w)^2}{4\eta_y t}} = \frac{1}{2\sqrt{\pi\alpha_D L_w}} \sqrt{\frac{\eta_x}{\eta_y}} e^{-\frac{y_D^2}{4t_D}} \tag{44}$$

and the proper time for this approximation to be applicable is:

$$t_D \leq \min \left[\frac{\left[\frac{(y_D y_{eD} + 2y_{wD})/y_{eD}}{20} \right]^2}{\left[\frac{(y_D y_{eD} + 2y_{wD} - 4)/y_{eD}}{20} \right]^2} \right] \tag{45}$$

Based on the short time approximations for the above three functions, the short time approximation for Eq. (34) can be written as the product of the three approximations:

$$P_D(x_D, y_D, z_D, z_{wD}, L_D, t_D) = \frac{1}{4L_D} \int_0^{t_D} \frac{1}{\tau_D} e^{-\frac{[y_D^2 + z_D^2]}{4\tau_D}} d\tau_D = -\frac{1}{4L_D} Ei \left(-\frac{y_D^2 + z_D^2}{4t_D} \right) \tag{46}$$

$$= \frac{1}{4L_D} \left(\ln \left(\frac{t_D}{y_D^2 + z_D^2} \right) + 0.80907 \right) \text{ when } Ei \left(-\frac{y_D^2 + z_D^2}{4t_D} \right) \leq 0.01$$

Long-time approximation

As the time increases, the exponential terms in Eq. (31), (32), and (33) approach zero. Therefore, the first instantaneous function can be approximated as follows:

$$S(x, t) = \frac{L_w}{x_e} \tag{47}$$

and the long limit of the time so that the pseudo steady state will take place is:

$$t_D \geq \frac{20}{\pi^2 x_e^2} \tag{48}$$

The approximation for the second source function and the time limit are:

$$S(y, t) = \frac{1}{2y_e} \tag{49}$$

$$t_D \geq \frac{20}{\pi^2 y_{eD}^2} \tag{50}$$

while the approximation and the time limit for the third function are:

$$S(z, t) = \frac{1}{h} \tag{51}$$

$$t_D \geq \frac{5}{\pi^2 L_D^2} \tag{52}$$

Therefore the long time approximation of Eq. (34) can be written as follow:

$$P_D(x_D, y_D, z_D, z_{wD}, L_D, t_D) = \frac{q}{2L_w \phi \mu} \int_0^{t_{D1}} S(x_D, \tau_D) \times S(y_D, \tau_D) \times S(z_D, \tau_D) d\tau_D + \frac{q}{2\phi \mu L_w} \int_{t_{D1}}^{t_D} \frac{Lw}{x_e y_e h} d\tau_D \tag{53}$$

$$= P_D(x_D, y_D, z_D, z_{wD}, L_D, t_{D1}) + \frac{\pi}{2} x_{eD} y_{eD} (t_D - t_{D1})$$

where:

$$t_{D1} \geq \text{Max} \left[\begin{array}{l} \frac{20}{\pi^2 x_{eD}^2} \\ \frac{20}{\pi^2 y_{eD}^2} \\ \frac{5}{\pi^2 L_D^2} \end{array} \right] \tag{54}$$

For long horizontal wells when $L_D \geq 20$, where the vertical fracture pressure behavior is expected to happen, the infinite plane source in slab reservoir can be presented as:

$$S(z_D, t_D) = \left[1 + 2 \sum_{n=1}^{\infty} \exp(-n^2 \pi^2 L_D^2 \tau_D) \cos(n\pi z_{wD}) \cos(n\pi(\bar{z}_D + z_{wD})) \right] \times \frac{1}{h} = \frac{1}{h} \tag{55}$$

Therefore the model for long horizontal wells in limited reservoirs can be written as follows:

$$P_D(x_D, y_D, z_D, L_D, x_{eD}, y_{eD}, t_D) = \frac{\pi}{2} x_{eD} y_{eD} \int_0^{t_D} \left\{ 1 + \frac{4}{\pi x_{eD}} \sum_{n=1}^{\infty} \frac{1}{n} \exp(-\frac{\pi^2 n^2 x_{eD}^2 \tau_D}{4}) \sin(n\pi \frac{x_{eD}}{2}) \cos(n\pi \frac{x_{wD}}{2}) \cos(\frac{n\pi}{2} (x_D x_{eD} + x_{wD})) \right\} \times \left[1 + 2 \sum_{n=1}^{\infty} \exp(-\frac{\pi^2 n^2 y_{eD}^2 \tau_D}{4}) \cos(n \frac{y_{wD}}{2}) \cos(\frac{n\pi}{2} (y_D y_{eD} + y_{wD})) \right] d\tau_D \tag{56}$$

The short time approximation and the applicable time limit for long horizontal wells in limited reservoirs are the same for long horizontal wells in infinite reservoirs. The long time approximation and the time limit are the same as the regular horizontal wells in limited reservoirs.

Pressure behavior

In general, the pressure response of horizontal wells acting in finite reservoirs shows five flow regimes: the early radial flow, early linear flow, pseudo- radial flow, channel flow (linear flow corresponding to the channel system when the pressure behavior is affected by the influence of the nearest parallel boundaries to the horizontal wells), and pseudo-steady state flow. The following classification for the pressure behavior can be noticed based on the distance to the boundaries.

1- Square reservoir:

The effect of the boundaries depends significantly on the distance to the nearest boundary which is normal to the direction of the wellbore in the case of square reservoirs. Four flow regimes are expected to develop: early radial, early linear, pseudo-radial and pseudo steady state for $x_{eD} = y_{eD} \leq 0.5$ as shown in **Fig. (5)** and **Fig. (6)**. For $x_{eD} = y_{eD} \geq 0.5$, pseudo-radial flow are disappeared and linear flow or channel flow for

$x_{eD} = y_{eD} = 1.0$ will be the dominant flow between the early radial and pseudo-steady state flow as shown in Fig. (7) and Fig. (8). For large square drainage area $x_{eD} = y_{eD} = 0.1$, pseudo-steady state flow is affected by wellbore length. The required time to reach pseudo-steady state increases as the wellbore length increases as shown in Fig.(5). However, when both x_{eD} and y_{eD} increase, the required time to reach pseudo-steady state becomes constant for all wellbore length as shown in Figs. (6), (7) and (8).

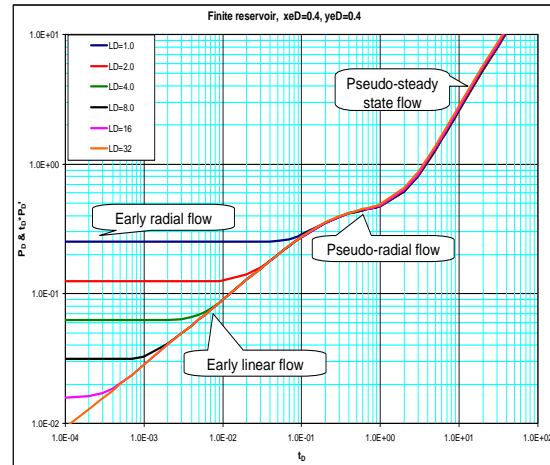
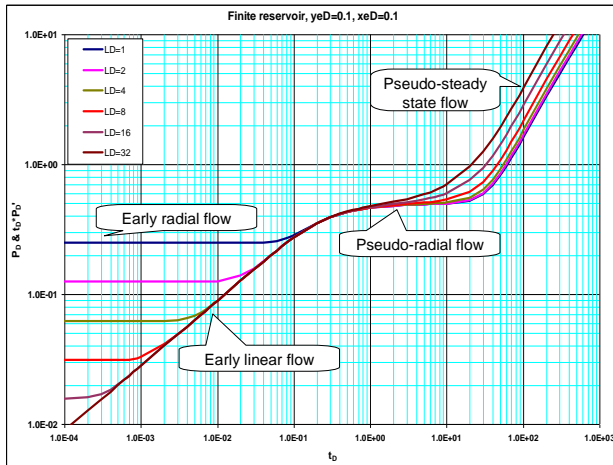


Figure 5: Pressure derivatives for different horizontal wells. Figure 6: Pressure derivatives for different horizontal wells.

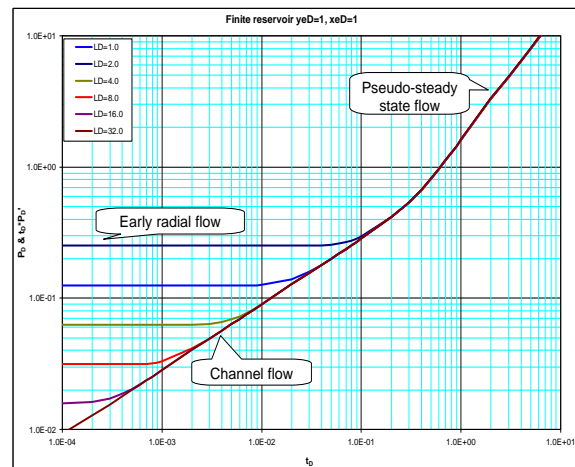
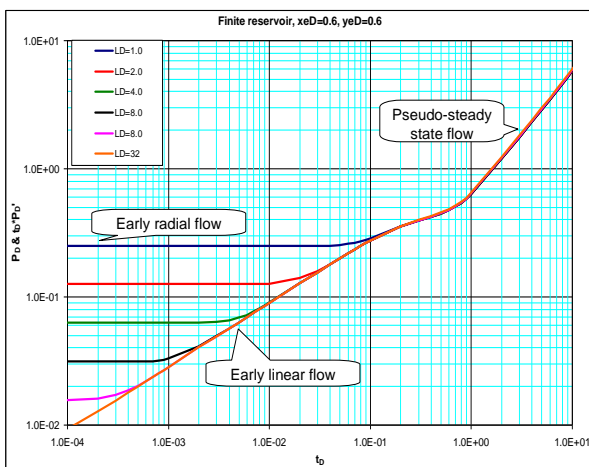


Figure 7: Pressure derivatives for different horizontal wells. Figure 8: Pressure derivatives for different horizontal wells

2- Rectangular reservoirs $0.1 < x_{eD} < 0.5$ and $0.1 < y_{eD} < 0.5$

Typically, early linear, pseudo-radial and pseudo-steady state flow are observed in addition to early radial flow for the case of $L_D \leq 20$. The required time to reach pseudo-steady state is affected by the distance to the boundaries. It increases as the distance increases regardless of the wellbore length as shown in Fig. (9) and (10).

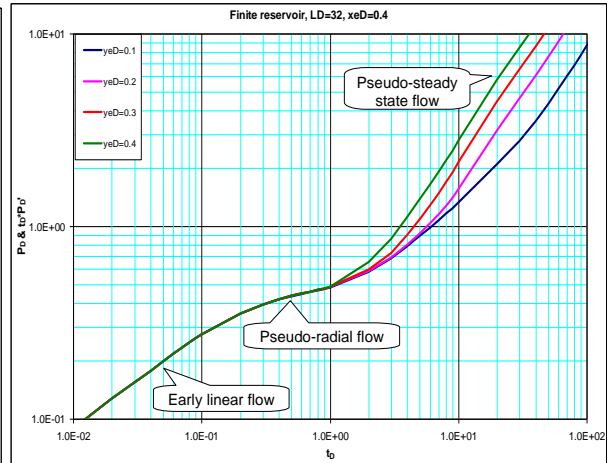
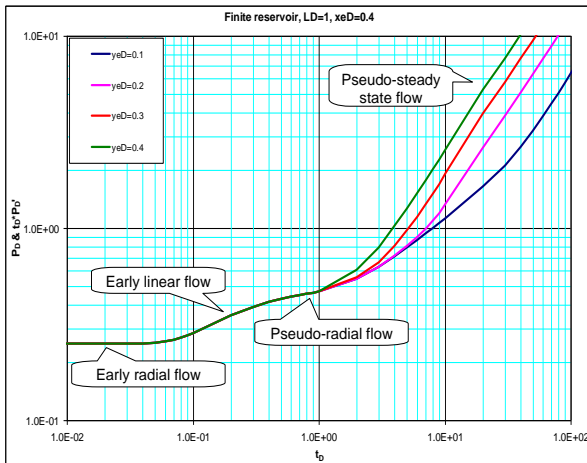


Figure 9: Pressure derivatives for different horizontal wells. Figure 10: Pressure derivatives for different horizontal wells.

3- Rectangular reservoirs $1 \leq xeD < 0.5$ and $1 \leq yeD < 0.5$

Two flow regimes are observed for horizontal well with $L_D \geq 20$, channel and pseudo-steady state flow as shown in Fig. (12). Early radial flow is observed for wellbore $L_D \leq 20$ as shown in Fig. (11) in addition to the channel and pseudo-steady state flow.

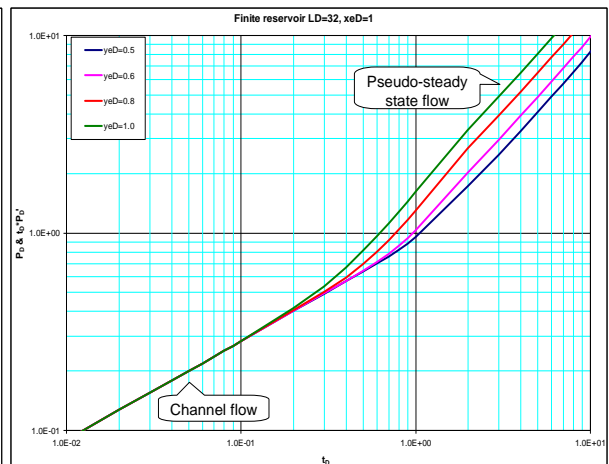
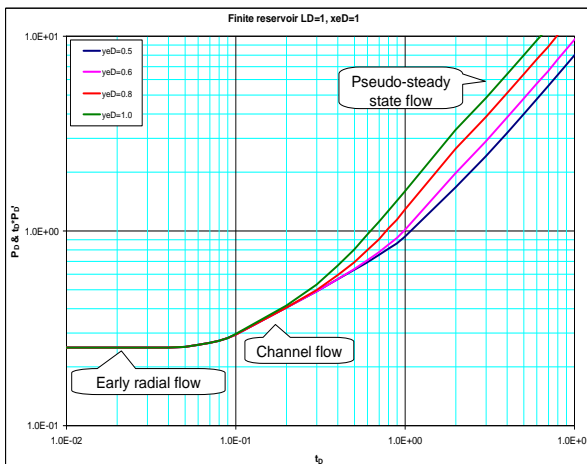


Figure 11: Pressure derivatives for different horizontal wells. Figure 12: Pressure derivatives for different horizontal wells.

Flow Regimes:

1- Early radial flow:

For horizontal wells with $L_D \leq 20$, early vertical radial flow is expected to develop at early time as the fluid flows radially from all directions in YZ plane into the wellbore as shown in Fig. (13). This flow regime is characterized by slope equals to $(1/4L_D)$ on pressure curves or having the following value on pressure derivative curves:

$$(t_D \times P_D')_{ER} = \frac{0.5}{2L_D} \tag{57}$$

therefore:

$$(t \times \Delta P')_{ER} = \frac{70.6q\mu B}{\sqrt{k_z k_y} L} \tag{58}$$

or:

$$(\Delta P)_{ER} = \frac{162.6q\mu B}{\sqrt{k_z k_y} L} \log(t) + C \tag{59}$$

where:

$$C = \ln\left(\frac{k_y}{\phi\mu cr_w^2}\right) - 7.43 + 2S_d \tag{60}$$

$$S_d = S \left(\frac{L}{h} \sqrt{\frac{k_z}{k_y}} \right) \tag{61}$$

Therefore, a semi-log plot of (ΔP) vs. (t) yields a straight line during the early data. The slope of this line can be used to calculate:

$$\sqrt{k_z k_y} = \frac{162.56q\mu B}{m_{ER} L} \tag{62}$$

2- Early linear flow:

After both upper and lower boundaries are reached, early linear flow is developed. Early linear flow represents linear flowing of reservoir fluids in the XZ plane toward the wellbore as shown in **Fig.(14)**. This flow is characterized by half slope on pressure derivative curves. The governing equation for early linear flow (Goode 1987) is:

$$(\Delta P)_{EL} = \frac{8.128qB}{Lh} \sqrt{\frac{\mu t}{k_y \phi c_t}} + C \tag{63}$$

Where:

$$C = \frac{141.2q\mu B}{L\sqrt{k_z k_y}} S_d \tag{64}$$

$$S_d = \frac{L\sqrt{k_z k_y}}{141.2q\mu b} \Big|_{\Delta P=0} - \ln\left(\frac{h}{r_w}\right) - 0.25 \ln\left(\frac{k_y}{k_z}\right) + 1.838 \tag{65}$$

Eq. (74) indicates that the plot of ΔP vs. $t^{1/2}$ yields a straight line. The slope of this line m_{EL} can be used to estimate k_y .

$$\sqrt{k_y} = \frac{8.128qB}{Lhm_{EL}} \sqrt{\frac{\mu}{\phi c}} \tag{66}$$

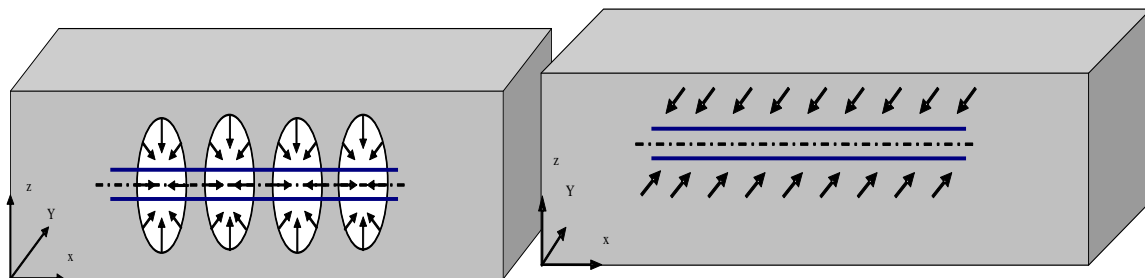


Figure 13: Early radial flow.

Figure 14: Early linear flow.

3- Pseudo radial flow:

Late or pseudo-radial flow takes place when the dimensionless time reaches the limits defined by Eq. (25) for horizontal well acting on an infinite reservoir or Eq. (54) for a finite reservoir. This flow represents

radial flowing of reservoir fluid in the XY plane toward the wellbore as shown in Fig. (15). For short distance to the boundary $1 \leq xeD < 0.5$ and $1 \leq yeD < 0.5$, pseudo-radial flow can not be observed. This type of flow is characterized by horizontal line on pressure derivative curve with:

$$(t_D \times P'_D)_{PR} = 0.5 \tag{67}$$

$$(t \times \Delta P')_{PR} = \frac{70.6q\mu B}{\sqrt{k_x k_y} h} \tag{68}$$

$$(\Delta P)_{PR} = \frac{162.6q\mu B}{\sqrt{k_x k_y} h} \log(t) + C \tag{69}$$

$$C = \frac{162.6q\mu B}{\sqrt{k_x k_y} h} \left[\log\left(\frac{k_x}{\phi \mu c L^2}\right) - 2.023 \right] + \frac{141.2q\mu B}{L \sqrt{k_y k_z}} S_d \tag{70}$$

$$S_d = 1.151 \sqrt{\frac{k_z}{k_x}} \frac{L}{h} \left[\frac{\Delta P_{1hr}}{m_{PR}} - \log\left(\frac{k_x}{\phi \mu c L^2}\right) + 1.76 \right] \tag{71}$$

A semi-log plot of (ΔP) vs. (t) yields a straight line during the pseudo-radial flow period. The slope of this line can be used to calculate:

$$\sqrt{k_x k_y} = \frac{162.6q\mu B}{m_{PR} h} \tag{72}$$

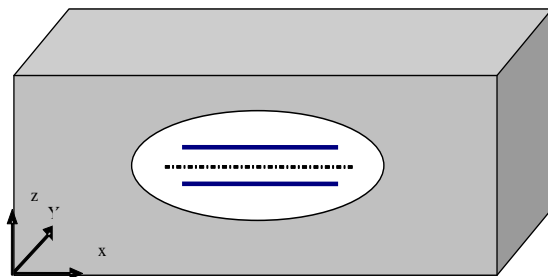


Figure 15: Pseudo-radial flow.

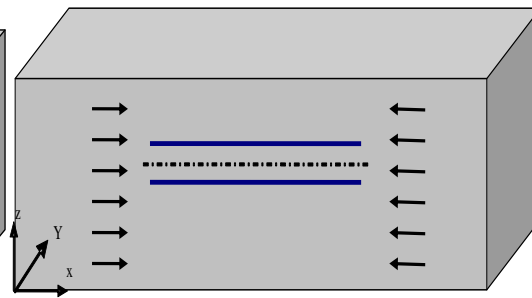


Figure 16: Channel flow.

4 - Channel Flow:

This flow starts when the pressure behavior is affected by the closest parallel outer boundaries of the reservoir. It takes place either in the XZ plane or YZ plane as shown in Fig.(16). It is characterized by slope of half on pressure derivative curves. The governing equation for this flow is (Goode 1987):

$$(\Delta P)_{CF} = \frac{8.128qB}{2hx_e} \sqrt{\frac{\mu t}{k_y \phi c_t}} + C \tag{73}$$

$$C = \frac{141.2q\mu B}{L \sqrt{k_z k_y}} S_t \tag{74}$$

$$S_t = \frac{L}{2x_e} \left[\frac{2x_e \sqrt{k_z k_y}}{141.2q\mu b} \Big|_{\Delta P=0} - S_p - \ln\left(\frac{h}{r_w}\right) - 0.25 \ln\left(\frac{k_y}{k_z}\right) + 1.838 \right] \tag{75}$$

where S_p represents the partial penetration skin factor.

The plot of ΔP vs. $t^{1/2}$ yields a straight line. The slope of this line m_{CF} can be used to estimate x_e .

$$x_e = \frac{8.128qB}{2hm_{CF}} \sqrt{\frac{\mu}{k_y \phi c_t}} \tag{76}$$

5- Pseudo-Steady State Flow:

For long producing time in a closed reservoir, a pseudo-steady state flow regime appears as a result of the pressure being influenced by all four closed boundaries at the same time. It is characterized by unit-slop line on the pressure derivative curve. The equation of this straight line is:

$$(t_D \times P_D')_{PSS} = 2\pi_{DA} \quad (77)$$

This flow can be used to estimate the drainage area of the reservoir:

$$A = \frac{0.2338qB}{\phi c_i h} \sqrt{\frac{k_x}{k_y} \left(\frac{t_{PSS}}{(t \times \Delta P')_{PSS}} \right)} \quad (78)$$

Application of Type Curve Matching:

As shown on the plots in Appendix (A), the pressure and pressure derivative have a unique shape for each combination of the distance to the outer boundaries x_e and y_e (reservoir configuration). These plots can be used for the type-curve matching technique to determine reservoir characteristics such as: permeability in the three directions and the distance to the boundaries. The following steps illustrate the procedures required in this technique:

- 1- Plot $(\Delta P$ vs. t) and $(t \times \Delta P'$ vs. t) on log-log paper.
- 2- Obtain the best match of the data with one of the type curves.
- 3- Read from any match point: $t_M, \Delta P_M, t_{DM}, P_{DM}, L_D, x_{eDM}, y_{eDM}$.
- 4- Calculate k_x, k_y, k_z from the following equations:

$$k_x = \frac{\phi \mu c_i L_w^2 t_{DM}}{0.0002637 t_M} \quad (79)$$

$$k_y = \frac{1}{k_x} \left[\frac{141.2 q \mu B P_{DM}}{h \Delta P_M} \right]^2 \quad (80)$$

$$k_z = \left(\frac{L_D^2 h^2}{L_w^2} \right) k_x \quad (81)$$

- 5- Calculate x_e using:

$$x_e = \frac{L_w}{x_{eDM}} \quad (82)$$

- 6- Calculate y_e using:

$$y_e = \frac{L_w}{y_{eDM}} \sqrt{\frac{k_y}{k_x}} \quad (83)$$

II. EXAMPLE

A pressure drawdown test data of a horizontal well acting on a finite reservoir are given in Table B-1 of Appendix (B). Other known reservoir and well data are:

$$\begin{aligned} q &= 500 \text{ STB/D} & \phi &= 0.1 & \mu &= 0.5 \text{ cp} \\ c_i &= 2 \times 10^{-6} \text{ psi}^{-1} & B &= 1.15 \text{ bbl/STB} & h &= 50 \text{ ft} \\ L &= 1600 \text{ ft} & r_w &= 0.63 \text{ ft} & p_i &= 9500 \text{ psi} \end{aligned}$$

Estimate formation permeability in all direction and the distance to the outer boundaries.

III. SOLUTION

1-The pressure and pressure derivative plot is shown in Fig. (17).

2- The matching process is shown in Fig. (18).

3- Read from the matching point:

$$t_M = 10, t_{DM} = 0.33, \Delta P_M = 10, P_{DM} = 0.078, L_{DM} = 8, x_{eDM} = 0.4, y_{eDM} = 0.3$$

4- The permeabilities in the x, y, z directions from Eqs. (79, 80, 81):

$$k_x = \frac{0.1 \times 0.5 \times 0.00002 \times 800^2 \times 0.33}{0.0002637 \times 10} = 8 \text{ md}$$

$$k_y = \left[\frac{141.2 \times 500 \times 0.5 \times 1.15 \times 0.078}{\sqrt{8} \times 50 \times 10} \right]^2 = 5 \text{ md}$$

$$k_H = \sqrt{k_x k_y} = \sqrt{8 \times 5} = 6.3 \text{ md}$$

$$k_z = k_V = \frac{8^2 \times 50^2 \times 8}{800^2} = 2 \text{ md}$$

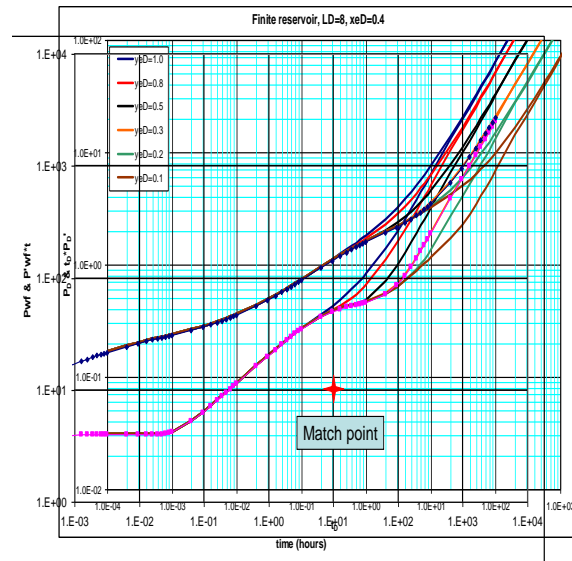
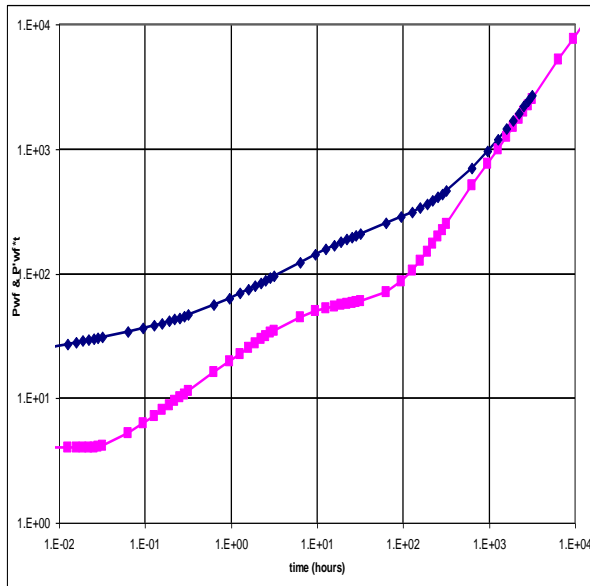


Fig. (17): Pressure & pressure derivative plots for Example.

Fig. (18): Type curve matching.

5-The distance to the boundary in the x-direction using Eq. (82):

$$x_e = \frac{800}{0.4} = 2000 \text{ ft}$$

6-The distance to the boundary in the y-direction using Eq. (83):

$$y_e = \frac{800}{0.3} \sqrt{\frac{5}{8}} = 2108 \text{ ft}$$

The above results can be compared with the results obtained by the conventional semilog method as follow:

1- The Cartesian plot of ΔP vs. \sqrt{t} , as shown in **Fig. (19)**, yields a straight line corresponding to the early linear flow data. This slope of this line $m_{EL} = 41$ can be used to obtain k_y using Eq. (66):

$$k_y = \left[\frac{8.128 \times 500 \times 1.15}{1600 \times 41 \times 50} \right]^2 \frac{0.5}{0.1 \times 0.000002} = 5 \text{ md}$$

2 - From early time data, the semi-log plot of the early radial flow, as shown in **Fig. (20)**, can be used to obtain k_z from the slope of the straight line $m_{ER} = 9.3$ using Eq. (62).

$$k_z = \left[\frac{162.6 \times 0.5 \times 500 \times 1.15}{9.3 \times 1600 \times \sqrt{5}} \right]^2 = 2 \text{ md}$$

3- From late time data, the semi-log plot of the pseudo-radial flow as shown in **Fig. (21)** can be used to obtain k_x from the slope of the straight line $m_{PR} = 147$ using Eq. (72).

$$k_x = \left[\frac{162.6 \times 500 \times 0.5 \times 1.15}{147 \times 50 \times \sqrt{5}} \right]^2 = 8 \text{ md}$$

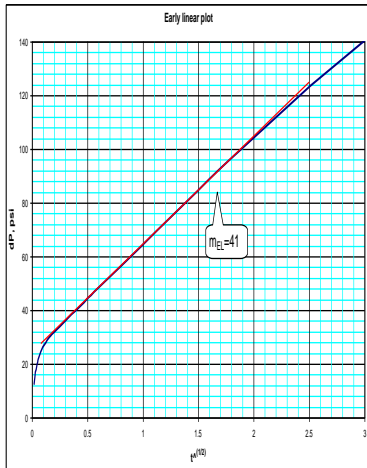


Fig. (19): Early-Linear plot

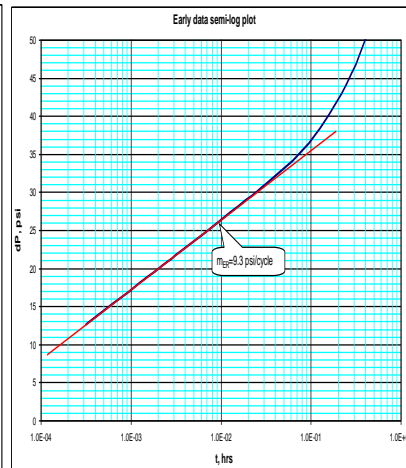


Fig. (20): Early-radial plot.

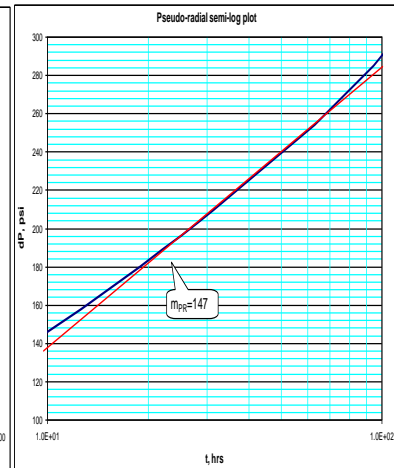


Fig. (21): Pseudo-Radial plot.

IV. CONCLUSIONS

1-Pressure behavior and flow regimes of horizontal wells acting in bounded reservoirs are affected significantly by the outer boundaries where the reservoir no longer maintains constant pressure when the production pulse reaches these boundaries.

2-The impact of the boundaries on pressure responses and fluid flow regimes occur at late time production. Pressure behaviors and flow regimes at early time production are not affected by the boundaries.

3-Wellbore length has noticeable effect on pressure behavior at late time for large square drainage area. However, this effect has not been observed for rectangular shape reservoirs.

4- Pseudo-steady state flow represents the flow resulted due to the impact of the boundaries. The starting time of this type of flow depends mainly on the distance to the boundaries and somehow a wellbore length. For the same wellbore length, it increases as the distance to the boundary increases.

5- Channel flow usually occurs for the following cases:

- The distance to one of the boundaries is significantly smaller than the second boundary.
- The wellbore penetrates completely the formation in the long horizontal direction.
- Square drainage area where the boundary in the normal plane to the wellbore can be reached before the other boundary which is parallel to the wellbore.

6-The pressure behavior of the long horizontal well, i.e. $L_D > 20$, is similar to the behavior of vertical fractures. Early radial flow can't be seen for long horizontal wells.

7- Permeabilities in all three directions and well location with respect to the boundaries can be estimated using type curve matching technique.

Nomenclature

- A drainage area, ft²
- B oil volumetric factor, RB/STB
- c_t compressibility, 1/psi
- h formation thickness, ft
- k_x Formation permeability in the X direction, md
- k_y Formation permeability in the Y direction, md
- k_z Formation permeability in the Z direction, md
- L total length of horizontal well, ft
- L_w half length of horizontal well, ft

m_{ER} slope of early radial flow line
 m_{EL} slope of early linear flow line
 m_{PR} slope of pseudo-radial flow line
 m_{CF} slope of channel flow line
 P pressure, psi
 P_D dimensionless pressure
 P_i initial pressure, psi
 P_{wf} flowing well pressure, psi
 Q oil well flow rate per unit length of horizontal well, B/D/ft
 q oil well flow rate, B/D
 r_w wellbore radius, ft
 S pseudo-skin factor
 t time, hr
 t_D dimensionless time
 t_p producing time, hr
 t_{pss} pseudo-steady state time, hr
 x_e half the distance to the boundary in the X direction, ft
 x_w the X coordinate of the production point.
 y_e half the distance to the boundary in the Y direction, ft
 y_w the Y coordinate of the production point.
 z_w the Z coordinate of the production point.

GREEK SYMBOLS

ϕ Porosity
 μ viscosity, cp
 $\square \square \square \square \square \square \square \square \square$ dummy variable of time

SUBSCRIPTS

CF channel flow
 ER early radial flow
 EL early linear flow
 PR pseudo radial flow
 PSS pseudo-steady state flow

V. REFERENCES

- [1]. Babu, D.K., and Odeh, A.S. 1988. Productivity of a Horizontal Well" SPE 18298 presented at the 63rd Annual Technical Conference, Houston, 2-5 October. doi: 102118/18334-MS.
- [2]. Carvalho, R.S., and Rosa, A.J. 1989. A Mathematical Model for Pressure Evaluation in an infinite-Conductivity Horizontal well. SPE Formation Evaluation 4 (4): 559-566. SPE 15967-PA. doi:102118/15967-PA.
- [3]. Clonts, M.D., and Ramey, H.J. 1986. Pressure Transient Analysis for Wells with Horizontal drainholes. SPE 15116 presented at the SPE Regional Meeting, California, 2-4 April. doi: 102118/15116-MS.
- [4]. Daviau, F., Mouronval, G., Bourdarot, G., et al. 1988. Pressure Analysis for Horizontal Wells. SPE Formation Evaluation: SPE Formation Evaluation: 717-724. SPE 14251-PA. doi: 102118/14251-PA.
- [5]. Escobar, Freddy H., Nestor F. Saavedra, Claudia M. Hernandez, et al. 2004. Pressure and Pressure Derivative Analysis for Linear Homogeneous Reservoirs without using Type-Curve matching. SPE 88874 presented at the 28th annual SPE technical conference and exhibition in Abuja, Nigeria, 2-4 August. doi: 102118/88874-MS.
- [6]. Economides, M.J., Brand, C.W., Frick, T.P. 1996. Well Configurations in Anisotropic Reservoirs. SPE Formation Evaluation. 257-262. SPE 27980-PA. doi: 102118/27980-PA.
- [7]. Giger, F. 1985. Horizontal Wells Production Techniques in Heterogeneous Reservoirs. SPE 13710 presented at the Middle East oil technical conference, Bahrain, 11-14 March. doi: 102118/13710-MS.
- [8]. Goode, P.A., and Kuchuk, F.J.: 1991. Inflow Performance of Horizontal Wells. SPE Reservoir Engineering. 319-323. SPE 21460-PA. doi: 102118/21460-PA.
- [9]. Goode, P. A. and Thambynaygam, R.K.M. 1987. Pressure Drawdown and buildup Analysis of Horizontal Wells in Anisotropic Media. SPE Formation Evaluation. 683-697. SPE 14250-PA. doi: 102118/14250-PA.
- [10]. Gringarten, A. C. 2010. Practical Use of Well Test Deconvolution," SPE 134534 presented at the 2010 annual technical conference, Florence, 20-22 September. Doi: 10218/134534-MS.
- [11]. Gringarten, A. C., Ramey, H. J. 1973. The Use of Source and Green's Function in Solving Unsteady-Flow Problem in Reservoir. SPEJ. 285-295. SPE 3818. doi: 102118/3818-PA.
- [12]. Gringarten, A.C., Von Schoreter, T., Rolfsavaag, T., et al. 2003. Use of Downhole Pressure Gauge Data to Diagnose Production Problems in a North Sea Horizontal Well. SPE 84470 presented at the 2003 annual conference, Denver, 5-8 October. Doi:102118/84470-MS.
- [13]. Guo, G., and Evans, R.D. 1993. An Economic Model for Assessing the Feasibility of exploiting Naturally Fractured Reservoirs by Horizontal Well technology. SPE 26676 presented at the 68th Annual technical Conference, Houston, 3-6 October. doi: 102118/26676 MS
- [14]. Hashemi, A., Laurent, M., and Gringarten, A.C. 2004. Well test Analysis of Horizontal Wells in Gas-condensate reservoirs. SPE 89905 presented at the SPE Annual Technical Conference, Houston, 26-29 September. doi: 102188/89905-MS.
- [15]. Ilk, D., Valko, P.P., and Blasingame. 2005. Deconvolution of Variable Rate Reservoir Data Using B-Spline. SPE 95571 presented at the 2005 annual conference, Dallas, 9-12 October. doi: 102118/95571-MS.

[16]. Joshi, S.D. 1986. Augmentation of Well Productivity Using Slant and Horizontal Wells. SPE 15375 paper presented at the 61th annual technical conference, New Orleans, 5-8 October. doi: 102188/15375-MS.

[17]. Khelifa, M., and Tiab, D. 2002. Multirate Test in Horizontal Wells. SPE 77951 paper presented at the SPE Asia Pacific Oil and gas conference, Melbourne, 8-10 October. doi: 102188/77951-MS.

[18]. Kuchuk, F.J., Goode, P.A., Wilkinson, D.J., Thambayagam, R.K. 1991. Pressure-Transient behavior of Horizontal wells with and without gas Cap or aquifer. SPE Formation Evaluation. 86-94. SPE 17413-PA. doi: 102118/17413-PA.

[19]. Odeh, A.S., and Babu, D.K. 1990. Transient Flow Behavior of Horizontal wells: Pressure Drawdown and Buildup analysis. SPE Formation Evaluation. 7-15. SPE 18802-PA. doi: 102118/18802-PA.

[20]. Ogunsanya, B.O., Oetama, T.P., Heinze, J.F., et al. 2005. A Physically Consistent Model for describing Transient Pressure Behavior of Horizontal drainholes. Canadian SPE 2005-071 presented at the 6th Canadian International Petroleum Conference, Calgary, Alberta, 7-9 June.

[21]. Ozkan, E., Raghavan, R., and Joshi, S.D. 1989. Supplement for SPE 16378, Horizontal Well Pressure analysis. SPE 20271 available from Richardson, TX 75083-3836.

[22]. Ozkan, E., Sarica, C., Haciislamoglu, M., et al. 1995. Effect of Conductivity on Horizontal Well Pressure behavior. SPE Advanced Technology Series Vol. 3, No.1. 85-94. SPE 24683-PA. doi: 102118/24683-PA.

[23]. Spivak, D. 1985. Pressure Analysis for Horizontal Wells. Ph.D. Dissertation, Louisiana Tech University, Louisiana (May 1985).

[24]. Verga, F.M., Beretta, E., and Albani, D. 2001. Transient Dual-Porosity Behavior for Horizontal wells draining Heterogeneous Reservoirs. SPE 68844 presented at the SPE western Regional Meeting, California, 26-30 March. doi: 102118/68844-MS.

[25]. Thompson, L.G., and Temeng, K.O. 1993. Automatic Type-Curve matching for Horizontal wells. SPE 25507 presented at the production operation symposium, Oklahoma City, 21-23 March. doi: 102118/25507-MS.

[26]. Von Schroeter, T., Hollaender, F., and Gringarten, A.C. 2004. Deconvolution of Well Test Data as a Nonlinear Total Least squares Problem. SPE Journal. 375-390. SPE 77688-PA. doi: 102118/77688-PA.

[27]. Whittle, T., Jiang, H., Young, S., and Gringarten, A.C. 2009. Well Production Forecasting by Extrapolation of the Deconvolution of the Well Test Pressure Transients. SPE 122299 presented at the 2009 SPE EUROPEC/EAGE conference, Netherland, 8-11 June. doi: 102118/122299-MS.

Appendix A

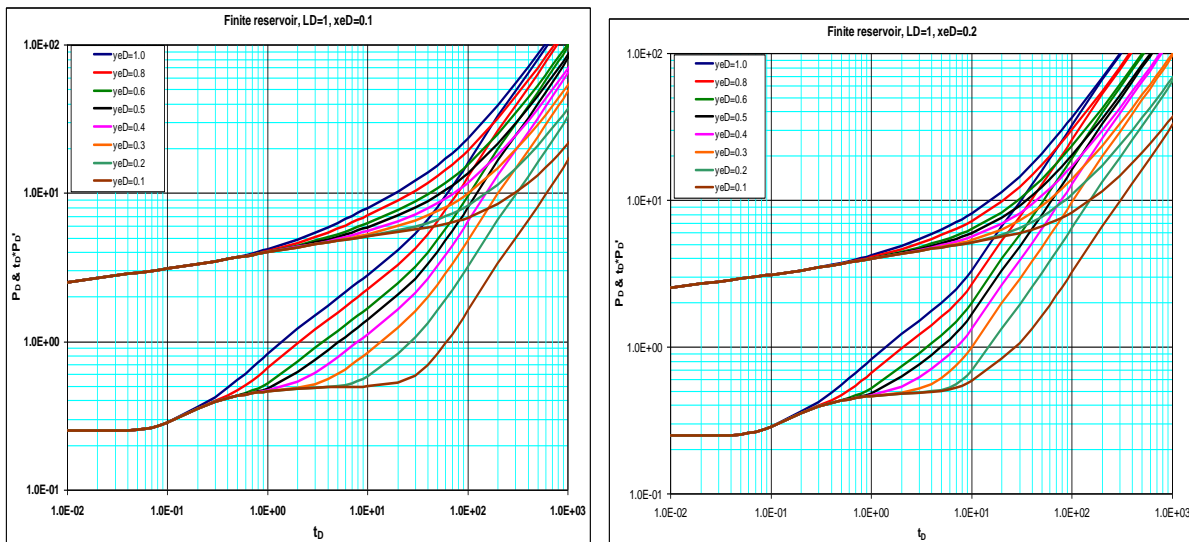


Fig. (A-1): Type curve for short horizontal well $L_D=1$ Fig. (A-2): Type curve for short horizontal well $L_D=1$.

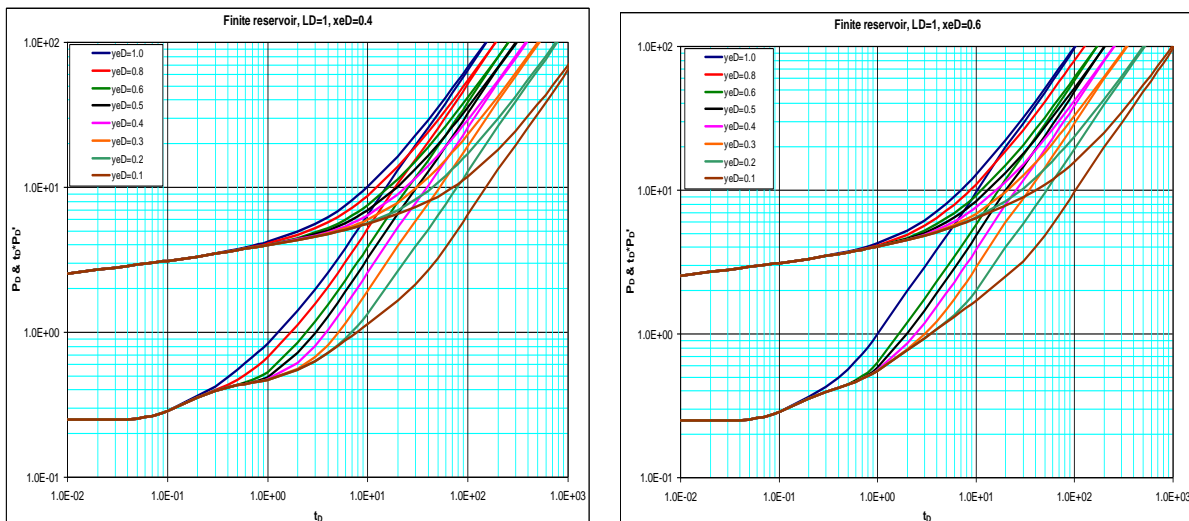


Fig. (A-3): Type curve for short horizontal well $L_D=1$.

Fig. (A-4): Type curve for short horizontal well $L_D=1$.

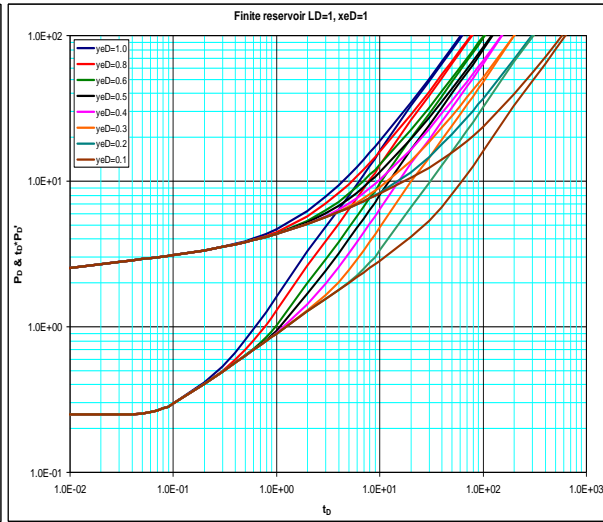
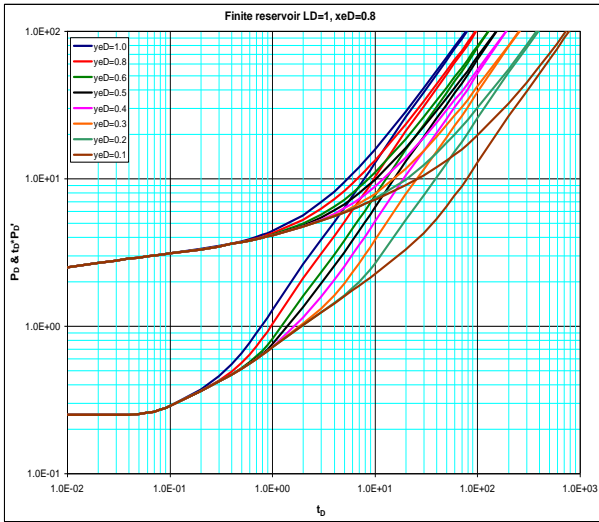


Fig. (A-5): Type curve for short horizontal well $L_D=1$.

Fig. (A-6): Type curve for short horizontal well $L_D=1$.

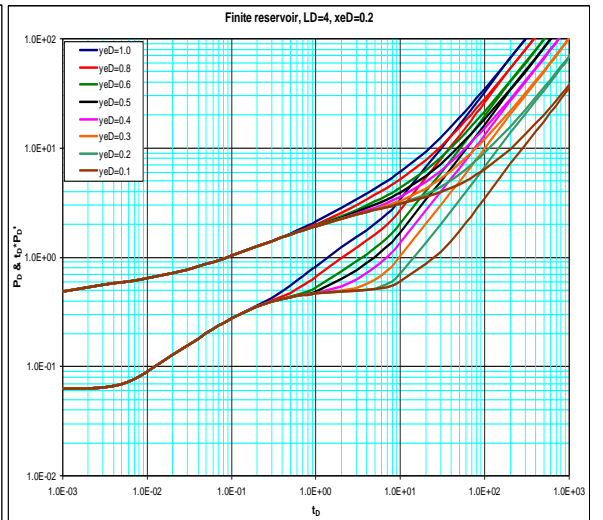
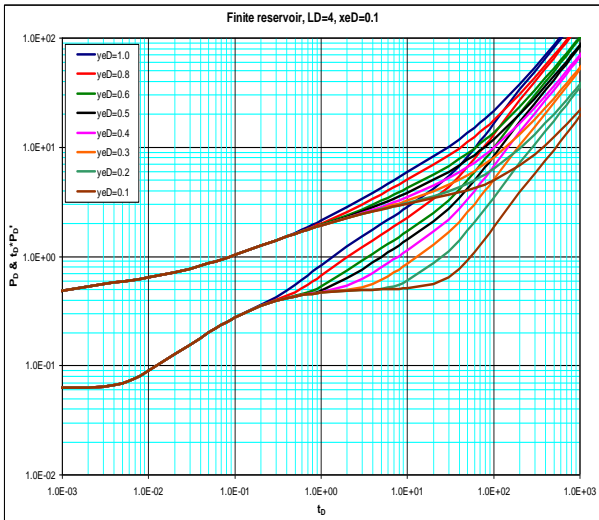


Fig. (A-7): Type curve for short horizontal well $L_D=4$.

Fig. (A-8): Type curve for short horizontal well $L_D=4$.

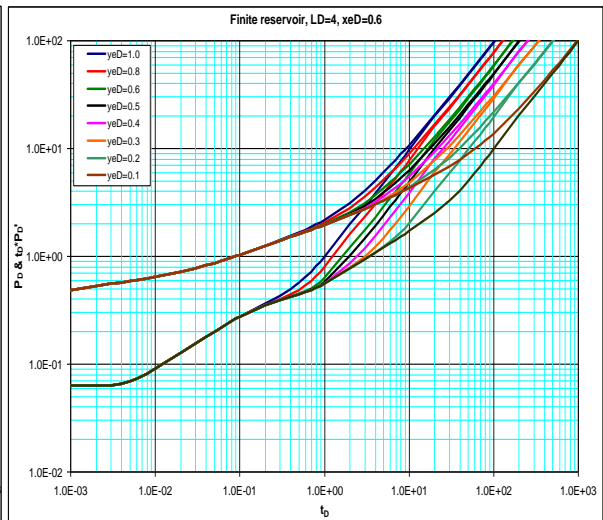
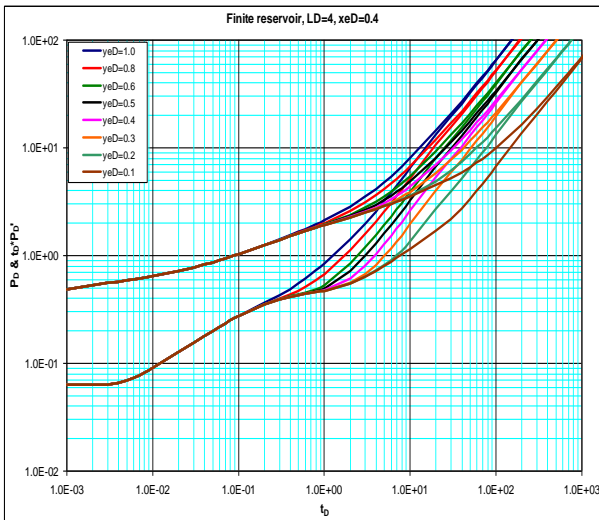


Fig. (A-9): Type curve for short horizontal well $L_D=4$.

Fig. (A-10): Type curve for short horizontal well $L_D=4$.

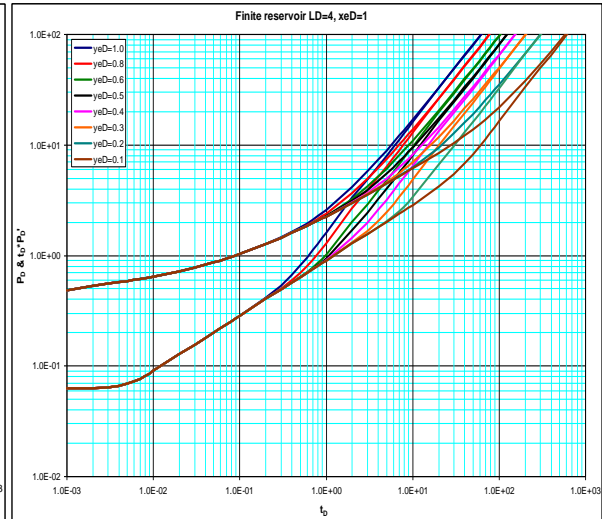
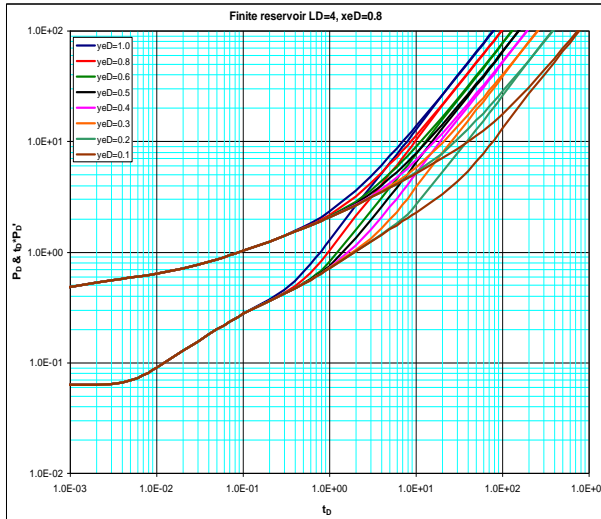


Fig. (A-11): Type curve for short horizontal well $L_D=4$. Fig. (A-12): Type curve for short horizontal well $L_D=4$.

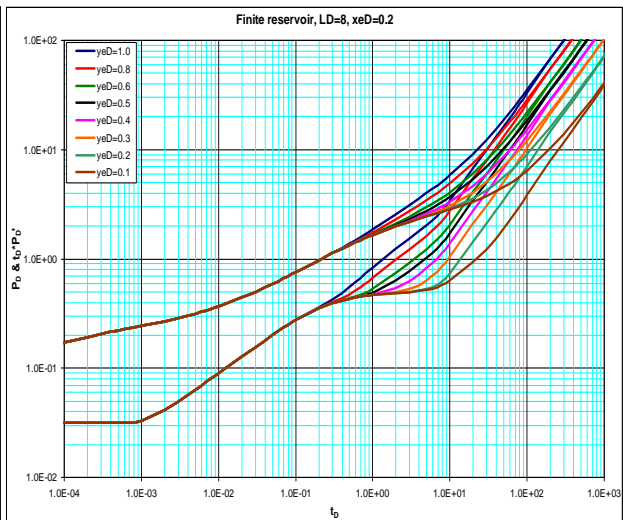
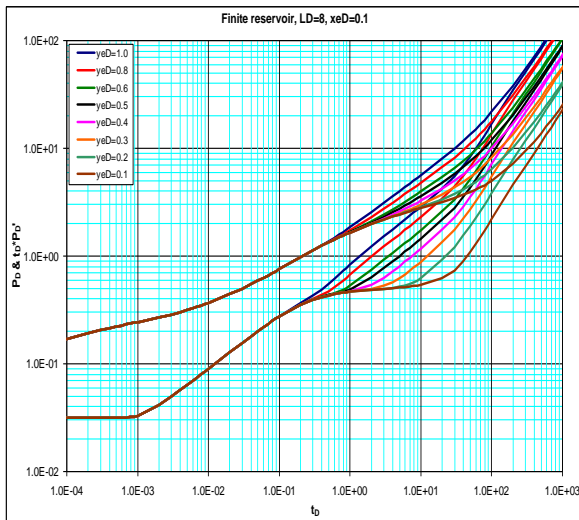


Fig. (A-13): Type curve for short horizontal well $L_D=8$. Fig. (A-14): Type curve for short horizontal well $L_D=8$.

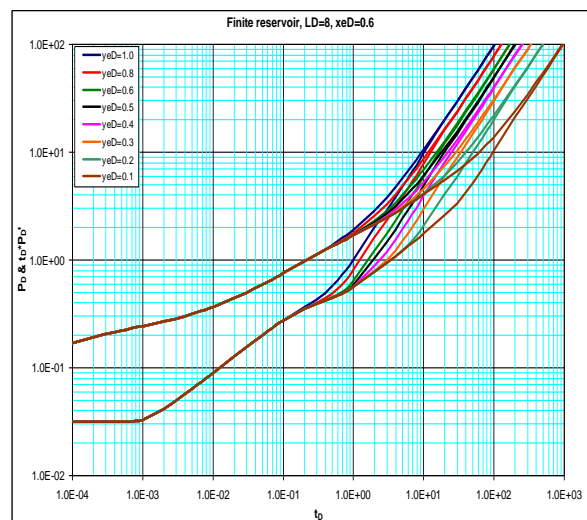
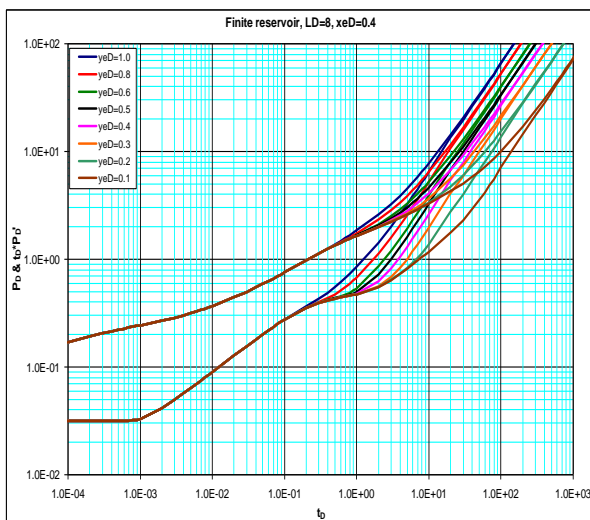


Fig. (A-15): Type curve for short horizontal well $L_D=8$. Fig. (A-16): Type curve for short horizontal well $L_D=8$.

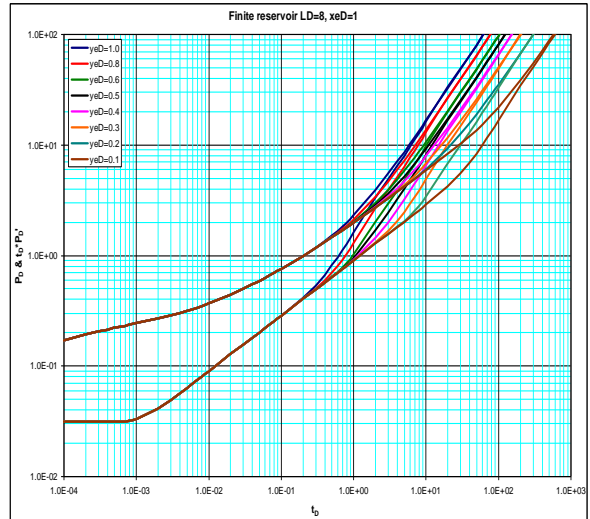
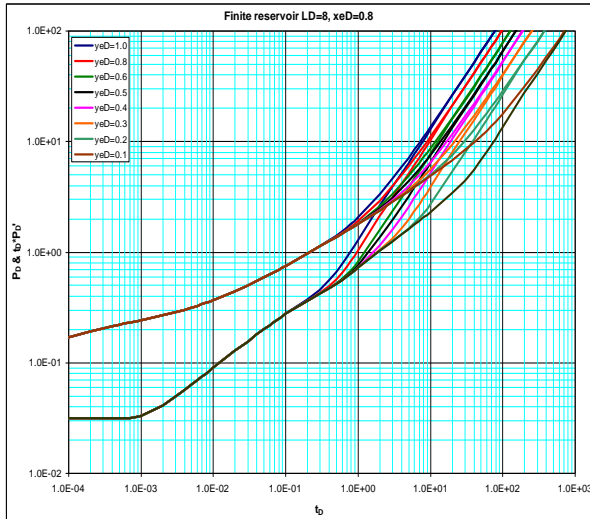


Fig. (A-17): Type curve for short horizontal well $L_D=8$. Fig. (A-18): Type curve for short horizontal well $L_D=8$.

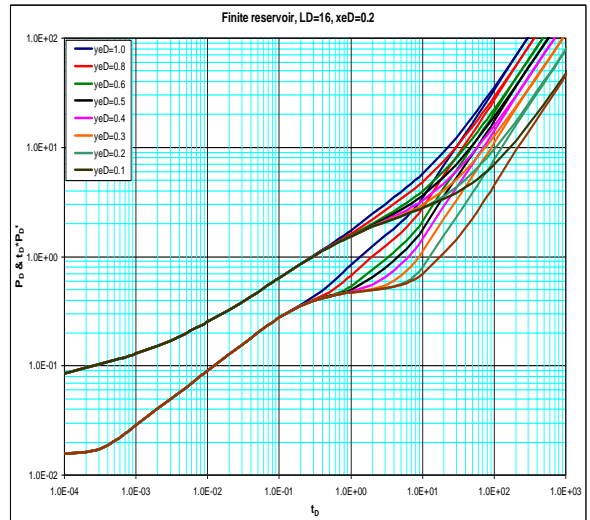
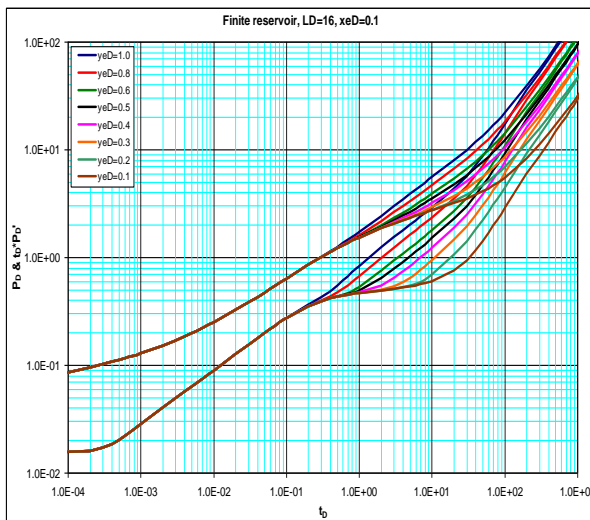


Fig. (A-19): Type curve for short horizontal well $L_D=16$. Fig. (A-20): Type curve for short horizontal well $L_D=16$.

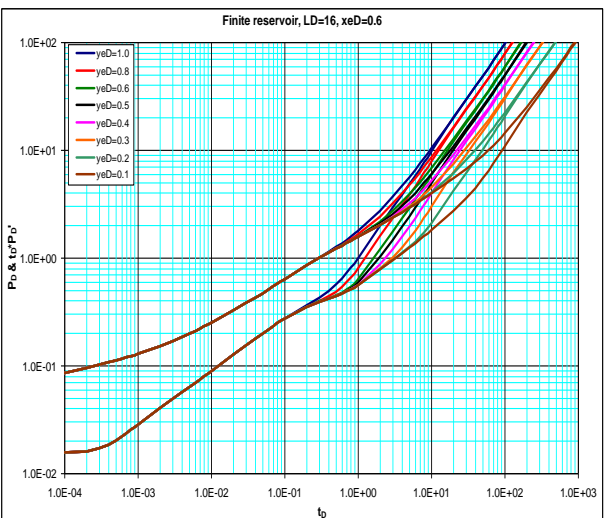
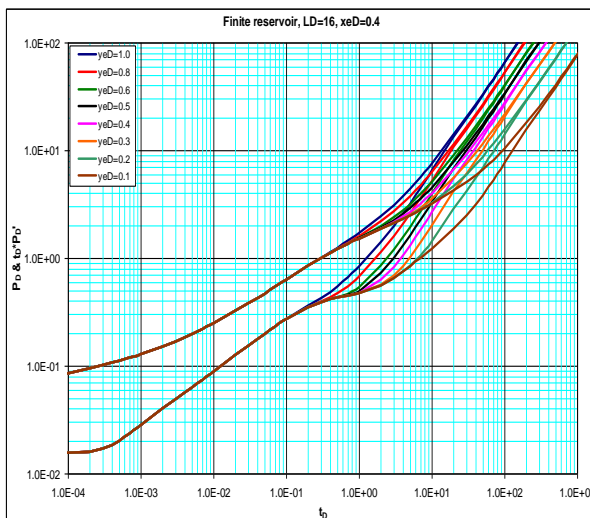


Fig. (A-21): Type curve for short horizontal well $L_D=16$. Fig. (A-22): Type curve for short horizontal well $L_D=16$.

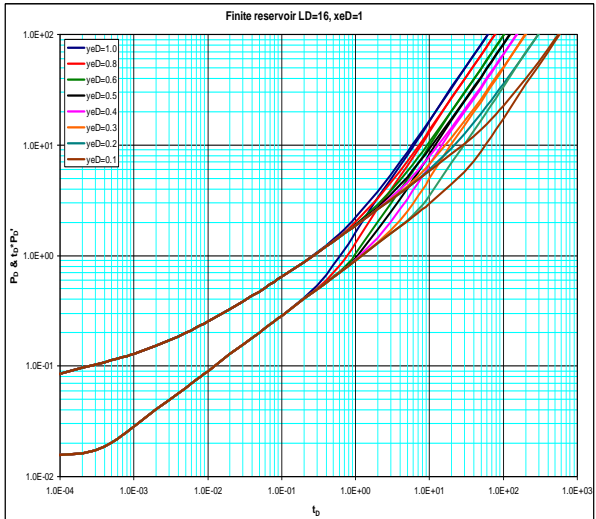
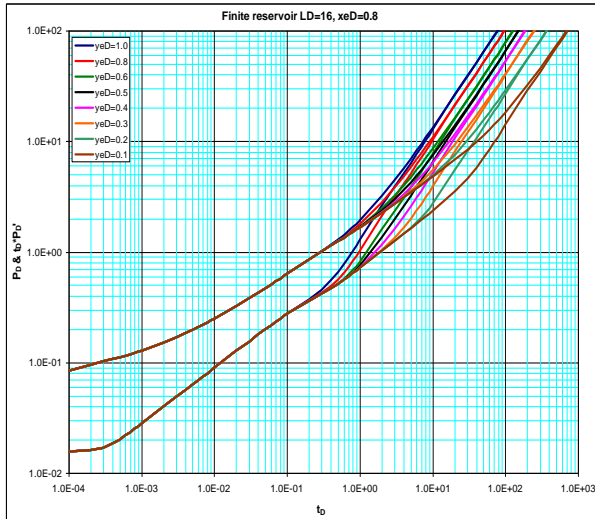


Fig. (A-23): Type curve for short horizontal well $L_D=16$. Fig. (A-24): Type curve for short horizontal well $L_D=16$.

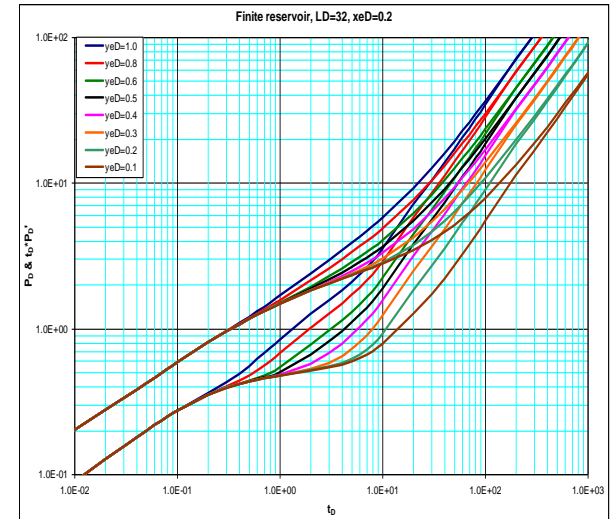
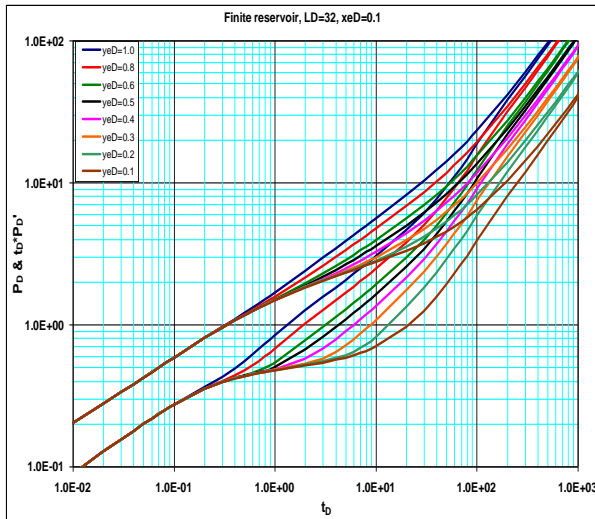


Fig. (A-25): Type curve for long horizontal well $L_D=32$. Fig. (A-26): Type curve for long horizontal well $L_D=32$.

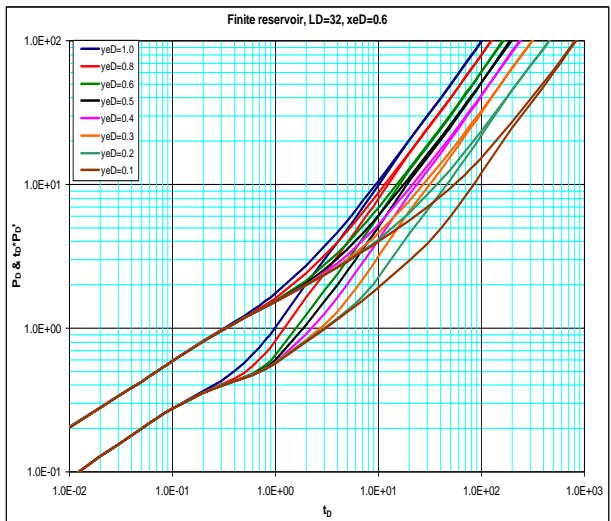
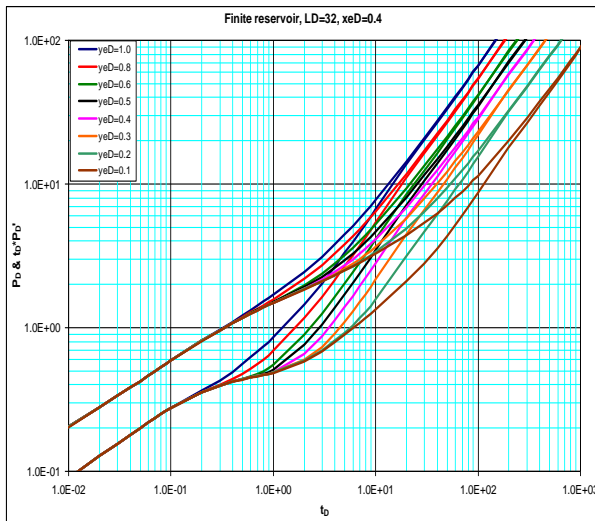


Fig. (A-27): Type curve for long horizontal well $L_D=32$. Fig. (A-28): Type curve for long horizontal well $L_D=32$.

Appendix B

Table B-1: Simulated Pressure Drawdown Data of Example.

t, hrs	Pwf, psi						
0	9500	0.031533	9469.02	6.306661	9376.40	945.9992	8544.48
0.000315	9487.42	0.063067	9465.85	9.459992	9357.07	1261.332	8296.37
0.000631	9484.69	0.0946	9463.55	12.61332	9342.22	1576.665	8048.00
0.000946	9483.11	0.126133	9461.62	15.76665	9330.16	1891.998	7799.44
0.001261	9481.96	0.157667	9459.92	18.91998	9320.01	2207.331	7550.73
0.001577	9481.06	0.1892	9458.39	22.07331	9311.24	2522.665	7301.91
0.001892	9480.33	0.220733	9456.97	25.22665	9303.50	2837.998	7052.98
0.002207	9479.71	0.252266	9455.66	28.37998	9296.59	3153.331	6803.97
0.002523	9479.18	0.2838	9454.42	31.53331	9290.32	6306.661	4311.03
0.002838	9478.70	0.315333	9453.26	63.06661	9246.18	9459.992	1815.31
0.003153	9478.28	0.630666	9443.83	94.59992	9215.33		
0.006307	9475.50	0.945999	9436.59	126.1332	9188.42		
0.00946	9473.87	1.261332	9430.49	157.6665	9162.94		
0.012613	9472.72	1.576665	9425.12	189.1998	9137.99		
0.015767	9471.82	1.891998	9420.28	220.7331	9113.24		
0.01892	9471.09	2.207331	9415.83	252.2665	9088.56		
0.022073	9470.47	2.522665	9411.72	283.7998	9063.91		
0.025227	9469.94	2.837998	9407.87	315.3331	9039.25		
0.02838	9469.45	3.153331	9404.26	630.6661	8792.19		

Evaluation of Relationship Between Mechanical Properties of High Strength Self Compacting Concrete

S.SeshaPhani¹, Dr.Seshadri Sekhar T², Dr.Srinivasa Rao³, Dr Sravana⁴

¹Deputy Executive Engineer, Tirumala Tirupathi Devasthanams, Hyderabad

²Principal Ashoka Institute of engineering and Technology

^{3,4}Jawaharlal Nehru Technological University, College of Engineering, Hyderabad, Andhra Pradesh,

Abstract: In the present experimental investigation an attempt is made to report relationship between compressive strength, Split tensile Strength and Flexural Strength of High Strength Self Compacting Concrete with mineral admixtures. It is well known that the properties of concrete are affected by cementitious matrix, aggregate and the transition zone between the two phases. Reducing water powder ratio and addition of pozzolona admixtures like Fly ash and Micro silica are often used to modify the micro structure of the matrix and to optimize the transition zone.

Keywords: Self Compacting Concrete, Segregation Resistance, Filling ability, Passing Ability, Water-Powder Ratio.

I. LITERATURE REVIEW

C. SELVAMONY et.al⁽¹⁾ involved evaluating the Effectiveness of various percentages of mineral admixtures in producing SCC. Okamura's method, based on EFNARC specifications, was adopted for mixed design. DR SRIRAVINDRARAJA H et.al⁽²⁾ investigated into the development of self-compacting concrete with reduced segregation potential. The fine particle content is increased by replacing partially the fine and coarse aggregates by low-calcium fly ash. S. VENKATESWARA RAO et.al⁽³⁾ aims at developing standard and high strength Self Compacting Concrete (SCC) with different sizes of aggregate based on Nansu's mix design procedure. Also, fly ash optimization is done in study with the graded coarse aggregate. OKAMURA⁽⁴⁾ proposed a mix design method for SCC based on paste and mortar studies for super plasticizer compatibility followed by trial mixes. However, it is emphasized that the need to test the final product for passing ability, filling ability, and flow and segregation resistance is more relevant. DR.SRINIVASA RAO. P⁽⁵⁾ had proposed the relationship between Splitting Tensile Strength and Compressive Strength by the test results and found that Split Tensile Strength is proportional to 0.78 power of Compressive Strength for normal concrete. DR.SESHADRI SEKHAR .T. P⁽⁶⁾ had proposed the mix design for high strength self compacting concrete of M100 mix using fly ash and Micro silica as Mineral admixtures. DR SESHADRI SEKHAR .T⁽⁷⁾ had proposed the relationship between Compressive Strength, Flexural strength and Splitting Tensile Strength for self compacting concrete mix of different grades ranging from M30 to M65. NIHAL ARIOGLU ET.AL⁽⁸⁾ had studied ratio of split tensile strength to cylinder compressive strength as a function of compression strength of concrete.

Research Significance

In fact, concrete researchers have shown that the true tensile strength, as determined from the split cylinder test, is between 65 and 75 per cent of the modulus of rupture for normal concrete. It has been well established that the splitting tensile test of the cylindrical specimen gives more reasonable tensile strength estimation than the direct tensile test or the modulus of rupture test. The acceptance of the split cylinder test is based on the fact that the stress distribution is reasonably uniform along the vertical diameter of the cylinder, which has been shown to be the plane of principle tensile stress for about 80 per cent of its length. In a number of recent investigations of the behaviour of actual concrete dams during earthquakes, it has become apparent that a limiting factor has been that the tensile strength of any concrete is only a fraction of its

compressive strength. However, ACI building code provisions are primarily based on tests of relatively mature concrete elements, and provisions may not provide consistent safety margins when applied to young concrete. In ACI, such strengths as modulus of rupture, shear, and splitting tensile strength of concrete are expressed in terms of the square root of the compressive strength. These empirical relationships were derived from tests on relatively mature concrete specimens, and the square root function was probably chosen as a matter of convenience so that calculations could be readily performed with a slide rule. However, recent research has shown that a square root relationship between splitting tensile strength and compressive strength is not the most appropriate relationship for maturing concrete. It is evident that most concrete researchers believe, from analyses of test data that the true test data is representative of power relation, which lies between 0.6 and 0.8.

For a newly development material like Self Compacting Concrete studies on Compressive, Split Tensile and Flexural strength are of paramount important for instilling confidence amongst the engineers and builders. The literature indicates that while some studies are available on the Compressive Strength, Split Tensile Strength and Flexural Strength of Self Compacting Concrete. Comprehension studies which involve relationship between the parameters Compressive Strength, Split Tensile Strength, Flexural Strength are not available High Strength Self Compacting Concrete Mixes. Hence, considering the gap in the existing literature, an attempt also has been made to obtain a relationship between the splitting tensile strength, Flexural Strength and Compressive strength.

Experimental Programme

The objectives of the experimental study that was conducted are given below.

- (i) To develop Mathematical Relationship between Compressive Strength, Split Tensile Strength and Flexural Strength.

II. MATERIALS

Cement

Ordinary Portland cement of 53 grade having specific gravity was 3.02 and fineness was $3200\text{cm}^2/\text{gm}$ was used in the investigation. The Cement used has been tested for various proportions as per IS 4031-1988 and found to be confirming to various specifications of IS 12269-1987.

Coarse Aggregate

Crushed angular granite metal of 10 mm size having the specific gravity of 2.65 and fineness modulus 6.05 was used in the investigation.

Fine Aggregate

River sand having the specific gravity of 2.55 and fineness modulus 2.77 was used in the investigation.

Viscosity Modifying Agent

A Viscosity modified admixture for Rheodynamic Concrete which is colourless free flowing liquid and having Specific of gravity 1.01 ± 0.01 @ 25°C and pH value as 8 ± 1 and Chloride Content nil was used as Viscosity Modifying Agent

Admixture

The Modified Polycarboxylated Ether (BASF Glenium™ B276 SURETEC) based super plasticizer which is pale yellow colour and free flowing liquid and having Relative density 1.10 ± 0.01 at 25°C , pH >6 and Chloride Ion content $<0.2\%$ was used as super plasticizer.

Fly Ash Type-II fly ash confirming to I.S. 3812 – 1981 of Indian Standard Specification was used as Pozzolana Admixture.

Micro Silica

The Micro silica having the specific gravity 2.2 obtained from Oriental Trexim, Private Limited was used in the present investigation

Test Specimens:

Test specimens consist of $150\text{X}150\text{X}150$ mm cubes, $150\text{ X }300$ mm cylinders and $100\text{X}100\text{X }500$ mm beams were casted for Mix 100 and tested as per IS 516 and 1199.

III. DISCUSSION OF RESULTS

Quantities of materials required per 1 cum of High Strength Self Compacting Concrete mixes

Table 1.0 gives the quantities of material required for High Strength Self Compacting mix of grade M 100. The Trail Mixes were carried by verifying the fresh state properties with EFNARC guidelines.

Fresh State properties of High Strength Self Compacting Concrete mixes

Table 2.0 provides a summary of the fresh state properties of High Strength Self Compacting Concrete of Mix 100. As it is evident, the basic requirements of high flow ability and segregation resistance as specified by guidelines on High Strength Self Compacting Concrete mixes by EFNARC are satisfied. The Rheological properties are maintained by adding suitable quantities of super plasticizers which satisfies the EFNARC⁽⁸⁾ guidelines.

Mathematical Relationship Between Mechanical Properties of High Strength Self Compacting Concrete Mix M 100

Table 3.0 gives the Compressive Strength, Flexural strength and Split Tensile Strength of M 100 grade of High Strength Self Compacting Concrete for 7, 28, 56, 90, 180 and 270 days. Based on the results of the specimens the mathematical equations were obtained expressing Compressive Strength, Split Tensile Strength and Flexural Strength for High Strength Self Compacting Concrete of Mix M 100. Fig 1.0 shows the graphical behaviour of Compressive Strength and Split Tensile Strength, fig 2.0 shows the graphical behaviour of Compressive Strength and Flexural strength. The mathematical relationship between both between Compressive Strength – Split Tensile Strength and Compressive Strength – Flexural Strength of Self Compacted Concrete depicts that they are obeying Power Law. Plate no 1, 2 and 3 gives the test setup for measuring Compressive Strength, Split tensile Strength and Flexural Strength.

The Relationship between Compressive Strength – Split Tensile Strength is given by
 $f_t = 0.043f_{ck}^{1.064}$ with coefficient of variation $R^2 = 0.990$

The Relationship between Compressive Strength – Flexural Strength is given by
 $f_{cr} = 0.031f_{ck}^{1.125}$ with coefficient of variation $R^2 = 0.989$

IV. CONCLUSIONS

- The Relationship between Compressive Strength – Split Tensile Strength is given by
 $f_t = 0.043f_{ck}^{1.064}$ with coefficient of variation $R^2 = 0.990$
- The Relationship between Compressive Strength – Flexural Strength is given by
 $f_{cr} = 0.031f_{ck}^{1.125}$ with coefficient of variation $R^2 = 0.989$
- The Relationship between Compressive, Split Tensile and Flexural Strength of High Strength Self Compacting Concrete are in accordance with power's law.
- The Water –Powder Ratio of .022 is used for getting High Strength Self Compacting Concrete of Mix M 100.

REFERENCES

- [1]. Selvamony C et.al., "Development of high strength self compacted self curing concrete with mineral admixtures" International Journal Design and manufacturing Technologies, Vol.3, No.2, July 2009, pp 103 -108.
- [2]. Dr. R. Sri Ravindrarajah, et.al "Development of high strength self compacting concrete with reduced segregation potential" Proceedings of the 3rd International RILEM Symposium, Reykjavik, Iceland, 17-20 August 2003, Edited by O. Wallevik and I. Nielsson, (RILEM Publications), 1 Vol., 1048 pp., ISBN: 2-912143-42-X, soft cover.
- [3]. S. Venkateswara Rao et.al "Effect of Size of Aggregate and Fines on Standard And High Strength Self Compacting Concrete", Journal of Applied Sciences Research, 6(5): 433-442, 2010.
- [4]. Hajime Okamura et.al, "Self Compacting Concrete", Journal of Advanced Concrete Technology, Vol 1, No 1,5-15, April 2003.
- [5]. Dr.P.Srinivasa Rao et.al "Relationship between Splitting Tensile and Compressive Strength of Concrete", Construction Review Journal June, 39-44.
- [6]. Dr T. Seshadri Sekhar et.al "High Strength self compacting concrete using mineral admixtures", Indian Concrete Journal March 2013 PP 42-48.
- [7]. Dr T. Seshadri Sekhar et.al "Relationship between Compressive, Split Tensile, Flexural Strength of Self Compacting Concrete" publication in International Journal of Mechanics and Solids, Volume 3, Number 2 (2008) pp 157-168.
- [8]. EFNARC, "Specifications and guidelines for self compacting concrete", www.efnarc.org

Table 1.0 Quantities of Materials for 1m³ of High Strength Self Compacting Concrete mix of M 100

Mix	Cement (Kg/m ³)	Fly ash (Kg/m ³)	Micro Silica (Kg/m ³)	Water (Kg/m ³)	Coarse Aggregate (kg/m ³)	Fine Aggregate (Kg/m ³)	SP (kg/m ³)	V.M.A (Kg/m ³)	Water /Powder Ratio
Mix 100	500	125	75	154	774.985	766.195	11.2	0.35	0.22

Table 2.0 Fresh Concrete properties of High Strength Self Compacting Concrete Mix M 100

	Mix 10	Permissible limits as per Efnarc Guidelines		
		Min	Max	
V-Funnel	12 sec	6 sec	12 sec	
Abrams slump flow	665 mm	650mm	800mm	
T _{50cm} slump flow	4.5 sec	2 sec	5 sec	
L-Box	H ₂ /H ₁	0.90	0.82	1.0
	T ₂₀	1sec	1sec	2 sec
	T ₄₀	2 sec	2sec	3sec
V-Funnel at T _{5 min}	14 sec	11 sec	15 sec	

Table 3.0 Compressive Strength, Flexural Strength and Split Tensile Strength of High Strength Self Compacting Concrete Mix M100

Sample ↓ Days ⇒	Compressive Strength (Mpa)						Split Tensile Strength(Mpa)						Flexural Strength(Mpa)					
	7	28	56	90	180	270	7	28	56	90	180	270	7	28	56	90	180	270
1	93.38	117.18	122.38	133.18	143.22	144.12	5.43	7.21	7.32	8.02	8.42	8.72	4.98	7.02	7.27	7.75	8.28	8.46
2	92.64	116.92	122.74	132.48	141.38	145.29	5.49	7.13	7.42	7.83	8.51	8.48	5.66	7.11	7.12	7.85	8.61	8.58
3	95.49	118.21	123.12	133.16	138.75	147.26	5.47	7.12	7.46	7.84	8.46	8.46	4.68	7.24	7.28	7.58	8.28	8.42
4	93.35	117.12	121.18	133.12	143.17	144.37	5.26	6.98	7.41	7.86	8.32	8.38	5.44	6.28	7.42	7.79	8.22	8.68
5	92.46	116.92	122.95	132.42	140.12	148.25	5.24	6.92	7.48	7.78	8.43	8.92	5.12	7.12	7.32	7.85	8.32	8.42
6	93.39	115.83	123.47	133.28	141.60	148.81	5.29	7.12	7.31	7.95	8.38	8.94	5.15	6.87	7.29	7.52	8.45	8.80
Average value	93.62	117.03	122.64	132.94	141.38	146.35	5.36	7.08	7.40	7.88	8.42	8.65	5.18	6.94	7.25	7.72	8.36	8.56

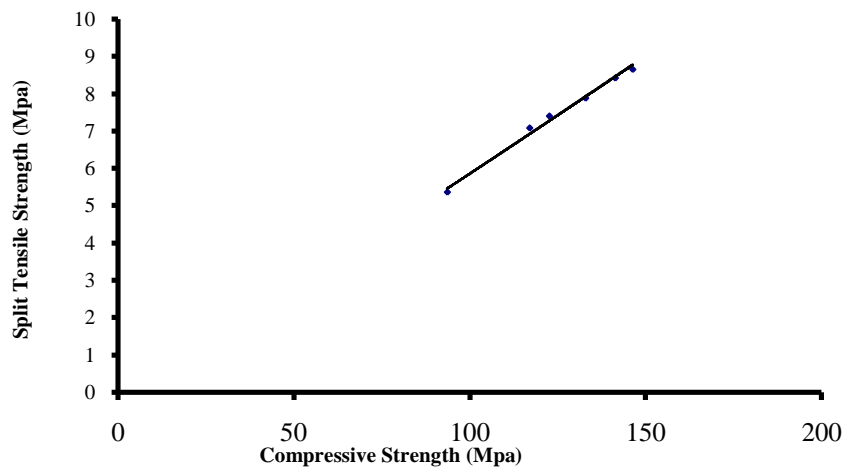


Fig 1.0 Relationship between Compressive Strength and Split Tensile Strength

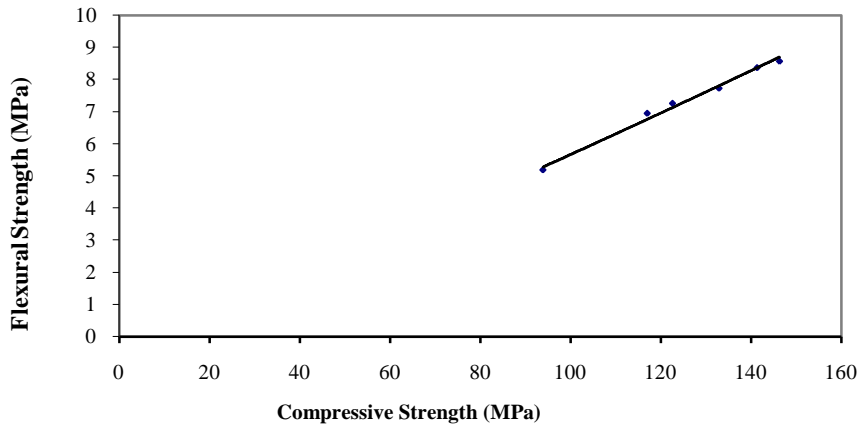


Fig 2.0 Relationship between Compressive Strength and Flexural Strength



Plate No1 Test Set up for measuring Compressive Strength



Plate No2 Test Set up for measuring Flexural Strength



Plate No3 Test Set up for measuring Split Tensile Strength

Carbon Emissions from air-Conditioning

Rajesh Kumar¹, RK Aggarwal², Dhirender Gupta³ Jyoti Dhar Sharma¹

¹Deptt. of Physics, Shoolini University, Bajhol, Distt. Solan (HP)- 173 212 (India)

²Deptt. of Environmental Science, University of Horticulture & Forestry, Solan (HP) -173230 (India)

³Deptt. of Physics, Govt P G College, Bilaspur (HP) – 174001 (India)

Abstract: This paper explores electricity consumption and carbon emissions associated with air-conditioning. The total heat load of a room fitted with air conditioner of 1.5 ton capacity has been calculated by calculating conduction and ventilation losses. Solar heat gain and internal gain were taken as the other two parameters for the total heat calculation.

Keywords: Heat gain, absorptance, transmittance, coefficient of performance.

I. INTRODUCTION

As the average temperature of the planet rises every year we also have started using the air conditioner more. The result is that we are heating up the environment even more. What happens is, whenever we turn on the air conditioner, it releases carbon into the air. And carbon has been identified as the element that insulates our planet and is a major contributor in global warming. The average world temperature of the Earth has increased by 1 degree Fahrenheit in just the last century. Compared to most other electric devices, the air conditioner consumes much more energy. We had considered a room of 6.7 m length, 5.5 m width and 3 m height. The room was maintained at 22°C temperature by an air-conditioner. Under the steady state approach (which does not account the effect of heat capacity of building materials), the heat balance for room air can be written as [1]:

$$Q_{\text{total}} = Q_c + Q_s + Q_i + Q_v \dots \dots \dots (1)$$

1.1 Conduction

The rate of heat conduction (Q_c) through any element such as roof, wall or floor under steady state can be written as

$$Q_c = AU\Delta T \dots \dots \dots (2)$$

where,

A = surface area (m^2)

U = thermal transmittance (W/m^2K)

ΔT = temperature difference between inside and outside air (K)

Mean hourly values of data for various places in India are available in the handbook by Mani [2].

1.2 Ventilation

The heat flow rate due to ventilation of air between the interior of a building and the outside, depends on the rate of air exchange. It is given by:

$$Q_v = \rho V_r C \Delta T \dots \dots \dots (3)$$

where,

ρ = density of air (kg/m^3)

V_r = ventilation rate (m^3/s)

C = specific heat of air (J/kgK)

ΔT = temperature difference ($T_o - T_i$) (K)

1.3 Solar Heat Gain

The solar gain through transparent elements can be written as :

$$Q_s = \alpha_s \sum A_i S_{gi} \tau_i \dots \dots \dots (4)$$

where,

α_s = mean absorptivity of the space

A_i = area of the i th transparent element (m^2)

S_{gi} = daily average value of solar radiation (including the effect of shading) on the i th transparent element (W/m^2)

τ_i = transmissivity of the i th transparent element

1.4 Internal Gain

The heat generated by occupants is a heat gain for the building; its magnitude depends on the level of activity of a person. Table 1.1 shows the heat output rate of human bodies for various activities [3]. The total rate of energy emission by electric lamps is also taken as internal heat gain. The heat gain due to appliances (televisions, radios, etc.) should also be added to the Q_i .

Table 1. Heat production rate in a human body [3]

Activity	Rate of heat production	
	(W)	(W/m ²)
Sleeping	60	35
Resting	80	45
Sitting, Normal office work	100	55
Typing	150	85
Slow walking (3 km/h)	200	110
Fast walking (6 km/h)	250	140
Hard work (filing, cutting, digging etc.)	More than 300	More than 170

$$Q_i = (\text{No of people} \times \text{heat output rate}) + \text{Rated wattage of lamps} + \text{Appliance load} \dots \dots \dots (5)$$

We have the following data available [3]:

Place: Solan (Himachal Pradesh)

Month: May

Ventilation rate: 2 h^{-1}

Artificial light: 18 Tubelights of 20 W each are continuously used

Occupants: Four persons (normal office work; 8hours occupancy)

Window: (1.8m X 4.8m) on South wall, single glazed

Window: (1.2m X 1.8m) on West wall, single glazed

Door: (0.9m X 3m) on South wall

Door: (0.9m X 3m) on West wall

$U_{\text{glazing}} = 5.8 \text{ W/m}^2\text{K}$ [4]

$U_{\text{wall}} = 3 \text{ W/m}^2\text{K}$

$U_{\text{roof}} = 2.3 \text{ W/m}^2\text{K}$ [3]

Daily average outside temperature in May: $28.2 \text{ }^\circ\text{C}$

Absorptance of external wall surfaces: 0.6

Outside heat transfer coefficient: $22.7 \text{ W/m}^2\text{K}$

Inside design temperature: $22 \text{ }^\circ\text{C}$

Mean absorptivity of the space: 0.6

Transmissivity of window: 0.8

Density of air: 1.2 kg/m^3

Specific heat of air: 1005 J/kgK

Using equations (2), (3), (4) & (5) in equation (1), we get

$$Q_{\text{total}} = Q_c + Q_s + Q_i + Q_v$$

$$\begin{aligned} Q_c &= 3 (16.2-11.3) [(28.3-22)] + 3 \times 19.8 [(26.9-22)] + 3 \times 16.2 [(27.4-22)] + 3 \times \\ &\quad (19.8-4.9) [(27.8-22)] + 2.3 \times 35.6 [(26-22)] + 5.7 \times 4.5 [(33.0-23.3)] \\ &= (3 \times 4.9 \times 6.3) + (3 \times 19.8 \times 4.9) + (3 \times 16.2 \times 5.4) + (3 \times 14.9 \times 5.8) + (2.3 \times 35.6 \times 4) + \\ &\quad (5.7 \times 4.5 \times 9.7) \\ &= 92.6 + 291.1 + 262.4 + 259.3 + 327.5 + 248.8 \\ &= 1481.7 \text{ W} \end{aligned}$$

$$Q_s = 0.6 \times [(11.3 \times 111.3) + (4.9 \times 155.2)] \times 0.8$$

$$\begin{aligned}
 &= 0.6 \times (1257.7 + 760.5) \times 0.8 \\
 &= 0.6 \times 2018.2 \times 0.8 \\
 &= 968.7 \text{ W} \\
 Q_i &= 4 \times 100 + 18 \times 20 \\
 &= 400 + 360 \\
 &= 760 \text{ W} \\
 Q_v &= 1.2 \times 1005 (2 \times 6.7 \times 5.5 \times 3/3600) (28.2 - 22) \\
 &= 1.2 \times 1005 \times 0.02 \times 6.2 \\
 &= 149.5 \text{ W} \\
 \text{Thus, } Q_m &= 1481.7 + 968.7 + 760 + 149.5 \\
 &= 3359.9 \text{ W} \\
 &= 33.6 \text{ kW}
 \end{aligned}$$

It represents that total heat entering the building is 33.6 kW.

The COP of a standard window air conditioner of 1.5 tons cooling capacity is about 2.8 [3]. So the power required is 12 kW (i.e., 33.6 kW/2.8). Suppose the machine was to be used for 8 hours a day; then it would consume 12 kWh per day (12 kW × 8 hours = 96) or 96 units (One kWh is equivalent to one unit) of electricity supplied by the power company [3]. At a rate of Rs. 2 per unit, expenses would amount to Rs. 192/- per day. The carbon component emitted by the use of 96 kWh hydroelectric power is 384 g [5] whereas per day emission of carbon by this ac is 5344 g [6]. Total carbon produced by using 1.5 ton AC is 5728 g = 5.7 kg per day, therefore per annum it will be 1368 kg if the air conditioner works for 20 days per month as an average [7].

II. CONCLUSION

Till the day we can use alternative forms of energy in a wide scale, turning on the air conditioner will always mean that the earth will be affected. The only way to limit the damage is by using high energy efficient air conditioners which require less power to run, and to keep the use of the air conditioners to the minimum level possible. Increasing awareness of environmental issues has led to development of a large number of energy conservation technologies for buildings, especially in more developed countries [6]. Energy savings potential (ESP) is a very important indicator for developing these technologies.

REFERENCES

- [1]. Nayak J.K. and Prajapati J.A., *Handbook on Energy Conscious Buildings*, Prepared under the interactive R & D project no. 3/4(03)/99-SEC between Indian Institute of Technology, Bombay and Solar Energy Centre, Ministry of Non-conventional Energy Sources, Government of India, May, 2006.
- [2]. Mani A. and Rangarajan S., *Solar radiation over India*, Allied Publishers, New Delhi, 1982.
- [3]. Bansal N.K., Hauser G. and Minke G., *Passive building design*, Elsevier Science, New York, 1994.
- [4]. SP: 41 (S&T) - Handbook on functional requirements of buildings, Bureau of Indian Standards, New Delhi, 1987.
- [5]. A tool for companies and office activities: the "Carbon Inventory" of ADEME may 2004.
- [6]. Chikada M., Inoue T., Evaluation of Energy Saving Methods in a Research Institute Building, CCRH. PLEA2001-The 18th Conference on Passive and Low Energy Architecture, Florianopolis-BRAZIL, pp. 883-888, 2001.
- [7]. <http://sciencerey.com/biology/ecology/dangers-facts-the-amount-of-carbon-in-the-household/>

Design and Analysis of an Efficient Primary Synchronization Signal Detector

Mathana.J.M¹, Ashvanth.R², Bhavanam Jagadish³, Ashok Robert.J⁴

Associate Professor, Department of Electronics & Communication Engineering, RMKCET, Chennai, India¹

Department of Electronics & Communication Engineering, RMKCET, Chennai, India²

Department of Electronics & Communication Engineering, RMKCET, Chennai, India³

Department of Electronics & Communication Engineering, RMKCET, Chennai, India⁴

Abstract: In this paper, we present a novel design for the detection of primary synchronization signal in a Long Term Evolution (LTE) system based device at the expense of low cost and low power. This is facilitated by using a matched filter architecture which incorporates parallel processing. The approach of a 1-bit analog-to-digital converter (ADC) with down-sampling is compared with that of a 10-bit ADC without down-sampling under multi-path fading conditions defined in LTE standard for user equipment (UE) performance test. A high performance primary synchronization signal detection method is derived in this paper.

Keywords: Low cost, low power, matched filter, primary synchronization signal (PSS).

I. INTRODUCTION

The LTE, also referred as EUTRA (Evolved UMTS Terrestrial Radio Access), is intended to enhance the 3g and 3.5g systems in order for them to adopt higher peak data rates with extremely high mobility support. The LTE, as one of the latest steps in an advancing series of mobile telecommunications system, can be seen to provide a further evolution of functionality, increased speeds and general improved performance comparing to the third generation systems [1]. The LTE specification provides downlink peak rates of at least 100 Mbps, and uplink of at least 50 Mbps. LTE supports scalable carrier bandwidths, from 1.4 MHz to 20 MHz and supports both frequency division duplexing (FDD) and time division duplexing (TDD). The long term evolution (LTE) is based on orthogonal frequency-division multiple access (OFDMA) in down-link and single-carrier frequency-division multiple access (SC-FDMA) in up-link [2]. It offers favorable features such as high spectral efficiency, robust performance in frequency selective channel conditions, simple receiver architecture and lower latencies.

The main reasons of developing LTE was to sustain packet switched traffic (IP traffic), voice traffic e.g. voice over IP. In addition it permits both frequency-division duplexing (FDD) and time-division duplexing (TDD) communication. Its support for multiple input multiple output (MIMO) technology gives it an advantage in the communication arena [3]. One interesting challenge in the physical layer of LTE is how the mobile unit immediately after powering on, locates a radio cell and locks on to it. This process is called "initial cell search" aimed at frequency and timing synchronization as well as parameters recognition [4]. This process consists of a series of synchronization stages by which the UE determines time and frequency parameters that are necessary to demodulate the downlink and to transmit uplink signals with the correct timing and the UE also acquires some critical system parameters. The synchronization signal is defined as the downlink physical signal which corresponds to a set of resource elements used by the physical layer but does not carry information originating from higher layers. The synchronization procedure makes use of two specially designed physical signals which are broadcast in each cell: the Primary Synchronization Signal (PSS) and the Secondary Synchronization Signal (SSS). The SSS carries the physical layer cell identity group and the PSS carries the physical layer identity. The detection of these two signals not only enables time and frequency synchronization, but also provides the UE with the physical layer identity of the cell and the cyclic prefix length, and informs the UE whether the cell uses Frequency Division Duplex (FDD) or Time Division Duplex (TDD). Synchronization sequence is more important because its detection affects not only search time but also performance of demodulation. The 3GPP working group decided to adopt Zadoff-Chu (ZC) sequences as the downlink primary synchronization signal

(PSS) and the uplink random access preamble. A Zadoff-Chu sequence is a complex-valued mathematical sequence which exhibits the useful property that cyclically shifted versions of it are orthogonal to each other. The ZC sequences have flat frequency domain autocorrelation property and the low frequency offset sensitivity [5]. The primary synchronization signal is detected by using a non coherent detection method since there is no reference information initially. Matched filter is the basic non coherent detection method that can used to detect PSS efficiently. Currently employed matched filters are computation-intensive since they involve a large number of constant complex multiplications.

The main objective of this paper is to propose an efficient matched filter architecture that involves less number of complex multiplications to occur. The system model and PSS definition are presented in Section II. A brief review of the matched filter approach is presented in Section III. Afterwards, both the method of 1-bit ADC with down-sampling and that of 10-bit ADC without down-sampling for PSS detection are discussed in Section IV. Section V addresses different implementation architectures of PSS detection. Whereas their simulation results are shown in Section VI Finally, conclusion remarks are given in Section VII.

II. SYSTEM MODEL AND PROBLEM DEFINITION

1.1. OFDM System Model with Carrier Frequency Offset (CFO)

3GPP adopt OFDM to improve spectrum efficiency. In OFDM systems, a sequence of complex data symbols is considered as orthogonal subcarriers during the k th OFDM blocks, the sequence of data symbols is defined as follows:

$$d(k) = [d_0(k), d_1(k), d_2(k), \dots, d_{N-1}(k)]^T \tag{1}$$

The sequence of data symbols is modulated using an N-point inverse discrete Fourier transform (IDFT) process that produces the sequence

$$x(k) = W d(k) \tag{2}$$

Where W is the normalized-by-N IDFT matrix and x(K) is

$$x(k) = [x_0(k), x_1(k), \dots, x_{N-1}(k)]^T \tag{3}$$

Consequently, the nth sample in the sequence x(k) can be expressed as

$$x_n(k) = \frac{1}{\sqrt{N}} \sum_{i=0}^{N-1} d_i(k) e^{j \frac{2\pi i n k}{N}}, n=0, 1, \dots, N-1 \tag{4}$$

In fading channels, a time-domain guard interval, which is named as cyclic prefix (CP), is created by copying the last samples of the IDFT output and appending them at the beginning of the OFDM symbol to be transmitted. So the transmitted OFDM block consists of (N + Ng) samples [7]. At the receiver side, after removing the first CP samples, the received sequence

$$y(k) = [y_0(k), y_1(k), y_2(k), \dots, y_{N-1}(k)]^T \tag{5}$$

Is obtained [9]

$$y(k) = e^{j \frac{2\pi \epsilon k (N+Ng)}{N}} A(\epsilon) W H(k) d(k) + N(k) \tag{6}$$

where ε represents the normalized CFO, and A(ε) represents the effect of the accumulated phase rotation caused by the CFO on the time domain samples

$$\epsilon \in (-0.5, 0.5) \tag{7}$$

$$A(\epsilon) = \text{diag} \left(\left[e^{j \frac{2\pi \epsilon}{N} x_0}, e^{j \frac{2\pi \epsilon}{N} x_1}, \dots, e^{j \frac{2\pi \epsilon}{N} x_{(N-1)}} \right]^T \right) \tag{8}$$

H(k) denotes the channel frequency response during the kth OFDM block.

$$H(k) = \text{diag}([H_0(k), H_1(k), H_2(k), \dots, H_{N-1}(k)]^T) \tag{9}$$

N(K) represents a zero-mean complex white Gaussian noise sample with variance N_σ . Assuming that the receiver sampling clock is aligned to that of the transmitter, then the nth element of y(K) can be expressed as

$$y_n(k) = \frac{e^{j \frac{2\pi \epsilon k (N+Ng)}{N}}}{\sqrt{N}} \sum_{i=0}^{N-1} d_i(k) H_i(k) e^{j \frac{2\pi \epsilon}{N} (i+\epsilon)} + N_n(k) \tag{10}$$

$$R_{\text{spat}} = R_{\text{cNB}} \otimes R_{\text{UE}} = \begin{bmatrix} 1 & \alpha^{\frac{1}{\nu}} & \alpha^{\frac{2}{\nu}} & \alpha^{\frac{3}{\nu}} \\ \alpha^{\frac{1}{\nu^*}} & 1 & \alpha^{\frac{1}{\nu}} & \alpha^{\frac{2}{\nu}} \\ \alpha^{\frac{2}{\nu^*}} & \alpha^{\frac{1}{\nu^*}} & 1 & \alpha^{\frac{1}{\nu}} \\ \alpha^{\frac{3}{\nu^*}} & \alpha^{\frac{2}{\nu^*}} & \alpha^{\frac{1}{\nu^*}} & 1 \end{bmatrix} \otimes \begin{bmatrix} 1 & \beta^{\frac{1}{\nu}} & \beta^{\frac{2}{\nu}} & \beta^{\frac{3}{\nu}} \\ \beta^{\frac{1}{\nu^*}} & 1 & \beta^{\frac{1}{\nu}} & \beta^{\frac{2}{\nu}} \\ \beta^{\frac{2}{\nu^*}} & \beta^{\frac{1}{\nu^*}} & 1 & \beta^{\frac{1}{\nu}} \\ \beta^{\frac{3}{\nu^*}} & \beta^{\frac{2}{\nu^*}} & \beta^{\frac{1}{\nu^*}} & 1 \end{bmatrix} \tag{11}$$

Where α and β is define in Table VI [5], and ⊗ denotes Kronecker product.

TABLE I DELAY PROFILES FOR E-UTRA CHANNEL MODELS

Model	Number of channel taps	Delay Spread (r.m.s)	Maximum excess tap delay (span)
Extended Pedestrian A (EPA)	7	45ns	410ns
Extended vehicular A (EVA)	9	357ns	2510ns
Extended Typical Urban	9	991ns	5000ns

TABLE II ROOT INDICES FOR THE PSS

NID ⁽²⁾	Root index u
0	25
1	29
2	34

2.2. PSS

The P-SCH is used for obtaining the time and frequency synchronization necessary for demodulating the S-SCH [6]. The UE achieves synchronization by correlating the received P-SCH signal with a replica of the transmitted signal (i.e., using a matched filter), thereby identifying a correlation peak at the proper symbol timing. The Primary Synchronization Signals are modulated using one of three different frequency domain Zadoff-Chu sequences. The sequence $d_u(n)$ used for the PSS is generated from a frequency-domain ZC sequence [1] according to

$$d_u = \begin{cases} e^{-j \frac{\pi u n(n+1)}{63}} & , n = 0, 1, \dots, 30 \\ e^{-j \frac{\pi u(n+1)(n+2)}{63}} & , n = 31, 32, \dots, 61 \end{cases} \quad (12)$$

Where the ZC root sequence index is given by Table II

The three different ZC sequences are orthogonal to each other, and each sequence corresponds to a sector identity which is in the range of 0 to 2. The Primary Synchronization signal first determines one of three cell identities (0, 1, 2), also represented by N (2) ID. Then the secondary synchronization signal is used to determine a cell ID between 0 and 167 represented by N (1) ID. A Zadoff-Chu sequence is a complex-valued mathematical sequence which exhibits the useful property that cyclically shifted versions of it are orthogonal to each other. Thus, it is easy to detect PSS during the initial synchronization because the ZC sequence has the flat frequency domain autocorrelation property and the low frequency offset sensitivity.

III. FUNDAMENTAL DETECTION OF PSS

The main function of PSS is to detect the boundary of a frame where non-coherent detection method has to be used at the receiver since there is no known reference information initially [7]. Matched filter is a basic non-coherent detection method that can be used to detect PSS efficiently. The sequence in (12) is mapped to the subcarriers around DC and transformed to time domain by 64-point IDFT. To detect this signal at the receiver, the correlation with the time domain signal of the ZC sequence is calculated [2]–[4]

$$C_u(m) = (W^H d_u)^H y \quad (13)$$

Where y is the successive 64-by-1 received signal vector, W is the DFT matrix, and d_u is 64-by-1 vector composed of punctured at DC.

Then, from (13), the coefficients of the matched filter can be obtained

$$C_{coeff} = (W^H d_u)^H \quad (14)$$

Where

$$C_{coeff} = [C_{coeff}(63) C_{coeff}(62) \dots C_{coeff}(1) C_{coeff}(0)] \quad (15)$$

and the matched filter can be expressed

$$MF = \sum_{k=0}^{63} C_{coeff}(k) y(t - k) \quad (16)$$

Where $y(k)$ is the received signal.

IV. PROPOSED DESIGN OF PSS

The receiver side of an OFDM system model ADC is present for digital representation of the received signal. 10-bit ADC is generally preferred to be used at the receiver. From the power consumption perspective, a 10-bit analog-to digital converter (ADC) uses more power than 1-bit ADC. Typically, the power consumption of a 1-bit 122.88 MHz ADC composed of one comparator is about 200 W, while the power consumption of a 10-bit 122.88 MHz pipelined ADC is about 50mW.

To come up with a low-power solution, a method of PSS detection using 1-bit ADC is proposed. PSS is transmitted periodically, twice per frame which lasts 10 ms [8]. The sampling rate of the receiver is 122.88 MHz; however, the data rate of input data to the matched filter is 1.92 MHz. Thus, 9600 samples at the output of the matched filter need to be buffered during the 5 ms period, which is not area and cost efficient. To come up with a low cost solution, a method of down-sampling by 8 is used at the output of matched filter.

4.1 Method without Down-Sampling by 8 for 10-Bit ADC

From the last section, the matched filter as expressed in (16) can be reformulated when using a 10-bit, 122.88 MHz pipelined ADC

$$MF_{qt} = \sum_{k=0}^{63} \text{coeff}(k) y_{qt}(t - k) \tag{17}$$

where $y_{qt}(k)$ is the received signal sampled by a 10-bit, 122.88 MHz pipelined ADC, and is obtained in (14) and (15). Every output of the matched filter is buffered since there is no down-sampling module, and it needs a large area buffer which is very costly.

TABLE III SIMULATION ASSUMPTIONS

PARAMETER	UNIT
Number of Rx Antenna	4
Number of Tx Antenna	4
Frequency offset	12.5 KHz
Carrier Frequency	2.5Ghz
Symbol detection	Replica-based
Root index	29

4.2 Method With Down-Sampling by 8 for 1-Bit ADC

Equation (16) can be reformulated when using a 1-bit, 122.88 MHz ADC

$$MF_{qo} = \sum_{k=0}^{63} \text{coeff}(k) y_{qo}(t - k) \tag{18}$$

Where $y_{qo}(k)$ is the received signal sampled by a 1-bit, 122.88MHz ADC, and is obtained in (14) and (15). Every output of the matched filter is down-sampled by 8

$$MF_{qod} = \max \begin{cases} MF_{qo}(8n), MF_{qo}(8n + 1), \\ MF_{qo}(8n + 2), MF_{qo}(8n + 3), \\ MF_{qo}(8n + 4), MF_{qo}(8n + 5), \\ MF_{qo}(8n + 6), MF_{qo}(8n + 7) \end{cases} \tag{19}$$

where MF_{qod} is the output of the down-sampling module. Now, only 1200 outputs need to be buffered during 5 ms with an additional comparator of 1 out of 8 implementing the down sampling module. This results in less area which translates to lower cost in a practical system. Its implementation architecture is discussed in next chapter [12].

V. HARDWARE IMPLEMENTATION

The implementation architecture of the proposed method is presented here along with the new matched filter architecture that reduces the complexity involved in existing methodology. The matched filter is an important component in the PSS detection. We use 64-tap time domain matched filter; hence 64 complex multiplication units per matched filter are used in the calculation in [16].

3.1. Existing Architecture of Matched Filter

In this architecture input data that is being received is processed serially. As per our simulation assumptions, 84 matched filters are required in the system. So a total of 5376 units of complex multiplication is needed. Instead we can use only one complex multiplication unit during 64 cycles instead of using 64 units of complex multiplication. As a result, 84 units of complex multiplication are enough for the whole system. But

the problem that it encounters is that since the data is processed serially, so significant amount of delay is encountered due to the shifting involved in it. This problem is overcome in our proposed method [19].

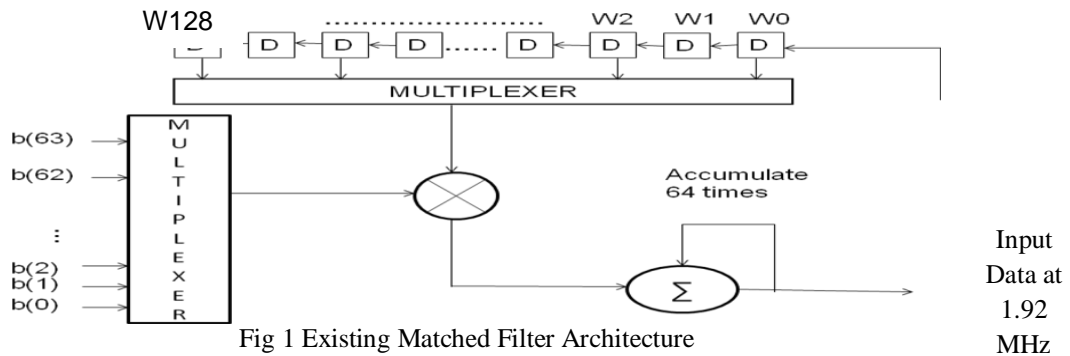


Fig 1 Existing Matched Filter Architecture

3.2. Proposed Architecture Matched Filter

In order to overcome the shortcomings of existing matched filter architecture, a matched filter architecture that incorporates parallel processing is proposed. The proposed architecture is shown in fig 3. Here the input data which is fed at 1.92MHz is processed parallelly. So, there is no shifting of input data during each input clock. As a result of it, the effect of propagation delay is overcome.

3.3. Architecture of PSS Detection

A mismatch of up to 14 part per million (ppm) can exist between the oscillators at the eNodeB and at the UE, so seven groups of matched filters are used to cover the range of 14 ppm, 14 ppm. Each group contains three matched filters to detect three different physical-layer IDs of value 0, 1, or 2 [21]. Therefore, there are 21 hardware units as shown in Fig. 2 for each receiver antenna. Since the system is MIMO 4-by-4 and there are 4 receiver antennas at the UE end, 84 such hardware units are involved in the architecture of the PSS detection. A total of 9600 samples during 5 ms and thus a single port RAM with 9600 addresses is needed.

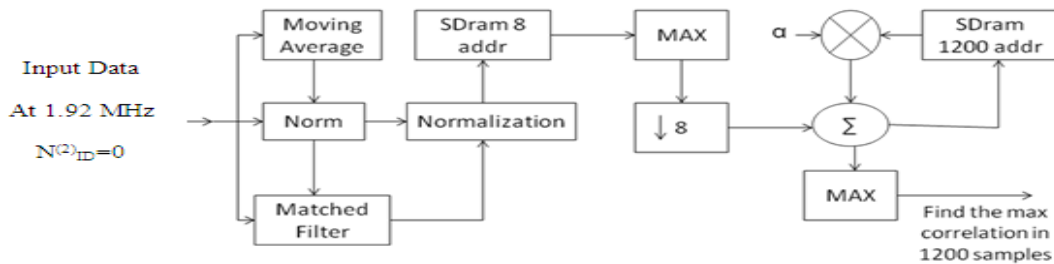


Fig 2 Architecture of PSS Detection

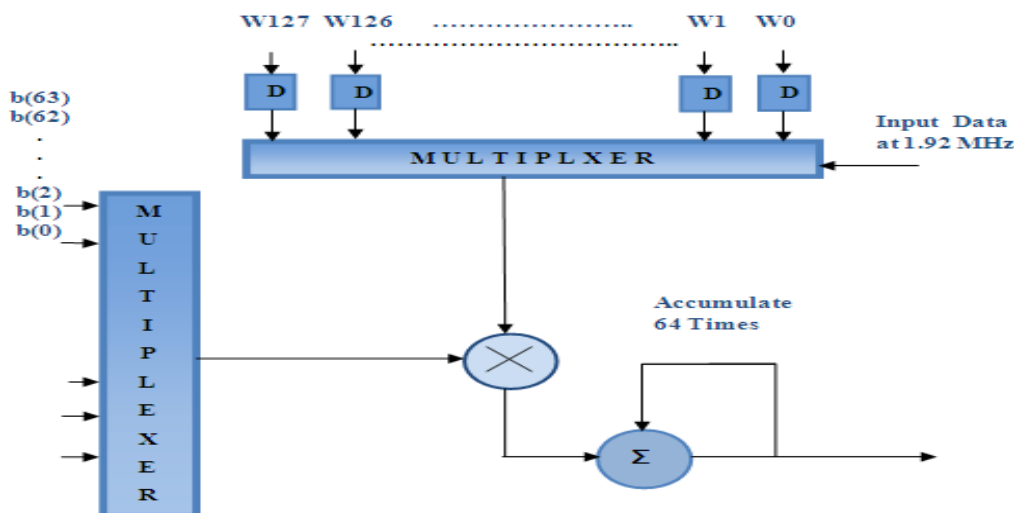


Fig 3 Proposed Matched Filter Architecture

As described above, there are 84 such RAMs in the system, and the area is too large for the UE chip; therefore an area efficient architecture is proposed as shown in Fig. 2. Compared to the architecture in Fig. 1, a small RAM with 8 addresses is added whose function is to find the maximum value of every eight correlations. As a result, only 1200 correlation values need to be stored in RAM with 1200 addresses, which reduce the RAM size of the whole system by a factor of almost 8 [22]. We can observe that the area of the area-efficient architecture is much smaller

than that of the original architecture, which reduces the Cost of the chip significantly. From the power perspective, not only the 1-bit ADC reduces the power consumption, but the hardware of digital logic also does.

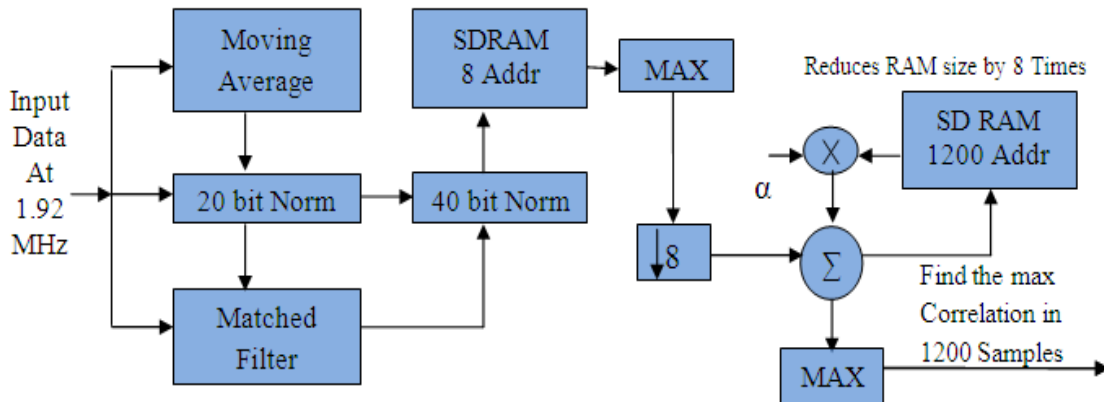


Fig 4 Original architecture of the whole PSS detection

VI. SIMULATION RESULTS

Primary synchronous signal is designed for cell search and handover in 3GPP LTE systems, which is transmitted every 5ms. Search time of PSS detection is an important criterion when measuring its performance. To compare the performance using a 10-bit 122.88MHz ADC without down-sampling and that using a 1-bit 122.88MHz ADC with down-sampling by 8, the parameters listed in Table III are used in the simulation [23].

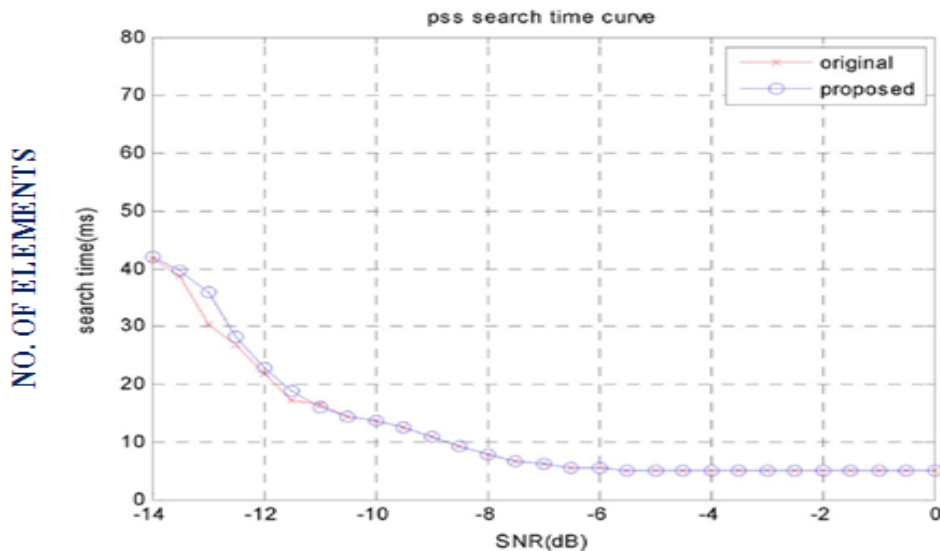


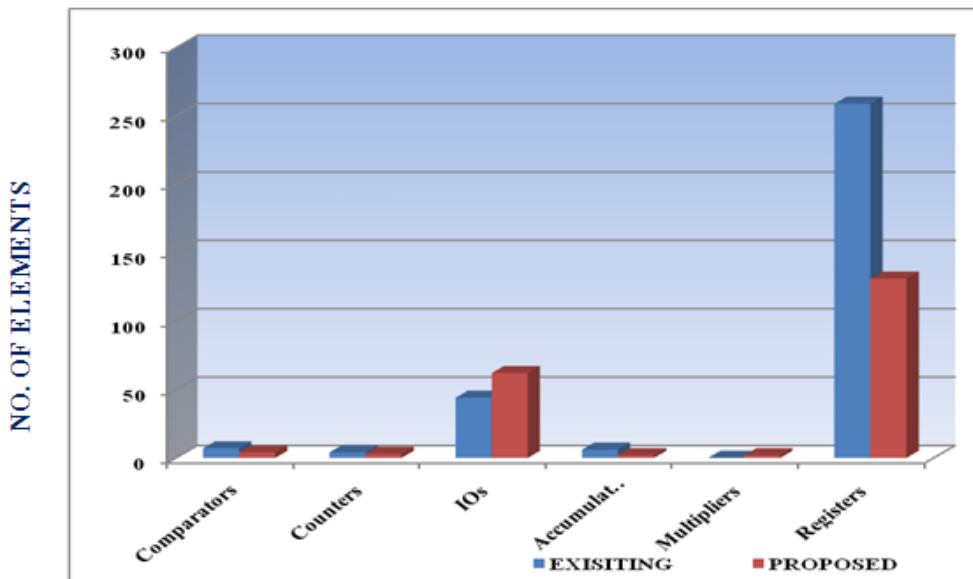
Fig 5 Performance of both methods using low correlation channel matrix and EPA 5 Hz channel model.

The simulation results for search time of both the methods under EPA 5 Hz channel model are shown. It is clear that the search time of both methods under EPA 5 Hz model with low correlation channel matrix, is very close to each other. The Existing and the proposed model is simulated using altera quartus software. The power and gate analysis are carried out for both the methods. The simulation results show that the performance of our proposed matched filter architecture which incorporates parallel processing is efficient in terms of power [24]. Furthermore, the implementation of our proposed architecture with the method of 1-bit adc with down sampling by a factor of 8 results in the reduction of overall gates required for it to be implemented in the user equipment. This is shown in table V.

TABLE IV HDL SYNTHESIS OF MATCHED FILTER ARCHITECTURE

LOGIC UNITS	EXISTING	PROPOSED
Comparators	7	4
Counters	4	3
Flip – flops	1472	1338
IOs	44	62
Accumulators	6	2
Multipliers	-	2
Registers	259	131

RESOURCE UTILIZED BY MATCHED FILTER



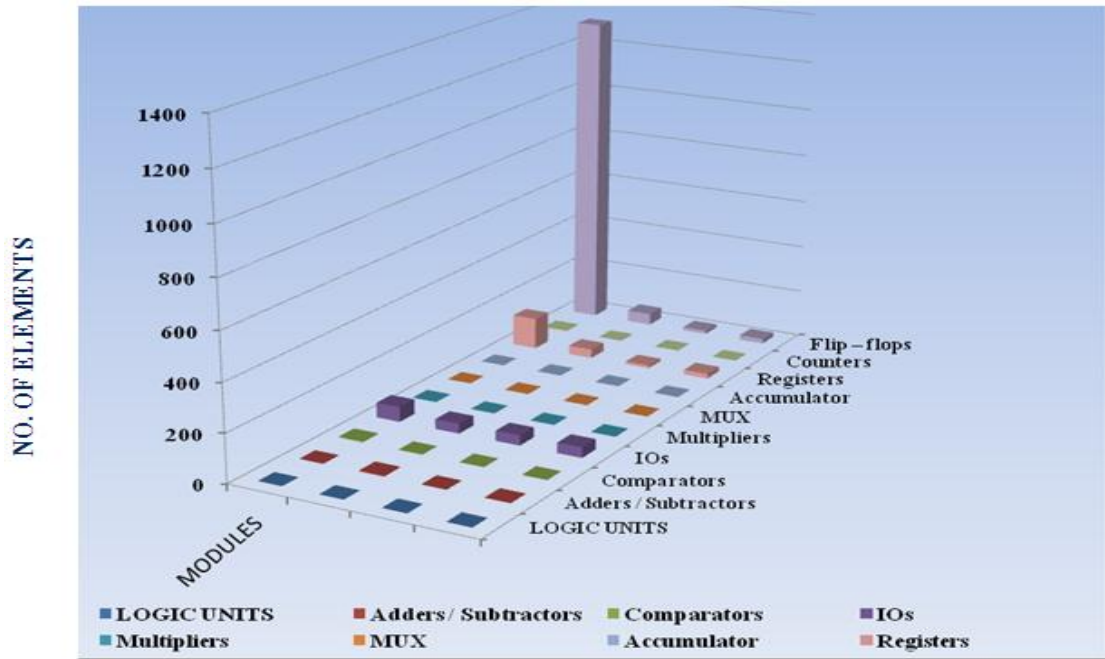
LOGIC UNITS

Fig 6 Resource utilized by Existing and Proposed matched filter

TABLE V RESOURCE UTILIZATION OF VARIOUS MODULES

LOGIC UNITS	MODULES			
	Matched Filter	Moving Average	40 Bit Norm	20 Bit Norm
Adders / Subtractors	-	5	1	2
Comparators	4	-	-	-
IOs	62	41	42	43
Multipliers	2	-	-	-
MUX	-	1	-	-
Accumulator	-	2	-	-
Registers	131	37	11	20
Counters	3	1	1	-
Flip – flops	1338	48	14	20

RESOURCE UTILIZED BY VARIOUS MODULES

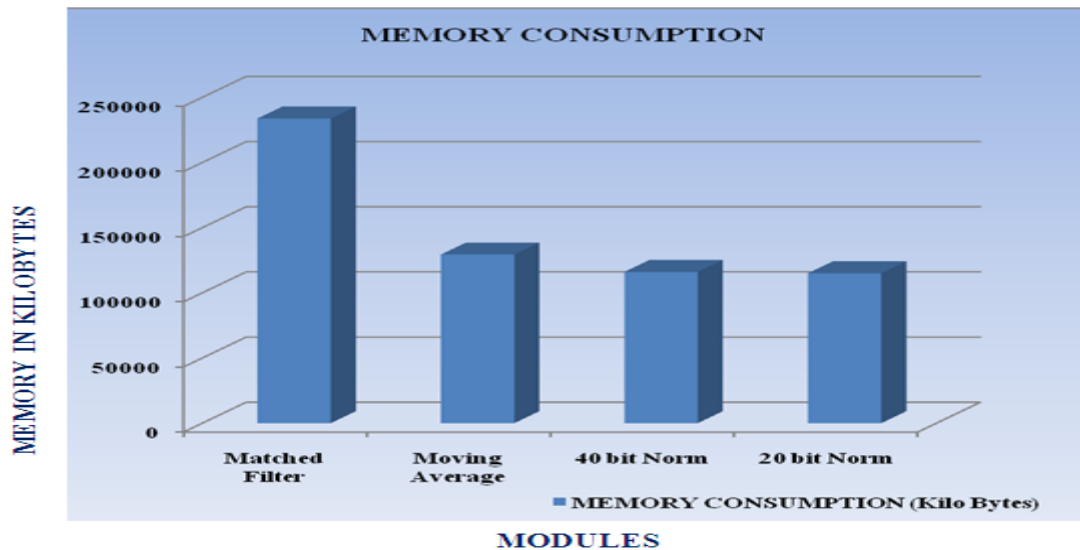


MODULES

Figure 7 Resource Utilization of Various Modules

TABLE VI MEMORY CONSUMED BY VARIOUS MODULES

MODULES	MEMORY CONSUMPTION (Kilo Bytes)
Matched Filter	233784
Moving Average	129400
40 bit Norm	116088
20 bit Norm	115064



MODULES

Fig 8 Memory Consumed By Various Modules

TABLE VII COMPARISON OF PROPOSED 1 BIT AND 10 BIT ADC

LOGIC UNITS	TEN BIT	ONE BIT
Adders / Subtractors	25	34
Comparators	3	3
Counters	16	16
Flip – flops	5115	1659
IOs	142	124
Multipliers	6	-
MUX	7	7
Accumulator	2	2
Registers	543	543
IO buffer	142	124
Memory in Kilo Bytes	447928	339896

TABLE VIII SIMULATION RESULTS FOR POWER

POWER	PROPOSED		EXISTING	
	One bit	Ten bit	One bit	Ten bit
Thermal Power	68.02mw	224.39mw	159.77mw	1009.47mw
Core Dynamic Power	1.94mw	16.48 mw	91.44mw	559.56mw
Core Static Thermal Power	46.36mw	46.88mw	46.45mw	48.10mw

VII. PERFORMANCE WITH EXISTING STATE-OF-THE-ART MATCHED FILTER ARCHITECTURE

The matched filter architecture, in the design [4] uses 84 matched filters and 5376 units of complex multiplication making the practical implementation difficult. The matched filter architecture in the design [22] requires only 84 units of complex multiplication and this is practically possible. But the cost for implementation is high. In the design [40], the matched filter architecture uses a serial mechanism and consumes more logic elements.

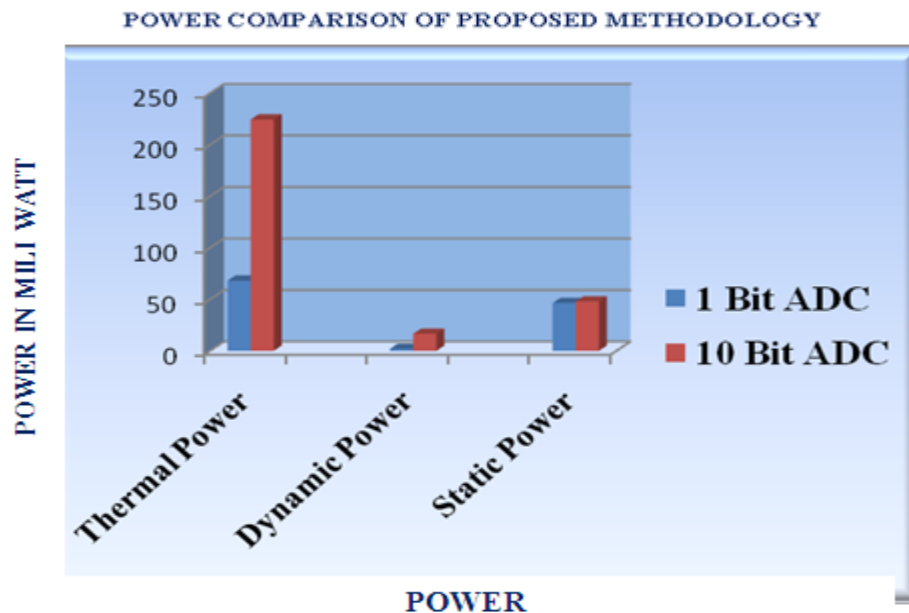


Fig 9 Power Comparison of Proposed Methodology

The proposed architecture is power and area efficient. In the proposed matched filter architecture, a parallel mechanism is used for inputting the data and the logic elements utilized is also significantly reduced. One bit ADC with down sampling by factor 8 consumes 339896 Kilo Byte and the power utilized is less when compared to design [40]. Ten bit ADC without down sampling, consumes 46.88Mili Watt as static power and 16.48Mili Watt as dynamic power. The logic elements utilized is also significantly reduced when compared to the existing state of architecture. The problem with the existing architecture is, since the data is processed serially a significant amount of delay is encountered due to the shifting involved in it. This occurs when one value is high and subsequent values are low, no matter what the shift is, the output of the MUX will be the same. This causes unnecessary multiplication to occur and also the delay that is involved affects the overall performance of the system. This problem is overcome in our proposed architecture which incorporates parallel processing. So, there is no shifting of input data during each input clock. As a result of it, the effect of propagation delay is overcome and the table 4.6 shows the comparison with the existing state architecture.

TABLE IX COMPARISON WITH PREVIOUS WORK

WORK	MEMORY (KILO BYTES)	STATIC POWER (MILI WATT)	DYNAMIC POWER (MILI WATT)	LOGIC ELEMENTS
Design [4]	-	-	-	84 Matched Filters (5376 Units Of Complex Multiplications)
Design[11]	-	-	-	84 Units Of Complex Multiplications
Design [9]				
Matched Filter	247224	-	-	2524
1 Bit ADC With Down Sampling	704696	46.45	91.44	2844
10 Bit ADC Without Down Sampling	454072	48.45	559.56	5660
Proposed Architecture				
Matched Filter	233784	-	-	1733
1 Bit ADC With Down Sampling	339896	46.36	1.94	2244
10 Bit ADC Without Down Sampling	447928	46.88	16.48	4877

VIII. CONCLUSION

The detection of PSS plays a primary role in mobile communication. Theoretically, detection with 1-bit ADC and with down-sampling would degrade the performance and prolong the detection time. However, due to the inherent advantage of the ZC sequence, simulation results show that the performance of the proposed method using a 1-bit ADC with down-sampling by 8 does not degrade much compared with that using a 10-bit ADC without down-sampling in the presence of frequency offset under several typical LTE propagation channels. Subsequently, two different implementation architectures of the PSS detection are presented. The area and the power consumption of the original implementation architecture are too large. Based on the simulation results in the proposed architecture, the PSS can be detected efficiently and accurately at a much lower power and lower cost which renders it feasible in the implementation of a UE chip.

IX. FUTURE WORK

As first phase of the project, primary synchronization signal (PSS) is simulated using Model Sim. In the future phase of the project, FPGA implementation is proposed to be carried and investigation of real-time performance metrics will also be carried out. Further, detection of Secondary synchronization signal (SSS) will also be done. In case of significant deterioration in the performance, hardware solutions will be investigated.

REFERENCES

- [1]. B. M. Popovic and F. Berggren, "Primary synchronization signal in E-UTRA," in Proc. IEEE 10th Int. Symposium. Spread Spectrum Technology. Applied (ISSSTA), 2008, pp. 426–430.
- [2]. 3rd Generation Partnership Project (3GPP), Sophia-Antipolis Codex, France, 3GPP TS 36.211 v8.9.0 3rd Generation Partnership Project; Dec. 2009, 3GPP.
- [3]. K. Melonakos, D. M. Gutierrez Estevez, V. Jungnickel, X. Wen, and C. Drewes, "A closed concept for synchronization and cell search in 3GPP LTE systems," in Processing. IEEE Wireless Communication Network Conference., 2009, pp. 1–6.
- [4]. S. Sepia, I. Tewfik, and M. Baker, LTE-The UMTS Long Term Evolution: From Theory to Practice. New York: Wiley, 2009.
- [5]. H.-G. Park, I.-K. Kim, and Y.-S. Kim, "Efficient coherent neighbor cell search for synchronous 3GPP LTE system," Electron. Letter, volume.44, no.21, Oct. 2008.
- [6]. Chixiang Ma, Hao Cao and Ping Lin 'A Low-Power Low-Cost Design Of Primary Synchronization Signal Detection'. IEEE Transactions On Very Large Scale Integration Systems, Vol. 20, No. 7, July 2012
- [7]. K. Melonakos, D. M. Gutierrez Estevez, V. Jungnickel, X. Wen, and C. Drewes, "A closed concept for synchronization and cell search in 3GPP LTE systems," in Proc. IEEE Wireless. Communication. Network. Conference, 2009, pp. 1–6.
- [8]. F. J. Harris, "Orthogonal frequency division multiplexing, OFDM," presented at Department of Electrical Engineering, San Diego State University, San Diego, CA, 2008.
- [9]. 3GPP TS 36.101 v8.9.0 3rd Generation Partnership Project; Technical Specification Group Radio Access Network; Evolved Universal Terrestrial Radio Access (E-UTRA); User Equipment (UE) Radio Transmission and Reception (Release 8), 3rd Generation Partnership Project, Technology Representation December 2009, 3GPP. 3GPP. (n.d.). 3GPP TR 25.913 - v7.3.0, Requirements for EUTRA and EUTRAN [Online].
- [10]. Available: <http://www.3gpp.org/ftp/Specs/archive/25%5Fseries/25.913/> European Telecommunications Standards Institute, 3GPP TS 36.211 version 9.1.0 Release 9, Sophia Antipolis, France: ETSI, 2010.
- [11]. G. Colavolpe and R. Raheli, "Noncoherent sequence detection," IEEE Transaction Communication, vol. 47, no. 9, pp. 1376–1385, Sep. 1999.
- [12]. R. Van Nee, and R. Prasad, OFDM for Wireless Multimedia Communications. Norwood, MA: Artech House Publishers, 2000.
- [13]. Y. Yao and G. B. Giannakos, "Blind carrier frequency offset estimation in SISO, MIMO and multiuser OFDM systems," IEEE Transaction Communication, vol. 53, no. 1, pp. 173–183, Jan. 2005.
- [14]. H.G. Myung, J. Lim, and D. J. Goodman, "Single Carrier FDMA for Uplink Wireless Transmission," IEEE Vehicular Technology Society. volume. 1, no. 3, pp. 30-38, Sept. 2006.
- [15]. Mobile Cell Search And Synchronization In LTE -A Thesis Presented to the Faculty of San Diego State University by Nalini Paravastu Samavedam.
- [16]. H.-G. Park, I.-K. Kim, and Y.-S. Kim, "Efficient coherent neighbor cell search for synchronous 3GPP LTE system," Electron. Letter, volume.44, no.21, Oct. 2008.
- [17]. J.-I. Kim, J.-S. Han, H.-J. Roh, and H.-J. Choi, "PSS detection method for initial cell search in 3GPP LTE FDD/TDD dual mode receiver," presented at the 9th International Symposium on Communications and Information Technology, Incheon, Korea, Sept. 2009.
- [18]. B. M. Popovic and F. Berggren, "Primary synchronization signal in E-UTRA," in Processing. IEEE 10th International. Symposium Spread Spectrum Technology. Application (ISSSTA), 2008, pp. 426–430.
- [19]. 3GPP Technical Specification 32.422, "Telecommunication management; Subscriber and equipment trace; Trace control and configuration management (Release 10), www.3gpp.org.

Data Warehousing Concept Using ETL Process for SCD Type-2

K.Srikanth¹, N.V.E.S.Murthy², J.Anitha³

¹(Computer Science and Systems Engineering, Andhra University, India)

²(Computer Science and Systems Engineering, Andhra University, India)

³(Computer Science and Systems Engineering, Andhra University, India)

Abstract: SCD type 2 will store the entire history in the dimension table. In SCD type 2 effective date, the dimension table will have Start_Date and End_Date as the fields. If the End_Date is Null, then it indicates the current row. Know more about SCDs at Slowly Changing Dimensions Concepts. The new incoming record (changed/modified data set) replaces the existing old record in target. We will see how to implement the SCD Type 2 Effective Date in informatica. If there are retrospective changes made to the contents of the dimension, or if new attributes are added to the dimension which have different effective dates from those already defined, then this can result in the existing transactions needing to be updated to reflect the new situation. As an example consider the Employee dimension.

Keywords: ETL; Metadata; Mapping; Transformation.

I. INTRODUCTION

The beauty of this approach is it will maintain two versions, you will find two records the older version and the current version. In other words it maintains history. The thing to be noticed here is if there is any update in the salary of any employee then the history of that employee is displayed with the current date as the start date and the previous date as the end date. As in case of any SCD Type 2 implementation[1], here we need to first find out the set of SCD2 records which qualify for either INSERT or INSERT/UPDATE. Based on this approach, a typical mapping will contain expression, router and update strategy transformations but will not contain any lookup transformation.

Again we can implement Type 2 in following methods

1. Versioning
2. Effective Dates
3. By setting Current Flag values/Record Indicators.
4. We will divide the steps to implement the SCD type 2 Effective Date mapping into four parts.

II. SCD TYPE 2 EFFECTIVE DATE IMPLEMENTATION

Here we will see the basic set up and mapping flow require for SCD type 2 Effective Date. The steps involved are

Implementation:

Source:

```
SQL> SELECT * FROM EMP;
```

EMPNO	ENAME	JOB	MGR	HIREDATE	SAL	COMM	DEPTNO
7369	SMITH	CLERK	7902	17-DEC-80	2300		20
7499	ALLEN	SALESMAN	7698	20-FEB-81	1600	300	30
7521	WARD	SALESMAN	7698	22-FEB-81	1250	500	30
7566	JONES	MANAGER	7839	02-APR-81	2975		20
7654	MARTIN	SALESMAN	7698	28-SEP-81	1250	1400	30
7698	BLAKE	MANAGER	7839	01-MAY-81	2850		30
7782	CLARK	MANAGER	7839	09-JUN-81	2450		10
7788	SCOTT	ANALYST	7566	19-APR-87	3000		20
7839	KING	PRESIDENT		17-NOV-81	5200		10
7844	TURNER	SALESMAN	7698	08-SEP-81	1500	0	30
7876	ADAMS	CLERK	7788	23-MAY-87	1100		20
7900	JAMES	CLERK	7698	03-DEC-81	950		30
7902	FORD	ANALYST	7566	03-DEC-81	3000		20
7934	MILLER	CLERK	7782	23-JAN-82	1300		10

14 rows selected.

Table 1: Oracle SQL Query On EMP Table

- Create the source and dimension tables in the database using Table 1.
- Open the mapping designer tool, source analyzer and either create or import the source definition.
- Go to the Warehouse designer or Target designer and import the target definition[2].
- Go to the mapping designer tab and create new mapping.
- Drag the source into the mapping[7].
- Go to the toolbar, Transformation and then Create.
- Select the lookup Transformation, Figure 1. enter a name and click on create. You will get a window as shown in the below image.

Figure 1: Creating Lookup Transformation ports logic

- Edit the lookup transformation, go to the ports tab and remove unnecessary ports. Just keep only Empkey, EMPNO and location ports in the lookup transformation. Create a new port (new_flag, update_flag) in the lookup transformation[3]. This new port needs to be connected to the output port of the Expression transformation.
- Go to the conditions tab of the lookup transformation and enter the condition as EMPNO= EMPNO1.
- Go to the properties tab of the LKP transformation and enter the below query in Lookup SQL Override[1]. Alternatively you can generate the SQL query by connecting the database in the Lookup SQL Override expression editor and then add the WHERE clause.

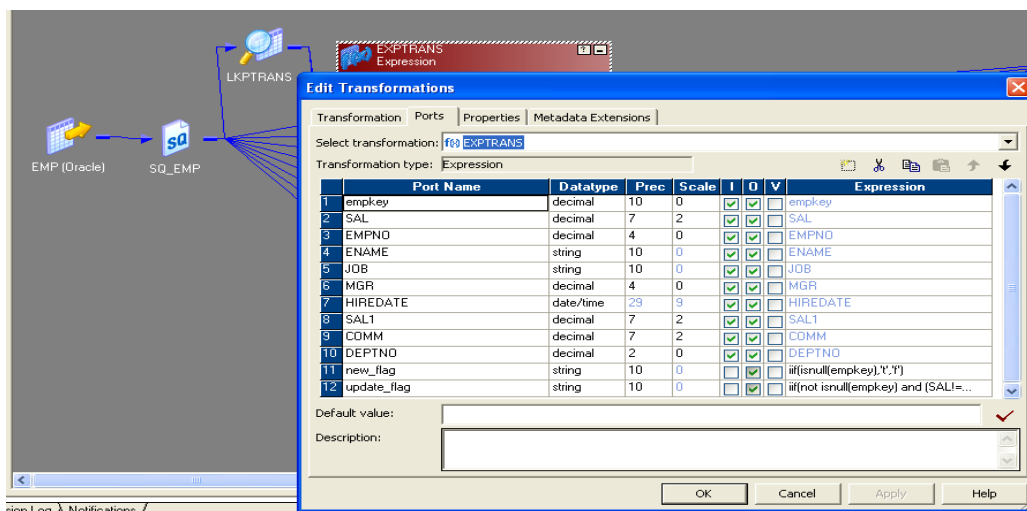


Figure 2: Creating Expression Transformation ports logic

You can add ports to expression transformation either by selecting and dragging ports from other transformations or by opening the expression transformation and create ports manually[4], Figure 2. We can add the port new_flag and update_flag using string datatype. In expression transformation implement the employee key either true or false.

1. IIF(ISNULL(EMPKEY),'T','F');
2. IIF(NOT ISNULL(EMPKEY) AND (SAL!=SAL1),'T','F');

II. SCD TYPE 2 EFFECTIVE DATE IMPLEMENTATION

In this part, we will identify the new records and insert them into the target with Begin Date as the current date. The steps involved are:

- Go the properties tab of filter transformation and enter the filter condition as New_Flag=T and Update_Flag=T[5].
- Edit Router Transformation select groups port writing the Group Filter Condition in the inset and update flags, Figure 3.

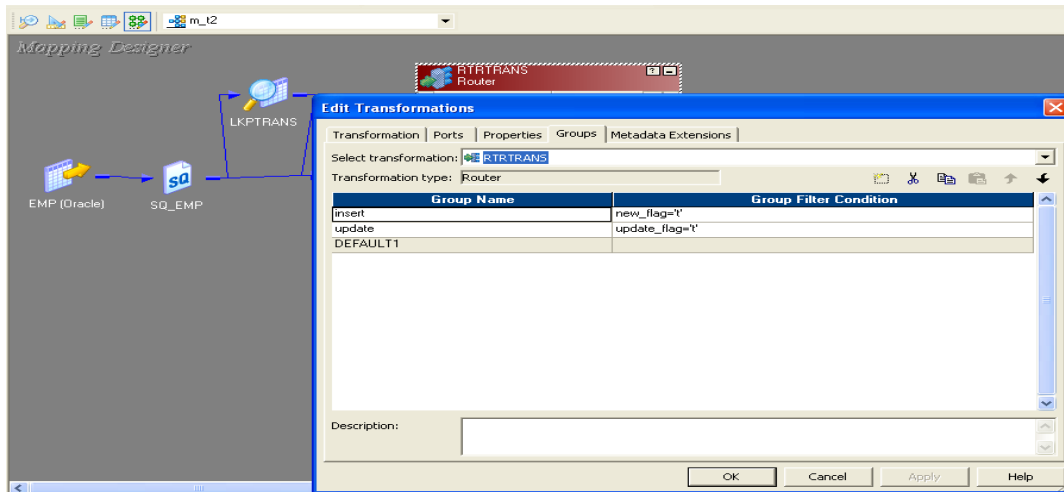


Figure 3: Creating Router Transformation Groups logic
 Insert : New_Flag='T' Update: Update_Flag='T'

III. SCD TYPE 2 EFFECTIVE DATE IMPLEMENTATION

In this part, we will identify the changed records and insert them into the target with Begin Date as the current date. Figure 4, The steps involved are:

- Now connect the ports of expression transformation (Nextval, Start_Date) to the Target definition ports (Emp_Key, End_Date)[6]. The part of the mapping flow is shown in the below image.
- Now drag the target definition into the mapping and connect the appropriate ports of update strategy transformation to the target definition.
- Drag and connect the NextVal port of sequence generator to the Expression transformation. In the expression transformation create a new output port (Start_Date and End_Date) and assign value SYSDATE to it.

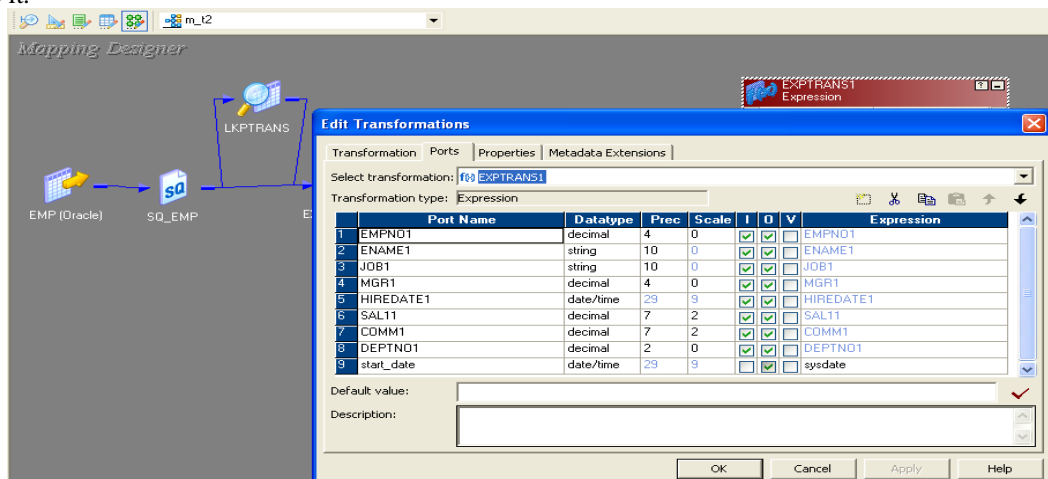


Figure 4: Creating Expression Transformation ports logic
 Start_date: Sysdate

IV. SCD TYPE 2 EFFECTIVE DATE IMPLEMENTATION

In this part, we will update the changed records in the dimension table with End Date as current date.

- Go to the ports tab of expression transformation and create a new output port (Start_Date and End_Date with date/time data type). Assign a value SYSDATE to this port[5].
- Now create an update strategy transformation and drag the ports of the expression transformation into it. Go to the properties tab and enter the update strategy expression as DD_UPDATE.
- Drag the target definition into the mapping and connect the appropriate ports of update strategy to it. Figure 5, The complete mapping image is shown below.

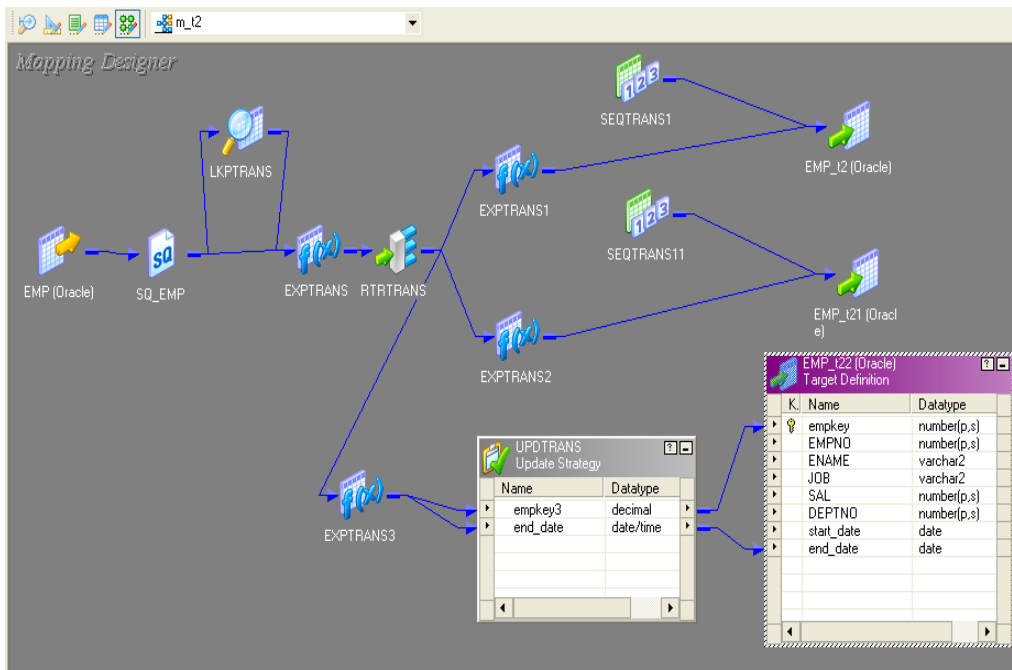


Figure 5: Update Strategy Transformation using End-Date
End_Date: Sysdate

The complete Slowly Changing Dimension Mapping Design flow, Figure 6. This flow will provide completion information of SCD-Type-2 source data how to load target, maintain the data processing.

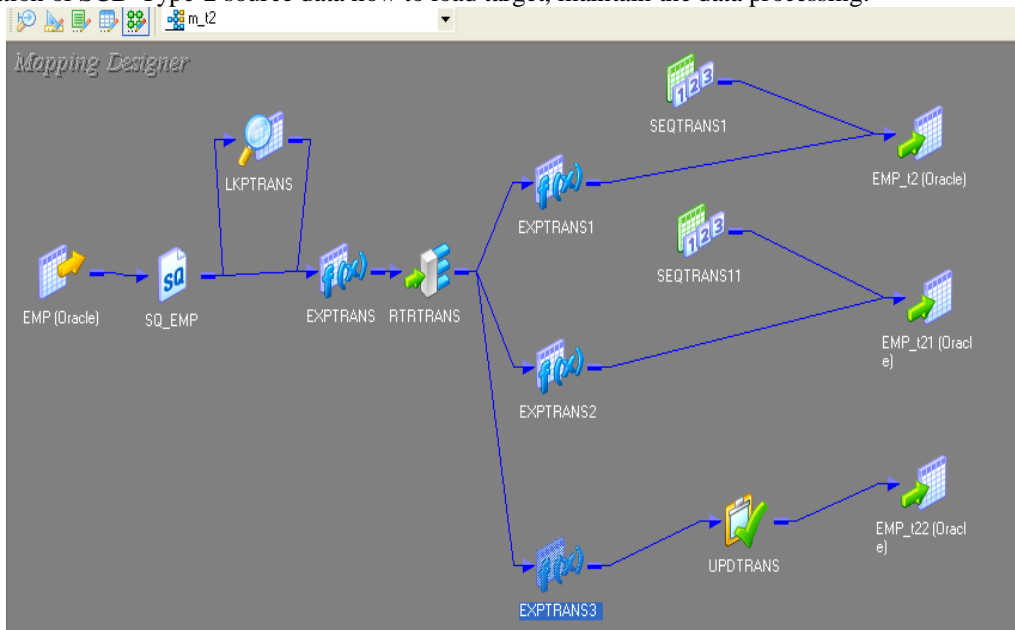


Figure 6: Slowly Changing Dimensions (SCDs) Flow

V. RESULTS

```
SQL> select * from emp_t2;
```

EMPKEY	EMPNO	ENAME	JOB	SAL	DEPTNO	START_DAT	END_DATE
1	7369	SMITH	CLERK	2300	20	02-FEB-12	
2	7499	ALLEN	SALESMAN	1600	30	02-FEB-12	
3	7521	WARD	SALESMAN	1250	30	02-FEB-12	
4	7566	JONES	MANAGER	2975	20	02-FEB-12	
5	7654	MARTIN	SALESMAN	1250	30	02-FEB-12	
6	7698	BLAKE	MANAGER	2850	30	02-FEB-12	
7	7782	CLARK	MANAGER	2450	10	02-FEB-12	
8	7788	SCOTT	ANALYST	3000	20	02-FEB-12	
9	7839	KING	PRESIDENT	5200	10	02-FEB-12	
10	7844	TURNER	SALESMAN	1500	30	02-FEB-12	
11	7876	ADAMS	CLERK	1100	20	02-FEB-12	
12	7900	JAMES	CLERK	950	30	02-FEB-12	
13	7902	FORD	ANALYST	3000	20	02-FEB-12	
14	7934	MILLER	CLERK	1300	10	02-FEB-12	
15	1111	SRIKANTH	PHD	9000	40	02-FEB-12	

15 rows selected.

Table 2: Oracle SQL Query On EMP Table Target Data

```
SQL> insert into emp values(2345,'dileep','dfd',2346,'23-feb-1986',467,455,40);
1 row created.
```

Once load the target data after write oracle queries in insert data and update the values Using connect the employee table. Table 2, Table 3. Below oracle table insert, update display the new type 2 complete updated data.

```
SQL> select * from emp_t2;
```

EMPKEY	EMPNO	ENAME	JOB	SAL	DEPTNO	START_DAT	END_DATE
207	7369	SMITH	CLERK	2300	20	02-FEB-12	
208	7499	ALLEN	SALESMAN	1600	30	02-FEB-12	
209	7521	WARD	SALESMAN	1250	30	02-FEB-12	
210	7566	JONES	MANAGER	2975	20	02-FEB-12	
211	7654	MARTIN	SALESMAN	1250	30	02-FEB-12	
212	7698	BLAKE	MANAGER	2850	30	02-FEB-12	
213	7782	CLARK	MANAGER	2450	10	02-FEB-12	
214	7788	SCOTT	ANALYST	3000	20	02-FEB-12	
215	7839	KING	PRESIDENT	5200	10	02-FEB-12	
216	7844	TURNER	SALESMAN	1500	30	02-FEB-12	
217	7876	ADAMS	CLERK	1100	20	02-FEB-12	
218	7900	JAMES	CLERK	950	30	02-FEB-12	
219	7902	FORD	ANALYST	3000	20	02-FEB-12	
220	7934	MILLER	CLERK	1300	10	02-FEB-12	
221	1111	SRIKANTH	PHD	2000	40	02-FEB-12	
222	2345	dileep	dfd	1200	40	02-FEB-12	02-FEB-12
223	2345	dileep	dfd	1000	40	02-FEB-12	

17 rows selected.

Table 3: Oracle SQL Query On EMP Table Updated Target Data

Source Data: Table 1
 Target Data : Table 2
 Updated Target Data: Table 3

VI. CONCLUSIONS

Extraction-Transformation-Loading (ETL) tools are pieces of software responsible for the extraction of data from several sources. In this paper, we have focused on the problem A Type One change updates only the attribute, doesn't insert new records, and affects no keys. It is easy to implement but does not maintain any history of prior attribute values. **Slowly Changing Dimensions (SCDs)** are dimensions that have data that changes slowly, rather than changing on a time-based, regular schedule. In SCD type 2 effective date, the dimension table will have Start_Date and End_Date as the fields. If the End_Date is Null, then it indicates the current row. Know more about SCDs at Slowly Changing Dimensions Concepts. The new incoming record

(changed/modified data set) replaces the existing old record in target. Comprehensive ETL criteria were identified. testing procedures were developed. and this work was applied to commercial ETL tools. The study covered all major aspects of ETL usage and can be used to effectively compare and evaluate various ETL tools. We can implement on SCD TYPE-2 based on SCD TYPE-1 and new fields like Versioning, Effective Dates, By setting Current Flag values/Record Indicators.

REFERENCES

Journal Papers:

- [1] I. William, S. Derek, and N. Genia, DW 2.0: The Architecture for the Next Generation of Data Warehousing. Burlington, MA: Morgan Kaufman, 2008, pp. 215-229.
- [2] R. J. Davenport, September 2007. [Online] ETL vs. ELT: A Subjective View. In Source IT Consulting Ltd., U.K. Available at: http://www.insource.co.uk/pdf/ETL_ELT.pdf.
- [3] T. Jun, C. Kai, Feng Yu, T. Gang, "The Research and Application of ETL Tools in Business Intelligence Project," in Proc. International Forum on Information Technology and Applications, 2009, IEEE, pp.620-623.

Books:

- [4] Kimball, R., Caserta, J.: The Data Warehouse ETL Toolkit: Practical Techniques for Extracting, loading, Conforming, and Delivering Data. John Wiley & Sons, 2004.
- [5] Informatica Power Center, Available at www.informatica.com/products/data_integration/power_center/default.htm

Theses:

- [6] ALKIS SIMITSIS , Dipl. Electrical and Computer Engineering (2000). Modeling and Optimization of Extraction-Transformation-Loading (ETL) Processes in Data Warehouse Environments

Proceedings Papers:

- [7] K.Srikanth, N.V.S.Murthy, J.Anitha : "Data Warehousing Concept Using ETL Process For SCD Type-1" Conf. on TIJCSA , Volume 1, No. 10, December 2012 ISSN – 2278-1080.

Influence of the Type of Measuring Device in Determining the Static Modulus of Elasticity of Concrete

Suélcio da Silva Araújo ^a, Gilson Natal Guimarães ^b e André Luiz Bortolacci Geyer ^c

^a Masters Degree in Civil Engineering from the Federal University of Goiás, Brazil (2011), School of Civil Engineering, Research Assistanship from CNPq - National Council of Scientific and Technological Development.

Address: Rua A, Número 141, Bairro Mato Grosso, CEP: 76.200-000, Iporá, GO – Brasil.

^b PhD., University of Texas at Austin, USA (1988). Full Professor at the Federal University of Goiás, Brazil. E-Address: Universidade Federal de Goiás, Escola de Engenharia Civil, Laboratório de Estruturas. Av. Universitária, Pça. Universitária, s/n, Setor Universitário, CEP 74640-220, Goiânia, GO – Brasil.

^c Doctorate in Civil Engineering from the Federal University of Rio Grande do Sul, Brazil (2001). Associate Professor II at the Federal University of Goiás.

Address: Universidade Federal de Goiás, Escola de Engenharia Civil, Laboratório de Materiais de Construção. Av. Universitária, Pça. Universitária, s/n, Setor Universitário, CEP 74640-220, Goiânia, GO – Brasil.

Abstract: This paper presents a comparative analysis of the results obtained in static modulus of elasticity tests of plain concrete cylindrical specimens. The purpose of this study is to identify and evaluate the influence of several factors involved in modulus of elasticity tests such as the strain measurement device used (dial indicators, electrical surface bonded strain gages, externally fixed strain gages and linear variation displacement transducer - LVDT), the type of concrete (Class C30 and Class C60) and cylindrical specimen size (100 mm x 200 mm and 150 mm x 300 mm). The modulus tests were done in two different laboratories in the Goiânia, GO region and were performed according to code ABNT NBR 8522:2008, which describes the initial tangent modulus test, characterized by strains measured at tension values of 0.5 MPa and 30% of the ultimate load. One hundred and sixty specimens were tested with statistically satisfactory results. It was concluded that the type of strain measurement device greatly influenced the modulus of elasticity results. Tests in specimens 100 mm x 200 mm showed highest statistical variation.

Keyword: Concrete; Specimen Size; Measurement; Modulus of Elasticity.

I. INTRODUCTION

The use of the modulus of elasticity is frequently related to displacement and deflection calculations in the design phase of a reinforced concrete structure. The structural engineer specifies a value for the modulus of elasticity of the concrete which he uses in his calculations to satisfy serviceability limit states. This value for the modulus of elasticity will be later verified during the construction phase by the construction engineer or the concrete contractor. An incorrect verification of the modulus of elasticity can have serious consequences for the structural design, for example, excessive deflections not foreseen during the design phase.

Several factors can influence the value of the concrete's modulus of elasticity [8,10,14] such as concrete compressive strength, concrete specimen casting process, loading and unloading speed of the testing apparatus, mortar content, type of strain measurement device, aggregate type and size, testing machine operator, concrete specimen size. This research had the objective to study and evaluate the influence of some of these variables on the static modulus of elasticity: influence of measurement device (dial or digital indicator, surface mounted strain gages, externally fixed strain gages or clip gages, linear variable differential transformer –

LVDT), concrete type (Class C30 and Class C60) and cylindrical specimen size (100 mm x 200 mm e 150 mm x 300 mm). Tests were conducted in two different concrete laboratories in the Goiânia, GO region.

The modulus of elasticity can be defined as a relation between the applied stress and the measured strain below yield stress. According to code ABNT NBR8522:2008 [3], the static modulus of elasticity for a concrete loaded in axial compression is determined by the inclination of the stress-strain curve obtained in testing cylindrical concrete specimens. The specimen is subjected to incrementally increasing loads and the strain is measured at each load increment. The types of modulus of elasticity are related to different loading stages and should be chosen based on the purpose of the test. Figure 1 shows the different types of static modulus of elasticity in concrete subjected to compression.

Briefly, the moduli of elasticity are:

- Initial tangent modulus: is given by the inclination of a tangent line at the origin of the stress-strain diagram. It is used to characterize concrete deflections at very low stresses.
- Tangent modulus at a given stress: is the inclination of a tangent line of the stress-strain diagram at any given stress. It is used to simulate the structure to loading or unloading at different loading stages. Loading and unloading can be applicable, for example, when a numerical structural analysis is needed due to large accidental loads.
- Secant modulus: is given by the inclination of a secant line obtained between any two points in the stress-strain diagram. Frequently the points chosen correspond to a stress of 0.5MPa and a stress at 50% of the ultimate stress. In this case, it simulates the structure during its initial loading stage when permanent loads prevail. The Brazilian Code for Design and Execution of Reinforced Concrete Constructions ABNT NBR 6118:2003 [4] proposes a value for the secant modulus as 85% of the initial tangent modulus. The secant modulus is frequently used by structural engineers in design.

In this work, the initial tangent modulus of elasticity was determined. It was done according to code ABNT NBR 8522:2008 [3] which prescribes, in this case, concrete strains at stress levels of 0.5 MPa and 30% of ultimate stress. This code prescribes an initial stress of 0.5 MPa, and not a zero value, to minimize the effect of specimen imperfections, testing machine variability and the accommodation process of the top and bottom plates of the testing machine, since these factors can generate in initial disturbance in the stress-strain diagram near zero stress.

The value of the initial tangent modulus of elasticity, E_{ci} , is given by the equation below:

$$E_{ci} = (\sigma_b - \sigma_a) / (\epsilon_b - \epsilon_a) \quad \text{(Equation 1)}$$

where:

σ_b is the higher stress and it is equal to 0.3 of the rupture stress;

σ_a is the basic stress and is equal to 0.5 MPa;

ϵ_b is the average strain of the specimen under the higher stress;

ϵ_a is the average strain of the specimen under the basic stress;

Contrary to strain measurements in steel rebars, strain measurements in concrete are much harder to obtain. In steel, strain measuring devices known as strain gages are widely used and give good quality and reliable results. But in concrete, the same does not happen and several researchers [6,7,8,9] and laboratories in Brazil and worldwide have search for other alternatives to obtain reliable strain measures with less statistical variability. Among these alternatives for measuring strains in concrete, the present research work verified the use of four different measuring devices [15,16]: dial indicator, surface bonded strain gages, externally fixed strain gages or clip gages, linear variable differential transformer – LVDT.

The digital or dial indicator is a mechanical measuring device where a small piston moves indicating the measurement. Both the strain gage and the clip gage work based on the same principle of changes in the electrical resistance of a coil during the deformation of the body to which they are attached. The difference is that the strain gage is bonded (glued) to the body surface and the clip gage is mechanically fixed to the surface through claws, permitting their reuse. The strain gage is disposable after the test. The linear variable differential transformer is better known by its acronym LVDT and it is an electro-magnetic displacement transducer. Figure 2 shows photos of these 4 measuring devices.

As far as loading speed, code ABNT NBR 8522:2008 [3] specifies a loading speed for the modulus of elasticity test at (0.45 ± 0.15) MPa/s. The laboratory where the test is undertaken chooses the loading speed. In the research, the loading speed used was 0.6 MPa/s at both labs.

II. EXPERIMENTAL PROGRAM

Considering the characteristics of the interlaboratory program, three variables were considered:

- Type of conventional concrete (class C30 and class C60);

- Type of strain measurement device (dial gages, strain gages, clip gages and linear variation displacement transducer - LVDT);
- Cylindrical specimen dimensions: 100 mm x 200 mm and 150 mm x 300 mm.

Tests with the dial gages and strain gages were done at Carlos Campos Laboratories and tests with clip gages and LVDTs were done at Furnas Centrais Elétricas Laboratories. It was not possible to conduct all tests at the same laboratory due to physical and operational constraints (equipment, operating hours, operator availability, storage) of the two laboratories involved and the quantity of specimens to be tested.

The loading stages known as Metodology A in code ABNT NBR 8522:2008 [3] was used for the modulus of elasticity tests. Cycles of loading and unloading were done. According to Figure 3, strain measurements were taken at stress levels of 0.50 MPa and 30% of the rupture stress (known as f_c) and the initial tangent modulus was calculated according to Equation 1.

Conventional concrete Class C30 and Class C60 were used. These were cast in concrete mixers with a maximum capacity of 450 liters using Portland cement Type V ARI (high initial strength) fabricated by CIMPOR. Silica fume, superplasticizers and polyfunctional additives were also used in the concrete mix. The properties of the additives and admixtures used are presented in Table 1. The mix proportions are presented in Tables 2 and 3. All specimens were cast at Carlos Campos Laboratories.

Ten cylindrical specimens were cast for compressive strength tests for each type of concrete (class C30 and C60), for each specimen dimension (100 mm x 200 mm e 150 mm x 300 mm) and for each laboratory, for a total of 80 specimens. These tests were done in the two laboratories (40 specimens tested in each laboratory) at 28 days after casting. The compressive strength test is needed prior to the modulus tests so the value of 30% of rupture stress can be calculated for use in the modulus tests and in Equation 1. The rupture stress was calculated as the average of the rupture stresses of the 10 specimens.

Ten cylindrical specimens were cast for the modulus of elasticity tests for each measurement device (4 different devices), for each type of concrete (class C30 and C60), and for each specimen dimension (100 mm x 200 mm e 150 mm x 300 mm), for a total of 160 (10x4x2x2) specimens. Tests using the dial indicators and strain gages were done simultaneously on the same concrete specimen, so not all specimens cast were used. This was possible, since, during the test, the analogical readings from the dial indicators were obtained visually by the operator, and the strain gage readings were digital and obtained using a microcomputer.

All tests were done 28 days after casting. The modulus test is nondestructive and the same specimen was then taken to rupture to obtain its compressive strength. The objective of testing the same specimen for compressive strength after the modulus test is to verify the homogeneity of the concrete and to allow statistical control. However, these compressive strength results were not used in Equation 1. The values used were obtained in the compressive strength tests mentioned earlier.

Specimens were cast and stored according to provisions in code ABNT NBR 5738:2008 [1], following guidelines in code ABNT NBR 5739:2007 [2]. To reduce the influence of specimen humidity, after 24 hours after casting, the specimens were identified and stored in water tanks for 28 days. After this, the specimens were removed from the storage tanks and stored at room temperature and humidity. Sulfur capping was used in all specimens.

The specimens were grouped in packages of 10 specimens and were randomized before the modulus of elasticity tests. Randomization was done to allow minimization of certain variables effects that could not or were not considered in the experiment such as: casting process, aggregate distribution in the concrete, testing device setup, among others. Also, if any dependency mechanism exists between subsequent experimental results, the randomizations of the tests allow this dependency to be diluted among all studied situations, thus not favoring a certain situation over another.

Statistical analysis of variance technique (ANOVA) was applied using software Statsoft Statistica 7[®], for concrete Class C30 and for concrete Class C60 specimens, separately and together. The test methodology consists in the application of Fisher's Test. This analysis indicated that the results should be analyzed together to be statistically significant.

III. PRESENTATIONS AND DISCUSSION OF RESULTS

In order to verify the homogeneity of the concrete used, the compressive strength results of the specimens taken to rupture right after the modulus of elasticity tests were first analyzed. These compressive strength results were analyzed by statistical methods in order to identify possible variances of the results and to verify the normal distribution (histogram) of the results. Figures 4 and 5 show the histograms of these compressive strength results for concrete classes C30 and C60, respectively. Concrete C30 showed an average compressive strength of 36.5MPa with a coefficient of variation of 10% and concrete C60 showed an average compressive strength of 69.3 MPa with a coefficient of variation of 11%. The comparison between the histograms and the normal distribution curve was analyzed by the Kolmogorov-Smirnov e Qui-square methods.

From a statistical point of view, a value of 10% is an acceptable level for variability for a measuring process.

Table 4 presents the averages, standard deviations and coefficients of variation of the results obtained in all of the situations studied with a 95% confidence interval from the average for the modulus of elasticity property. A statistical analysis of variance (ANOVA) was done with the modulus of elasticity results to determine the statistically significant factors with a 95% confidence level. Some values were removed, since they did not fit the confidence interval and they were eliminated by the Chauvenet criteria.

Table 4 shows that the measuring devices that presented the smallest dispersions were the strain gages and the clip gages since the total coefficients of variation of these devices were 11.0% and 14.4%, respectively, and the total coefficients of variation of the dial indicators and the LVDTs were 16.1% and 18.2%, respectively.

Table 4 also shows that the specimens with 100 mm x 200 mm dimensions presented higher dispersion of results, because their total coefficient of variation was 24.4% and the total coefficient of variation of the specimens with 150 mm x 300 mm dimensions was 13.1%.

Since ANOVA revealed that the specimen size, type of measuring device and type of concrete were statistically significant, grouping homogeneous averages by the Duncan method was done to observe the differences and similarities of the results obtained.

This method demonstrated that the two specimen sizes influenced the values of the modulus of elasticity of the concrete because the average of the modulus for specimens 100 mm x 200 mm and 150 mm x 300 mm were 24.4 GPa e 26.2 GPa, respectively. That is, the specimens 150mm x 300mm had an average 7% higher than the average obtained for specimens 100mm x 200 mm.

The Duncan method also demonstrated that the strain gages presented results similar to the dial indicators, since their averages for the modulus tests were 27.6 GPa e 27.5 GPa, respectively, and the averages for the clip gages and the LVDTs were 26.3 GPa e 19.8 GPa respectively.

For 100mm x 200 mm specimens, modulus results (see Figure 6) obtained using strain gages had averages of 24.6 GPa and 30.6 GPa and their respective coefficients of variation were 13.2% and 1.9% for concrete classes C30 and C60. Results obtained with dial indicators had averages of 24.1 GPa and 31.6 GPa and their respective coefficients of variation were 16.1% and 17.7% for concrete classes C30 and C60. Results obtained with clip gages had averages of 22.0 GPa and 29.8 GPa and their respective coefficients of variation were 4.0% and 2.5% for concrete classes C30 and C60. Results obtained with LVDTs had averages of 14.9 GPa and 20.3 GPa and their respective coefficients of variation were 13.5% and 7.9% for concrete classes C30 and C60. For 100mm x 200 mm specimens, modulus results obtained from dial indicators and LVDTs presented larger variability.

For 150mm x 300 mm specimens, modulus results (see Figure 6) obtained using strain gages had averages of 26.6 GPa and 29.8 GPa and their respective coefficients of variation were 2.6% and 4.0% for concrete classes C30 and C60. Results obtained with dial indicators had averages of 26.9 GPa and 27.9 GPa and their respective coefficients of variation were 3.8% and 7.6% for concrete classes C30 and C60. Results obtained with clip gages had averages of 23.5 GPa and 30.8 GPa and their respective coefficients of variation were 4.1% and 1.5% for concrete classes C30 and C60. Results obtained with LVDTs had averages of 20.6 GPa and 23.2 GPa and their respective coefficients of variation were 1.4% and 12.6% for concrete classes C30 and C60. For 150mm x 300 mm specimens, modulus results obtained from dial indicators and LVDTs presented larger variability. Results obtained using LVDTs presented lowest modulus.

Since 100 mm x 200 mm specimens showed larger variability in the modulus results, the variable "specimen size" was investigated in further with more results shown in Figures 7 and 8. Figure 7 shows the effect of specimen size and the effect of concrete type with concrete class C60 showing higher modulus results. Modulus results obtained with 100 mm x 200 mm specimens had averages of 21.6 GPa and 27.6 GPa and their respective coefficients of variation were 21.6% and 20.5% for concrete classes C30 and C60. Modulus results obtained with 150 mm x 300 mm specimens had averages of 24.5 GPa and 27.7 GPa and their respective coefficients of variation were 10.8% and 12.2% for concrete classes C30 and C60.

Figure 8 show the effect of measuring device interacting with specimen size and the behavior explained earlier is the same. Again, highest variability is shown in results obtained with LVDTs. For 100mm x 200 mm specimens, modulus results (see Figure 8) obtained using strain gages had an average of 26.8 GPa and the coefficient of variation was 14.7%. Results obtained with dial indicators had an average of 27.7 GPa and the coefficient of variation was 21.9%. Results obtained with clip gages had an average of 25.7 GPa and the coefficient of variation was 15.9%. Results obtained with LVDTs had an average of 17.7 GPa and the coefficient of variation were 18.5%. For 100mm x 200 mm specimens, modulus results obtained from dial indicators and LVDTs presented larger variability.

For 150mm x 300 mm specimens, modulus results (see Figure 8) obtained using strain gages had an average of 28.3 GPa and the coefficient of variation was 6.6%. Results obtained with dial indicators had an average of 27.4 GPa and the coefficient of variation was 6.2%. Results obtained with clip gages had an average of 26.8 GPa and the coefficient of variation was 12.9%. Results obtained with LVDTs had an average of 22.0

GPa and the coefficient of variation were 11.3%. For 150 mm x 300 mm specimens, modulus results obtained from clip gages and LVDTs presented larger variability.

IV. CONCLUSION

The analysis of the results obtained before considered the influence of measuring device, concrete class and specimen size. The most important conclusions of this study were:

1. The two specimen sizes used in this study had an effect on the concrete static modulus of elasticity since the average modulus obtained from 100 mm x 200 mm and 150 mm x 300 mm specimens were 24.4 GPa and 26.2 GPa, respectively. The average modulus obtained from 150 mm x 300 mm specimens were 7% higher. However, code ABNT NBR 8522:2008 [3] sets tolerance limits in item 8.2 which allows variation in results of up to 10%.
2. Results using strain gages were similar to results using dial gages since their average modulus were 27.6 GPa and 27.5 GPa, respectively. The results for clip gages and LVDTs showed average modulus of 26.3 GPa and 19.8 GPa, respectively.
3. For specimen size 100 mm x 200 mm, results showed largest variability when dial gages and LVDTs were used. For 150mm x 300 mm specimens, modulus results obtained from clip gages and LVDTs presented larger variability.
4. For the two concrete types, 100 mm x 200 mm specimen results showed larger variability than 150 mm x 300 mm specimen results. The 150 mm x 300 mm specimens had smaller coefficient of variability in the modulus tests.
5. Modulus values obtained using dial gages and strain gages were higher than results obtained with clip gages and much higher than those obtained with LVDTs.
6. Values obtained with LVDT were smallest than those obtain with the other 3 devices. In general, LVDT was considered the less accurate (greatest coefficient of variation among the 4 devices), and harder to use due to its analog readings, need of constant maintenance, equipment fragility, calibration difficulties and manual control by the testing operator.
7. In general, the strain gages and clip gages had more consistent readings and lowest coefficients of variation and showed important advantages such as a smaller need of external intervention during testing and minimization of reading errors by the operator. In case of strain gages, the bonding of the gage to the concrete surface has various aspects that should be closely watched, making its use more difficult. Also, the strain gages have to be discharged after their use, and a second use is not allowed, which increases testing costs. The clip gages have the advantage of measuring both longitudinal and transverse strains, show digital readings and are less susceptible to calibration procedures. Clip gages are more practical, can be reused several times and setting them up on the specimen is easy and no great operator expertise is required.

Modulus of elasticity tests using different measuring devices showed that even when following the criteria specified in code ABNT NBR 8522:2008 [3], variations in test results are relatively significant.

V. ACKNOWLEDGEMENTS

The authors wish to express special thanks to Laboratory Carlos Campos Consultoria e Construções Ltda., to Laboratório de Furnas Centrais Elétricas, to Realmix Concreto S.A., to Conselho Nacional de Desenvolvimento Científico e Tecnológico – CNPq and to Procad/CAPEs.

REFERENCES

- [1] ASSOCIAÇÃO BRASILEIRA DE NORMAS TÉCNICAS – ABNT. **NBR 5738**: Concreto – Procedimento para moldagem e cura de corpos de prova. Rio de Janeiro: ABNT, 2008.
- [2] **NBR 5739**: Concreto – Ensaio de compressão de corpos de prova cilíndricos. Rio de Janeiro: ABNT, 2007.
- [3] **NBR 8522**: Concreto – Determinação do módulo estático de elasticidade à compressão e Diagrama Tensão-Deformação – Método de Ensaio. Rio de Janeiro: ABNT, 2008.
- [4] **NBR 6118**: Projeto e Execução de Obras de Concreto Armado. Rio de Janeiro: ABNT, 2003.
- [5] CUPERTINO, M. A.; PEREIRA, A. C.; INÁCIO, J.J.; ANDRADE, M.A.S. **Avaliação de Fatores de Ensaio que Interferem nos Resultados de Módulo de Elasticidade do Concreto**. In: 49º CONGRESSO BRASILEIRO DO CONCRETO, 2007, Bento Gonçalves - RS. Anais 49º Congresso Brasileiro do Concreto. 2007. CD-ROM.
- [6] MARTINS, D. G. **Influência do tamanho do corpo de prova nos resultados de ensaios de módulo de deformação e resistência à compressão e suas correlações para concretos produzidos em Goiânia-GO** [manuscrito] / Danilo Gomes Martins. – 2008. Dissertação (Mestrado) – Universidade Federal de Goiás, Escola de Engenharia Civil, 2008.
- [7] RODRIGUES, G. S. S. **Módulo de deformação estático do concreto pelo método ultra-sônico: estudo da correlação e fatores influentes**. Dissertação de Mestrado. Escola de Engenharia Civil, Universidade Federal de Goiás. 2003. 234 p.
- [8] ARAÚJO, SUÉLIO DA SILVA. **Influência do tipo de medição na determinação do módulo estático de elasticidade do concreto** - 2011. 212 f.: il., figs, tabs. Orientador: Prof. PhD. Gilson Natal Guimarães; Co-orientador: Prof. Dr. André Luiz Bortolacci Geyer. Dissertação (Mestrado) – Universidade Federal de Goiás, Escola de Engenharia Civil, 2011.
- [9] FIGUEIREDO, E. J. P.; SOUZA, F. L. S.; DE FIGUEIREDO, A. D. **Medidas de deformação através de strain gages**. Trabalho da disciplina de tecnologia avançada no estudo do comportamento do concreto. São Paulo, 1989. 57 p.

- [10] METHA, P. K.; MONTEIRO, Paulo J. M. “Concreto-Microestrutura, Propriedades e Materiais.” 1ª Ed. Português, IBRACON, São Paulo, 2008.
- [11] MONTIJA, Fernando Celloto. **Aspectos da Variabilidade Experimental do Ensaio de Módulo de Deformação do Concreto.** 2007. Dissertação (Mestrado em Engenharia de Construção Civil e Urbana) – Escola Politécnica, Universidade de São Paulo, São Paulo, 2007.
- [12] SHEHATA, L. D. Deformações Instantâneas do Concreto. In: IBRACON, **Concreto: Ensino, Pesquisa e Realizações.** Editor: ISAIA, G. S. IBRACON, São Paulo, 2005. cap. 21, p. 633-654. ISBN 85-98576-03-4.
- [13] NBR 8953 – **Concreto para fins estruturais – Classificação por grupos de resistência.** Rio de Janeiro, 2009.
- [14] BARBOSA, Isa Lorena Silva. **Influência dos agregados graúdos da região de Goiânia no módulo de deformação tangente inicial do concreto** - 2009. 133 f.: il., figs, tabs. Orientador: Prof. Dr. André Bortolacci Geyer. Dissertação (Mestrado) – Universidade Federal de Goiás, Escola de Engenharia Civil, 2009.
- [15] PORTNOI, M. **Extensometria: história, usos e aparelhos.** Disponível em: http://locksmith.orcishweb.com/academic-files/extensometria.html#_Toc511736064. Acesso em 15 jun. 2009.
- [16] UNIVERSITY OF COLORADO AT BOULDER. **Transducers.** 1999. Disponível em: http://civil.colorado.edu/courseware/struct_labs/transducer.html. Acesso em 15 jun. 2011.

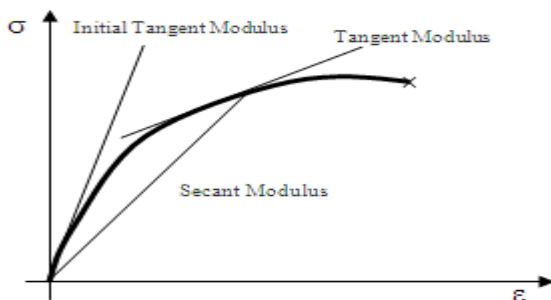


FIGURE 1 – Different types of modulus of elasticity in the stress-strain curve



FIGURE 2 – Dial Indicators (a) Strain gage (b), Clip gage (c) and LVDT (d)

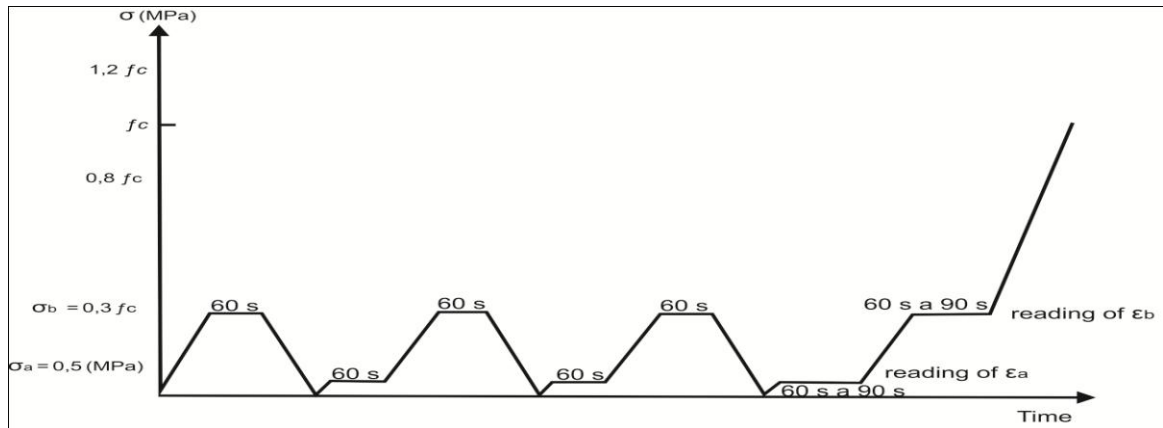


FIGURE 3 – Loading history for determining the modulus of elasticity – Method A (ABNT NBR 8522:2008)

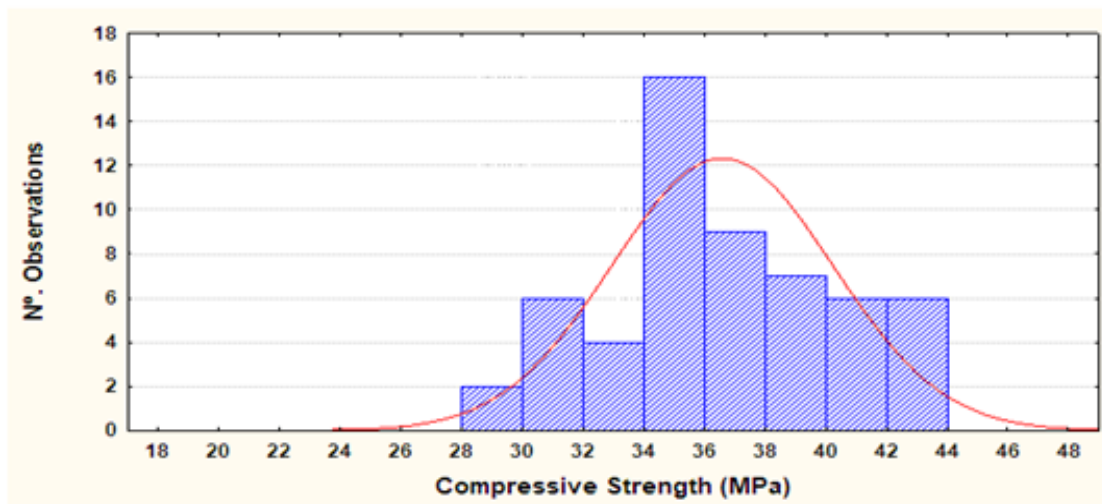


FIGURE 4 – Histogram of the compressive strength results obtained from concrete class C30 specimens

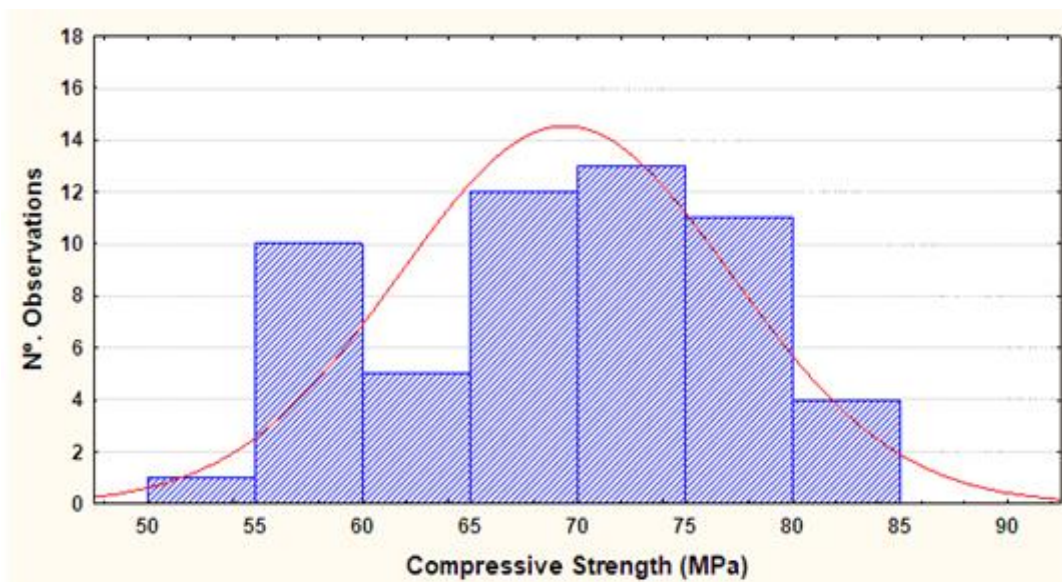


FIGURE 5 – Histogram of the compressive strength results obtained from concrete class C60 specimens

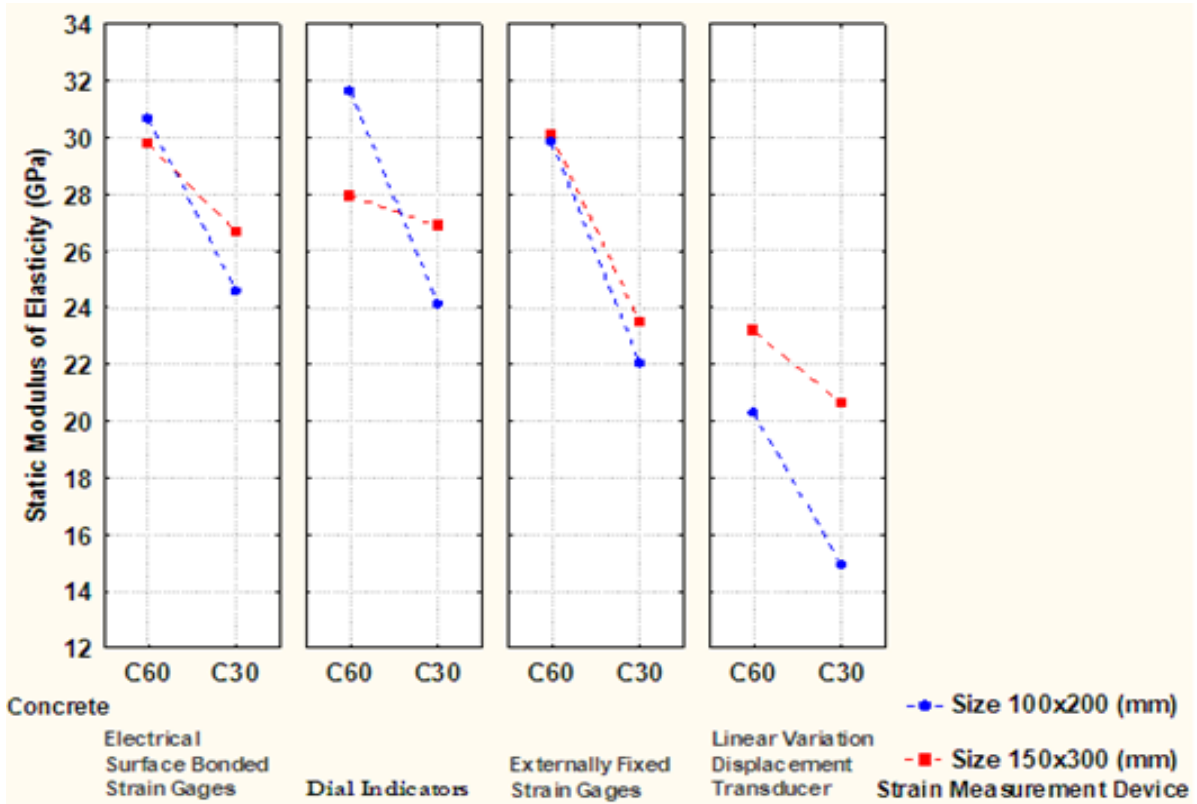


FIGURE 6 – Static modulus of elasticity versus specimen size, type of concrete and strain measurement device

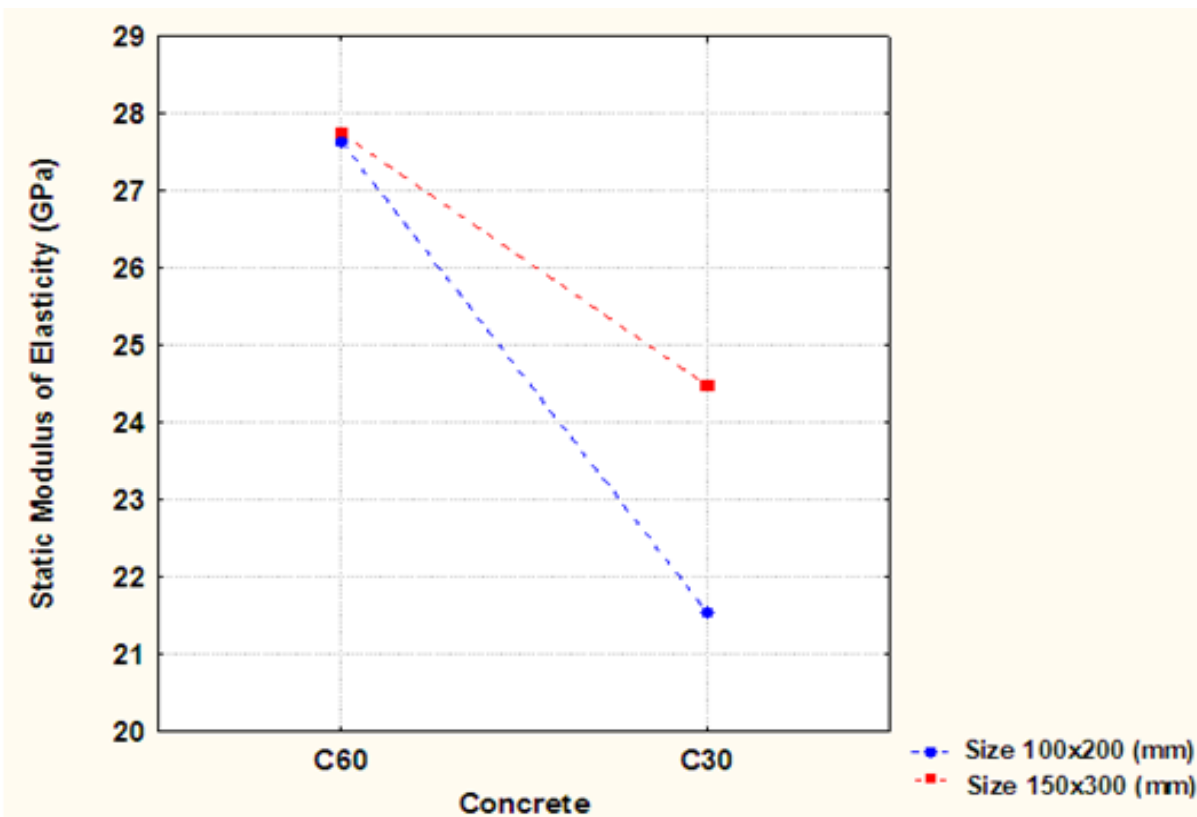


FIGURE 7 – Modulus of elasticity versus concrete type and specimen size (includes all measuring devices)

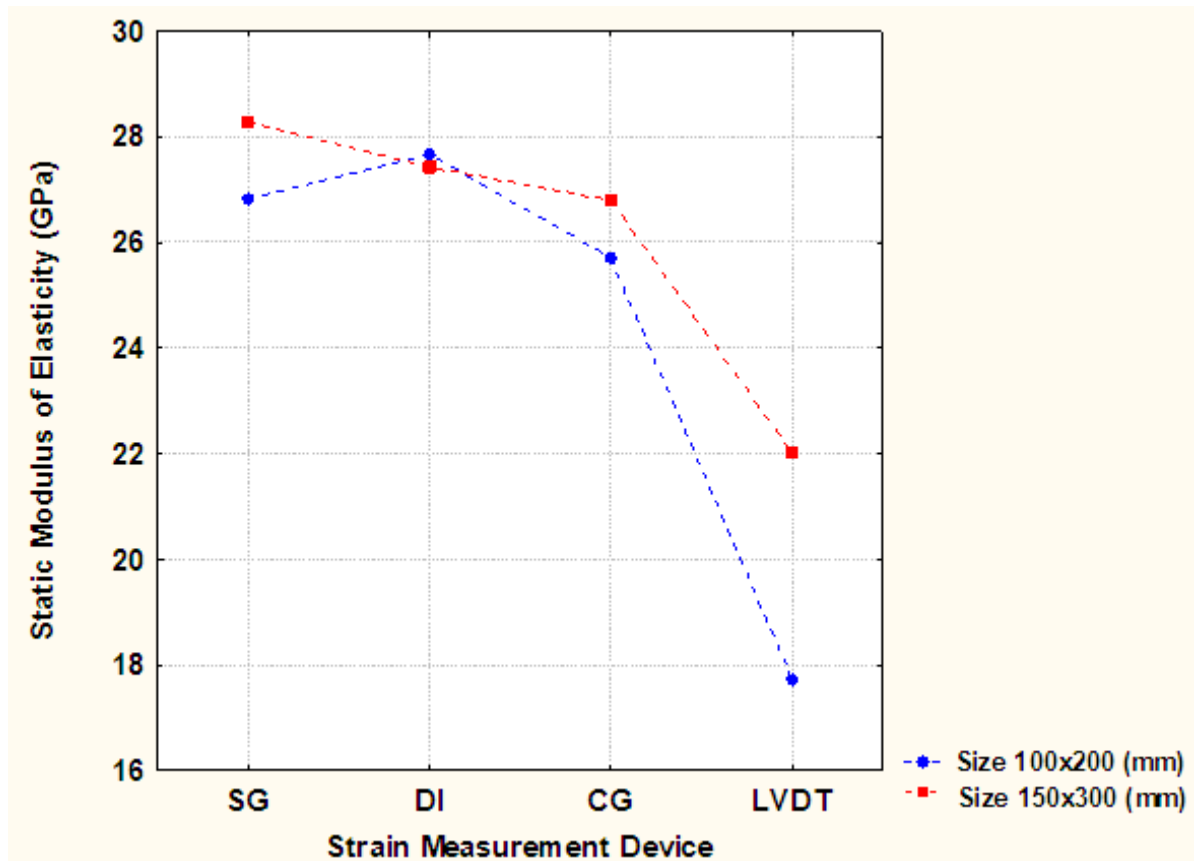


FIGURE 8 – Modulus of elasticity versus strain measurement device and specimen size (SG – strain gage, DI - dial indicator, CG - clip gage and LVDT)

TABLE 1 – Properties of additives and additions used in the concrete

Properties	Material		
	Additive GLENIUM 51	Additive Sikament PF 171	Silica Fume Silmix
Main Function:	3 rd Generation Superplasticizer	Polifunctional Additive	Filler
Chemical Basis	Polycarboxilate	Sodium Lignosulfonate	Amorphous Silica
Appearance:	Viscous Liquid	Liquid	Powder
Color:	Beige	Dark brown	Light or dark gray
Density (g/cm ³)	1.067 to 1.107	1.13 to 1.17	2.2
pH:	5 to 7	4 to 6	8 to 10

Materials	Conventionally Vibrated Concrete
	Quantity per m ³
Cement CP V ARI	236 kg
Artificial sand	891 kg
Gravel size 1 (19 mm)	999 kg
Water	172 kg
Polyfunctional Additive	1.65 kg (0.7% of cement)
Superplasticizer	0.94 kg (0.4% of cement)
Silica Fume	18.9 kg (as replacement for 8% of cement in weight)
Fresh Concrete Properties:	
Consistency	130 mm
Air	2 %

TABLE 3 - Concrete mix for $f_c = 60$ MPa

Material Proportioning by m^3 of concrete Mix design (1 : 1.928 : 2.58)
W/C ratio = 0.42

Materials	Conventionally Vibrated Concrete	
	Quantity per m^3	
Cement CP V ARI	398 kg	
Artificial sand	765 kg	
Gravel size 1 (19 mm)	1028 kg	
Water	167 kg	
Polyfunctional Additive	2.79 kg (0.7% of cement)	
Superplasticizer	1.59 kg (0.4% of cement)	
Silica Fume	31.87 kg (as replacement for 8% of cement in weight)	
Fresh Concrete Properties:		
Consistency	120 mm	
Air	1.5 %	

TABLE 4 – Statistical Analysis of Test Results – Static Modulus of Elasticity

Situation of Study			N°. of Specimen	Static Modulus of Elasticity (GPa)		
Size (mm)	Type of strain measurement device	Type of Concrete		Average (GPa)	Standard Deviation (GPa)	Coefficient of Variation (%)
—	Dial Indicators	—	37	27.5	4.4	16.1
—	Electrical Surface Bonded Strain Gages	—	35	27.6	3.05	11.0
—	Externally Fixed Strain Gages	—	39	26.3	3.8	14.4
—	Linear Variation Displacement Transducer - LVDT	—	37	19.8	3.6	18.2
100X200	—	—	73	24.4	5.96	24.4
150X300	—	—	75	26.2	3.4	13.1
100X200	Dial Indicators	C30	10	24.1	3.9	16.1
	Dial Indicators	C60	9	31.6	5.6	17.7
	Electrical Surface Bonded Strain Gages	C30	10	24.6	3.2	13.2
	Electrical Surface Bonded Strain Gages	C60	6	30.6	0.58	1.9
	Externally Fixed Strain Gages	C30	10	22.0	0.88	4.0
	Externally Fixed Strain Gages	C60	9	29.8	0.74	2.5
	Linear Variation Displacement Transducer - LVDT	C30	9	14.9	2.004	13.5
	Linear Variation Displacement Transducer - LVDT	C60	10	20.3	1.6	7.9
150X300	Dial Indicators	C30	9	26.9	1.02	3.8
	Dial Indicators	C60	9	27.9	2.1	7.6
	Electrical Surface Bonded Strain Gages	C30	9	26.6	0.69	2.6
	Electrical Surface Bonded Strain Gages	C60	10	29.8	1.2	4.0
	Externally Fixed Strain Gages	C30	10	23.5	0.96	4.1
	Externally Fixed Strain Gages	C60	10	30.1	0.46	1.5
	Linear Variation Displacement Transducer - LVDT	C30	8	20.6	0.29	1.4
	Linear Variation Displacement Transducer - LVDT	C60	10	23.2	2.9	12.6

OBS.: - Concrete types: concrete class C30 for dimensions 100 mm x 200 mm and 150 mm x 300 mm and concrete class C60 for dimensions 100 mm x 200 mm and 150 mm x 300 mm.
- Twelve of the individual results were considered as spurious values.

Inspection of Buildings in Rio de Janeiro-Brazil: Proving the greater tendency of corrosion at the base of reinforced concrete columns using potential corrosion technique

Marcelo Henrique Farias de Medeiros¹; Mikko Knuutila², Eduardo Pereira³; Paulo Helene⁴

¹(Department of Civil Engineering, Federal University of Paraná, Brazil)

²(Graduate student, Oulu University of Applied Sciences, Finland)

³(Department of Civil Engineering, State University of Ponta Grossa, Brazil)

⁴Department of Civil engineering, Polytechnic School, University of São Paulo

Abstract: Monitoring the corrosion of steel embedded in concrete is a way to assess the degradation of civil structures. A technique used for this is the measurement of corrosion potential, which includes the use of a reference electrode, connected to a high input impedance voltmeter. There are many factors influencing the measurement of corrosion potential, such as: degree of concrete moisture content, the oxygen access, existence of micro fissures, chloride penetration, carbonation and concrete cover thickness. This study aims to analyze the measurement of corrosion potential for the copper/copper sulfate (Cu/CuSO₄) electrode obtained in the inspection work of four residential buildings located in Barra da Tijuca, Rio de Janeiro, Brazil. The evaluation aims to investigate the difference in measurements of corrosion potential in the middle and bottom of each inspected column. The reason for the research is to explain a practical realization: the reinforcement corrosion can be seen more often at the columns base than in the remaining of this type of structural element. General data for all the 4 buildings inspected indicates that 77% of all 109 inspected columns have more negative corrosion potential values at the base. The reasons for this discovery are discussed throughout this paper.

Keyword: inspection; corrosion potential; reinforced concrete; reference electrode

I. INTRODUCTION

Having started in the United States of America around the 70's, the use of the method for evaluating the corrosion potential in inspecting reinforced concrete structures, became widely used in U.S.A and also in Europe in recent years. One good use for this method is mapping the values of corrosion potential as these mappings enable the identification of compromised areas and areas with steel depassivation [1].

The corrosion potential can be identified in places with thermodynamic conditions which enable the beginning of electrochemical corrosion in the steel reinforcements of the concrete even though the corrosion has not yet manifested visibly in the surface of the reinforcement steel.

Actually, there are also other methods based on electrochemistry which not only enable identification of these areas but also provide quantitative data on the kinetics of the corrosion process, for example, the methods for evaluating corrosion speed by electrochemical impedance or by the resistance of linear polarization. These procedures which combine the interpretation of corrosion potential values with corrosion speed are currently most recommended for monitoring the durability of reinforcements of reinforced concrete structures.

This study aims to analyze the measurement of corrosion potential for the copper/copper sulfate (Cu/CuSO₄) electrode obtained in the inspection work of four residential buildings located in Barra da Tijuca, Rio de Janeiro, Brazil. The evaluation aims to investigate the difference in measurements of corrosion potential in the middle and bottom of each inspected column. The motive for the research is to explain a practical realization: that the reinforcement corrosion can be seen more often at the columns base than at the remaining of this type of structural element.

Real cases are still in a learning phase and models are being developed and adjusted to make service life predictions more accurately. This work is inserted in this context, disseminating data obtained from on-site inspection of reinforced concrete structures that were weather-exposed to a marine environment for years, helping to understand the work in service of real reinforced concrete structures.

II. DETAILS OF THE METHOD

The tendency of any metal to react with an environment is indicated by the potential it develops in contact with the environment. In reinforced concrete structures, concrete acts as an electrolyte and the reinforcement will develop a potential depending on the concrete environment, which may vary from place to place [2]. The method for evaluating corrosion potential includes the use of a reference electrode connected to a high input impedance voltmeter as shown in Figure 1.

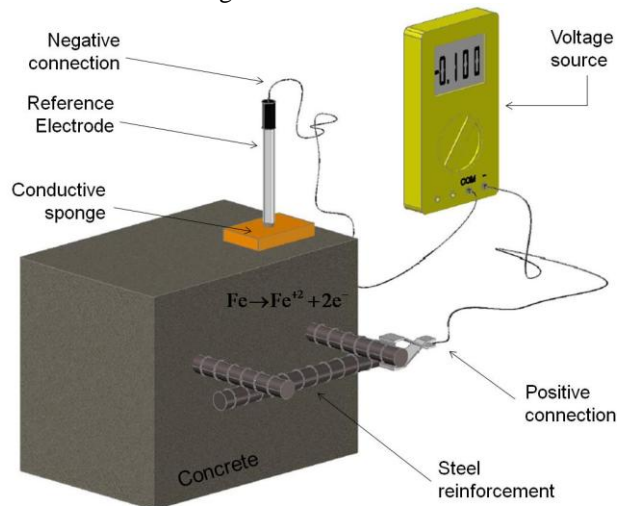


Figure 1 – Schematic of the technique being applied to study corrosion potential [3].

The test is generally performed in sample pieces or in reinforced concrete structures for monitoring or punctual evaluation, in case of an inspection where there is no time to monitor the readings over a long time. Thus, it is necessary to have a reference electrode (usually a copper/copper sulfate - Cu/CuSO4) where the potentials are referred to.

The readings of corrosion potential provide evidence of corrosion risks as indicated in Table 1.

Table 1 – Criteria for evaluating measurements of corrosion potential [4].

The corrosion potential related to the reference electrode (Cu/CuSO4) - (Ecorr)	Probability of Corrosion (%)
< - 350 mV	90
Between - 350 and - 200 mV	Uncertain
> - 200 mV	10

Using the method, a measurement of electrochemical potential difference is made at certain points of the structure, between an unstable electrolyte system (steel/concrete) and another stable one which is the reference electrode. When the device is applied they create an electrochemical cell formed by the two systems previously mentioned.

Generally, what is observed in electrode potential measurements made in reinforced concrete is a current flow going from the reinforcement to the reference electrode, closing the circuit between the two parts occurring in an ionic way through a highly conductive interface.

Normally, the obtained values are negative regardless the state of the reinforcement because the potential of the reference copper/copper sulfate electrode is nobler (more positive values) than the steel/concrete system potential.

The reference electrode can be moved over the concrete surface to create a potential map that shows the possible locations of active corrosion in the structure. This tool has been widely used in the field because it provides a fast and low cost way to identify areas of steel depassivation that require analysis or repair. However, test results may be affected by the following factors:

Concrete moisture content: The corrosion in reinforced concrete is an electrochemical process and therefore depends on the existence of an electrolyte, or in other words, a sufficient level of humidity in the capillary pores of concrete. Hence corrosion will occur only when there is a minimal level of humidity and the highest the level is, the higher the mobility of ions participating in the electrochemical process. Therefore, strong additional moistening or preferably saturation of concrete is recommended before starting the potential reading. The ideal situation would be concrete saturation, at least one hour before the start of readings to ensure the correct measurement [5]. According to Poursaeed and Hansson [6], potential measurements begin no sooner than 15 minutes after the first measurement area is wet.

Depending on the concrete moisture content (or on its resistivity) at the moment when the inspection is performed, the steel embedded in a reinforced concrete structure, carbonated or contaminated by chlorides, may be classified according to the criteria of ASTM C876 [4] as being either in an active or in a passive state of corrosion [7].

Aeration (access to oxygen): In order to have electrochemical corrosion with formation of ferruginous and expansive products (rust), it is necessary to have an access to oxygen. Oxygen is required for the reaction forming oxides/hydroxides of iron, porous and expansive. These products from corrosion may have variable colors such as black, green, reddish and rusty brown denoting different levels of oxygen availability, the black color on the beginning of the process (and unstable) and brown being the end of the process and a stable environment with normal access to oxygen. Thus the existence of more negative potentials in cases with low access to oxygen is possible (before fissures and in saturated concrete), compared to fissured regions or with detached concrete (highly deteriorated regions) [5]. This means that not always the corrosion potential values are directly proportional to the rate or level of corrosion. Saturated concrete, for example, has high conductivity, high tendency to more negative potentials, but limited access to oxygen which results in low corrosion rate.

Micro fissures: Local electrochemical corrosion can be accelerated or facilitated by micro fissures which also reduce the ionic resistivity of the concrete, affecting the measurement of corrosion potential [8].

Chloride penetration: According to Browne et al. [9], chlorides on the surface layer of concrete may result in different values of potential for more negative rates, since the chlorides improve the ionic movement in the concrete porous solution, an essential part of the electrochemical corrosion process.

Carbonation: increases the electrical resistivity of carbonated concrete and makes the corrosion potential less negative.

Thickness of concrete cover: the greater the thickness is, the less negative the values of corrosion potential are. Figure 2 shows an image illustrating the effect of concrete cover thickness in the readings of corrosion potential.

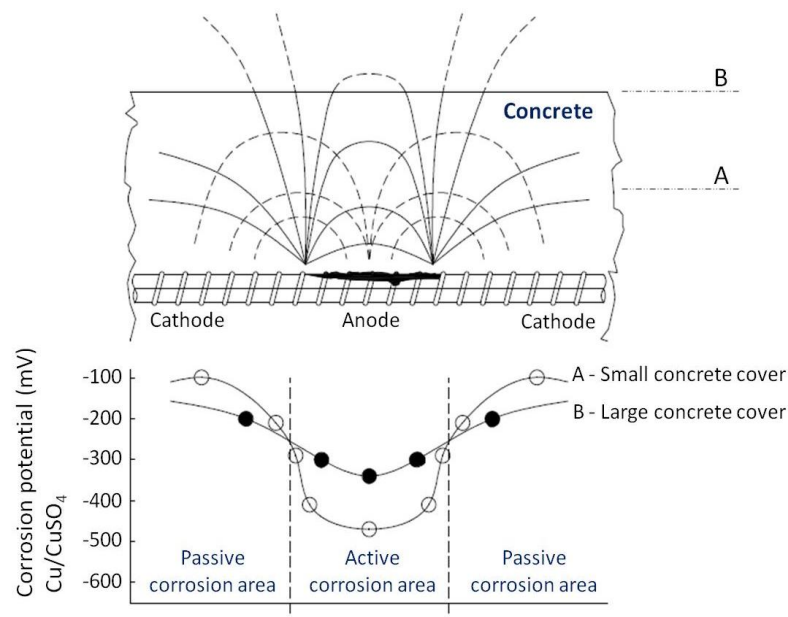


Figure 2 – Influence of concrete cover on readings of corrosion potential [5].

For the reasons specified by ASTM C 876 [4] the criteria from Table 1 must be taken carefully, with restrictions in special situations such as: very dry concrete, deeply carbonated, having a painted or film coated surface or when the reinforcement has a galvanized metal coating or epoxy paint. Although this method of half-cell potential is widely applied, it must be noted that it is not quantitative, since the corrosion rate is not determined.

When there is a protective layer on the concrete, such as epoxies, polyurethane, acrylic, among others, the electrical contact between the reference electrode and the concrete surface is impaired and the technique should not be used unless the protection is removed, even locally, for measurements [10]. Figure 3 shows a general scheme of activities sequence forming the method for evaluating corrosion potential.

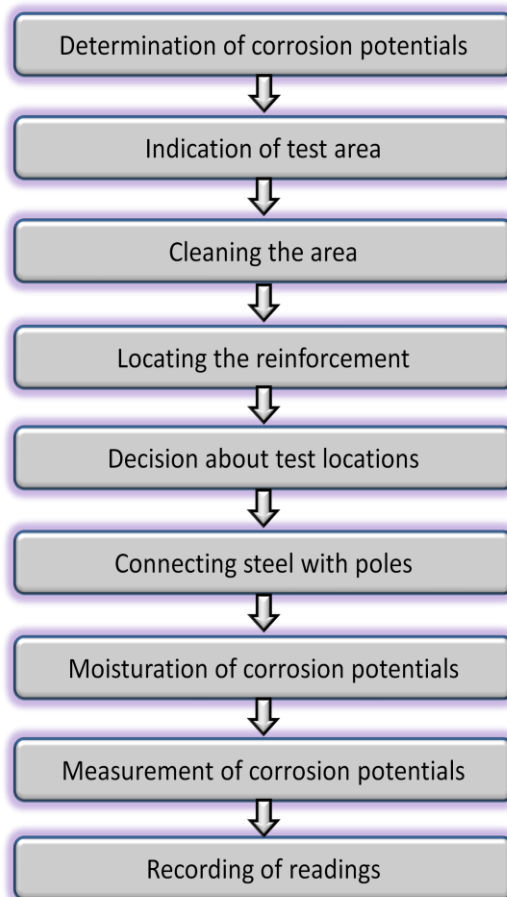


Figure 3 – Flow diagram of process [11].

III. METHODOLOGY

An inspection work is much more than just reading corrosion potentials. However this study focused on evaluating this method in four residential buildings where the inspection work was completely carried out. Table 2 shows details of buildings that were part of this work.

Table 2 – Identification of buildings of this study.

Details	
Building 1	A building with 14 residential floors + 2 (2-floors apartment) + ground floor + 2 basement floors = total 21 floors
Building 2	A building with 35 residential floors + 1 (2-floors apartment) + floor with home machines + ground floor + 2 basement floors = total 40 floors
Building 3	A building with 14 residential floors + 2 (2-floors apartment) + ground floor + 2 basement floors = total 21 floors
Building 4	A building with 14 residential floors + 2 (2-floors apartment) + ground floor + 2 basement floors = total 21 floors

All of the buildings are located in Barra da Tijuca, Rio de Janeiro, Brazil about 700m from the seashore. The environment where all four buildings are located is considered as a strongly aggressive environment according to NBR 6118 [12]; EN 1992-1-1 [13]; EN 206-1 [14], ACI 201.2R [15].

The measurements of corrosion potential were conducted on the columns of the inspected buildings and the site of every reading was saturated beforehand. The saturation procedure was done with a constant supply of water to the surface of the columns. Water was allowed to penetrate into the concrete by the absorption mechanism by capillary suction. In every analyzed column the readings were taken both at the column base and at the height of 1.5m from the floor slab as illustrated in Figure 4.

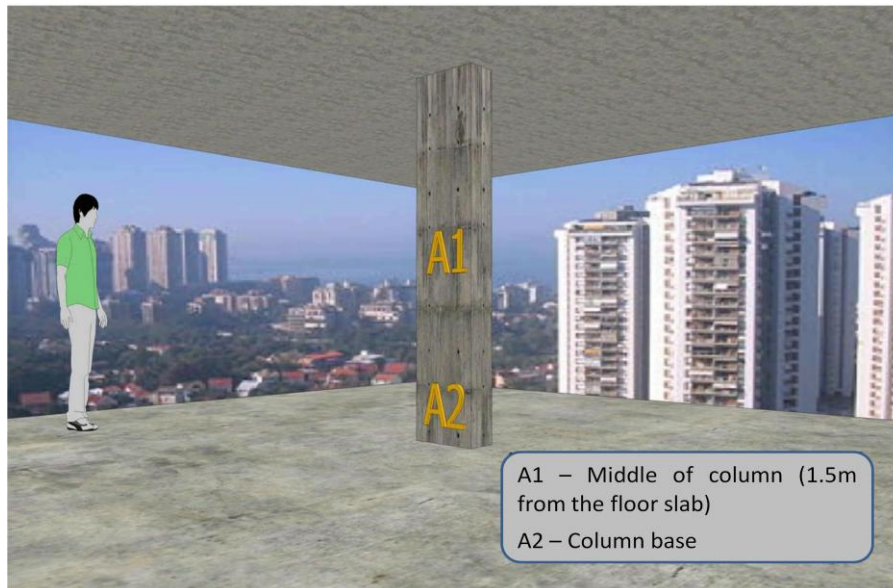


Figure 4 – Positioning schematic for readings taken.

Sampling was done from the inspection work in four buildings and the sample space in each building is shown in Figure 5. The number of sampled columns was limited due to the time available for inspection work as indicated on the work contract. However, it can be considered a great opportunity to use practical experience in order to learn about the functioning of reinforced concrete structures. Figure 5 shows a total of 109 columns that were inspected in the four buildings.

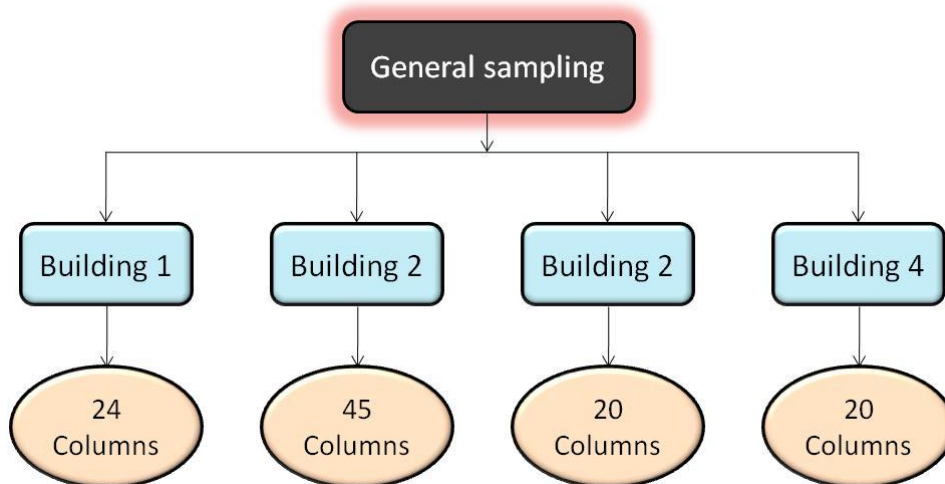


Figure 5 - General overview of sampling.

IV. RESULTS AND DISCUSSION

4.1 Building 1

Figure 6 has the obtained results from every column and floor where the values of corrosion potential were registered in Building 1. It is easy to notice that in this building there is a tendency for the existence of more negative corrosion potential values at the columns bases.

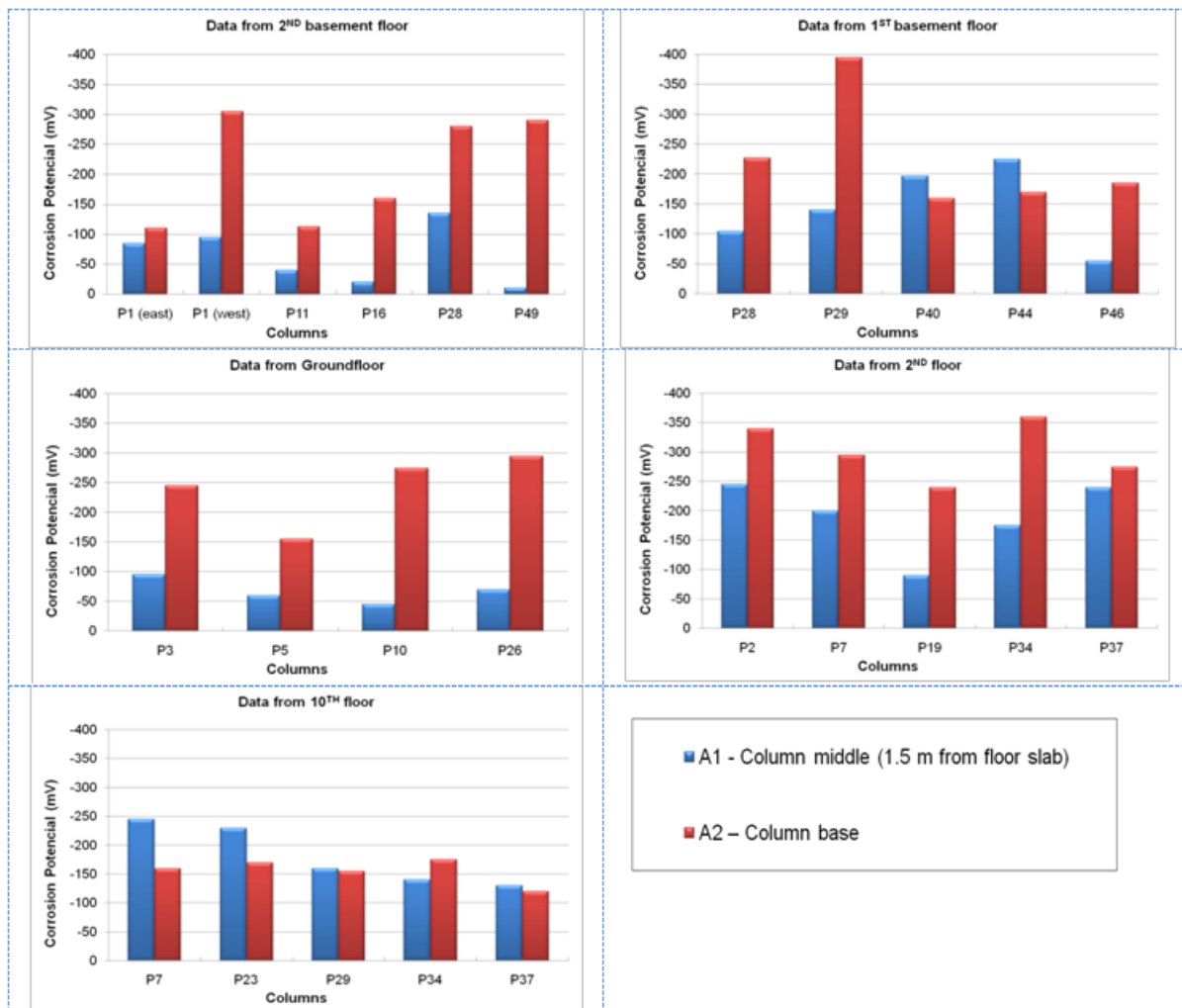


Figure 6 – The corrosion potential (E_{corr}) data for building 1.

This is more evident in Figure 7 showing the percentages for the more negative corrosion potential values in the columns bases (A2) and at the columns central region (A1). In this case, it was shown that 75% of the more negative corrosion potential values were in the columns bases.

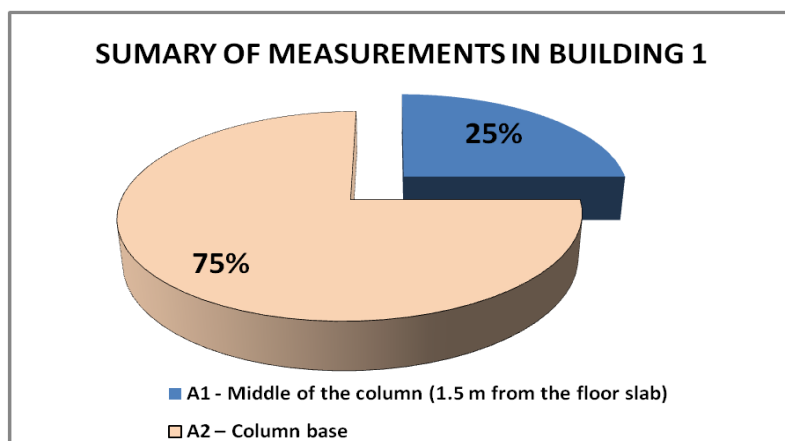


Figure 7 – Percentage of columns with more potential values of negative corrosion in base and central region of inspected columns in Building 1.

4.2 Building 2

Figure 8 presents the results obtained for each one of 45 columns sampled along the floors where the readings of corrosion potential were recorded in Building 2. It is clear that the results trend is contrary to the

results from Building 1. Figure 9 shows an overview of these results indicating that in this building the values of more negative corrosion potential are concentrated in the columns middle (at height of 1.5m).

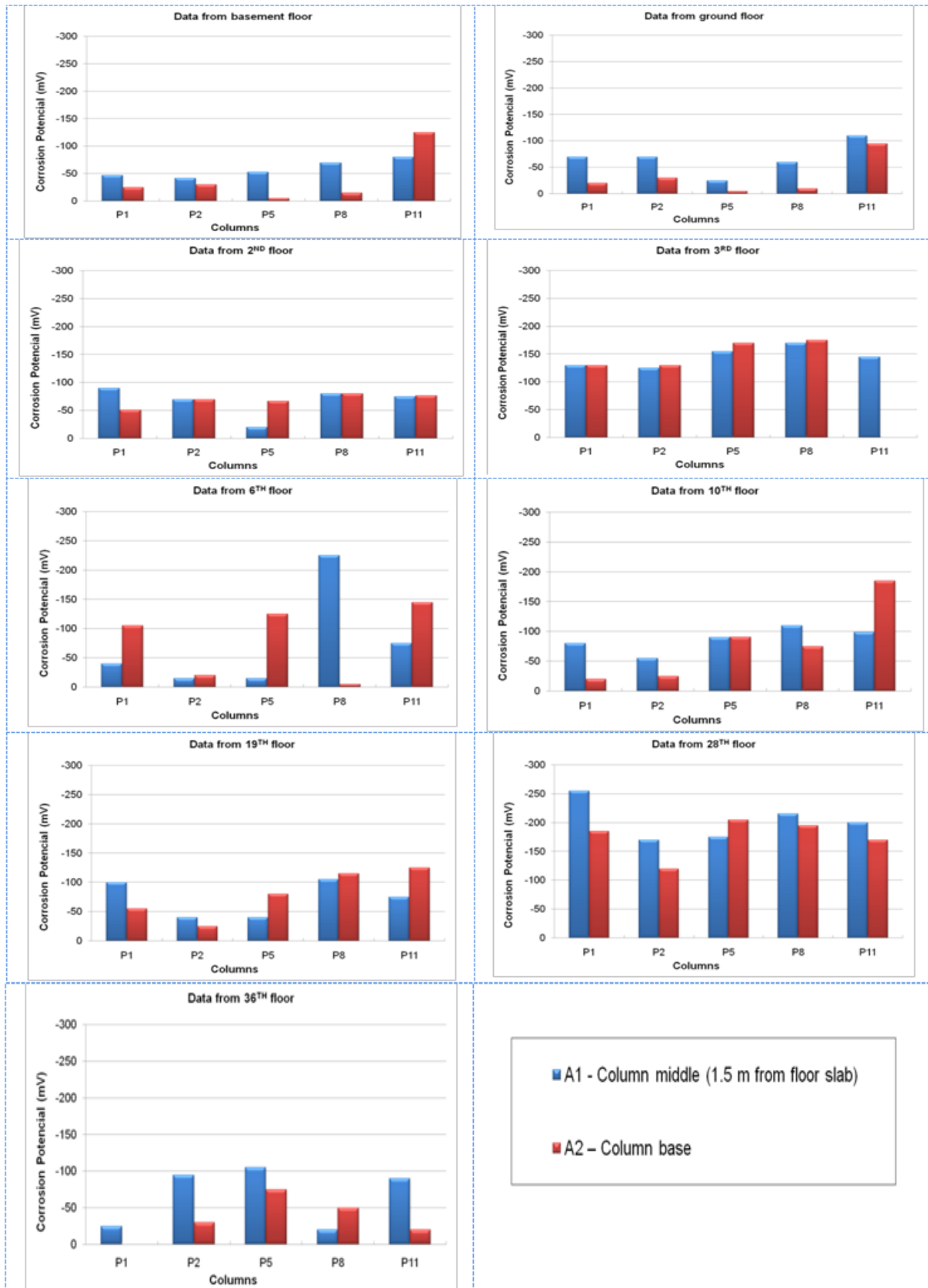


Figure 8 – Corrosion potential (E_{corr}) data for building 2.

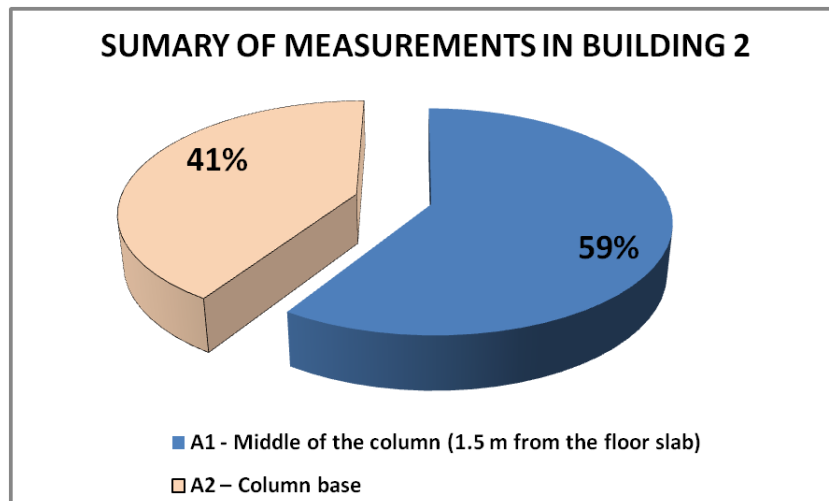


Figure 9 – Percentage of columns with more potential values of negative corrosion in base and central region of inspected columns in Building 2.

4.3 Building 3

Figures 10 and 11 indicate the same trend as results from Building 1. It is important to notice that in this case the value of corrosion potential at the base is more negative than in the middle in 100% of the inspected columns. This result is in accordance with the obtained in Building 1.

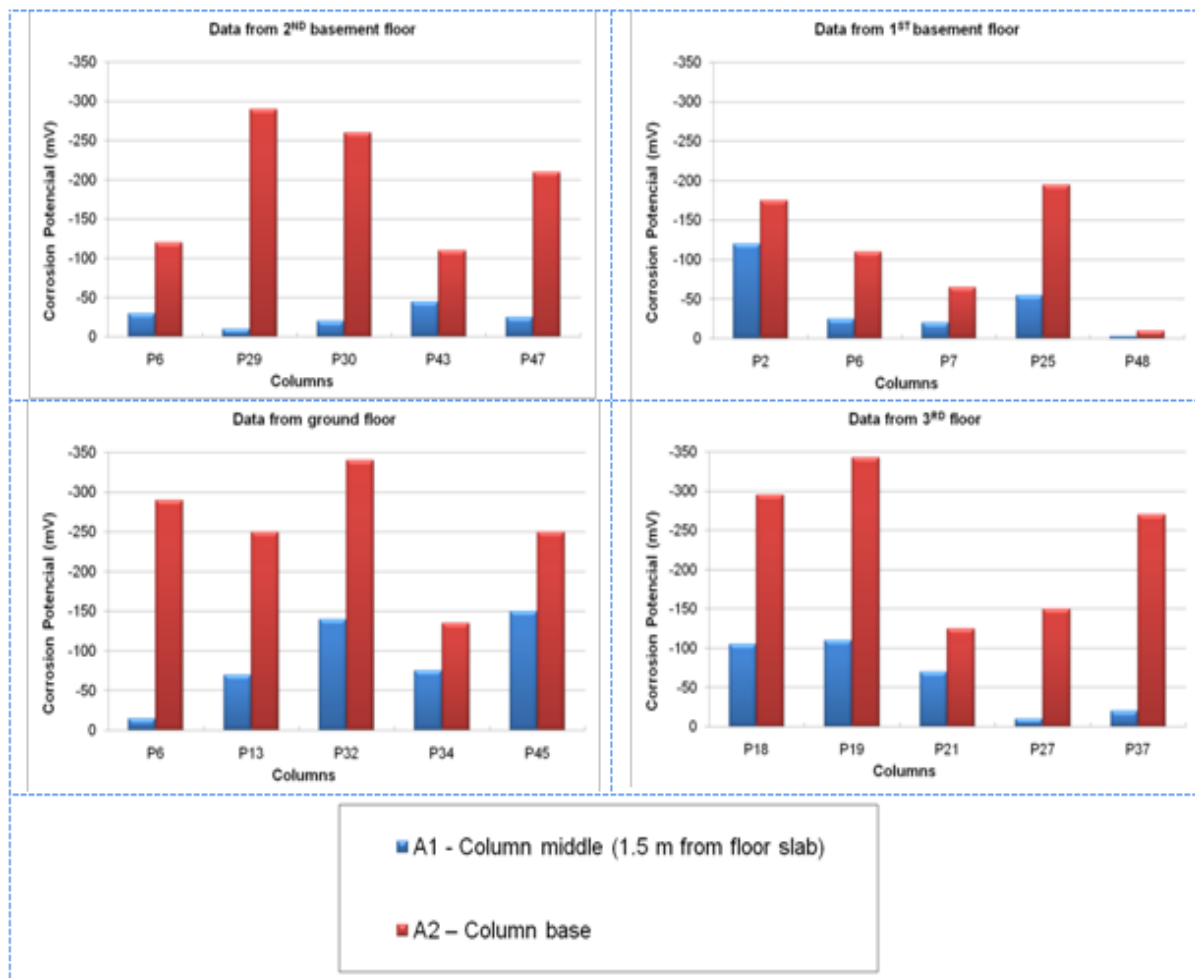


Figure 10 – Corrosion potential (E_{corr}) data for building 3.

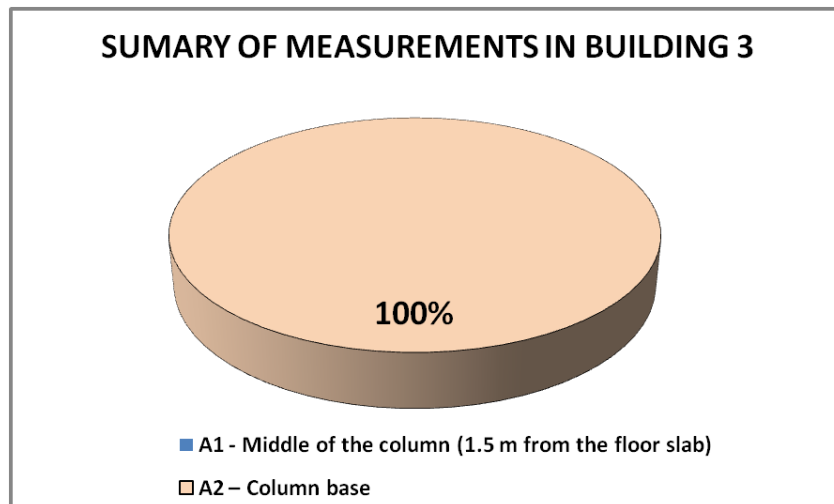


Figure 11 – Percentage of columns with more negative corrosion potential values in the base and the central region of inspected columns in Building 3.

4.4 Building 4

Finally, Building 4 indicates the same trend as buildings one and three. As Figures 12 and 13 show, the individual results for each column inspected and an overall outcome of this study is presented respectively. It is noteworthy that in 75% of the cases the most negative values of corrosion potential are located at the columns base in Building 4 as showed in Figure 13.

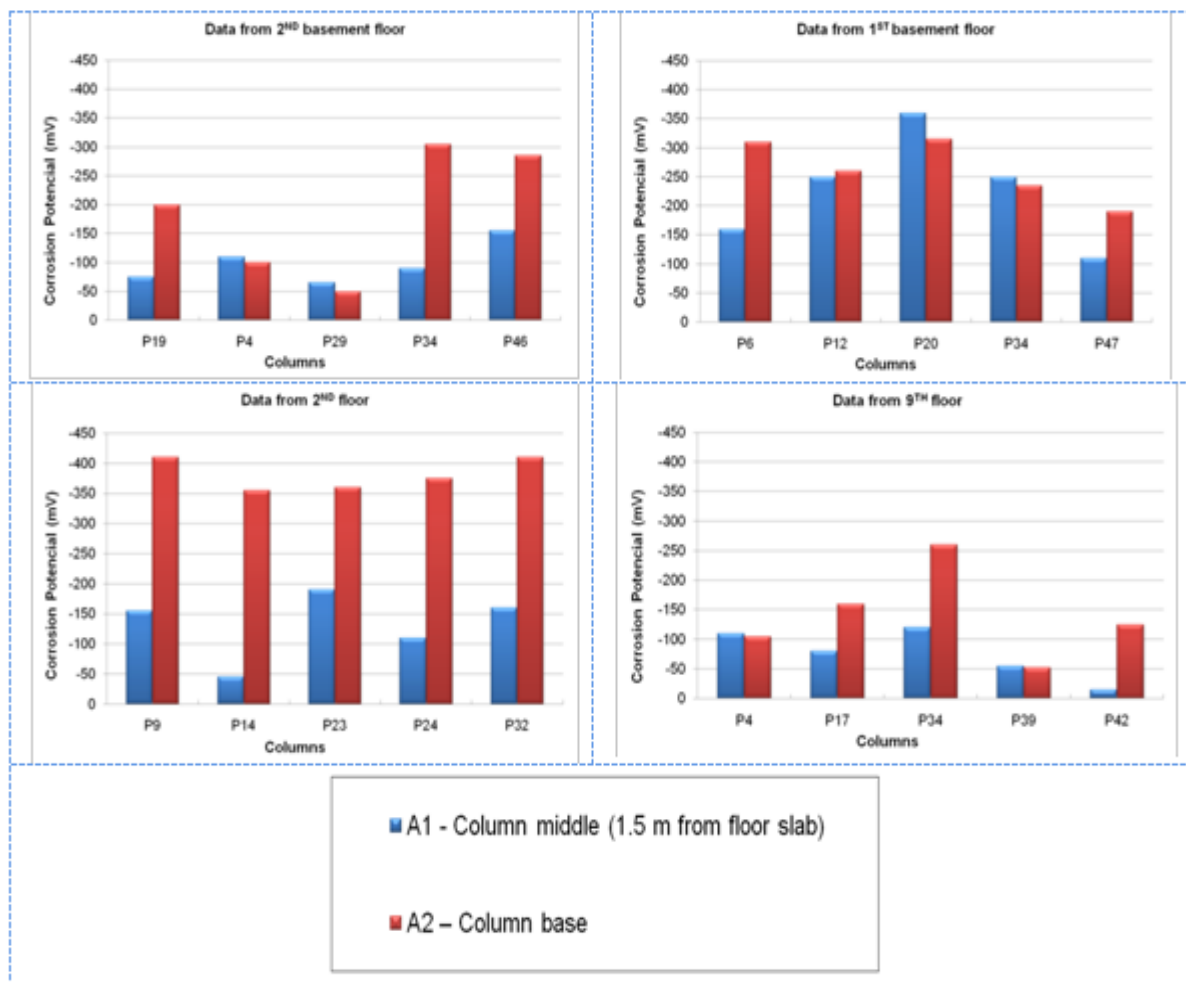


Figure 12 – Corrosion potential (E_{corr}) data for Building 4.

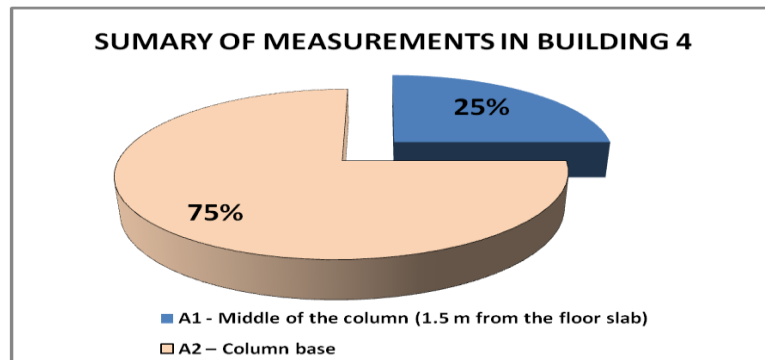


Figure 13 – Percentage of columns with more negative corrosion potential values in the base and the central region of the inspected columns in Building 4.

4.5 Discussion of results

Figure 14 shows general data for all 4 buildings inspected indicating that 77% of all 109 inspected columns have more negative corrosion potential values at the columns bases. This result is a very relevant amount, indicating high prevalence of this presented occurrence.

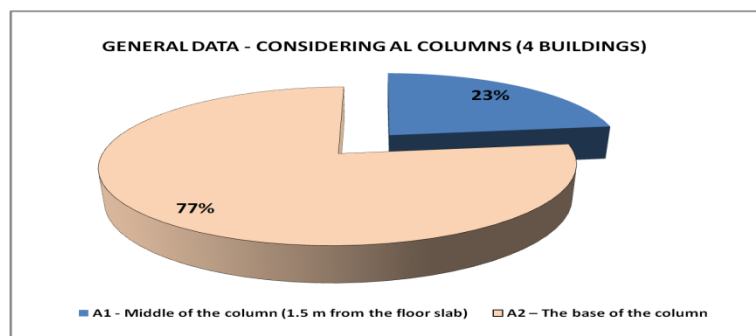


Figure 14 – General percentage of columns with more negative corrosion potential values in the base and the central region of the inspected columns.

In addition, Figure 15 shows that, in 75% of the inspected buildings, the trend to have a tendency to negative values of corrosion potential in the columns bases was validated.

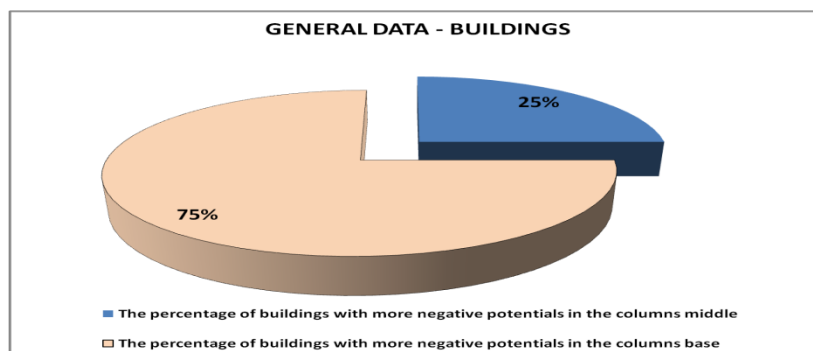


Figure 15 – Percentage of the buildings that follow the tendency of columns with more negative corrosion potential in the base.

As shown in most cases, the corrosion potential is more electronegative in the column base than in the central region. Some theories to explain this trend follow:

- 1) *Placement of concrete*: There is a consensus that placement of concrete from a height without extra care may lead to segregation, which tends to happen mainly in the columns base. As a result, there is a larger concentration of aggregates in the base region of many columns. This creates a region with richer cement and a region with poor cement. The poorer region is precisely located in the columns base where a tendency exists for more negative values of corrosion potential.

- 2) *High concentration of steel reinforcements*: The column base consists of a region with a higher quantity of steel bars because it is the connection area of the reinforcement. This fact can complicate the densification of concrete in the columns bases and is also an influencing factor in the values of corrosion potential.
- 3) *Humidity*: When exposed to the environment during longer periods of time, the water inside the columns has a tendency to accumulate in their bases because of gravity. Thereby, it is known that a humid column dries faster near the roof slab than in the base, near the floor. This also explains the negative values of corrosion potential at the columns bases.
- 4) *Synergy between 1, 2 and 3*: The effects of nature and the synergy between the factors mentioned earlier also explain the trend of results. If the concrete in the column base has a tendency to be more porous because of segregation and difficulties in densification because of the high quantity of steel reinforcement, it is easy to conclude that this is a region with a tendency to suffer more contamination of chloride ions and carbon dioxide. Consequently, these regions also suffer from faster corrosion of steel. As already argued, it is a region with a tendency to have a higher level of humidity which, for its part, also advances the development of corrosion in the reinforcement in this area.

V. CONCLUSIONS

The data presented here is a result from an inspection of reinforced concrete structures directly exposed for weathering during more than five years. It is possible to conclude, according to presented facts, that there is a strong trend to have more negative values of corrosion potential in the columns base. This was verified in 77% of the 109 concrete columns inspected. This also explains the fact that the reinforcement corrosion occurs more often at the columns base.

The method of evaluating corrosion potential proved to be an important tool to detect changes in the state of the steel, helping to realize when the state of the reinforcement changes from passive to active corrosion and vice versa, confirming that the method is an useful tool in inspection services and evaluation of the durability of reinforced concrete structures.

It is important to highlight that the considerations made here need validation supported by a more detailed experimental study. This is due to the fact that in a real structure there are several variables that are not controlled, such as: uniformity in concrete mixture and proportioning, changes along the building, changes in cement, humidity rate in the measurements, thickness of concrete cover, temperature and others. Thus, this work results should be seen as a reference of a practical experience that triggers laboratory studies.

VI. ACKNOWLEDGEMENTS

The authors would like to thank the Polytechnic School of the University of São Paulo (POLI-USP) and the Federal University of Paraná (UFPR) for making this study possible.

REFERENCES

- [1] T. Parthiban, R. Ravi, G. T. Parthiban, Potential monitoring system for corrosion of steel in concrete, *Advances in Engineering Software* 37, 2006, 375-381.
- [2] H. Song, V. Saraswarthy, Corrosion monitoring of reinforced concrete structures – A review, *International Journal of Electrochemical Science* 2, 2007, 1-28.
- [3] F. C. Rocha, Potential corrosion in concrete structures: Influence of water/cement ratio, temperature, chloride contamination, thickness concrete cover and moisture content of the concrete, MSc Thesis, Federal University of Paraná, Curitiba, Brazil, 2012.
- [4] American Society for Testing and Materials, *Standard test method for half-cell potentials of uncoated reinforcing steel in concrete*, C 876, ASTM, Philadelphia, EUA, 2009.
- [5] P. R. L. Helene, "Contribution to the study of steel corrosion in reinforced concrete structures," Habilitation thesis, Escola Politécnica, University of São Paulo, São Paulo, Brazil, 1993.
- [6] A. Poursaee, C. M. Hansson, Potential pitfalls in assessing chloride-induced corrosion of steel in concrete, *Cement and Concrete Research* 39, 2009, 391-400.
- [7] J. A. González, J. M. Miranda, S. Feliu, Considerations on reproducibility of potential and corrosion rate measurements in reinforced concrete, *Corrosion Science* 46, 2004, 2467-2485.
- [8] P.K. Mehta; P. J. M. Monteiro, *Concrete: microstructure, properties and materials* (New York: McGraw-Hill Companies ed. 3, 2006).
- [9] R. D. Browne, M. P. Geoghegan, A. F. Baker, *Corrosion of Reinforcement in Concrete Construction* (Society of Chemical Industry, London, 1983).
- [10] P. Gu, B. Arsenault, J. J. Beaudoin, J. G. Legoux, B. Harvey, J. Fournier, Polarization Resistance of Stainless Steel-Coated Rebars, *Cement and Concrete Research* 28, 1998, 321-327.
- [11] O. T. Rincón, A. R. Carruyo, C. Andrade, P. R. L. Helene, I. Díaz, *Manual for inspection, evaluation and diagnosis of corrosion in reinforced concrete structures* (RED IBEROAMERICANA XV.B, Rio de Janeiro, Brazil, 1998).
- [12] Associação Brasileira de Normas Técnicas, *Analysis and design of concrete structures*, NBR 6118, Rio de Janeiro, 2007.
- [13] European Committee for Standardization, Eurocode 2: *Design of concrete structures - Part 1-1: General rules and rules for buildings*, EN 1992-1-1, Europe, 2004.
- [14] European Committee for Standardization (CEN), *Betão: Parte 1 – Especificação, desempenho, produção e conformidade*, EN 206-1, Portugal, 2007.
- [15] American Concrete Institute. *Guide to Durable Concrete: reported by ACI Committee 201* (ACI 201.2R, 2008).

Analyzing of urban green spaces development process with emphasis on sustainable principles (Case study: Mashhad metropolitan)

Maryam Ebrahimpour, Hamid Reza Saremi, Baratali Khakpour

Architecture & urban planning Department, Science and Research branch, Islamic Azad University, Boroujerd, Iran

Professor Department of Art and Architecture, Tarbiyat Modares University, Tehran, Iran

Assistant Professor Department of Geography, Ferdowsi University, Mashhad, Iran

Abstract: Urban green spaces are an important element in structure of cities. From these spaces can be named as the urban breathing lungs that they have various functions such as: City beautification, environmental modulators and leisure. Public land uses in many cities especially urban green spaces aren't successful due to some factors such as: high population density, imbalance in land use location, neglect to radial access for providing services and etc. Today, it isn't enough that we increase service centers also effort to achieve the standard and urban per capita because it is possible that all citizen haven't appropriate access to land use (parks & urban green space) due to imbalance of their location. Due to urbanism phenomenon grow sharply, so analyzing of appropriate location and its geographical distribution is very useful in development and future of cities.

In this research has been studied urban green space development process. This study is applied and the research method is "descriptive – analytical". Also data collected is documents. The findings show, the process of green space growth is well but don't adapt with global standards. So, should be attempted in this issue.

Key word: Green space, urban management, land-use, Mashhad metropolitan

I. INTRODUCTION

Green spaces are as a complement of urban physical structure. These spaces are a type of urban land-use that has ecologic and social traits. On the other hand, today planning and design is adaption green space networks (Ericson, 2004). Today, urban green spaces are introduced as appropriate method for promotion of life quality due to impressive social and ecological influences (Barker, 1968). So, an urban green space is important issue due to creating beautiful landscape, also it is as obstacle air pollution in cities.

Last years in Iran, don't achieve sustainable cities especially in Mashhad metropolitan due to development of cities with out regard to infrastructure such as green spaces. In different section of cities exist problems such as air pollution, terrific, shortage of green spaces. Appropriate planning & effective management in urban green section are necessary for eliminating these problems. Effective management is led to promotion of humane life quality in cities. Some countries in world are successful to decline shortage of green spaces by implementing different plans of developing green spaces.

Development of green spaces in Mashhad

Old Mashhad according to natural condition has numerous trees and pastures. Old Mashhad is introduced as green city at previous time. But, green spaces have changed in last centuries due to development of city. According to research, in Mashhad the ratio of green spaces to city area is high at Qajar¹ age. In 1922 decade (Pahlavi² age) decrease this ratio due to physical development of city. After that, Mashhad had grown sharply in 1962 & 1972 decades due to immigration of rural that was led to destroying of gardens and green spaces and making apartments. This issue introduced green spaces as important topic in urban issues. On the other hand, by developing of Mashhad the garden and agriculture lands that has been located around the city,

were combined with its .the figure (1), shows these changes clearly. Last years have destroyed many of green spaces and have replaced buildings and other urban equipment.

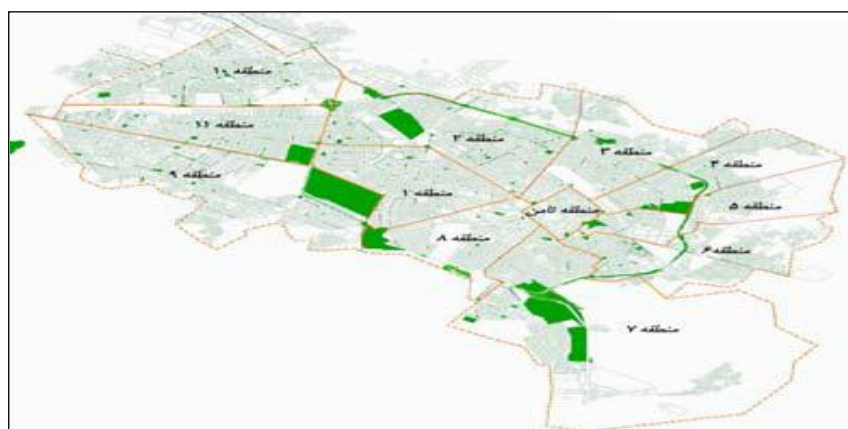


Figure (1): the plan of green spaces in Mashhad

In this stage decrease the area of green space land-use due to lack of appropriate plan. The results of plans and program in this stage show the lack of land has been led to increasing the value of lands so, has changed green space land-use to other land-uses. There are heterogeneous in distribution of green spaces due to high expenditure of making green spaces. Even, in some cities per capita of green space land-use is low from optimum range. The green spaces development process of Mashhad show that the first modern green space is national garden. It has been made in 1952. Then, in order to balancing between green spaces land-use and other land-uses (such as: residential, commercial, administrative and etc) were made parks in 1962 decade. The studies show urban green spaces increase to 11.1 km² in 1998 that the numbers of parks are 184 (*Vista & Pars consultant engineers*). In 2003, the numbers of parks increase to 672 and the area of parks is 12076761 hectare (*Mahmudian, 2006:134*).

After that urban green spaces development is important in 2006 & 2007 due to increasing air pollution. The area of green spaces in 2006 & 2007 are 6882 & 7244 hectare. In 2008, the area of urban green spaces increase to 7990 hectare that consist 130% of city area (*Zokae, 2008:230*).

Table (1): The indicators of urban green spaces (2006 – 2009)

2009	2008	2007	2006	Green spaces
80403	79903	72443	68822	The area of green spaces (1000 m ²)
13.25	13	12.2	11.6	The ratio of area green spaces to city rea
11.6	11.2	10.8	10.25	Per capita of green space

The figure (2) shows, the process of urban green spaces development increase between "2006 to 2009".

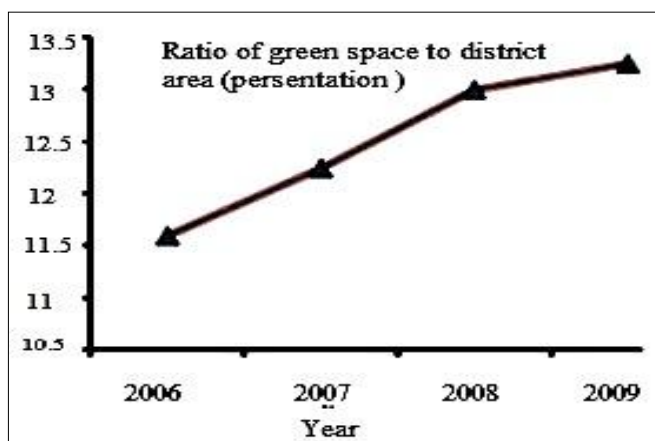


Figure (2): ratio of green space to district area (presentation)

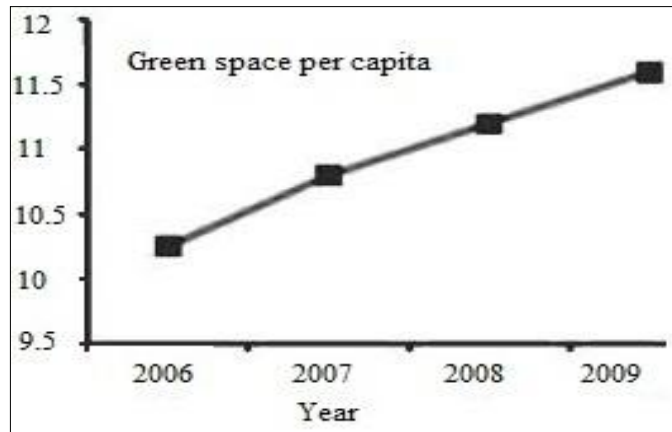


Figure (3) : green space per capita

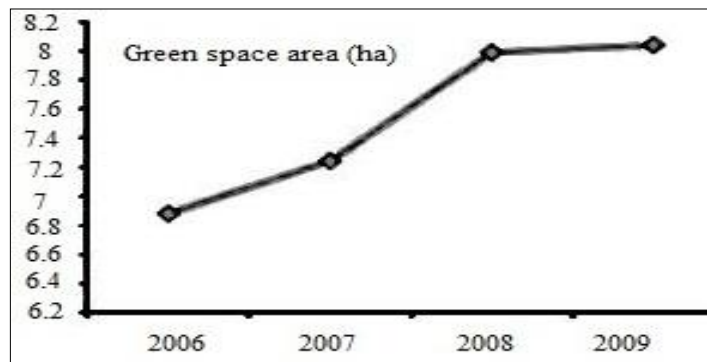


Figure (4): green

space area (ha)

Current condition of Mashhad green spaces

The green spaces management of Mashhad has been from 1972. area of urban green spaces is nearly 142375 hectare. Also, the averages of per capita green spaces in 12 of Mashhad districts are 12.01 m². On the other hands, the most per capita is in district 12 (17.97m²) and the least per capita is district 10 (1.97 m²). So, the distribution of green spaces in Mashhad is heterogeneous. According to report of parks organization, for balancing of green space in city, was suggested that was made parks, green roof, vertical green spaces and etc. Regional and neighborhood parks are appropriate place for citizen as entertainment places. According to the World Health Organization, park spaces can provide physical and social health of people in city. On the other hands, these spaces strengthen urban landscape. So in last decades have been made in city due to important role. Figure 6 show sharp growth of urban green spaces in last years.

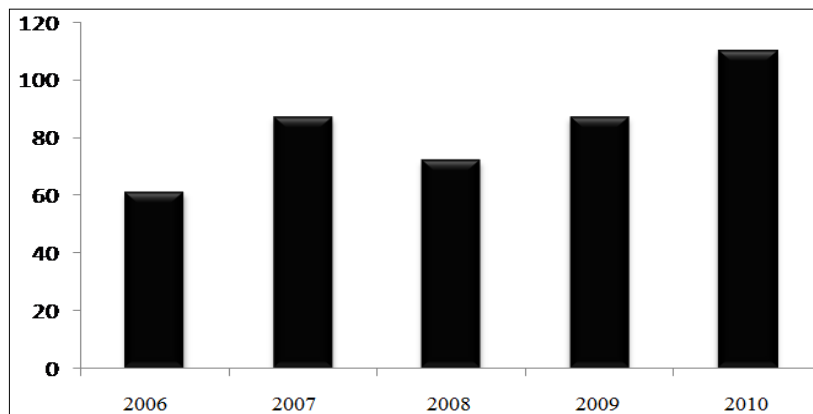


Figure (5): information of parks in Mashhad (2006-2010) Source: parks & green space organization of Mashhad, 2010

Table (2): parks information of Mashhad Source: parks & green space organization, 2010

Parks of Mashhad		
(ha) Total Area	Number	Area
1042	1499	<5hectare
168	28	5-7 hectare
929	44	>7hectare
2140	1571	Total

Table (3): information of Mashhad parks Source: parks & urban green space of Mashhad, 2010

Park area (hectare)	number	district	Park area (hectare)	number	district
67.5	47	12	9.90	88	1
47.3	60	13	124	140	2
79.6	51	14	111	83	3
339	95	15	156.1	174	4
143.2	46	16	156.5	160	5
39.6	60	17	81.7	46	6
150.7	74	18	21.8	43	7
180.4	54	19	30.7	73	8
120.9	122	20	19.3	20	9
77.2	31	21	19.3	31	10
32.3	45	22	49.6	27	11
2138.4			1571		Total

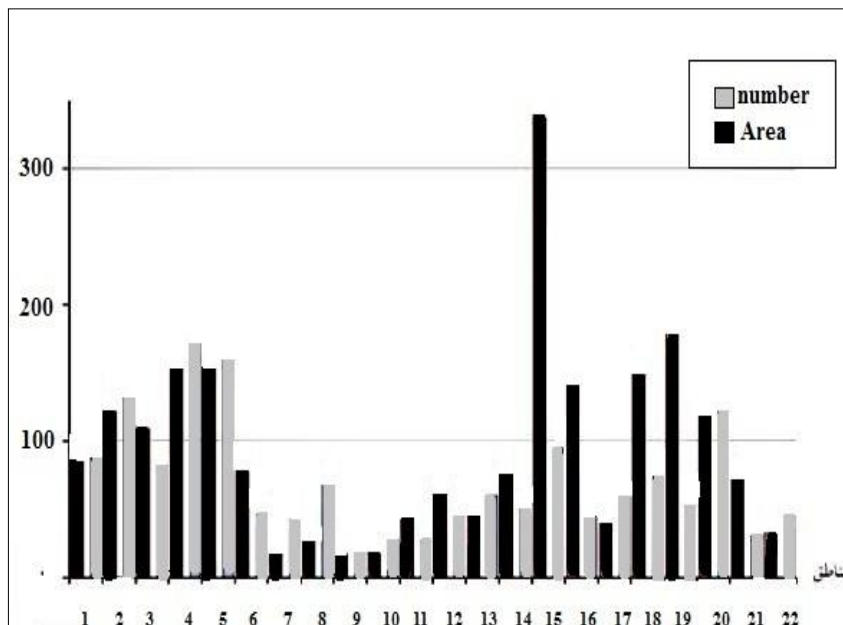


Figure (6): Number & parks area in Mashhad

Developing of Mashhad and necessity of urban green space

The studying of physical-spatial changes show, Mashhad growth sharply. The population in 1967 is 1.53 million and it increase to 6.4 million in 1987. In 2002 the population increase to 1.8 million and then in

2008 the population of Mashhad was 2.9 million. On the other hand, the area of Mashhad was 500 km² in 1972. But in 2008, the area of Mashhad was 730 km² (Iran census center 1967- 2008).

While developing of Mashhad, the land-use was distributed heterogeneous. Creating public and social spaces are important urban issues. Due to high centralization of population in Mashhad, developing of green spaces is necessary. Building of green spaces is the basic issue for achieving sustainable city. Also green space is important due to ecologic effect and emotion of human life (laqae, 1995:6). So, both quality and quantity of green spaces of Mashhad is important. Indeed, parks & green spaces organization hasn't succeeded yet. On the other hand, Mashhad has been located in imbalance slope, so natural conditions affect to green space management (Parivar, 2008: 49).

Figure 7 shows, total area of indoor and outdoor green spaces is 19.7 hectare. By comparing of area green spaces and other land-uses can understand that the amount of green spaces is low.

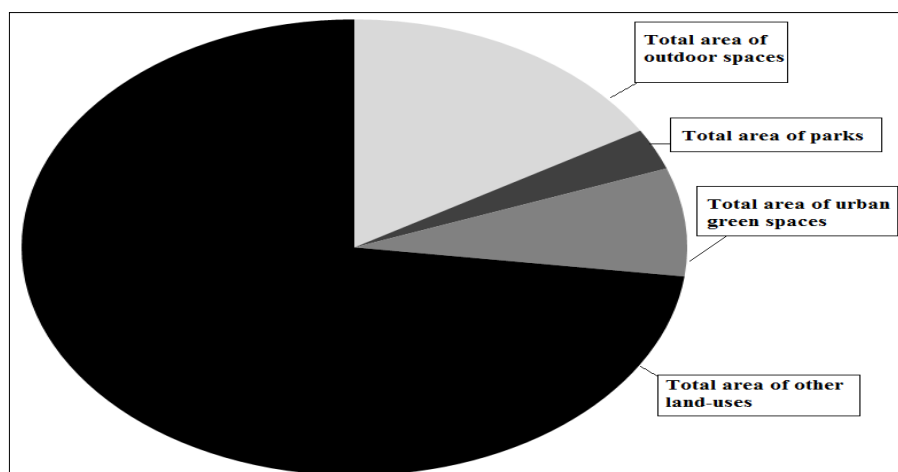


Figure (7): comparison area of land-uses Source: parks & green space organization, 2010

Now, per capita of urban green spaces is 12.6 m² in Mashhad. Mashhad located in dry region and preparing water is difficult. So, Mashhad faces natural elimination. On the other hands, the total area of urban green spaces is 2.28%. According to Presented standards by the UN and other international officials, per capita of green spaces is low with comparison other countries (figure 10).

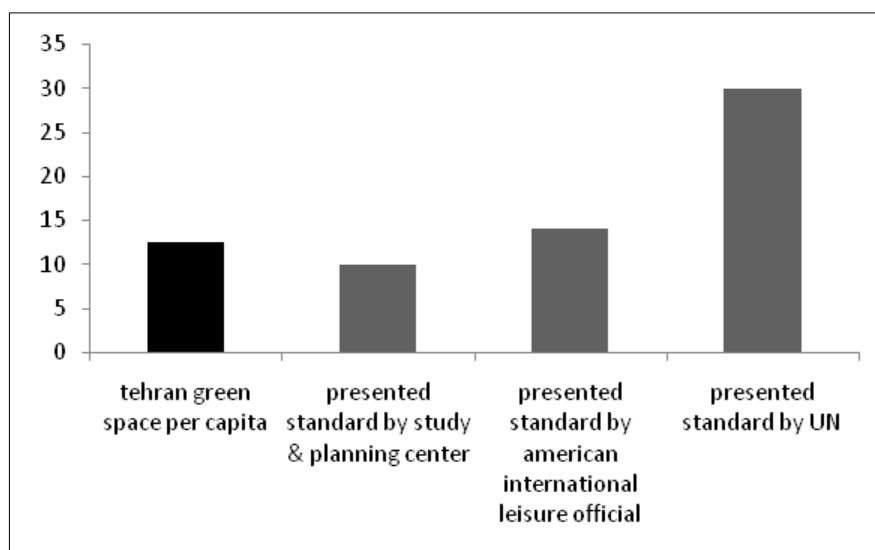


Figure (8): comparison Mashhad per-capita with other presented per-capita

The organizations structure of green spaces management in Mashhad metropolitan

The administration of city has been distributed between organizations. But there isn't cooperation between organizations. So, the organizations need to cooperate each other. However, there are some organizations for administrating of city, but also the main organization is parks & green spaces organization.



Figure (9): the structure of organizations

For promoting of green space management, gardens official was established in 1961. After that, change to parks and green space organization in 1964. Also, the basic changes were created in structure. The traditional methods were removed and were replaced modern technique for administrating city. The basic proposes of this organization are :

- creating appropriate places for spending leisure times
- preparing desirable places for promoting people health and comfort
- creating happy space for resident
- creating beautiful urban landscape and decreasing air pollution
- presentation microclimate that is led to reducing sound pollution
- controlling and protecting parks and green spaces The necessary policy of parks & green spaces organization are: updating equipment and methods of promoting urban green spaces
- developing resident partnership in urban green space introducing economical, social, cultural and environmental values of urban green spaces
- utilization of functional and biological elements for improving urban green spaces.

II. RESULT

Preservation of green space and implementation urban plans in Mashhad show, process of green spaces development is appropriate. Indeed, developing of urban green spaces is the best solution for achieving sustainable city. Implementing of urban green spaces development plans have important role in urban life especially in Mashhad city. In these city urban management both should create urban green spaces and should protect green spaces. Appropriate and systematic plans are necessary for developing of cities. On the other hands , studying of urban plans show , green spaces are the best solution for decreasing air pollution , mental diseases and social problems in metropolitan cities (such as Mashhad) . So has been emphasized to promoting of green spaces. thus , parks & green space organization have done basic programs in order to developing urban

green spaces (such as : preparing water , using of native plants , utilization of modern techniques and etc) These plans are led to creating new green space center in neighborhoods . Also, using of right and efficient management by adaption to current conditions is other important method.

Studied plans show a lot of points, they are:

- The important issue is unification between organizations. Increasing of citizen partnership via increasing public information about behavior between human and environment Utilization of professional xperts in research centers for improving urban life.
- Preparing comprehensive plan of green spaces.
- Revival structure of organization and creating new rules for promoting of urban green spaces.
- Correction of old laws that had been approved in previous time.
- Preparing financial sources for using modern equipments and technique.
- Making standard in urban management.
- Codification urban forest plan.
- Presenting of different models and other urban green spaces plans.
- Creating urban green spaces should be adapted to unique system.
- Strengthening of natural scopes that have been located in Mashhad.
- Prevention of mountainous open space by using native plants
- Changing industrial land-uses to green space land-use.
- Rivers is the most important natural element. so must be prevented from destroying them .

III. NOTE

- 1- Qagar age is the historical period in Iran that was started in 1786 - 1847.
- 2- Pahlavi age is the historical period in Iran that was started after Qagar age .

RESOURCE

- [1]. parivar, parasto(2008): analyzing ecologic structure of Tehran for codification of promotion environment , no51
- [2]. khorasani , (2004): ecologic characterize some appropriate trees for planting in Mashhad , publication of parks & green space organization of Mashhad
- [3]. Zokaee , Mohammad (1999-2008): study & research center of Tehran
- [4]. Parks & green space organization (1999): studying of Mashhad city in order to creating green space.Census center of Mashhad (2002)
- [5]. Sadr (1991): principle of urbanity, Baharestan publication.
- [6]. Dorsay (1994) : sound pollution and Mashhad green space , publication of parks & green space organization of Mashhad
- [7]. Mashhad comprehensive plan (2010)
- [8]. Leqae (1995): planning urban green space , no5&6
- [9]. Mahmudian ,Akbar (2006) , looking to Mashhad , geographic publication
- [10]. Barbosa, Olga etal, 2007, who Benefits from Access to Green Space. A Case Study from Sheffield, UK, Landscape and Planning Journal.
- [11]. Barker, R.G. 1968. Ecological Psychology, Stanford Ca: Stanford University Press.
- [12]. Burel, F, J. Baudry. 2003. Landscape Ecology Concepts Methods and Application. Sience Publishers. INS
- [13]. Baschak, LA & Brown, RD. 1995, "An ecological framework for the planning, design and management of urban river greenways", Landscape and Urban Planning, vol. 33, no. 1-3, pp. 25-211.
- [14]. Dingxi Huang, Chuanting Lu, Guanxian Wang. 2009. Integrated Management of Urban Green Space, The Case in Guangzhou China. 45th ISOCARP Congress 2009.
- [15]. Retieved, 2010. Extrem Temperatures around the world.
- [16]. Tjallingii, S.P. 2000. Ecology on the Edge: Landscape Ecology between Town and Country, Landscape and Urban Planning.
- [17]. Th. Brinkhoff, 2010. The principal agglomerations of the world – population statistics.
- [18]. United Nations. Dept. of Public Information. 1993, Agenda 21: programme of action for sustainable development: Rio Declaration on Environment and Development: Statement of Forest Principles, United Nations Department of Public Information, New York.
- [19]. LI, F & WANG, R. 2004, "Recearc advance in ecosystem service of organ green space", Chinese Journal of Applied Ecology, vol. 15, no. 3, pp. 527-31.

Context of qos In Web Service Selection

Nabil Keskes

Computer science Department, University of Sidi Bel Abbes, Algeria

Abstract: In the recent year, web service selection is becoming more and more prominent due to the large impact the web service in e-commerce. In selecting best services, several candidate services with similar capabilities are provided by different service providers. The question is, how upon a request over a B2B integration scenario, the system chooses a service among several candidate services offering a capability satisfying its requests? The Quality of service presents the key factor to answer this question. In this paper, we continue our work, we emphasize on the effect of increasing the number of qualities (higher than three), and the effect of increasing the number of services (higher than six) on the process of selection of web services based on both context and the QoS ontology for multi dimensional QoS. Finally, some experiments are run so to demonstrate consistency and effectiveness of the proposed method.

Keywords: Selection of services, semantic Web service, quality of service, QoS Ontology, context Ontology, matching.

I. INTRODUCTION

Actually, the Web Service plays an important role in large field for the development of the e-science, e-commerce, and e- education. Still, not all is good. One serious consequence is to delivering relevant service to the user. The web semantic solves these problems, it structures information, adds the logic, it expresses the sense by the ontology, however, there is a certain difficulty concerning semantic heterogeneity and conflicts semantics. Clearly it is not sufficient for the semantic Web to resolve all problems related to the use of ontology. The Pragmatic Web plays an important role to solve these problems especially it describes the semantic of information in their context. The pragmatic Web services are located at the cross roads of two major research areas of the net technology: the pragmatic Web and Web services. The aim of pragmatic Web services is to create a pragmatic Web service whose properties, capabilities, interfaces and effects are unambiguously described and used by machines with introduce pragmatic technologies. Our goal is to find the best provider of e-service that responds to a request for service. To achieve that, the following steps are required:

- Submit the query with terms and values of quality without and within their context.
- Compare the qualities of provider services with the qualities of request.
- Select the best provider service.

In the last step, to select the best provider, we first compute the matching degree of published qualities and required qualities for each service without using the context of quality. Second, we make use of the context of quality and compare the two cases [1] [2]. In our last work, we are showed the importance of context in interpreting the concepts of qualities in selecting processes. In this paper, we present a service selection based on both the context and the QoS ontology where QoS is multi-dimensional. We emphasize on the effect of increasing the number of qualities, and the effect of increasing the number of services on the process of selection of web services. The rest of this paper is organized as follows: Section 2 presents web service selection and related works in the current literature, Section 3 presents some concepts on the context and QoS, Section 4 presents the proposed approach, Section 5 is devoted to experiments and Section 6 concludes this article.

II. WEB SERVICE SELECTION AND RELATED WORKS

From a semiotic point of view, there are two ways to deal for Web services: first, an approach based on Web Socio semantic [3], and second an approach based on the pragmatic web [4].our work focus in the second way. We can group the approaches of selection into several categories:

Selection based on the Matchmaking: Classification of services deals with ranking. This is by determining the degree of similarity between the requested and the provided services. [5][6]

Selection based on Quality of Service (QoS): The classification of services is done by evaluating criteria such as response time, cost, and reputation for delivering such service. Major techniques in the current literature are based on the quality of service, some approach based on one dimension [7] [8] [9] [10] and the others on multi dimensional.

Selection based on context:

Most relevant concepts found in the current literature are summarized as follows: [Gandon F and al 2004]: Stress the need to consider knowledge about user preferences and contextual characteristics to seek information. Their approach is based first on a server context that contains information about preferences, and second, the access rights of a user [11]. [Behr G and al 2004]: propose a framework that operates on four profiles that describe the characteristics of the content or media (type, format, size, location where the media is stored) of the user (preferences), the device (hardware and software capabilities), network and service (media format supported, network connection, bandwidth, latency and performance [12]. [Pashtan and al 2004]: propose to adjust the content delivered by the web service through processing of Extensible Stylesheet Language Transformations (XSLT) [13]. [Keidl M and al 2004]: proposed an integration of the definition of Simple Object Access Protocol (SOAP) in order to find a web service that is able to meet user needs [14].

Selection based on Configurable Web Services

The selection algorithm ranks the offered services and their configurations according to the requester's preferences and thus facilitates personalized selection strategies. In addition, the approach leverages existing Web standards to provide a maximal degree of interoperability between services. Providers and their customers leading to significant efficiency gains. The approach is implemented prototypically and the performance is evaluated by means of a simulation [15].

Selection based on communities

There are two ways for this category: first, an approach a reputation-based Web services community architecture and define some of the performance metrics that are needed to assess the reputation of a Web service community as perceived by the users and providers [16] and second an approach based on the model of communities whose main objective is to allow client applications to select the services which better meet a set of non-functional properties such as quality of service. The model of communities is formalized by a set of abstract data types. Types provide operations which enable service providers to register services to a community and client applications to select services, either at design time or at run time, and those that meet their needs [17].

Selection based on negotiation between Requester and Provider

In this approach, authors propose an agent negotiation framework towards Pragmatics Web Service. First, they abstract the rule and policy for access control to private information about context, preference towards the Pragmatics Web Service. Second, they have formalized the access control rules, context information and preference policy, and stored them in the service ontology base possessed by service agent [18].

III. QOS AND CONTEXT

Selection of service still is an important challenge, especially, when a set of services fulfilling user's capabilities requirements have been discovered, among these services which one will be eventually invoked by user is very critical, generally depending on a combined evaluation of qualities of services (QoS) [19]. Due to the increasing number of Web Services, which provide similar functionality, the non-functional properties are becoming more important during the selection of the best available service. Non-functional properties describe Quality of Service (QoS) as well as context of service execution. Although there are many approaches considering only QoS or context during service discovery and selection, there is a lack of systems taking both non-functional categories into account [20]. In our work, we always associate context to quality. Moreover, this condition justifies the adoption of a use of context; we can define "the context of Quality includes all internal or external elements which is relative to the quality that is necessary to the correct interpretation of the Concept of quality". For reason of simplicity, we choose an approach for modeling of context proposed by [21]. This approach consists to store the context using a set of couples (attribute, value), mainly because of the diversity of the contexts in a multi dimensional QoS. Furthermore, we may say that a formal and practical model of the context is not available, big efforts are provided to define how to capture the context to the system. Our goal is

to give an answer of how to combine the QoS with the context. This is where this paper is supposed to give contribution.

IV. THE PROPOSED SOLUTION

Our work is based on the use of the notion of context to facilitate the process of selection between services. We already have proposed an architecture which uses different qualities of services, and gives the appropriate interpretation for these qualities in their respective context. But remember we introduce some relevant related basic concepts.

4.1 Similarity measures

Measure based on the interpretation of concepts

In [22] the authors proposed a similarity measure of the concepts described in logic, and defined as follows:

$$s(C,D) = \frac{|C \cap D|^I}{|C|^I + |D|^I - |C \cap D|^I} \times \max\left(\frac{|C \cap D|^I}{|C|^I}, \frac{|C \cap D|^I}{|D|^I}\right) \quad (1)$$

Where $(.)^I$ is a function of interpretation and $|.|$ is the cardinal of a set. This measure is interesting because it verifies the semantic properties such as the similarity between two equivalent concepts ($C \equiv D$) is equal to 1.

4.2 The proposed architecture

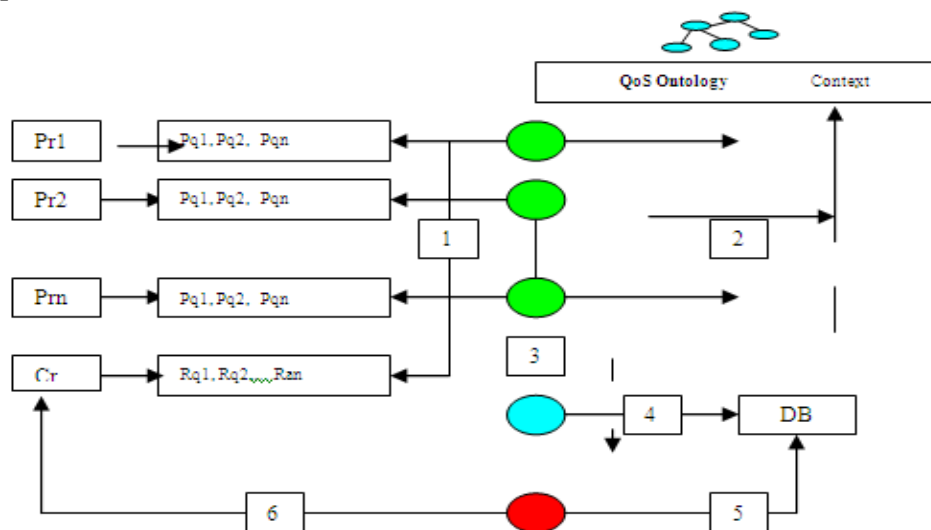
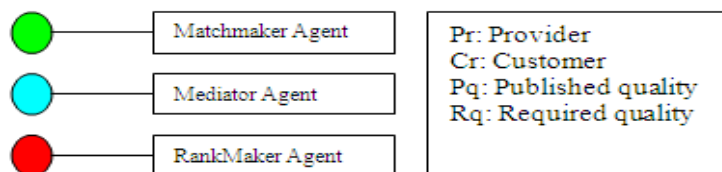


Figure 1: The proposed architecture



Our architecture consists of a set of agents: Matchmaker Agents, Mediator Agent, and a Rankmaker Agent. The process of selection is described as follows:

- 1- Matchmaker Agent consults the required qualities and the published qualities.
- 2- Matchmaker Agent uses QoS ontology to match the required qualities and the published qualities.
- 3- This Agent sends the result by a message to the mediator agent.
- 4- Mediator Agent receives the message that contains the result and stocks it in a Database. This agent connects with Database by using the pilot jdbc: odbc.
- 5- Rankmaker Agent consults this Database and makes the ranking by using Algorithm [23] in two stages without using context and using it.
- 6- Finally, RankMaker sends the result to the consumer.

The primary task of this architecture is ranking through using the proposed algorithm in [23] in two stages without using context and with context. This is resumed as below:

The 1st stage [without using context]

We assume that $Q_R = \{r_1, r_2, \dots, r_k\}$ expresses the profile of a user's quality requirements, which includes k quality metrics. Similarly, the quality profile of m candidate services in set S is denoted as

$Q_S = \{Q_{A1}, Q_{A2}, \dots\}$ Where $Q_{Ai} = \{q_{i1}, q_{i2}, \dots, q_{ij}\}, i, j \in N$. Therefore, the matrix of QoS for service matchmaking $M_Q = \{Q_R, Q_{A1}, \dots, Q_{Am}\}$ with the quality requirements Q_R in the first row, and the quality information of candidates services in the other rows. For uniformity, matrix M_Q has to be normalized [23], i.e., the elements of the matrix are real numbers in the range [0, 1], the result matrix is $M_{Q'}$. Finally, we compute the evaluation result for each quality metrics by summing the values of each row. These abstract values are taken as a relative evaluation of each service's QoS.

$$M_{Q''} = M_{Q'} \times W = \sum_{i=1}^M (q_{ij} \times w_j) \quad (2)$$

$W = \{w_1, w_2, \dots, w_n\}$, Where w represents the weighted value for each quality metrics.

The 2nd stage [use of context]

We use the semantic distance (equation 1) because this distance may introduce the required interpretation in this method.

We assume C_j The Context of Quality r_j for customer

We assume C'_{ij} The Context of Quality q_{ij} for service

The interpretation of required quality in context is: C_j^I

The interpretation of published quality in context is: C'_{ij}^I

We apply equation (1)

$$S(C_j, C'_{ij}) = \frac{|C_j \cap C'_{ij}|^I}{|C_j|^I + |C'_{ij}|^I - |C_j \cap C'_{ij}|^I} \times \max\left(\frac{|C_j \cap C'_{ij}|^I}{|C_j|^I}, \frac{|C_j \cap C'_{ij}|^I}{|C'_{ij}|^I}\right) \quad (1)$$

The degree of match with context for q_{ij} present by the average between the normalize value of q_{ij} and semantic distance $S(C_j, C'_{ij})$, after we compute the evaluation result for each quality metrics with context by summing the values of each row (equation 2). These abstract values are taken as a relative evaluation of each service's QoS with context. In our case the context presents additional information, therefore we compute the degree of matching without use QoS ontology, then we take the average match degree that specifies the relation existing between the context and the quality of service.

V. EXPERIMENTAL RESULTS

In the last paper [2], we showed the performance of selecting web services using three quality services is similar to the one using up to seven quality services, and we proved the selection of web services using three qualities (price, ComRat, Repu) is well adapted up to six services. This paper emphasize on the effect of increasing the number of qualities (higher than three), at beginning we take four qualities (price, ComRat, PenRat, Repu).

Table1: experiment data with five qualities.

	Pri	CompRat	PenRat	Execu	Repu
s1	25	0,7	0,3	100	2,0
s2	25	0,8	0,1	40	2,3
s3	40	0,2	0,8	200	2,5
s4	55	0,6	0,5	104	4,0

Table2: Normalization

Pri	CompRat	PenRat	Execu	Repu	
1,000	0,799	0,287	0,625	0,000	6,510
0,998	1,000	0,000	1,000	0,167	7,324
0,497	0,000	1,000	0,000	0,235	3,458
0,000	0,735	0,601	0,597	1,000	4,668

Table3: result of selection with 5 qualities

s2	7,324
s1	6,510
s4	4,668
s3	3,458

We repeat with four qualities (price, ComRat, PenRat, Reput)

Table4: experiment data with four qualities

Pri	CompRat	PenRat	Repu	
1,000	0,799	0,287	0,000	5,885
0,998	1,000	0,000	0,167	6,324
0,497	0,000	1,000	0,235	3,458
0,000	0,735	0,601	1,000	4,071

The result of ranking is:

Table5: experiment data with four qualities

s2	6,324
s1	5,885
s4	4,071
s3	3,458

In table 3 we can find the results of ranking procedure with 5 qualities, and in table 4 we can find The results of normalization and QoS with four qualities (price, ComRat, PenRat, Reput), and table 5 shows results of ranking procedure with four qualities. Through this example, we observe that for these four services, the result with four qualities is the same as with five. To check this hypothesis, we apply the Kolmogorov-Smirnov test:

Table6: Kolmogorov-Smirnov test for 4 services

1,00	0,50	0,33	0,25	0,20	
0,0417	0,001736	7,2E-05	3,01E-06	1,25587E-07	
0,9583	0,498264	0,33326	0,249997	0,199999874	0,958333333

In table 6 we repeated this experiment five times with random values generated by function "runif" of language R as mentioned before. For entries n=4 and $\alpha=0.05$, the value of doorstep according the statistics table Kolmogorov-Smirnov is 0.6239. In our experiment $D = \max |F_n(x) - F(x)| = 0,958333333$; that is higher than 0.6239. This shows that the result for five qualities is the same as for with four qualities. We repeated this experiment for 5, 6, 7, 8 services.

Table 7: Kolmogorov-Smirnov test for 5,6,7,8 services

N=number of services	D
5	0,999999421
6	0,998611111
7	0,999801587
8	2,48016E-05

The table 7 resumes the results. Through those experiments, it is shown that when the number of services is higher than seven, the value of D is smaller than 0.6239, therefore we may say that the hypothesis is accepted up to seven services, that is the selection of web services using four qualities (price, ComRat, PenRat,Repu) is well adapted up to seven services. Finally, to illustrate this approach, we propose a purchasing scenario so to demonstrate consistency and effectiveness of the proposed method. In table 14, there are six providers S1 to S6, all of them providing the same services. The evaluation of quality of services is made by multi-dimensional QoS. The second, third, and fourth columns represent respectively price, Compensation Rate, and Reputation. The fifth, sixth, and seventh columns represent the normalization of quality; the eighth column is the current values of each QoS. Following the proposed method in section 4.2, we first start with identifying the effect of the context on the selection of services based on QoS. In the first time, the context is not used; the results obtained after calculating QoS are illustrated in the figure2 Following this step, we rely on the context to select the best service for a particular request. The results obtained are illustrated in the figure3. In Figure 2, the best service is S3 and in Figure 3 it is S2. Through this example, we notice that the context affects the process of selection. Furthermore, we repeat this experiment thirty one times. We try to check the dependencies existing between the two major variables: QoS modality with context and QoS modality without context. In all those experiments, we observed that the ranking procedure without context is different that with context. We make use of the χ^2 test. In this experiment, the observed frequency is 31, the theoretical frequency is 31. This means that we can accept the hypothesis of dependencies. We may assert that the QoS depends on the context. Future work will emphasize on extending the proposed method by increasing the number of services in the selection process. We implemented computer simulation of several scenarios using jade [http://jade.tilab.com] for implementing agents and Jena [http://jena.sourceforge.net] for interaction with ontology, and finally R language for generating random values.

VI. CONCLUSION

This paper continued our work of selection of web services based on both context and the QoS ontology. This is done by proposing an architecture that makes an automatic selection of best service provider that is based on mixed context and QoS ontology for a given set of parameters of QoS. We first showed that the performance of selecting web services using four quality services is similar to the one using up to seven quality services. Moreover, other experiments demonstrate that the QoS is strongly dependent of the context. Furthermore, future work may emphasize on the effect of increasing the number of qualities, and the effect of increasing the number of services on the process of selection of web services based on both context and the QoS ontology.

REFERENCES

- [1]. Nabil keskes, Ahmed Lehireche, and Abdellatif Rahmoun. (2010). Web Services Selection Based on Context Ontology and Quality of Services, International Arab Journal of e-Technology, Vol. 1, No. 3, January 2010.
- [2]. Nabil keskes, Ahmed Lehireche, and Abdellatif Rahmoun. (2011) Web Services Selection Based on Mixed Context and Quality of Service Ontology, Computer and Information Science ,Vol. 4, No. 3; May 2011
- [3]. Manuel Zacklad. (2005). Introduction aux ontologies sémiotiques dans le Web Socio Sémantique In :JAULENT,M,-C, 16emes journées francophones d'ingenerie des connaissances,30-03 avril 2005,NICE.Grenoble : PUG, 2005,p12
- [4]. Aldo de Moor, van den Heuvel. (2004). Web service selection in virtual communities, System Sciences
- [5]. Proceedings of the 37th Annual International Conference, Hawaii, on Volume, Issue Page(s): 10, [Online]Available: <http://doi.ieeecomputersociety.org/10.1109/HICSS.2004.1265468>
- [6]. Christophe Rey. (2002). Dynamic discovery of e-services: a Description Logics based approach.Symposium on the Effectiveness of Logic in Computer Sciences (ELICS02) in Honour of Moshe Vardi Poster Presentation. March 4 - 6, Saarbruecken. Germany, ISBN:1-59593-046-9 doi>10.1145/1060745.1060823.
- [7]. Michael C. Jaeger, Stefan Tang. (2004). Ranked Matching for Service Descriptions using DAML-S,
- [8]. pp217-228,Workshops: Riga, Latvia - Vol. 3, [Online] Available:<http://citeseerx.ist.psu.edu/viewdoc/summary?doi=10.1.1.88.3787>.
- [9]. Y.Liu, A. H.H. Ngu. (2004). QoS Computation and Policing in Dynamic Web Service Selection, Proceedings of the 13th international World Wide Web conference on Alternate track papers & posters. New York, NY, USA, pp 66 - 73, [Online] Available: <http://citeseerx.ist.psu.edu/viewdoc/summary?doi=10.1.1.2.1739>.
- [10]. Padovitz, S. Krishnaswamy, S. Wai Loke. (2005). Towards Efficient Selection of Web services, 17th IEEE
- [11]. International Conference on Volume, Issue, 16-16 Nov, Page(s):5 pp. – 376, [Online] Available: <http://doi.ieeecomputersociety.org/10.1109/ICTAI.2005.122>.
- [12]. Bonatti, P. Festa. (2005). On Optimal Service Selection, Proceedings of the 14th international conference on
- [13]. World Wide Web, Chiba, Japan, pp.530 – 538, ISBN:1-59593-046-9 doi>10.1145/1060745.1060823
- [14]. Maximilien and P. Singh. (2004). Multi agent System for Dynamic Web Services Selection, IEEE InternetComputing. _Volume 8, Issue 5, pp84- 93, [Online] Available:<http://citeseerx.ist.psu.edu/viewdoc/summary?doi=10.1.1.67.2076>.
- [16]. Gandon F. Sadeh N. (2004). Semantic Web Technologies to Reconcile Privacy and Context A wareness. Journal
- [17]. of Web Semantic, vol .1, n3,pp.241-260, doi:10.1016/j.websem.2003.07.008 Key: citeulike:1019436.

- Behr G, Brunei L., Pierson J.M. (2004). Modeling Service-Based Multimedia Contents Adaptation in Pervasive Computing, Actes de la 1ere Conference Computing Frontiers, Ischia, Italie, ACM Press, pp 60-90, ISBN:1-58113-741-9 doi>10.1145/977091.977102.
- [18]. Pashtan A. Heusser A, Sheuermann P. (2004). Personal Service Areas For Mobile Web Applications. IEEE Internet Computing, vol .8, n 6, pp 34-39, doi:10.1109.
- [19]. Keidl M., Kemper A. (2004). Toward Context-Aware Adaptable Web Services, Actes de 13eme conference WWW, New York, ,USA, pp. 55-65, ISBN:1-58113-912-8 doi>10.1145/1013367.1013378.
- [20]. Steffen Lamparter, Anupriya Ankolekar. (2007). Automated Selection of Configurable Web Services Proceedings of the 16th international conference on World Wide Web, ACM New York, NY, USA, ISBN: 978-1-59593-654-7, pp.441-458, [Online] Available: <http://citeseerx.ist.psu.edu/viewdoc/summary?doi=10.1.1.73.6109>.
- [21]. Hamdi Yahyaoui and al. (2008). On the Reputation of Communities of Web Services, NOTERE 2008 June 23-27, 2008, Lyon, France, ACM pp. 9-16, ISBN: 978-1-59593-937-1 doi>10.1145/1416729.1416735.
- [22]. Marie-Christine Fauvet. (2008). Sélection dynamique de services Web – une approche à base de communautés; projet Web Intelligence - Cluster ISLE - Région Rhône-Alpes; France; pp. 505-520.
- [23]. Sheping, Z., Zengzhi, L., & Juanli, W. ,“Negotiation between requester and provider based on Pragmatics Web Service”,Proc. 2009 WRI Int. Conf. on Communications and Mobile Computing, IEEE Computer Society.vol. 3, pp. 583-587, 2009.
- [24]. Xia Wang and al. (2006). A QoS-aware Selection Model for Semantic Web Services, ICSOC 2006 ,Volume 4294, pp 390-401, Spring-Verlag Berlin Heideberg, [Online] Available:<http://citeseerx.ist.psu.edu/viewdoc/summary?doi=10.1.1.93.4360>.
- [25]. Iris Braun, Anja Strunk, “ConQo – A Context- And QoS -Aware Service Discovery “Proceedings of the IADIS International Conference on WWW/Internet ,Freiburg, Germany, 2008.
- [26]. Dey A. K., Salber D. and Abowd G. D. (2001). A Conceptual Framework and a Toolkit for Supporting the Rapid Prototyping of Context-Aware Applications. Human-Computer Interaction Journal 16(2-4), pp. 97-166,doi>10.1207/S15327051HCI16234_02.
- [27]. D’amatoc, fanizzi. (2006). A dissimilarity measure for ALC concept descriptions, SAC’06: Proceedings of the ACM symposium on Applied computing, New York, USA, ACM Press, pp 1695–1699,ISBN:1-59593-108-2 doi>10.1145/1141277.1141677.
- [28]. Xia Wang and al. (2006). A QoS-aware Selection Model for Semantic Web Services, ICSOC 2006 ,Volume 4294, pp 390-401, Spring-Verlag Berlin Heideberg, [Online] Available:<http://citeseerx.ist.psu.edu/viewdoc/summary?doi=10.1.1.93.4360>.

Treatment of Municipal Wastewater by using Rotating Biological Contractors (Rbc's)

Prashant A.Kadu¹, Amruta A.Badge², Dr.Y.R.M.Rao³

¹Associate Profesor, Department of Civil Engineering, Prof. Ram. Meghe Institute of Technology & Research, Badnera, Amravati,(M.S.) India.

²Lecturer, Department of Civil Engineering, G.H.Raisoni polytechnic Amravati, (M.S.) India.

³Principal, Dr. Paul's college of Engineering, Vannur, Villupuram, Dist., Tamil Nadu, India.

Abstract: The rotating biological contactor process offers the specific advantages of a biofilm system in treatment of wastewater for removal of soluble organic substances. It is a unique adaptation of the moving-medium biofilm system which facilitates easy and effective oxygen transfer. Media in the form of several large flat or corrugated discs with biofilm attached to the surface is mounted on a common shaft partially submerged in the wastewater and rotated through contoured tanks in which wastewater flows on a continuous basis. The compactness of the system and its economical operation makes it a viable option specially suited for decentralized wastewater treatment technologies. The process optimisation and adaptability under different environmental conditions and influent characteristics remain challenging tasks for the efficient use of this technology. Oxygen is accepted to be one of the most important and often limiting substrates in an aerobic treatment process. Oxygen transfer through the water film developed on a rotating disc revealed that the oxygen transfer coefficient varies with the rotational speed and the location on the exposed disc surface. Increase of ambient temperature resulted in decrease of the oxygen mass transfer rate. The biofilm model was implemented for a three stage rotating biological contactor based on a laboratory-scale experimental set-up. The process kinetics was adopted from the Activated Sludge which represents a mixed culture biomass environment.

Keywords: Empirical Correlation, Factors affecting performance, Bioflim system, Influent, Behavior of overall oxygen transfer

I. INTRODUCTION

The consumption of resources and energy based on human activities followed by huge amount of wastes has being one of the most serious problems all over the world. It leads to terrible destruction of the global or regional environment, and its negative effects on human being's health as well as global ecosystem are appearing evidently. It is therefore necessary to establish the effective technology, i.e., prevention of emissions and saving resources and energy. Water is our most precious resource. The cleanliness of our lakes, rivers and oceans is one of the pressing goals for environmental protection. The balance of nature depends therefore on the comprehensiveness of our approach to solve the problem of wastewater disposal. If water of high organic matter content or biochemical oxygen demand (BOD) value flows into a river, the bacteria in the river will oxidize the organic matter consuming oxygen from the water faster than it dissolves back in from the air. If this happens, fish will die from lack of oxygen, a consequence known as fish kill. A stream must have a minimum of about 2 mg/l of dissolved oxygen to maintain higher life forms. In addition to this life-sustaining aspect, oxygen is important because the end products of chemical and biochemical reactions in anaerobic systems often produce aesthetically displeasing colours, tastes and odours in water [1]. The implementation of suitable methods for the disposal of wastewater dates back to the times of Roman civilization. However, it was only in the later part of the 19th century that a spurt of activity in the realm of wastewater treatment took place. The growth of the human population, urbanization and industrialization necessitated the treatment of wastewater. It became evident that the untreated wastewater which was discharged directly into water bodies caused pollution and posed health hazards. The objective of sewage treatment is to produce a disposable effluent without causing

harm to the surrounding environment and prevent pollution. For it analysis of the effluents COD and BOD need to be carried out and the values obtained used to establish an empirical relation for easy conversion of COD to BOD5. Comparison of BOD with COD assesses whether the compound is readily biodegradable. For BOD5, an indication is that a COD:BOD ratio of greater than 100 means that the compound is relatively non-biodegradable and a ratio of less than 10 that it is relatively degradable. However, low BOD5 may merely mean that the test microbes need longer than the test period to begin breaking the compound down and therefore ultimate BOD or other biodegradation testing is generally much more reliable [9]. The results obtained would provide the tool for effective monitoring and evaluation of the effluent by the selected industries and the monitoring agencies. In addition, this work will facilitate rapid effluent assessment or process control by the industries once the chemical oxygen demand is measured or vice versa.

II. RBC UNIT

Rotating biological contactors (RBCs) are mechanical secondary treatment systems, which are robust and capable of withstanding surges in organic load. The rotating disks support the growth of bacteria and micro-organisms present in the sewage, which break down and stabilize organic pollutants. To be successful, micro-organisms need both oxygen to live and food to grow. RBC consist of parallel, deformed discs mounted perpendicularly on a shaft that is slowly rotated in a tank through which the wastewater to be treated is passed. The shaft is mounted above the water level in the tank. Oxygen is obtained from the atmosphere as the disks rotate. As the micro-organisms grow, they build up on the media until they are sloughed off due to shear forces provided by the rotating discs in the sewage. Effluent from the RBC is then passed through final clarifiers where the micro-organisms in suspension settle as sludge. The sludge is withdrawn from the clarifier for further treatment [2]. The rotor has to turn continuously without any longer interruption that could harm the function of the bacteria and thus lower the efficiency. The bacteria need a continuous food source provided by a constant inflow of effluent from the reactor or wastewater. Therefore, the RBC inflow tank (Fig 1) is filled up with the needed amount of daily inflow. The tank is filled manually with the free submersible pump. To fill the inflow tank by pump power must be on. The upper layer on the tank indicates the fill level. The treated effluent is disposed off through the free pump directly to the environment. Make sure that the pipe outlet is placed outside the shed, at a place, where the disposal does not cause any inconvenience [3].

2.1 Factors affecting performance

Overall performance of RBC systems for nutrient removal from wastewater depends upon several factors:

- Influent wastewater characteristics
 - Hydraulic loading rate
 - Organic loading rate
 - Ammonium loading rate
 - pH
- System configuration
 - Rotational speed
 - Specific surface area of discs
 - Disc submergence
 - Number of stages
 - Recirculation rate
 - Drive mechanisms
 - Shaft arrangement (common shaft with single rpm or separate shaft for each stage)
- Oxygen transfer rate
- Ambient and wastewater temperature
- Media density

The most important physical factors affecting the overall removal efficiency of the system are oxygen mass transfer rate and temperature. Oxygen transfer rate is again dependent on operating temperature and physical set-up of the system. The thickness of the biofilm is controlled by the availability of nutrients and surface turbulence due to rotational speed. However, during scale-up, it is the peripheral speed on the discs which is the governing factor in the growth of the biofilm and the resultant thickness. Usually the peripheral velocity at the rim of the disc needs to be below 20cms-1[4]

2.2 Operating problems

- Shaft failures,
- Media breakage,

- Bearing failure and
- Odor problems

2.3 Biofilm system

Over the years, the treatment of wastewater using biofilm technologies has been established to be an efficient and proven technology with relatively stable end-products. They offer an ideal alternative, mainly as a secondary or tertiary biological treatment unit for the simultaneous removal of organic substances, nitrogen and other nutrients in municipal wastewater. Biofilm systems may be broadly divided into two categories: fixed-medium systems and moving-medium systems [5]. During the treatment process, microbes that remove the organic material in the wastewater (by using the organic material as a food source) attach themselves to the disc surfaces. They grow in a thin biofilm, whose thickness is controlled by the shearing force of the discs being rotated through the water. By rotating out of the water into the atmosphere, the microorganisms, growing on the disc, are provided oxygen. The surplus microorganisms that are sheared off the discs are carried with the wastewater to clarifiers where they are separated from the treated wastewater by settling out. The settled solids are then pumped from the bottom of the clarifier for further processing, most commonly, for use as fertilizer or soil amendment [6].

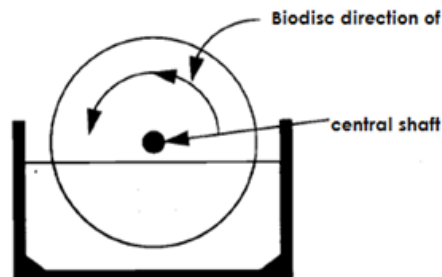


Fig 1: rotating biological contactor

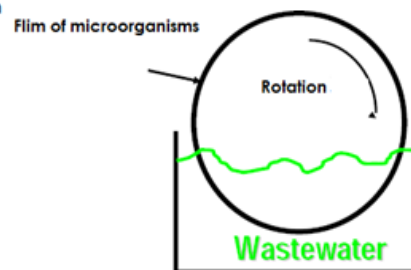


Fig 2: biofilm formation

2.3.1 Biofilm system offers the following advantages [7]

- High biomass packing density and reactor compactness due to a large specific surface area
- Short contact periods and co-habitation of aerobic and anoxic micro-organisms within the ameecosystem
- Reduced sludge bulking and better sludge thickening qualities
- Lower sensitivity and better recovery from shock loadings
- Low energy requirements and more economy in operation and maintenance
- Low sludge production and superior process control
- Simple in operation and maintenance

III. MATERIALS AND METHODS

In operation, a media, consisting of a series of circular disks of different diameter sets are mounted side by side on a common shaft is rotated through the wastewater flow. The shaft continually rotates at 3 to 16 rpm, and a layer of biological growth 2 to 4 mm thick is soon established on the wetted surface of each disk. The organisms in the slime remove organic matter from the wastewater for aerobic decomposition. Typically, a single contactor is not sufficient to achieve the desired level of treatment, so a group of contactors are used in series. Each individual contactor is called a stage and the group is known as a train.

3.1 Materials

The acrylic sheet surface was made rough with the help of sand paper. PVC pipe (shaft) of diameter 20 mm having length 60 cm for each stage was mounted at the top of semi circular pipe with the help of bearings. The disks were fixed equidistant from each other on the shaft. These disks were fixed with the help of screws. The two pulleys were created with the help of card boards. The pulleys were fixed at either side of the shaft. The AC motors were fixed on the semi-circular rectangular shaped card – board sheet on the either side. Plastic pulleys were attached to the motor. Due to the pulleys on two motor and two pulleys on two shafts, two rubber belts were mounted on each motor and one shaft. Electric supply from source to the electric motor was passed through the transformer and the current regulator.

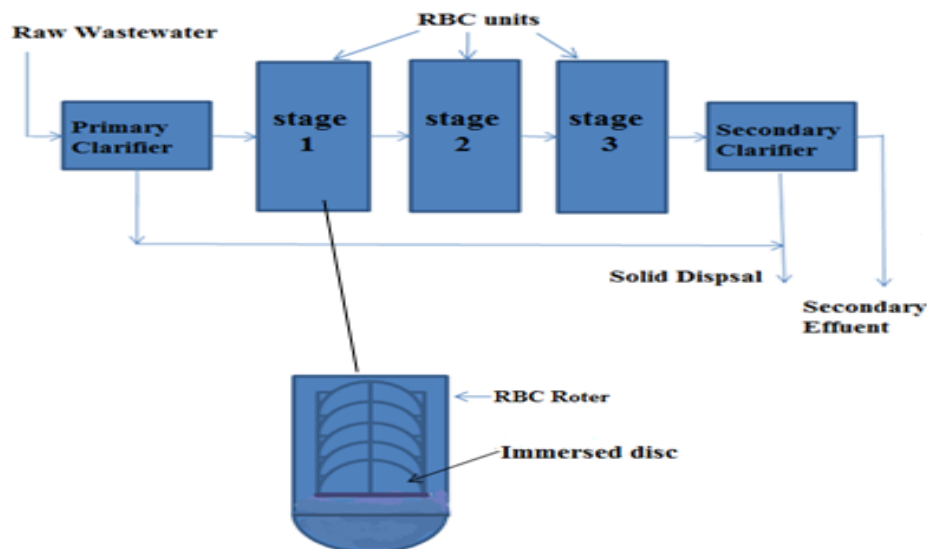


Fig 3: layout of the three-stage rotating biological contactor.

1.2 Methods

The samples collected before and after treatment were analyzed for pH, TSS, BOD₅ and COD by using standards methods.

3.2.1 Five-Day Biochemical Oxygen Demand (The Dilution Method)

The dissolved oxygen content of liquid was determined by the Azide modification of the Winkler's method before and after incubation for five days at 20°C. The difference gave the BOD₅ of the sample after allowance had been made for the dilution, if any, of the sample. For optimum biochemical oxidation, the pHs of the samples for analysis was 6.5 to 8 [8]. pH value was determined by pH meter.

3.2.2 Chemical Oxygen Demand (COD) Using the Open Reflux Method

The sample, to be measured, was oxidized under reflux with a known amount of potassium dichromate in strong sulphuric acid with silver sulphate as a catalyst. Organic matter reduced part of the dichromate and the remainder was determined by titration with iron (II) ammonium sulphate or iron (II) sulphate using ferroin as indicator. Interferences from chloride were suppressed by the addition of mercuric sulphate to the reaction mixture. The chemical oxygen demand (COD) was expressed as milligrams of oxygen absorbed from standard dichromate per liter of sample [8].

3.2.3 Total suspended Solids (TSS) Using the Gravimetric after filtration

Dry a glass fiber filter in an aluminum foil dish to constant weight at 103 °C, cool it in desiccators and weigh it and the dish. Filter a known volume of sample water through the filter. Place the wet filter and trapped solids in the dish again it in the oven to constant weight at 103 °C again and weigh it again. Subtract the first weight from the second weight and divide by volume of sample in liters to get suspended solids in mg/lit [8].

IV. RESULTS AND DISCUSSION

The objective of study is to find out the variation in overall oxygen transfer coefficient and aeration efficiency by varying the parameters- no. of disks, diameter of disks, rpm of disks, supplemental aeration etc. The purpose of different scales was to observe the variation in performance efficiency with scale-up operation. Each RBC reactor configuration has three stages separated by baffles to prevent mixing and initiate desired removal processes. The experimental work described here consists of series of controlled experiment on wastewater (from nalla around the Amravati City premises) taken in oxidation ditch using mechanical submerged aerators only.

4.1 Source of influent and Duration of Work

Influents were taken from the sewer (nalla) containing municipal sewage (wastewater) located in the Amravati campus. For the analysis three points were decided for the wastewater collection. Sampling of wastewater was done from Aug. 1 -30, 2012 for Sample-A (no heavy organic loading), Sept 1 -30, 2012 for

Sample-B (higher COD as well as TSS) and Oct 1 – 30, 2012 for Sample-C (higher BOD). The entire period of the study was four months, spanning from July to Oct. 2012. Data were collected from a RBC reactor over a period of four months. The result of the study is given below. The tables are represented graphically for better appreciation of the results.

It was observed that the results various with dissolved oxygen level, rotational speed, numbers of disks, diameter of disks. For every set of observation, BOD₅, COD, and TSS are computed and its behavior is studied with respect to other variables. The tables are represented graphically for better appreciation of the results. The results obtained during the effluent analysis from the selected source are depicted in Fig: 3.

Table 1: Characteristics of municipal wastewater

Sample		A		
Diameter of disk (cm)		24		
No. of disk		12		
r.p.m.		8		
HRT (hrs)	Stages	BOD (mg/l)	COD (mg/l)	TSS (mg/l)
0	Influent	131.72	268.82	159.25
2	PST	120.4	246.4	145.7
4	I stage	58.39	132.81	83.78
6	II stage	34.19	85.75	54.2
8	III stage	19.75	61.35	35.99
10	Effluent	12.28	49.28	28.41

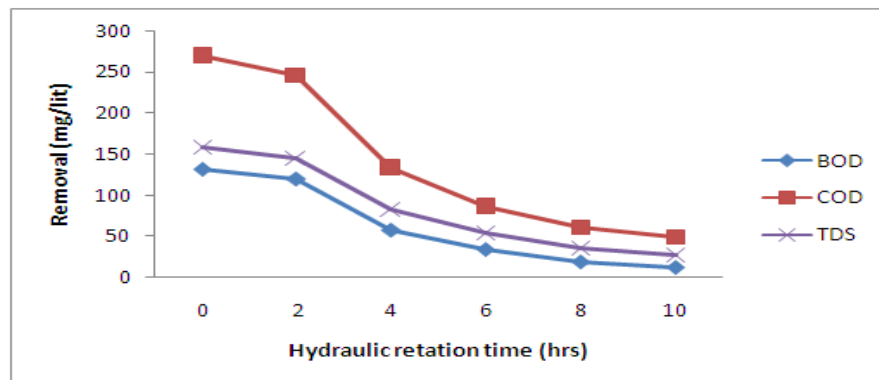


Fig 3: Optimum removal (mg/lit)

4.2 Behavior of overall oxygen transfer

4.2.1. Behavior of overall oxygen transfer with speed (rpm):

From the graphs, it is clear that result for O₂ transfer increases with the speed of 8 r.p.m. The maximum removal of BOD₅ in sample A was observed of 12.28 mg/l (89.8%). For waste water treatment, by rotating biological contractor, normally the rotational speed cannot be made very high. This checks the high peripheral velocities, which may cause shearing off the liquid film and consequently substrate limitations in the biofilm. Keeping this in mind, the rotational speed was restricted to 10 r.p.m. But the % removal rate was again get decreases with increasing or decreasing rotational speeds i.e with 10 r.p.m. and 6 r.p.m.

4.2.2 Behavior of overall oxygen transfer with surface area of the disks:

For the experimental work, the disks of 20cm, 22 cm, and 24cm diameter were used. It has been observed that the surface area of the disks increases; the value of oxygen transfer also increases. The maximum removal rate for BOD₅, COD and TDS for 24cm diameter a disk was observes as 89.8%, 80%, 55.5% and 80.5% respectively when 12 numbers of disks were rotated at 8 r.p.m.

Similarly, the maximum value of removal for 22cm diameter disks was observed as 84.2%, 77.3%, 46.5% and 75.3% respectively and for 20cm diameter disks was observed as 80.2%, 75%, 45.1% and 70.9% respectively when 12 numbers of disks were rotated at 8 rpm.

V. CONCLUSION

The RBC is an efficient method of treating wastewater because of its simplicity to maintain and operate, low energy consumption, ability to withstand shock or toxic load, freedom from odors and good sludge settling properties. RBC energy consumption is equivalent to or less than extended aeration activated sludge plants, and it requires less maintenance and operational skill. For small wastewater treatment plant, the capital cost of RBC is lower than activated sludge plant; therefore, RBC can result in more savings for small communities. Owing to the low loading rate of sewage, biofilm was fully developed only in the first stage.

The influent with an initial BOD₅ of 131.72 mg/l was reduced to a BOD₅ of 58.39 mg/l in the first stage, a reduction of 51.5%. The average BOD₅ of the effluent over a period of 10 hours was 12.28mg/l, a reduction of 89.8%. Initial COD of the influent 268.82 mg/l was reduced to 46.1% i.e. 132.81 mg/l in the first stage and effluent COD was observed as 49.28 mg/l i.e. nearly 80% removal. TSS removal rate was nearly 80% overall. But the sludge handling from primary and secondary clarifiers requires stabilization and disposal. Also the system requires daily attendance to biological process and maintenance of the equipment.

Typical Applications of RBC:

- Municipal wastewater treatment
- Food and Beverage wastewater treatment
- Landfill leachate
- Refinery and petrochemical wastewater treatment
- Pulp and paper wastewater treatment
- Septage treatment

REFERENCES

- [1]. Hach, C.C., Klein, R.L. Jr. and Gibbs, C.R., 1997. Introduction to Biochemical Oxygen Demand; Technical Information Series – Booklet No. 7. Hach Company, U.S.A.
- [2]. Boyles, W. 1997. Manganese III Chemical Oxygen Demand; Technical Paper. Hach Company, U.S.A.
- [3]. Metcalf and Eddy, Inc., 1995. Wastewater Engineering: Treatment, disposal and reuse. 3rd Edition. Tchobanoglous G. and F.L. Burton F.L. [eds.]. Tata McGraw-Hill Publishing Company Ltd., New Delhi.
- [4]. Boyles, W. 1997. The Science of Chemical Oxygen Demand; Technical Information Series, Booklet No. 9. Hach Company, U.S.A.
- [5]. DUTTA, S.: Mathematical Modeling of the Performance of a Rotating Biological Contactor for Process Optimisation in Wastewater Treatment. Karlsruhe 2007 (Verlag Siedlungswasserwirtschaft Karlsruhe).
- [6]. Ayyub, B.M. and McCuen, R.H., 1997. Probability, Statistics and Reliability for Engineers. CRC Press LLC, N.Y. U.S.A.
- [7]. Tchobanoglous, G. and Burton, F. (1995). “Wastewater Engineering-Treatment, disposal and reuse”, Metcalf and Eddy, Inc. 3rd edition, McGraw-Hill, New York.
- [8]. APHA. 1992. Standard Methods for Water and Wastewater Examination 18th Edition. American Public Health Association, Washington, D.C. www.cefic.com

Strength of Ternary Blended Cement Sandcrete Containing Afikpo Rice Husk Ash and Saw Dust Ash

L. O. Ettu¹, O. M. Ibearugbulem², K. O. Njoku³, L. Anyaogu⁴, and S. I. Agbo⁵
^{1,2,3,4,5}Department of Civil Engineering, Federal University of Technology, Owerri, Nigeria.

Abstract: This work investigated the compressive strength of ternary blended cement sandcrete containing Afikpo rice husk ash (RHA) and sawdust ash (SDA). 105 sandcrete cubes of 150mm x 150mm x 150mm were produced with OPC-RHA binary blended cement, 105 with OPC-SDA binary blended cement, and 105 with OPC-RHA-SDA ternary blended cement, each at percentage OPC replacement with pozzolan of 5%, 10%, 15%, 20%, and 25%. Three cubes for each percentage replacement of OPC with pozzolan and the control were tested for saturated surface dry bulk density and crushed to obtain their compressive strengths at 3, 7, 14, 21, 28, 50, and 90 days of curing. The 90-day strengths obtained from ternary blending of OPC with equal proportions of RHA and SDA were 11.80N/mm² for 5% replacement, 11.20N/mm² for 10% replacement, 10.60N/mm² for 15% replacement, 10.00N/mm² for 20% replacement, and 9.10N/mm² for 25% replacement, while that of the control was 10.90N/mm². This suggests that very high sandcrete strength values could be obtained with OPC-RHA-SDA ternary blended cement with richer mixes, high quality control, and longer days of hydration. Thus, OPC-RHA-SDA ternary blended cement sandcrete could be used for various civil engineering and building works, especially where early strength is not a major requirement.

Keywords: Binary blended cement, ternary blended cement, compressive strength, sandcrete, pozzolan, rice husk ash, sawdust ash.

I. INTRODUCTION

Gross inadequacy of accommodation for the densely populated areas of South Eastern Nigeria and many other parts of Africa has constrained researchers to continue to seek ways of reducing the cost of building projects. Agricultural by-products regarded as wastes in technologically underdeveloped societies could be used as partial replacement of Portland cement to achieve this purpose. Bakar, Putrajaya, and Abdulaziz (2010) assert that Supplementary cementitious materials prove to be effective to meet most of the requirements of durable concrete and that blended cements are now used in many parts of the world. During hydration of Portland cement, lime or calcium hydroxide [Ca(OH)₂] is obtained as one of the hydration products. When a pozzolanic material is blended with Portland cement it reacts with the lime to produce additional calcium-silicate-hydrate (C-S-H), which is the main cementing component. Thus the pozzolanic material reduces the quantity of the deleterious Ca(OH)₂ and increases the quantity of the beneficial C-S-H. Therefore, the cementing quality is enhanced if a good pozzolanic material is blended in suitable quantity with OPC (Dwivedia et al., 2006). At temperatures around 40°C and in the presence of water, the amorphous silica contained in pozzolans such as rice husk ash (RHA) reacts with Ca(OH)₂ to form more C-S-H gel (Poon, Kou, and Lam, 2006). Much has been reported on binary blended systems whereby OPC is blended with different percentages of a pozzolan in making cement composites (Adewuyi and Ola, 2005; Elinwa and Awari, 2001; De Sensale, 2006; Saraswathy and Song, 2007). Attempts have been made to produce and use pozzolanic RHA commercially in several countries (Cisse and Laquerbe, 2000). Malhotra and Mehta (2004) have reported that ground RHA with finer particle size than OPC improves concrete properties as higher substitution amounts result in lower water absorption values and the addition of RHA causes an increment in the compressive strength. Mehta and Pirtz (2000) investigated the use of rice husk ash to reduce temperature in high strength mass concrete and concluded that RHA is very effective in reducing the temperature of mass concrete compared to OPC concrete. Cordeiro, Filho, and Fairbairn (2009) carried elaborate studies of Brazilian RHA and rice straw ash (RSA) and demonstrated that grinding increases the pozzolanicity of RHA and that high strength of RHA, RSA concrete makes production of

blocks with good bearing strength in a rural setting possible. Their study showed that combination of RHA or RSA with lime produces a weak cementitious material which could however be used to stabilize laterite and improve the bearing strength of the material. Sakr (2006) investigated the effects of silica fume and rice husk ash on the properties of heavy weight concrete and found that these pozzolans gave higher concrete strengths than OPC concrete at curing ages of 28 days and above. Agbede and Obam (2008) investigated the strength properties of OPC-RHA blended sandcrete blocks. They replaced various percentages of OPC with RHA and found that up to 17.5% of OPC can be replaced with RHA to produce good quality sandcrete blocks. Rukzon, Chindaprasirt, and Mahachai (2009) studied the effect of grinding on the chemical and physical properties of rice husk ash and the effects of RHA fineness on properties of mortar and found that pozzolans with finer particles had greater pozzolanic reaction. Wada et al. (2000) demonstrated that RHA mortar and concrete exhibited higher compressive strength than the control mortar and concrete. Habeeb and Fayyadh (2009) investigated the influence of RHA average particle size on the properties of concrete and found that at early ages the strength was comparable, while at the age of 28 days, finer RHA exhibited higher strength than the sample with coarser RHA. Cordeiro, Filho, and Fairbairn (2009) also investigated the influence of different grinding times on the particle size distribution and pozzolanic activity of RHA obtained by uncontrolled combustion in order to improve the performance of the RHA. It was expected that the reduction of RHA particle size could improve the pozzolanic reactivity by reducing the adverse effect of the high-carbon content in the ash and increasing the homogeneity of the material. The study revealed the possibility of using ultrafine residual RHA containing high-carbon content in high-performance concrete. A number of researchers have also worked on sawdust ash and found good prospects in using binary blended cements made with sawdust ash (Elinwa, Ejeh, and Mamuda, 2008; Elinwa and Abdulkadir, 2011). A few researchers have also investigated the possibility of ternary blended systems in order to further reduce the quantity of OPC in blended cements. Elinwa, Ejeh, and Akpabio (2005) investigated the use of sawdust ash in combination with metakaolin as a ternary blend with 3% added to act as an admixture in concrete. Frías et al. (2005) studied the influence of calcining temperature as well as clay content in the pozzolanic activity of sugar cane straw-clay ashes-lime systems. All calcined samples showed very high pozzolanic activity and the fixation rate of lime (pozzolanic reaction) varied with calcining temperature and clay content. Rukzon and Chindaprasirt (2006) investigated the strength development of mortars made with ternary blends of OPC, ground RHA, and classified fly ash (FA). The results showed that the strength at the age of 28 and 90 days of the binary blended cement mortar containing 10 and 20% RHA were slightly higher than those of the control, but less than those of FA. Ternary blended cement mixes with 70% OPC and 30% of combined FA and RHA produced strengths similar to that of the control. The researchers concluded that 30% of OPC could be replaced with the combined FA and RHA pozzolans without significantly lowering the strength of the mixes. Fadzil et al. (2008) also studied the properties of ternary blended cementitious (TBC) systems containing OPC, ground Malaysian RHA, and FA. They found that compressive strength of concrete containing TBC gave low strength at early ages, even lower than that of OPC, but higher than binary blended cementitious (BBC) concrete containing FA. At long-term period, the compressive strength of TBC concrete was comparable to the control mixes even at OPC replacement of up to 40% with the pozzolanic materials. Their results generally showed that the TBC systems could potentially be used in the concrete construction industry and could be particularly useful in reducing the volume of OPC used.

The above works on ternary blended cements were based on the ternary blending of OPC with an industrial by-product pozzolan (i.e. FA) and an agricultural by-product pozzolan (i.e. RHA). Being majorly agrarian, many communities in South Eastern Nigeria have continued to generate tons of agricultural and plant wastes such as rice husk and sawdust as efforts are intensified toward food production and local economic ventures. This work investigated the suitability of using two agricultural by-products in ternary blend with OPC for sandcrete making. The compressive strength of ternary blended cement sandcrete containing Afikpo rice husk ash and sawdust ash was specifically investigated. The successful utilization of rice husk ash and sawdust ash in ternary combination with OPC for making sandcrete would further add value to these wastes. Moreover, by reducing the volume of OPC required for making sandcrete, it will also reduce the cost of civil engineering and building works that make much use of sandcrete blocks.

II. METHODOLOGY

Rice husk was obtained from rice milling factories in Afikpo, Ebonyi State and Saw dust from wood mills in Owerri, Imo State, all in South Eastern Nigeria. These materials were air-dried and calcined into ashes in a locally fabricated furnace at temperatures generally below 650°C. The rice husk ash (RHA) and sawdust ash (SDA) were sieved and large particles retained on the 600µm sieve were discarded while those passing the sieve were used for this work. No grinding or any special treatment to improve the quality of the ashes and enhance their pozzolanicity was applied because the researchers wanted to utilize simple processes that could be easily replicated by local community dwellers.

The RHA had a bulk density of 770 Kg/m^3 , specific gravity of 1.84, and fineness modulus of 1.48. The SDA had a bulk density of 810 Kg/m^3 , specific gravity of 2.05, and fineness modulus of 1.89. Other materials used for the work are Ibeto brand of Ordinary Portland Cement (OPC) with a bulk density of 1650 Kg/m^3 and specific gravity of 3.13; river sand free from debris and organic materials with a bulk density of 1590 Kg/m^3 , specific gravity of 2.68, and fineness modulus of 2.82; and water free from organic impurities. A simple form of pozzolanicity test was carried out for each of the ashes. It consists of mixing a given mass of the ash with a given volume of Calcium hydroxide solution $[\text{Ca}(\text{OH})_2]$ of known concentration and titrating samples of the mixture against H_2SO_4 solution of known concentration at time intervals of 30, 60, 90, and 120 minutes using Methyl Orange as indicator at normal temperature. For each of the ashes the titre value was observed to reduce with time, confirming the ash as a pozzolan that fixed more and more of the calcium hydroxide, thereby reducing the alkalinity of the mixture. The chemical analysis of the ashes showed they both satisfied the ASTM requirement that the sum of SiO_2 , Al_2O_3 , and Fe_2O_3 should be not less than 70% for pozzolans.

A standard mix ratio of 1:6 (blended cement: sand) was used for the sandcrete. Batching was by weight and a constant water/cement ratio of 0.6 was used. Mixing was done manually on a smooth concrete pavement. For binary blending with OPC, each of the ashes was first thoroughly blended with OPC at the required proportion and the homogenous blend was then mixed with the sand, also at the required proportions. For ternary blending, the two ashes were first blended in equal proportions and subsequently blended with OPC at the required proportions before mixing with the sand, also at the required proportions. Water was then added gradually and the entire sandcrete heap was mixed thoroughly to ensure homogeneity. One hundred and five (105) sandcrete cubes of $150\text{mm} \times 150\text{mm} \times 150\text{mm}$ were produced with OPC-RHA binary blended cement, one hundred and five (105) with OPC-SDA binary blended cement, and one hundred and five (105) with OPC-RHA-SDA ternary blended cement, each at percentage OPC replacement with pozzolan of 5%, 10%, 15%, 20%, and 25%. An equal combination of RHA and SDA was used in the ternary blended system. Twenty one control cubes with 100% OPC or 0% replacement with pozzolan were also produced. This gives a total of 336 sandcrete cubes. All the cubes were cured by water sprinkling twice daily in a shed. Three cubes for each percentage replacement of OPC with pozzolan and the control were tested for saturated surface dry bulk density and crushed to obtain their compressive strengths at 3, 7, 14, 21, 28, 50, and 90 days of curing.

III. RESULTS AND DISCUSSION

The particle size analysis showed that both the RHA and the SDA were much coarser than OPC, the reason being that the ashes were not ground to finer particles. Therefore, the compressive strength values obtained using them can still be improved upon when the ashes are ground to finer particles. The pozzolanicity test confirmed both ashes as pozzolans since they fixed some quantities of lime over time. The compressive strengths of the OPC-RHA and OPC-SDA binary blended cement sandcrete as well as the OPC-RHA-SDA ternary blended cement sandcrete are shown in tables 1 and 2 for 3-21 and 28-90 days of curing respectively.

As can be seen in tables 1 and 2, the results show that sandcrete produced from ternary blend of OPC with equal proportions of RHA and SDA have compressive strength values in between those of binary blends of OPC and RHA on one hand and OPC and SDA on the other hand for all percentage replacements and curing ages. Also, the variation of strength for sandcrete produced from ternary blended cements is similar to those of sandcrete produced from binary blended cements for all percentage replacements and curing ages. More significantly for civil engineering and building construction purposes, the 90-day strengths obtained from ternary blending of OPC with equal proportions of RHA and SDA were 11.80N/mm^2 for 5% replacement, 11.20N/mm^2 for 10% replacement, 10.60N/mm^2 for 15% replacement, 10.00N/mm^2 for 20% replacement, and 9.10N/mm^2 for 25% replacement, while that of the control was 10.90N/mm^2 . Thus, the 90-day strength values for 5-10% replacement are higher than that of the control and those for 15-25% replacement are not much less than that of the control. This suggests that very high sandcrete strength values could be obtained with OPC-RHA-SDA ternary blended cement with richer mixes, high quality control, and longer days of hydration.

Table 1. Compressive strength of blended OPC-RHA-SDA cement sandcrete at 3-21 days of curing

OPC Plus	Compressive Strength (N/mm ²) for					
	0% Poz.	5% Poz.	10% Poz.	15% Poz.	20% Poz.	25% Poz.
	Strength at 3 days					
RHA	3.30	2.40	2.40	2.20	2.10	2.10
SDA	3.30	2.40	2.30	2.20	2.10	1.90
RHA & SDA	3.30	2.40	2.30	2.20	2.10	2.00
	Strength at 7 days					
RHA	5.60	3.60	3.50	3.10	2.90	2.10
SDA	5.60	3.40	3.30	3.10	3.00	2.70
RHA & SDA	5.60	3.50	3.40	3.10	2.90	2.70
	Strength at 14 days					
RHA	7.70	5.00	4.60	4.10	3.80	3.40
SDA	7.70	4.80	4.40	4.00	3.60	3.20
RHA & SDA	7.70	4.90	4.50	4.00	3.70	3.30
	Strength at 21 days					
RHA	8.60	5.80	5.40	4.60	4.40	3.80
SDA	8.60	5.60	5.10	4.60	4.20	3.60
RHA & SDA	8.60	5.70	5.30	4.60	4.30	3.70

Table 2. Compressive strength of blended OPC-RHA-SDA cement sandcrete at 28-90 days of curing

OPC Plus	Compressive Strength (N/mm ²) for					
	0% Poz.	5% Poz.	10% Poz.	15% Poz.	20% Poz.	25% Poz.
	Strength at 28 days					
RHA	9.90	8.20	7.00	6.40	5.60	4.70
SDA	9.90	7.90	6.60	5.90	5.30	4.50
RHA & SDA	9.90	8.00	6.80	6.10	5.40	4.60
	Strength at 50 days					
RHA	10.30	10.40	9.50	8.60	7.70	6.80
SDA	10.30	9.60	8.70	8.00	7.50	6.70
RHA & SDA	10.30	10.00	9.10	8.40	7.60	6.70
	Strength at 90 days					
RHA	10.90	11.90	11.40	10.70	10.10	9.40
SDA	10.90	11.80	11.10	10.60	10.00	8.90
RHA & SDA	10.90	11.80	11.20	10.60	10.00	9.10

As would be expected, 100% OPC sandcrete (the control) strength increased steadily till the age of about 28 days, after which it increased only gradually until the age of about 90 days. Table 1 shows the very low strength of OPC-RHA-SDA ternary blended cement sandcrete relative to the strength of the control concrete at early ages of 3 to 21 days. The poor early strength gets more pronounced with increase in percentage replacement of OPC with RHA-SDA combination as shown in table 2. For example, whereas the 3-day strength at 5% replacement is 2.40N/mm², it is 2.00N/mm² at 25% replacement. This very low early strength could be due to the fact that pozzolanic reaction was not yet appreciable at early ages. The pozzolanic reaction set in after some days and increased with days of curing/hydration such that the strength of blended cement sandcrete increased more and more with age than that of the control. Table 1 clearly shows that very high strength could be achieved for ternary blended cement sandcrete containing OPC, RHA, and SDA with 10 to 15% replacement of OPC with pozzolans at 50 to 90 days of curing. By way of comparison, it can be seen from tables 1 and 2 that the strength values of OPC-RHA binary blended cement sandcrete are greater than those of OPC-SDA binary blended cement sandcrete at all percentage replacements of OPC with pozzolan and at all curing ages. The strength value of OPC-RHA-SDA ternary blended cement sandcrete consistently lies in-between the two for all percentage replacements and curing ages. This suggests that a disproportionate blending of the two pozzolans should be in favour of RHA for optimization of the strength of the ternary blended cement sandcrete.

IV. CONCLUSIONS

Ternary blended cement sandcrete produced from blending OPC with equal proportions of RHA and SDA have compressive strength values in between those of binary blended OPC-RHA and OPC-SDA cement sandcrete for all percentage replacements and curing ages. Also, the variation of strength for OPC-RHA-SDA ternary blended cement sandcrete is similar to those of OPC-RHA and OPC-SDA binary blended cement sandcrete for all percentage replacements and curing ages. More importantly, similar to the results of binary blending, the 90-day strengths of OPC-RHA-SDA ternary blended cement sandcrete are higher than the control values for 5-10% replacement of OPC with pozzolans and close to the control values for 15-25% replacement. The implication of this is that very high values of OPC-RHA-SDA ternary blended cement sandcrete strengths could be obtained if high target strength is intentionally designed for and good quality control is applied such as the quality control measures used in producing 100% OPC (control) sandcrete with very high strength values. Thus, OPC-RHA-SDA ternary blended cement sandcrete could be used for various civil engineering and building works, especially where early strength is not a major requirement.

REFERENCES

- [1]. Adewuyi, A.P., & Ola, B. F. (2005). Application of waterworks sludge as partial replacement for cement in concrete production. *Science Focus Journal*, 10(1): 123-130.
- [2]. Agbede, I. O., & Obam, S. O. (2008). Compressive Strength of Rice Husk Ash-Cement Sandcrete Blocks. *Global Journal of Engineering Research*, Vol. 7 (1), pp. 43-46.
- [3]. Bakar, B. H. A., Putrajaya, R. C., & Abdulaziz, H. (2010). Malaysian Saw dust ash – Improving the Durability and Corrosion Resistance of Concrete: *Pre-review. Concrete Research Letters*, 1 (1): 6-13, March 2010.
- [4]. Cisse, I. K., & Laquerbe, M. (2000). Mechanical characterization of sandcretes with rice husk ash additions: study applied to Senegal. *Cement and Concrete Research*, 30 (1): p.13– 18.
- [5]. Cordeiro, G. C., Filho, R. D. T., & Fairbairn, E. D. R. (2009). Use of ultrafine saw dust ash with high-carbon content as pozzolan in high performance concrete. *Materials and Structures*, 42: 983–992. DOI 10.1617/s11527-008-9437-z.
- [6]. De Sensale, G. R. (2006). Strength development of concrete with rice-husk ash. *Cement & Concrete Composites*, 28: 158–160.
- [7]. Dwivedia, V. N., Singh, N. P., Das, S. S., & Singh, N. B. (2006). A new pozzolanic material for cement industry: Bamboo leaf ash. *International Journal of Physical Sciences*, 1 (3): 106-111.
- [8]. Elinwa, A. U., & Abdulkadir, S. (2011). Characterizing Sawdust-ash for Use as an Inhibitor for Reinforcement Corrosion. *New Clues in Sciences*, 1: 1-10.
- [9]. Elinwa, A. U., & Awari, A. (2001). Groundnut husk ash concrete. *Nigerian Journal of Engineering Management*, 2 (1), 8 - 15.
- [10]. Elinwa, A. U., Ejeh, S. P., & Akpabio, I. O. (2005). Using metakaolin to improve sawdust-ash concrete. *Concrete International*, 27 (11), 49 - 52.
- [11]. Elinwa, A. U., Ejeh, S. P., & Mamuda, M. A. (2008). Assessing of the fresh concrete properties of self-compacting concrete containing sawdust ash. *Construction and Building Materials Journal*, 22: 1178 - 1182.
- [12]. Fadzil, A. M., Azmi, M. J. M., Hisyam, A. B. B., & Azizi, M. A. K. (2008). Engineering Properties of Ternary Blended Cement Containing Rice Husk Ash and Fly Ash as Partial Cement Replacement Materials. *ICCBT*, A (10): 125 – 134.
- [14]. Fri'as, M., Villar-Cocin' a, E., Sa' nchez-de-Rojas, M. I., & Valencia-Morales, E. (2005). The effect that different pozzolanic activity methods has on the kinetic constants of the pozzolanic reaction in sugar cane straw-clay ash/lime systems: Application of a kinetic–diffusive model. *Cement and Concrete Research*, 35: 2137 – 2142.
- [16]. Habeeb, G. A., & Fayyadh, M. M. (2009). Saw dust ash Concrete: the Effect of SDA Average Particle Size on Mechanical Properties and Drying Shrinkage. *Australian Journal of Basic and Applied Sciences*, 3(3): 1616-1622.
- [17]. Malhotra, V. M., & Mehta, P. K. (2004). *Pozzolanic and Cementitious Materials*. London: Taylor & Francis.
- [18]. Mehta, P. K. & Pirtz, D. (2000). Use of rice husk ash to reduce temperature in high strength mass concrete. *ACI Journal Proceedings*, 75:60-63.
- [19]. Poon, C. S., Kou, S. C., & Lam, L. (2006). Compressive strength, chloride diffusivity and pore structure of High Performance metakaolin and silica fume concrete. *Construction and building materials*, 20: 858 – 865.
- [20]. Rukzon, S., & Chindapasirt, P. (2006). Strength of ternary blended cement mortar containing Portland cement, rice husk ash and fly ash. *J. Eng. Inst. Thailand*, 17: 33-38 (547-551).
- [21]. Rukzon, S., Chindapasirt, P., & Mahachai, R. (2009). Effect of grinding on chemical and physical properties of saw dust ash. *International Journal of Minerals, Metallurgy and Materials*, 16 (2): 242-247.
- [22]. Sakr, K. (2006). Effects of Silica Fume and Rice Husk Ash on the Properties of Heavy Weight Concrete. *Journal of Materials in Civil Engineering*, 18(3): 367-376.
- [23]. Saraswathy, V., & Song, H. (2007). Corrosion performance of rice husk ash blended concrete. *Construction and Building Materials*, 21 (8): p.1779–1784.
- [24]. Wada, I., Kawano, T., & Mokotomaeda, N. (2000). Strength properties of concrete incorporating highly reactive rice-husk ash. *Transaction of Japan Concrete Institute*, 21 (1): p. 57–62.

Traffic and Transportation Problems of Metro Cities: Case of Meerut, Uttar Pradesh

Vijay kumar* , Dr R.K.Pandit**

Abstract: Metro cities in India are facing acute traffic and transportation problems leading to deteriorated quality of life and weak socio-- economic structure. The problems range from inefficiency of roads and transport infrastructure to deal with exorbitantly increasing in magnitude of vehicles especially the personal ones , lack of mass transportation systems , encroachments on roads ,lack of pedestrian facilities and weak traffic management systems. This paper focuses these problems contextual to Meerut city, one of the priority town of NCR. The probable solution to this gigantic problem can be creation of an independent, “Traffic and Transportation Authorities” at city level which should be technically strong in equipments, technology, and trained manpower & experts. Beside this comprehensive traffic and transportation plan should be made mandatory for all cities along with efficient management strict enforcement.

I. INTRODUCTION

Metro towns in India especially the old ones are facing acute Traffic and transportation problems and inspite of making efforts and investments, cities have not been able to cope up with this gigantic problem. The population in towns is regularly increasing but the road area especially in the existing part of the cities and in city cores, remains the same, making the situation grim by increasing the congestion in central and the other important part of cities. Mass transportation systems are generally neglected or do not provide regular, adequate, safe and reliable quality of services there by people relying on the private vehicles, which leads to extreme congestion, increase in pollution, accidents and add to general deterioration of quality of life in cities. In metro cities there are about 15% car users and as 75% of the transport budget is used for widening roads, which primarily benefits the car and two wheelers and not the mass transportation systems. Beside this increase of commercial and institutional activities in central built up areas ,temporary and permanent encroachment on roads ,unauthorized parking of tempos ,Rickshaws , use of same road lanes by slow moving vehicles, intermediate transport systems and fast speed vehicles , poor traffic management add to the problem. The problem can be addressed by preparation of a comprehensive traffic and transportation plan for the town along with appropriate placement/locating various land uses in the Master Plan. This paper is focuses on studying the problems of Traffic and transportation problems of Meerut one of the important historical and priority town of NCR and an important divisional headquarter of state of Uttar Pradesh, India.

II. MEERUT: GENERAL BACKGROUND

Meerut is one of the largest town of Western Uttar Pradesh. Beside a district headquarter it is a divisional headquarter. It is a major commercial, industrial, educational and a city of Archaeological importance. It has got a pride of being largest town in the NCR region after Delhi.

Location

Meerut Town is situated on Delhi -Sahranpur railway line and well connected to Delhi, Saharanpur, Muzaffarnagar, Hapur, Bulandshahar The Distance of Meerut from Delhi is 70 km and from Ghaziabad 50 km Meerut. 360kms from Kanpur , It is situated on state high way No. 45.Meerut town is situated on 29° - 41' North and longitude 77° - 45'-3" East.Meerut is situated at the heart of upper Ganges Yamuna Doab and has a mean sea level between 734.46 - 739.30 feet.

Meerut enjoys a strategic importance from the defense point of view, which is a foremost quality possessed by Meerut, since the dawn of Mughal Dynasty and imperialism and this particular quality was instrumental in the choice of location for military base.

Meerut Town: A Brief Historical Background

There are traces which depict that the settlement in Meerut was surrounded from all sides by a wall and a depression (Khai). It had nine gates, out of which 8 were old and one of the gates was new. It is said that Meerut is a historical town which started developing at the period of Ramayana. As per the mythology available, Meerut was capital of "Mayrastra". It is also said that prince Mandodra of this city was married to king of Lanka Ravana. Battle of Mahabharata took place near this town. There are number of monuments of the times of Mahatma Buddha, Hindu, & Muslim kings. One of the important such monument is Surajkund, "Shapeer Ki Dargah", Makbara of Mohammad Kamboh etc. Also Indian Mutinies of 1857 started from this city. Prior to 1881 it was ruined and almost settled again. In 1806 the cantonment was established and at present is an important centre of regimental unit. In 1881 the population of Meerut city was 60,948 excluding that of cantonments Meerut is a historical city. Number of remains have been found near this city. As per the experts these remains are of period approximately 1300 to 1500 BC and settlement existed here much before the king Ashok. The famous fort in Meerut was got constructed by king Haridutt and he constructed a moat around the fort and a river also with in the premises of fort. This fort spread in the area of 127 hectare, still exists in the city. Maratha Sardar Raghunath Rao captured this fort and Ahmad Shah Abdali looted the fort. In 1818 Meerut was made the District headquarter and a large cantt. area was established. By 1829 the cantonment was fully developed and natives of Meerut were crushed administratively. In 1847 Meerut was established as important center against British Govt. and consequently in 1857 mutiny started from Meerut. The 54th annual meeting of 1942 "Bharat Chodo Andolan" was organized at this place. Beside this Meerut contributed in Indian freedom at many occasions.

In the initial of twentieth century, Meerut city was developed in interior part of old fort. In west towards Delhi Saharanpur, Railway line and areas near main spines connecting District headquarter has sparsely populated; but after independence the settlement developed near the main roads Meerut-Hapur, Meerut-Delhi and Meerut-Roorkee road. In 1965 Meerut Municipal area and area 8 km around this were declared as controlled regulated area under section 3 of "Uttar Pradesh Nirman karya Viniyam Adhiniyam 1958". Later in 1976 afore said area was declared as Meerut Development area and Meerut Development authority was constituted & in 1978 the first Master plan of Meerut was prepared.

Regional Setting

Meerut lies in almost **geometrical centre of District Meerut**. Reason for becoming a centre for commerce and industry in western UP is its nodal location. It is situated on a land which is highly fertile agricultural area but devoid of any significant minerals, and very less section of the entire population is urban. Besides the major portion of Meerut tehsil, portion of Sardhana, Mawana, Baraut, Ghaziabad, Bulandshahar, Hapur and Southern portion of Muzaffarnagar fall within the region of Meerut.

The services rendered by Meerut are grouped into two categories

- **Local services** such as retail business recreation and personal community services, municipal govt. etc. which are meant for the consumption mostly by the local population.
- **Regional services** such as whole sale business and technical services, administrative services etc. which are meant for the consumption of both the regional components is usually predominant. **Meerut is the biggest employment centre** in the region where job opportunities exist not only for local population but also for the people of densely settled region. The labour supply zone, all around the town even extends up to Hapur Bulandshahar and Ghaziabad region from where the journeys are completed within 90 minutes in road and railway. The commuters from the surrounding rural region visit the city to seek employment in its industrial, commercial and services establishments.

Climate

The climate of Meerut is moderate, with winter minimum temperature 3°C to 5°C, The summer of city are generally hot with maximum temperature reaching up to 45°C to 47°C and average rainfall level is 775 mm to 820 mm, which is generally from June to September. In autumns also there happens

some rains which is generally very useful for agriculture . City has good amount of forest land which is in village Rithani near Delhi road and is about 550 hectare.

Soil and Vegetation

Meerut has plain topography and with clay loamy soil . It has very fertile agricultural land with high water table, quality of water is good and because of close vicinity to shivalik hills , it has appropriate level of humidity ,which makes it suitable for healthy habitation . Meerut is situated in between Ganga and Yamuna with river Ganga canal approximately 10 km away from main city, and so all small rivers and drains lead in to it. On East there is Kali “Nadi“ in which all liquid waste of city is disposed in as general slope of city is from North West to South East.

Socio- Economic Characteristics

Status of Housing Stock: Meerut City

YEAR	POPULATION	NO HOUSES	OF	NO OF FAMILIES	OF	AVERAGE SIZE OF FAMILIEs	SHORTAGE OF HOUSE
1971	3,71,760	54914		62158		5.98	7244
1981	536615	101222		101584		5.28	7362
1991	8,49,799	122957		131476		6.46	8519
2001	10,74,869	1,74595		184581		5.82	9986

From above it is evident that there is a shortage of 10 thousand houses where as housing board and Meerut Development Authority has floated many housing colonies , which are lying vacant because -

- Costly houses out of the reach of common people .
- Away from city .
- Availability of unauthorised , cheap,land available near the city built up area.

No of unauthorised colonies by 31.03.2001 as surveyed by M.D.A is 69 . Further 43 more unauthorised colonies were earmarked . So total of unauthorised colonies are 112 and total colonies regularized are 38.

City Economics & Occupation

Types of Industries	No of units	total % labour	skilled % worker	semi skilled % worker	unskilled % worker
Large scale & medium scale industries	39	4683 (6.31%)	235 (.32%)	796 (1.07%)	3652 (4.92%)
Smallscale industries	15510	61254 82.52	1838 2.48	15313 20.63 %	44103 59.41 %
house hold industries	7922	8295 11.17	141 0.19	995 1.34	7159 9.64
	23471	74232 100	2214 2.99	17104 23.04	54914 73.97

Demographic Characteristics

Meerut is a second number of town in terms of population in NCR region.As per 2001 census the population of Meerut is 11,70,985.The population of Meerut city exorbitantly increased which

was less than 5.5 lakhs in 1981 and nearly 8.5 lakhs until 1991(in period 71-91 ,In 71-81 the increase was 44.34 % and in 81-91 was 58.36 %). In these two decades the increase in population of Meerut and national increase in urban population are 40.39 % and 46.14 % respectively. The reason for this growth is because of increase in housing stock , provided by Govt. agencies on large scale through housing board and Meerut .Development. Authority, Industrial development in the city and development was of comparatively better infrastructure The increase of population in period 91-2001 is 37.79% which is less as compared to previous one but slightly more than national increase of 36.19% .. The recorded increase in the population during 1991-2001 was 37.8%, which was slightly less than that of the previous two decades and is lightly more than the national average of 36.17%. The reason in lower increase is because of good availability of housing facilities in smaller town & nearby town of Ghaziabad , Noida having proximity with Delhi NCR-Plan envisaged Meerut city as one of the regional centre and large no of offices and commercial activities will be shifted to this city in the process of decentralization, but it could not happen. In the central areas of Meerut City the population density is as high as 200 persons per hectare and in other built up areas near major road is about 500 persons per hectare. Thickly populated central built up areas are generally unhygienic & unhealthy and have acute traffic and transportation problems

III TRAFFIC AND TRANSPORTATION INFRASTRUCTURE OF MEERUT: AN OVER VIEW

The Meerut town is developed in organic pattern ,number of regional highways pass through this city ,Delhi- Roorkee road , Meerut –Baghpat road, Meerut – Bijnor road, Meerut -Garh road meet at central hub point commonly known as “Begum Bridge”. All these major state /regional /national highways pass through the central built up area of city. So the city has naturally grown concentric pattern of circulation network

Analysis of Effectiveness of Planning Proposals for Traffic and Transportation Infrastructure in Various Master Plans

III(a) Proposals of First Meerut Master Plan 1971- 91

Road Pattern And Typology

The first Master Plan of Meerut 1971-91 respected the organic Growth pattern of the city and further proposed concentric and radial pattern of roads In the total Regulated Area of Meerut considering only the major master plan road system , the percentage of land under transportation use will be about 5.35% In case the rural tract is deducted out of the regulated area the land under major transport use including the roads is about 7.67 % .To this if we add about 9.32 % of land under the existing and future roads below 100ft width located with in the residential and other use zones the total land under transport use will work out to be 17.00% , which is in accordance to generally accepted standards .So traffic has been managed through network of road of 250ft, 200ft´ . Roads of 120ft´ and 100ft´ are arterial roads which further connects to collector roads .The Meerut - Baghpat , Delhi-Mussoorie road , Meerut - Hapur road are part of the National Capital Region transportation Grid focusing on Meerut so right of way has been fixed to 250ft In trans nauchandi area about 196 acre (79.5 hectare) of land is under transportation use , 64.4 hectare will be covered by roads , while bus and truck terminals shall cover the rest about 15.1 hectare of land

In Master Plan 1971-91 two kinds of roads were proposed-

(1) To provide access to various areas of the town , to individual properties and to collect and distribute the various categories of traffic from and to various areas of the town.

For this a system of access streets up to 30mts in width was prepared comprising of

- (a) Pedestrian foot path and cycle tracks
- (b) Local streets
- (c) Collector streets

(2) To provide thorough fast and safe movement to vehicles traveling from one part of the town to other and for traffic passing through the town on way to destination out side the city.

For this thorough movement Master plan road more than 30 meter wide have been incorporated comprising of

- (a) Arterial streets and ring roads
- (b) Network of high ways and bye passes

In this category there are mainly **Delhi- Nitipas national highway no.58 , Meerut- Badaun , State Highway 22 , Garh- Meerut - Karnal State highway ,Meerut- Baghpat –Sonepat State highway ,Meerut –Bijnor – Pouri State highway , Meerut - Baraut , Meerut- Praikshitgarh road**

Bus Stands and Truck Terminus

- About 9.9 hectare of land for Bus Terminal and Truck Parking was proposed in the Abdullapur Planning Units
- In Kankarkhera land was reserved for Zonal City Bus Terminal.
- In Partapur Planning Unit about 11.3 hectare for local City Bus Terminal and 7.7 hectare for Truck Parking .
- In Trans Nauchandi Planning Unit about 196 acre (79.5 hectare) of land is under transportation use , the Bus and Truck Terminals were proposed in about 15.1 hectare of land

Railway Infrastructure

In the Partapur Planning District out of total area of 153 hectares, 24.3 hectare was earmarked for development of Railway Facilities

Analysis of Effectiveness & Outcome of Proposals of First Meerut Master Plan 1971- 91 for Traffic and Transportation Infrastructure

The proposals of Master plan were found not be very effective and very partially addressed the traffic problems of city

- Master plan 71-91 proposed widening of 29 roads with in the built up area , but it was not practically possible to widen these roads as there were already large encroachments and few commercial complex plans have been sanctioned with in the road widening area also.
- There has been large encroachment on internal roads and near the crossing and junction of unauthorized path of Rikshaws etc is further magnifying the problem
- Acute traffic issues of built up area could not be addressed. In the entire central area there were problems of traffic jams ,unauthorized parking, extremely low average traffic speed

However the Regional infrastructure was improved

The Regional roads Meerut –Roorkee (200)Meerut - Bijnor (200) ,Meerut -Parikshat garh (120) ,Meerut –Garh (250), Meerut -Hapur (250) ,Mmeerut -Delhi (250), Meerut –baraut (250), Meerut –baghpat (250) ,Meerut -Bhola (150) ,Meerut -sardhana (150), and beside above ,important town roads Begumpul to Hapur chowk (120) ,Begumpul to university (150) ,Gagoal road (200), Transport nagar road (150). These **afore said roads can be widened .**

Status of Mass Transportation modes by the end of Meerut Master Plan 1971-91 period

- There were 175 roadways busses 5.6 busses running in agreement with U.P roadways
- 481 private busses running in which 52,502 passengers came to Meerut city and 51190 passengers more out of the city .

III(b) Proposals of Second Meerut Master Plan 2001

Road Pattern and Typology

- (1) Meerut Master Plan- 2001 recommended development of radial and concentric framework of roads , Existing radial pattern of road was maintained through three ring cordons
- (2) So Roads in three cordons were proposed:
 - **Internal cordon** for transport movement with in the city and to connect different parts& areas of the city
 - **Middle cordon** to take care of regional traffic and to connect outer and new areas of town ,

- **Outer cordon** to take care of movement of goods and regional traffic
- (3). For Implementation of above cordons , undeveloped portion of the respective rings were to be developed , as per the requirement and priority.

Bus Stands and Truck Terminus

- MMP-2001, proposed to Shift Existing Bus Stand to decentralize and proposed four bus stands at the meeting points of middle cordon with Delhi - Roorkee , Bye Pass Road , Roorkee road , Mawana road, Garh road , Hapur road ,
- On all major roads bus stand has been proposed to take care of regional traffic and internal traffic of respective sides .Since the existing transport nagar is located in busy area so two new transport nagar have been proposed on Baghpat road and Garh road

Railway Infrastructure

- .MMP -2001 recommended additional truck terminus beside one existing keeping in extra requirement
- MMP-2001 recommended development of railway stations of Meerut city , ,Meerut cantt. , Pawli khas ,Noor nagar for passengers and for the purpose of goods . Partapur Railway station has to be developed. An additional railway station also proposed near Vedvyaspuri residential scheme .

Analysis of Effectiveness & Outcome of Proposals of First Meerut Master Plan 2001 for Traffic and Transportation Infrastructure

The proposals of Master plan 2001 were found not be very effective and very partially addressed the traffic problems of city During the Master Plan 2001 period no substantial development for enhancement of traffic and transportation facilities took place, out of proposed 1374.90 hectare of land, only 31.47% ie 432.60 hectare was developed. The development & construction of proposed five bustands didn't take place ,similarly the development and construction of Transport nagar was not taken up the development of outer ring road ,middle cordon an inner cordon couldn't take place except at some points. Also at number of places encroachments and unauthorised growth took place.

III(c) Proposals of Third Meerut Master Plan 2021

Road Pattern and Typology

In Meerut Master Plan 2021 a total of 10% of land ie 1550 hectare of land was earmarked for Transportation Land Use

- The major recommendations of Meerut Master Plan 2021 regarding roads are
- Development of Ghaziabad –Meerut Expressway,
- Widening of all regional roads, and Fly Overs
- Development and enhancement of Main Intersections,
- Improvement of Local Bus Service,
- Development of Parking Spaces,
- Development of Comprehensive Traffic Management Plan
- Improvement of Meerut-Baghpat- Sonipat State Highway

Bus Stands and Truck Terminus

- Development of bus stands near Railway stations. Shifting of all bus stands located in inner parts of city to outer areas, development of transport nagar near Baghpat and Garh Road
- Proposal of two Transport Stations have been made on Garh road and Baghpat road
- The roads which catres to local and regional traffic can be developed in participation with private pwnres.
- In the areas where there is probability of development , a proper Zonal Plan may be prepared and accordingly the road may be constructed by the betterment charges obtained from the plot owners of that area.
- Improvement of all intersections and construction of Railway over bridges

Railway Infrastructure

- Improvement of Delhi-Sahran pur and Meerut –Hapur Rail Way Line including Electrification,
- Development of Rapid Rail Network Between Delhi and Meerut,
- development of Cargo near Mohiddinpur, construction of Railway Over Bridges

- development of Ghaziabzd -Meerut –Saharanpur Railway Line

IV PRESENT STATUS OF TRAFFIC AND TRANSPORTATION FACILITIES:

Meerut Road Statistics: Meerut

The roads in Meerut town are developed , constructed & maintained by different agencies. The National Highway is developed and maintained by Central Public Works Deptt. & National Highway Authority of India where as the State Highways are developed and taken care of by State PWD department.

S.NO.	Particulars	Road Length (Km)	%age of Road Length	Jurisdictions
1	National Highway	112.5	0.98	NHAI
2	State Highway	243	19.05	PWD
3	District Roads	100	7.85	
	Sub total	355.5	27.88	
4	Municipal Roads (Pucca)	425.61	3.36	M. Corp
5	Municipal Roads (Kutchra)	425.61	33.36	M. Corp.
	Cantonment Roads	65.18	5.10	Cantonment Board
	Ground total	1275.66	100	

Source: Meerut Municipal Corporation & CDP Meerut

The total length of National and State Highway is 365 kms of which 65 kms is in the Cantt. Area . Meerut Municipal Corporation take care of 970 kms. The internal roads are maintained by Municipal Corporation ,MDA, Builders and Housing Boards . The total road length of road in Meerut city is 1391 Kms. Road covers about 7.76 % of Meerut Town Area which amounts to about 1.08 m per person. The regular maintenance of 67%roads are taken care by Meerut Municipal Corporation and about only 50% of roads metalled roads

The Meerut city is located on National Highways 58 which is on the western side of the city. Other important intercity / regional roads

- Meerut -Bidaun (State Highway 22)
- Garhmukteshwar-Meerut-Karnal (State Highway),
- Meerut—Bagpath—Sonipat (State Highway),
- Meerut—Bijnor—Pandi road
- Meerut –Parikshitgarh road.

These roads primarily cater to the ‘thorough traffic’ and some amount of ‘destined traffic Important city arterial road include Abu lane road, PL Sharma Road, Lal Kurti Road, Burhana Road, Ghanta Ghar Road. These roads take care of huge internal traffic

Traffic Characteristics

Various traffic studies for the city of Meerut reveal that peripheral/ outskirts areas of city witness about 80% of the trips being performed by fasts vehicles, this phenomenon decreases to 50% in the inner parts of the city. It is also indicated in these studies that two wheelers account for about 1/3rd of the total vehicular traffic while heavy vehicles constitute 25%. IPT (primarily cycle rickshaw) on the whole constitute 15% of the total vehicular trips. The role of public transport in serving the city’s travel demand is marginal which is substantiated by various para transit modes like tempos, shared jeeps, cycle rickshaws. Traffic volume count data for the inter city roads (regional roads) in the city of Meerut reveals that majority of roads carry traffic in excess of 10,000 vehicles with Dilli road witness the highest amount of traffic (21,835 PCU) while Baraut road

account for the least amount of traffic (7,566 PCU). In terms of composition it is seen that private vehicles constitute the highest category in all the road sections with Car/Jeep/Van having largest share.

Motor Vehicles Volumes

There is regular increase in the number of vehicles in the Meerut city , the number of vehicles enhanced from 64.6% to 70,175 in 2005

Daily Traffic Volume on Various Regional Roads (2002)

Transport System Plan for Meerut – 2011, a study carried out by School of Planning and Architecture (1994) reveals that outer cordon traffic in the year 1992 was heaviest on Delhi Road (24109 PCU) followed by Roorkee Road (15802 PCU). Least Traffic was observed on Bhola Road (1856 PCU).

Traffic surveys carried out at different time slabs reveal that there has been steady growth traffic on various important road corridors. Apart from Delhi Road and Roorkee Road, traffic has grown on all major road corridors. The decrease in traffic along Delhi and Roorkee road could be attributed to the construction of Meerut Bypass (National Highway 58) that has resulted in shifting of ‘through traffic’ from these roads to the new alignment. It is clear from

that on an average traffic has grown at the rate of 6.98% and 4.48% in terms of simple and compound growth rates respectively. The largest growth rate was observed on Sardhana Road followed by Mawana and Parikshit Garh Road respectively.

Sl. No.	Vehicle Type	Occupancy
1	Car	2.95
2	Two Wheeler	85
3	Auto Rickshaw	3.29
4	Tempo/Mini Bus	20.64
5	Bus	42.59
6	Cycle	1.25
7	Cycle Rickshaw	1.86

Vehicle Occupancy

Source: Transport System Plan for Meerut – 2011, School of Planning and Architecture

Road Name	Outer Cordon Count - 1992	Outer Cordon Count – 2002	Annual Growth Rate (Simple)	Annual Growth Rate (Compound)
Roorkee Road	15,802	16,227	0.27%	0.27%
Mawana Road	4,834	12,600	16.07%	10.05%
Parikshit Garh Road	2,649	5,967	12.53%	8.46%
Grah Mukhteshwar Road	11,672	12,414	0.64%	0.62%
Hapur Road	8,115	10,026	2.35%	2.14%
Dilli Road	24,109	21,835	-0.94%	-0.99%
Baghpat Road	9,462	10,900	1.52%	1.42%
Baraut Road	4,370	7,566	7.31%	5.64%
Sardhana Road	4,459	14,767	23.12%	12.72%
Average			6.98%	4.48%

Growth of Traffic along Regional Road Corridors

Source:CDP Meerut

It is clear from the table above that on an average traffic at the outer cordon has grown at the rate of 4.48% (compound) per annum. However in order to assess traffic on the inner cordon a growth rate of 3.5% (compound) has been adopted on the basis the fact that land use within the city area would not have undergone a significant change. The projected traffic on the city arterials have been summarized in Peak Hour Traffic estimation (PCU)

Peak Hour Traffic estimation (PCU)

Sl. No.	Road Name	Estimated Traffic (PCU)
1	Begum Bridge	7,867
2	Commissioner Crossing	1,609
3	Jail Chungi Crossing towards Quila	2,253
4	Jail Chungi Crossing towards Uni.	2,054
5	Garh Bus Stand	4,209
6	Hapur Bus Stand	3,979
7	Boomiya Pul	2,731
8	Dilli Gate	4,731
9	Baghpat Crossing	2,420
10	City Railway Station	486
11	Railway Crossing (Barnaut.Road)	1,504
12	Sadar Thana	1,905
13	Abu Lane	4,453
14		

The traffic of Meerut city is predominantly is mostly of personal/ private the public transport modes include rikshaws, autorikshawas, local busses. The auto rikshaws are the most used public transport mode. The local buses ply on nine routes on which the permits have been issued

Year	Tractor	Two Wheelers	Car Tax Free (Govt)	Reserved Bus	Contract Bus	UPS RTC	Trucks (less than 60 Quintal)	Trucks (more than 60 Quintal)	Tempo/ Taxi	Car/Jeep Private	Others	Total
2001	50761	1,31,098	313	859	299	406	1,352,	2753	701	135	210	2,02,887
2002	50864	1,44,199	330	860	314	419	1,396	2972	742	15,679	210	2,17,985
2003	51224	338	683	683	275	454	1,398	2964	994	17,216	221	2,46,922
2004	51647	1,73,240	232	683	214	448	1,224	2826	1,242	19,099	246	2,51,101
2005	52273	1,90,310	243	656	283	349	1,160	1765	2,515	21,502	151	2,71,207

Source: Meerut Municipal Corporation & CDP ,Meerut

There are 18 bus terminals present in the city, the existing city bus routes along with the Details of licenses / permits are shown in

Sl. No.	City with Population in Millions	Share of Public Transport (%)
1	0.5 – 1.0	25
2	1.0 – 2.0	30-40
3	2.0 – 3.0	50-60
4	3.0 – 5.0	60-70
5	5.0 plus	70-85

Share of Public Transport in Indian Cities Source: Traffic and Transportation Policies in Urban Area in India, Ministry of Urban Development – GOI

Status of Public Transport facilities In Meerut :

Local Buses Details of City Bus Service Routes

1. Medical College to City Railway Station via University ,Garh road
2. Medical College to Cant Railway Station via university Jail chnugi
3. Medical College – Kanshi
4. Medical College – Daraula via Modipuram
5. Rajpura – Modinagar via Mohiddinpur
6. Gandhi Ashram – Kithaur via University ,shashtri nagar
7. SSD College – Dabthua
8. Medical College–Tajbari Intersection– L Bolck Junction–PAC Bypass – Partapur Bypass – Modinagar
9. Medical College–Tajbari Intersection–L Block Junction – PAC Bypass – Partapur Bypass – Katai Mill – Gangol – Chandsara
10. SSD College – Shradhapuri – Khirwajalapur – Bypass – Shubhartipuram
11. SSD College – Company Bagh – PAC Bypass – Shubhartipuram
12. Begumpul – Railway Morh Crossing – Metro Plaza – Partapur – Modipuram Bypass – Shubhartipuram
13. Telephone – Exchange – SSD College – City Railway Station – Rohta Level Crossing – Shobhpur Bypass – Shubhartipuram
14. City Railway Station – Bhansauli Bus Stop – Begumpul – SSD College Intersection – Kashmir Junction – Defense Colony – Ganga Nagar Road – Jailchungi – Medical College
15. City Railway Station – Railway Road Intersection – Begumpul – SSD College – Jailchungi – Medical College – Sarai Kazi Morh
16. Begumpul – Bhainsali Bus Stand – Metro Plaza – TP Nagar –Maliana Over Bridge –Baghpat Bypass – Subhartipuram
17. SSD College – Lalkurti – Telephone Exchange – Commissioners Residence – Tejarhi Junction – Shohrabgate Bus Stand
18. City Station – Railway Road Junction – Begumpul – HSD College Crossing – Telephone Exchange – Commissioners Residence –
19. Tejgadhi – Medical College – Jagrati Vihar Sector 6 – A Block Shastri Nager – PAC Electricity Bamba – Patapur Bypass – Subhartipuram

Tempo – Taxi, a seven seater vehicle is also visible in the city of Meerut. These vehicles are licensed for a route length of 16 km. It was assessed that the city would require 600 vehicles in order to fulfill the demand, out of which 583 licenses / permits have been issued to various private operators. Auto Rickshaws also ply in city of Meerut but are confined within the municipal limits of the city. The exact requirements (demand) of these vehicles have not been worked out for the city but 543 permits / licenses have been issued so far. It is estimated that about 13- 15% of the total trips in the city are performed by the available public transportation modes which is far below the desired share of public transport as recommended by the Traffic and Transportation Policies in Urban Area in India by Ministry of Urban Development. It can be seen from the table above the share of urban transport in the city of Meerut is far less than optimal when compared against the recommended shares by the Ministry of Urban Development, highlighting the importance of urban transportation.

STATUS OF INTER CITY BUS SERVICES LS FOR MEERUT CITY

Sl. No.	Routes	No. of Permits / Licenses Issues
1	Meerut – Baghpat – Baraut – Chhaprauli	72
2	Meerut – Rohta – Baraut	74
3	Meerut – Baraut – Kotana	03
4	Meerut – Mawana – Meerapur – Bijnaur	108
5	Meerut – Parikshitgarh – Asifabad – Laliyana	42
6	Meerut – Hapur – Bulandshahar	102
7	Meerut – Ambala	09
8	Meerut – Jaani – Siwal – Khanpur – Lohara	03
9	Meerut – Sardhana – Binauli	38

Source: Meerut Municipal Corporation & CDP, Meerut

V. TRAFFIC & TRANSPORTATION PROBLEMS IN MEERUT

The following problems have been observed and identified by people, residing in the city ,daily commuters and people frequent to this city to pursue business and other affairs:

• General Problems Related To Traffic and Transport facilities

1. **Capacity Constraint: Most** of the roads have Capacity Constraint: the width of road especially in inner built up areas, inner cordon roads and even at some points the regional and outer cordon roads have lesser width/related infrastructure in context to the traffic volume they have to bear.
1. **Inadequate Road hierarchy:** Road hierarchy is not as per the acceptable level ,so the traffic movement is not smooth , the primary corridors ,secondary corridors do not follow the norms
2. **Encroachments:** Most of the roads in the are encroached by permanent temporary encroachments, leading to reduction of width and capacity of roads: at most of the places the hoardings ,shop displays ,advertising panels are placed in ROW even on the Mattelled areas. The roads have also been encroached chajja projections, ramps and other civil features constructed in the ROW.
3. **Mixed Traffic:** The most of the roads in the city are subjected to mixed kind of traffic , the slow ,very slow ,fast moving traffic move on the same roads /traffic corridors, due to which the average speed of city is lowered down.
4. **Traffic management:** The city has very weak traffic management; the traffic is regulated by traffic police, which is mostly untrained/not properly trained in traffic affairs, which fails in regulating traffic.
5. **Absence of Traffic Management Plan :** No comprehensive Traffic Management Plan is prepared for the city , the only methodology adopted is the traffic plan by police which is done in non technical way.
6. **Poor road quality:** The quality of roads in inner cordon ,middle cordon ,outer cordon as well as regional roads are of poor quality in terms of surfacing , gradients.
7. **Weak Traffic infrastructure:** The entire infrastructure is weak to cater to the magnitude of traffic
8. **Slow average traffic speed:** The average speed of traffic in the city is very low leading to deterioration of efficiency of city.
9. **Inadequate Pedestrian facilities :** The Pedestrian facilities on all most all the roads of different levels are inadequate , promoting less of pedestrian movement and more of traffic
10. **No provision for bicycles:** In the entire city there is hardly any provision required infrastructure to promote cycle movement in the city
11. **Lack of safety:** Proper considerations have not been kept for safety of people on the roads, especially for pedestrians, cyclists and people moving on two wheeler. Speed controls, use of helmet are not in practice, the traffic violators are hardly panelized.
12. **Enforcement of Traffic rules:** The traffic rules are not properly enforced, the reason being the lack of willingness in administration and extremely less and untrained manpower deputed for this purpose.
13. **Street furniture:** The street furniture on various roads are not adequate ,railings for pedestrians, seating facility , tree guard , bus shelters are hardly available.
14. **Problem of informal marketing on road side:** Hawkers ,road side vendors, informal markets: Hawkers, road side vendors , informal squatting of vegetable /grocery item vendors are a serious problem in the city , affecting the road efficiency .

• Problems Related Planning Issues

Meerut is an old and historical town, the core of the city has natural growth pattern and the street width ,geometry ,alignment and design is not compatible to accommodate the high speed and larger volume of traffic as well to provide vehicular access to the premises ,buildings ,complexes located in built-up area ,So the **Traffic Movement in the City Built-Up Core** is Highly Problematic the traffic and transportation infrastructure in City Old Built Up areas needs specific attention ,design , management ,which has generally been not addressed in the Master Plan ,Zonal Plans ,and building regulations . Master plan ,Zonal plan preparing team do not have **Experts In Traffic and Transportation** Engineers, Traffic/Transportation Planners , no consultation are generally made with the traffic rules /management team the local police force while finalizing the plans. Proposals of Master Plan, Zonal Plans are not based on detailed Traffic & Transportation surveys.

The permissions for development /building activities are allowed without any consideration of Traffic problems ,which include granting permissions to schools ,institutions ,offices ,cinema halls and other land uses /buildings which attract /generate traffic on important traffic corridors /roads in competent to hold the kind of Traffic&parking issues, they are subjected to .This kind of problem is on all major roads Gar Road ,Delhi Road ,inner cordons ,middle cordon ,outer cordon.. Concept of Mixed Land use and Allowing Commercial Activities on main corridors have enhanced the problems

- **Problems Related To Parking Issues**

Problems of Parking, unorganized and unauthorized parking are located at following points in the city: A large number of markets, commercial and other activity centers on various roads in Meerut are suffering from inadequate parking facilities. On most of these stretches, the root cause of the congestion on the street is caused due to on street parking. List of such areas with severe parking problems is furnished : The both sides of Begum bridge road up to Eves Chowraha ,both sides of Sadar bazaar,Sarrfa Market ,PL Sharma Road up to court complex ,both sides of Shahstri Marg, in roads of area near Budhana Gate ,Khair Nagar Market ,Old Gantaghar Area, Eastern and Western Kachehri Road ,Bhagpat Road ,the area around Kabari Bazaar, Sharda Road , Transport Nagar Garh Road ,Hapur Road,

- **Problems Related Intersections, Round About& Junctions**

The detailed traffic and transportation surveys were got conducted by the authorities and concluded that some of the intersections and crossings had number of problems leading to huge clogging of traffic and slowing down of average speed

1 **Begumpul** : This intersection having improper road Geometry, ,there are number of educational institutions leading to huge traffic at peak hours, temporary and permanent encroachments ,problem of huge member of road side vendors , parking of rikshaw , and private vehicles leading to inefficient intersection

2 **Bachcha Park** This intersection having improper road Geometry, ,there are number of temporary and permanent encroachments ,problem of huge member of road side vendors , parking of rikshaw ,tempos ,busses and private vehicles leading to inefficient intersection

3 **Hapur Adda** This intersection is also used as Hapur bus stand so is having huge traffic beside thi sit is having having improper road Geometry, ,there are number of temporary and permanent encroachments ,problem of huge member of road side vendors , parking of rikshaw ,tempos ,busses and private vehicles leading to inefficient intersection

4 **Eves Chupala** This intersection is surrounded by number of colleges and commercial establishments and so is having huge traffic beside this it is having improper road Geometry, ,there are number of temporary and permanent encroachments ,problem of road side vendors , parking of rickshaws ,tempos ,busses and private vehicles leading to inefficient intersection

5 **Kchahari chowk** : This intersection is having court complex and so is having huge traffic beside this it is having improper road Geometry, ,there are number of temporary and permanent encroachments ,problem of road side vendors , parking of rickshaws ,tempos ,busses and private vehicles leading to inefficient intersection

6 **Nauchandi**: This intersection is surrounded by number of commercial establishments, fair ground , thickly populated residential areas and so is having huge traffic beside this it is having improper road Geometry, ,there are number of temporary and permanent encroachments ,problem of road side vendors , parking of rickshaws ,tempos ,busses and private vehicles leading to inefficient intersection

7 **Ghantaghar**: This intersection is surrounded by number of commercial establishments, educational institutions , , thickly populated residential areas hugr commercial markets and so is having huge traffic beside this it is having improper road Geometry, ,there are number of temporary and permanent encroachments ,problem of road side vendors , parking of rickshaws ,. Private vehicles leading to inefficient intersection, Huge number of Pedestrian

8 **Baghpath Chowraha**: This intersection is surrounded by number of commercial establishments ,retail shoppings, thickly populated residential areas commercial markets ,vegetable market and so is having huge traffic beside this it is having improper road Geometry, ,there are number of temporary and permanent encroachments ,problem of road side vendors , parking of rickshaws , private vehicles leading to inefficient intersection, Huge number of Pedestrian

9 **Bhumiapul** : This intersection is surrounded by number of small commercial establishments, thickly populated residential areas so is having huge mixed kind of traffic, beside this it is having improper road hierarchy of roads Geometry, there are number of temporary and permanent encroachments ,problem of road side vendors , parking of rickshaws , private vehicles leading to inefficient intersection, Huge number of Pedestrian.

10 **Meerut Bus Stand**: The road/ Carriageway width is less with inefficient Geometry, number of small commercial establishments along the Delhi road , thickly populated residential areas in the vicinity, so is having huge mixed kind of traffic, beside this this area is having improper road hierarchy of roads, there are number of temporary and permanent encroachments ,problem of road side vendors , parking of rickshaws , private vehicles leading to inefficient transport system, Huge number of Pedestrian with no facilities adds to the problem.

11. **Thapar Nagar** : The road/ Carriageway width is less with inefficient Geometry, number of small commercial establishments/commercial strip development along the main roads , thickly populated residential areas in the vicinity, so is having huge mixed kind of traffic, beside this this area is having improper road

hierarchy of roads, there are number of temporary and permanent encroachments ,problem of road side vendors , parking of rickshaws , private vehicles leading to inefficient transport system, Huge number of Pedestrian with no facilities adds to the problem.

12. Jail Road : The road leads to Bijnour and its width is less, number of small commercial establishments/commercial strip development along the main roads near the existing settlements , residential areas in the vicinity, so is having huge mixed kind of traffic, beside this the area is having improper road hierarchy of roads, there are number of temporary and permanent encroachments ,problem of road side vendors , parking of rickshaws , private vehicles leading to inefficient transport system, Huge number of Pedestrian with no facilities adds to the problem , Hawking and Encroachment, On-street Parking

13 Commissionery choaraha: This is located at major intersection near Divisional commissioners office though the Geometry is comfortable but because of its vicinity to the Meerut College and other important offices ,court offices the capacity of road and intersection is week.

14 Sardana Bus Adda: This is located at Meerut –Roorkee Road , though the Geometry is comfortable but because of its vicinity to the central hub ,markets begum pul ,Abu lane and this place acts as local bus stand to Modipuram area and other important offices ,court offices the capacity of road and intersection is week. so is generally acute traffic problem because of hawkers, vendors roadside Rikshaw parking ,tempo ,local busses and heavy pedestrian movement

Problems Related To Road Safety / Accident Characteristics

- The Roads of the city of Meerut have to cater to mixed kind of vehicles very slow ,slow moving, intermediate ,and fast moving vehicles ,there is regular interface and mixing of very slow and fast moving vehicles like rickshaws ,bullock carts and SUV/cars ,busses which actually makes the situation worse

Year	INJURIES			FATALITIES			GRAND TOTAL
	Male	Female	Total	Male	Female	Total	
2001	421	83	504	271	37	308	812
2002	387	64	451	197	29	226	677
2003	469	73	542	253	21	274	816
2004	395	56	451	222	26	248	366
2005	599	71	670	212	19	231	901

Source: Meerut Municipal Corporation & CDP ,Meerut

Road Traffic Injuries and Fatalities Details for Meerut City

- The width of the Roads ,Geometry ,Alignment is not appropriate /capable to house and to cater to the magnitude of vehicle ,they have to carry especially the State Highways, Regional Highways passing the Central Built Up Area, inner ring road another local streets ,there is problem of heavy commercial traffic ,extreme congestion.
- There are on an average 250 deaths & fatalities and 500 injuries in an year because of road accidents.
- Year 2005 faced maximum about 900 cases of death and serious injuries due to road accidents in an year**

VI. RECOMMENDATIONS TO ADDRESS THE TRAFFIC AND TRANSPORTATION PROBLEMS OF MEERUT

- There is a requirement of creation of a “Traffic and Transport Authority” at city level in Meerut. This authority should have the comprehensive responsibility of Planning, Execution, Monitoring, Policing and Managing the Traffic System. This authority should have the responsibility for Development &Construction of the entire infrastructure related to Transport &Traffic including the roads, flyovers, intersections, pedestrian facilities etc. This authority should have the specially trained requisite manpower viz Civil Engineers ,Architects , Traffic Planners ,police officials ,Public Health Engineers, Structural Engineers, Electrical Engineers Landscape Architects, IT experts to manage the electronic &advanced equipments etc
- The Traffic and Transport Authority should have the responsibility and authority to prepare and implement the Comprehensive Traffic Management System & plan including the Traffic Signaling Design &Control, policing the traffic etc.
- The traffic and transportation problems needs to be addressed at various levels viz. Master Plan , Zonal &local plan level. There is a need for the conduct of detailed traffic and transportation surveys periodically, to understand the problematic issues. and the Master Plan and Zonal plan document should

have a separate section to address these areas. Master plan should recommend/proposes the phase wise improvement of Traffic and transportation infrastructure.

- The Master plan should integrate the network of land uses with the Traffic and Transportation plan. The land uses like vegetable market on Delhi roads, retail shops cinema generating & attracting traffic should be shifted to other locations.
- The temporary and permanent encroachments on roads especially in existing built up areas, Master Plan Roads, Inner, Middle and Outer Cordon are one of the prime reason which decrease the efficiency of roads. Encroachments should be removed through strong drive. The green belts and buffer zone should be earmarked on both sides of proposed Major Roads.
- A Comprehensive Traffic and Transport Management Plan for Meerut is required to manage different types of traffic, people, goods vehicles. Parking issues, managing pedestrians etc. which should be regularly updated to make necessary modification if required
- There is need for improving Pedestrian facilities in the entire city viz. construction of pedestrian pathways, underpasses, over bridges, bus stops, planting trees along the road /pathways, development of pedestrian infrastructure like resting /seating facilities, railing, bus stops, toilets, drinking water etc.
- Promotion of Bicycles: The Meerut city settlement has a diameter of about 15-20 kms and the internal movement in the city can be comfortably managed by bicycles, so this mode needs to be promoted in the city.
- In most of the roads especially on National Highway, State Highways and on main arteries of the city, there is a requirement for segregation of fast and slow moving traffic. Slow traffic should only be allowed on internal roads
- A Traffic and Transportation Plans for Meerut needs to be evolved The road & Intersection Geometry especially in old built up areas are not proper, which needs to be improved this process may require some acquisition of near by areas.
- There is need for improvement of Road Graphics, like zebra crossing, directions, road markings, lanes, road boundaries etc
- The Facilities of physically challenged people on roads, highways are categorically missing, which should be incorporated
- The Traffic signaling system in the city needs to be improved /strengthened, it should be integrated with latest technology for better efficiency of roads
- All the major Arteries of the city should have Security surveillance measures planted to check any violation of traffic rules, jam, clogging of roads and safety etc
- There is need for Improvement and enhancement of Mass Transportation modes the tempos, and local buses. The private players should be made to ensure that the quality of service should be adequate.
- The Comprehensive Traffic and Transportation Plan should have Multi Modal Transportation Approach
- Improvement & regular maintenance of roads, pathways and traffic infrastructure is important.
- There is a need for special mass/ Public awareness programmes to motivate use of Mass Transportation Systems & bicycles, promote maximum pedestrian movement in the city. Knowledge of traffic rules and maintaining discipline on roads
- Traffic rules should be strictly followed
- Public authority should develop parking plazas, multistoried car parking and the special incentive should be given to private players developing multistoried parking plazas
- Truck Terminus and Transport Nagar as proposed in the Master Plan needs to be developed at priority.
- The Railway Infrastructure needs special attention huge of population from Meerut and near by areas depend on railways for movement, so there is need for immediate development of proposals in Master plan to develop the railway infrastructure.

REFERENCES

- [1]. Meerut MASTER PLAN 1971-91: Town and Country Planning Deptt, Meerut
- [2]. Meerut MASTER PLAN 2001: Town and Country Planning Deptt, Meerut
- [3]. Meerut MASTER PLAN 2021: Town and Country Planning Deptt, Meerut
- [4]. City Development Plan :2006 under JNNURM, Meerut Development Authority

ABOUT AUTHORS:

*Vijay Kumar is a Professor, Faculty of Architecture, Urban and Town Planning in D.C.R University of Sc.&Tech., Murthal, Haryana, India

**Dr. R.K.Pandit is a Professor, Deptt. of Architecture, MITS, Gwalior, Madhya Pradesh, India

The Effect of Temperature on Mechanical Properties of M100 Concrete

A. Sreenivasulu¹, Dr. K. Srinivasa Rao²

1. Associate Professor, Department of Civil Engineering, PVP Siddhartha Institute of Technology, Vijayawada

2 Associate Professor in Civil Engineering, College of Engineering, Andhra University, Visakhapatnam.

Abstract: Concrete is generally an excellent fire proofing material. As concrete is exposed to elevated temperature in accidental building fire, an operating furnace, coke oven batteries or a nuclear reactor, its mechanical properties such as Compressive strength, Split tensile strength, Modulus of rupture and Modulus of elasticity for M100 concrete may be decreased reasonably. Since M100 concrete is a relatively a new type of concrete, knowledge about the performance of M100 subjected to fire is limited in comparison with conventional concrete. The behavior of M100 concrete differs from that of Conventional concrete under the same temperature exposure. An attempt has been made in this work to study the effect of elevated temperatures on Compressive strength, Split tensile strength and Flexural strength (modulus of rupture). The cubes of 150 mm side, the beams of 500 mm x 100mm x 100mm and the cylinders of 150mm dia and 300 mm height are used for this study. They were exposed to different temperatures of 50 to 250⁰ C in intervals of 50⁰C for different durations of 1h, 2h, 3h, 4h and 5hours. After these specimens were heated, they were tested for the above mechanical properties in hot state. The effect of elevated temperature on those properties was observed.

Keywords: Ultra strength concrete, Silica fume, Rheobuild, Modulus of rupture, Split tensile strength, Conventional concrete.

I. INTRODUCTION

Exposed to elevated temperature causes physical changes including large volume changes due to thermal dilations, thermal shrinkage and creep related to water loss. The volume changes can result in large internal stresses and lead to micro-cracking and fracture. Elevated temperatures also cause chemical and micro-structural changes such as water migration, increased dehydration, interfacial thermal incompatibility and the chemical decomposition of hardened cement past and aggregate. In general, all these changes decrease the stiffness of concrete and increase the irrecoverable deformation. Various investigations indicate that the strength and stiffness of concrete decrease with increasing temperature, exposure time and thermal cycles. High strength concrete is typically made with high binder contents, low water-to-binder ratios. Supplementary mineral and chemical admixtures. All of these combine to form a very dense matrix that restricts the ability of moisture to escape from the concrete during a fire. As heating progresses, there is a buildup of pore pressure in the concrete that continues to increase until the internal stress becomes so great that explosive spalling results. The present paper which focuses on the Flexural strength, Youngs modulus of M100 concrete and it gives the information about the behavior of M100 concrete under elevated temperatures.

II. OBJECTIVE

The objective of this work is to understand the behavior of M100 concrete when exposed to elevated temperatures. The experimentation was carried out to study the changes in Compressive strength, Split tensile strength and Flexure strength of Ultra strength concrete subjected to elevated temperatures for different durations of exposure.

III. RESEARCH SIGNIFICANCE

Concrete properties are changed by fire exposure. The mechanical properties must be accurately predicted after the fire as they are crucial for the further usage of concrete structures affected by fire. Despite the fact that certain models have already been proposed for the prediction of Compressive strength, Split tensile strength, Flexure strength as they have limitations or lower statistical performances. A unique and comprehensive empirical model is needed to predict loss with high statistical values for which the database of test results is required. This study aims to fulfill the need.

IV. LITERATURE REVIEW

1. Scott T Sherley et al performed fire tests on slab specimens with high strength concrete with and without silica fume and normal strength concrete and concluded that fire endurances of all five specimens were not significantly different.
2. Sujit Ghosh et al concluded through their research that compressive strength and Young's modulus of 20 and 60% Flyash and 10% Silica fume concrete decreased with a rise in temperature from 21.4 to 232⁰C for different pressures and this decrease was attributed to a gradual deterioration of the binding matrix with rise in temperature.
3. M.Saad et al concluded that concrete specimens containing 10% silica fume possess lower porosity values and the highest compressive strength values at all temperatures of thermal treatment as more CSH is formed with stronger binding forces and a sufficient thermal stability.
4. R. Ravindra rajaiah et al through their research concluded that the residual compressive and tensile strengths for high strength concrete with blended cement after heating to 800⁰C and water quenched were 31% of initial strengths whereas the corresponding residual strengths for concrete with ordinary Portland cement was 44%.
5. Potha raju et al investigated the effect of elevated temperature on the flexural strength of flyash concrete of different grades of M28, M33 and M35. Concrete specimens 100 x 100 x 50 mm with partial replacement cement by flyash were heated to 100, 200 and 250⁰C for 1, 2 and 3h durations. The specimens were tested for flexural strength in the hot condition immediately after removing from the oven. It was concluded that flyash content up to 20% showed improved performance compared with the control specimens by retaining greater amount of its strength.
6. Geogre C Hoff et al conducted research to study the effect of elevated temperature effects on high strength concrete residual strength. They concluded that there appeared to be a slight improvement in residual strength at 200⁰C (392⁰F) exposure when subjected to 100⁰C (212⁰F) exposure. At constant temperatures of 300⁰C (572⁰F) there is a significant loss of strength. At temperatures 900⁰C (1652⁰F) and after, all concretes essentially had no structural integrity residual strengths of HSC at exposed temperatures of 300⁰C (72⁰F) or higher are significantly different than residual strength for NSC.

Experimental Program

Preliminary investigations were carried out to develop M100 grade concrete. The mix proportion arrived as per ACI 211.1¹ was 1:0.556:1.629 by weight with w/c ratio as 0.25. The estimated batch quantities per cubic meter of concrete were: cement, 671.81 kg; fine aggregate, 373.33 kg; coarse aggregate, 1094.4 kg and water, 167.95 litres. The optimum dosages of Mineral and Chemical admixtures were identified as 6% and 1.5% of quantity of cement respectively.

Rheobuild 1100

The basic components of RHEOBUILD 1100 are synthetic polymers which allow mixing water to be reduced considerably and concrete strength to be enhanced significantly, particularly at early ages. Rheobuild 1100 is a chloride free product. It allows the production of very flowable concrete, with a low water/cement ratio. Concrete with Rheobuild shows strengths higher than concrete without admixture having the same workability.

Silica Fume (Micro Silica)

It is a by product of producing silicon metal or ferrosilicon alloys. Because of its chemical and physical properties, it is a very reactive pozzolana. Concrete containing silica fume can have very high strength and can be very durable. Silica fume is available from suppliers of concrete admixtures and when specified, is simply added during concrete production. Placing, finishing and curing silica fume concrete require special attention on the part of the concrete contractor. Silicon metal and alloys are produced in electric furnace. The raw materials are quartz and wood chips. The smoke that results from furnace operation is collected and sold as silica rather than being land filled.

Casting and curing specimens

The test specimens were demoulded after a lapse of 24 hours from the commencement of casting and submerged in water until the time of testing.

Exposing the specimen to elevated temperatures

An oven with a maximum temperature of 300°C was used for exposing the specimens to different elevated temperatures. It was provided with a thermostat to maintain constant temperatures at different ranges. The specimens were kept in the oven as shown in fig.2 for a specified duration after the temperature in the oven reached the defined temperature. The specimens were heated to different temperatures of 50, 100, 150, 200 and 250°C for different durations of 1, 2, 3 and 4 hours at each temperature. The specimens were tested for their strengths with minimum delay after removing from the oven in a hot state under unstressed condition.

Table 1 : Compressive and % Residual compressive strengths of cubes after exposing to elevated temperature

Temperature (°C)	Compressive Strength (N/mm ²)				% Residual Compressive strength			
	1 hour duratio	2 hours duratio	3 hours duratio	4 hours duratio	1 hour duratio	2 hours duratio	3 hours duratio	4 hours duratio
27	131.67	131.67	131.67	131.67	100.0	100.0	100.0	100.0
50	140.39	146.93	134.29	138.65	106.62	111.59	101.99	105.3
100	148.24	136.47	143.01	125.57	112.58	103.65	108.61	95.37
150	144.75	134.94	138.43	122.95	109.93	102.48	105.13	93.38
200	136.25	131.24	135.16	117.29	103.48	99.67	102.65	89.08
250	120.77	144.32	130.58	124.70	91.72	109.61	99.17	94.71

Table 2: Split and % Split tensile strengths of cylinders after exposing to elevated temperature

Temperature (°C)	Split Tensile Strength (N/mm ²)				% Residual Split Tensile strength			
	1 hour duratio	2 hours duratio	3 hours duratio	4 hours duratio	1 hour duratio	2 hours duratio	3 hours duratio	4 hours duratio
27	30.79	30.79	30.79	30.79	100.00	100.00	100.00	100.00
50	38.50	36.83	35.72	32.53	125.04	119.62	116.01	105.65
100	44.62	26.83	36.28	33.36	144.92	87.14	117.83	108.35
150	35.38	29.89	27.87	20.50	114.91	97.08	90.52	66.58
200	26.41	28.50	20.71	16.40	85.77	92.56	67.26	53.26
250	20.43	18.63	17.38	14.73	66.35	60.51	56.45	47.84

Table 3: Flexure and % Residual flexure strengths of beams after exposing to elevated temperature

Temperature (°C)	Flexural Strength (N/mm ²)				% Residual Flexural strength			
	1 hour duratio	2 hours duratio	3 hours duratio	4 hours duratio	1 hour duratio	2 hours duratio	3 hours duratio	4 hours duratio
27	5.34	5.34	5.34	5.34	100.00	100.00	100.00	100.00
50	5.57	6.44	6.00	5.81	104.41	120.59	112.50	108.82
100	6.32	6.87	7.22	7.02	118.38	128.68	135.29	131.62
150	7.73	8.04	7.18	6.98	144.85	150.74	134.56	130.88
200	4.79	5.65	6.00	5.77	89.71	105.88	112.50	108.09
250	4.24	4.12	3.85	3.49	79.41	77.21	72.06	65.44



Fig. 1 Cubes on Vibrating table during Compaction



Fig. 2 Cube in Oven while heating



Fig. 3 Testing of Cylinder during split tensile strength test



Fig. 4 Tested Concrete cube

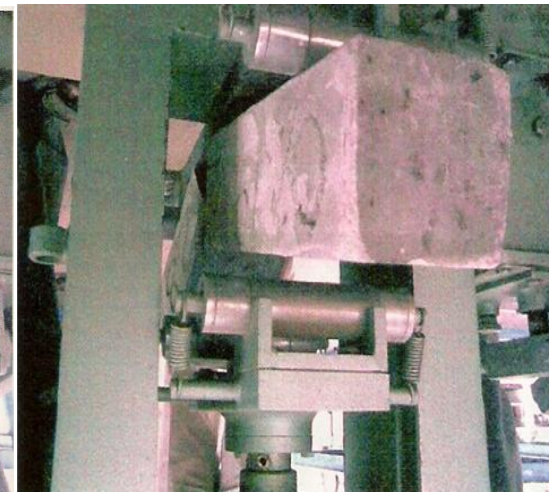


Fig.5 Testing of M100 Concrete beams for Flexure

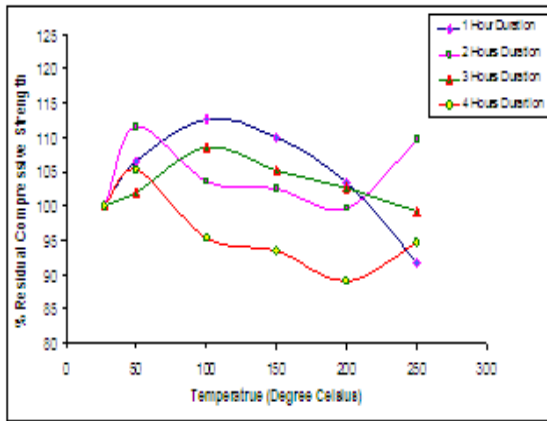


Fig.6 Variation of % Residual Compressive strength with temperature

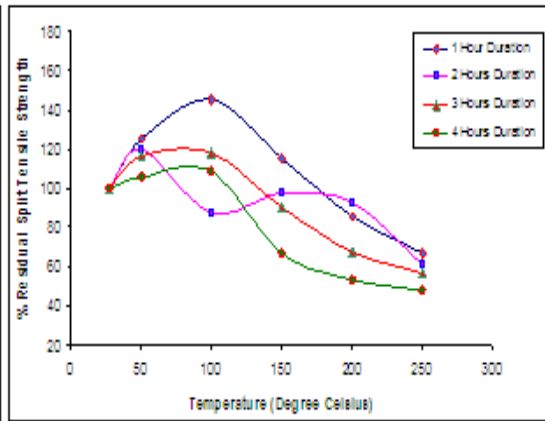


Fig. 7 Variation of % Residual Split tensile strength with temperature

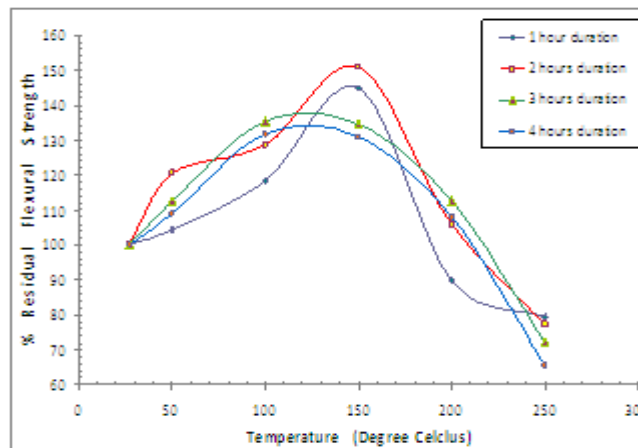


Fig. 8 Variation of % Residual Modulus of Rupture with temperature

V. RESULTS AND DISCUSSIONS

Compressive strength

The factors that influence the compressive strength of Ultra strength concrete when exposed to elevated temperatures are temperature and time of exposure. The test results are presented in Table 1. The variation of % Residual Compressive strength with temperature for different exposure durations is shown in Fig.6. The compressive strength at any temperature is expressed as the % of Compressive strength at room temperature. The heated specimens are tested in hot condition for compressive strength according to IS: 516-1959²

Split Tensile strength

Residual splitting tensile strength of concrete was found to be influenced by the temperature to which it was exposed and the duration of exposure. Residual splitting tensile strength of all heated specimens at any exposure time was expressed as the percentage of 28 days split tensile strength of unheated concrete specimens. The test results are presented in Table 2. The variation of % Residual Split tensile strength with temperature for different exposure durations is shown in Fig.7. The Split tensile strength at any temperature is expressed as the % of Split tensile strength at room temperature.

Modulus of Rupture

Flexural strength of M100 concrete was noticed to increase continuously upto 150°C and beyond that there is rapid decrease in Modulus of rupture. The Residual Modulus of rupture is also calculated at different temperatures for 100x100x500 mm size concrete beams. The variation of modulus of rupture w.r.t to temperature is also shown in the graph from the Fig.8.

VI. CONCLUSIONS

On the basis of the experimental work with ranging temperature from 50 to 250⁰C, the following conclusions are drawn.

- a) The compressive and split tensile strengths of M100 concrete are increased initially upto a temperature of
- b) 50- 100⁰C and beyond that they got reduced rapidly with increasing the temperature
- c) It was observed that major part of loss in split tensile strength is taking place in the first 1 hour exposure.
- d) The compressive and Split tensile strengths are lost very much when they are heated at 250⁰C
- e) Modulus of rupture was increased gradually upto a temperature of 150⁰C and beyond that it was observed to decrease continuously.

REFERENCES

- [1]. ACI 211.1-91 - Standard Practice for Selecting Proportions for Normal, Heavyweight and Mass Concrete. IS : 516-1959 - Indian Standard Methods of tests for Strength of concrete
- [2]. M.S Shetty Text book of Concrete Technology, S. Chand & Co. Ltd.
- [3]. A.M. Neville, Properties of Concrete, Longman. Said Irvani, "Mechanical properties of High Performance Concrete", ACI Mat. V.93, No.5, 1996, pp. 416-426.
- [4]. Richard Gagne, Alain Boisvert and Michel Pigeon, "Effect of Super plasticizer dosage on Mechanical properties, Permeability and Freeze-Thaw durability of High strength concrete with and without silica fume", ACI Mat. Journal, Volume 93, No.2, 1996, pp.111-120.
- [5]. Brandt. A.M. and Kucharska, L, "Mechanical properties and Applications of High Performance concrete", Proceedings of International Symposium on innovative world of concrete (ICI-IWC-93), pp. KN3-KN2.
- [6]. Xie, J., AE Elwi and MacGregor, J.G., "Mechanical Properties of three High strength concretes containing Silica fume", ACI Material Journal, V.92, No.2, 1995, pp. 135-145.
- [7]. Flyod Slate, O., Arthur Nilson H., Salvador Martinez, "Mechanical properties of High strength light weight concrete", ACI Journal, July-August 1986, pp. 603-613.
- [8]. V.K.R.Kodur and L.T. Phan (1996), "Fire performance of high-strength concrete", National Institute of Standards and Technology, Gaithersburg.

Properties of Reactive Compatibilized Dika Nutshell Powder filled Recycled Polypropylene (PP)/Polyethylene Terephthalate (PET) Biocomposites using Maleated Polypropylene and Epoxy Resin Dual Compatibilizers.

G. N. Onyeagoro¹, C. M. Ewulonu², M. D. Ayo³

¹Department of Polymer and Textile Engineering, Federal University of Technology, Owerri, NIGERIA.

²Department of Polymer and Textile Engineering, Nnamdi Azikiwe University, Awka, NIGERIA.

³Department of Polymer Technology, Auchi Polytechnic, Auchi, NIGERIA.

Abstract: Dika nutshell powder (DNS) filled – recycled polypropylene (PP)/polyethylene terephthalate (PET) biocomposite was prepared by reactive compatibilization using maleic anhydride-grafted-polypropylene (MAPP) and epoxy resin (EPR) as dual compatibilizers. The mechanical and rheological properties, as well as sorption behavior of the compatibilized biocomposites were studied at filler loadings of 0, 2, 4, 6, 8, and 10 phr (parts per hundred parts of resin). PP/PET composition was fixed at 30/70 wt. %. The results show that when MAPP alone was used as compatibilizer, property improvements were not substantial due to the low reactivity between MAPP and PET, which produces insignificant amount of copolymers as coupling agent at the interfaces. Effective compatibilization was achieved by adding epoxy resin (EPR) as suggested by impressive improvement in the properties investigated. Outstanding property improvements, especially oil resistance, tensile and impact strengths (higher values), and elongation at break (lower value) were obtained with increases in EPR and filler loadings.

Keywords: Biocomposite, compatibilization, dika nutshell powder, polyethylene terephthalate, polypropylene, recycling.

I. INTRODUCTION

Polypropylene (PP) and polyethylene terephthalate (PET) have been widely used in packaging applications and are frequently encountered in urban and industrial plastics wastes. Recycling offers an alternative solution for handling plastic wastes. Although there exist, easy and inexpensive separation methods for these plastics, yet a mechanical recycling method which involves blending of the plastics gives rise to secondary materials with interesting properties. It has been reported that blends of polyolefins (particularly polyethylene (PE) and PP) and PET can display good mechanical and permeation characteristics [1]. However, PP and PET are incompatible and immiscible leading to poor interfacial adhesion and mechanical properties, and this has greatly limited the search for PP – PET blend [2]. Compatibilization through a third component, acting as a bridge between the two incompatible phases, becomes necessary to stabilize the blend and to improve its mechanical performance. Two procedures have proved successful in compatibilization of immiscible blends: (1) addition of a block copolymer (BC) or a graft copolymer, which tends to migrate and concentrate at the interface as an interfacial emulsifier and (2) use of functionalized polymers or reactive compatibilizers to form chemical bonds between the blend components [3]. The choice of a block or graft copolymer is based on the miscibility of its segments with the blend components, and such copolymers usually require a separate preparation step, and some of them are difficult to synthesize. Besides, these copolymers may not have enough time to migrate and reside at the interface under a typical melt processing condition [4].

In recent times, the in-situ-formed compatibilizers in blend systems have been used as an alternative to replace the conventional block or graft copolymers. The in-situ reaction occurs during melt processing to form block or graft copolymers at interfaces. These in-situ-formed copolymers tend to reside along the interface to

reduce the interfacial tension at melt and increase interfacial adhesion at solid state, thus resulting in substantial improvement in the physico-mechanical properties of the resultant blend [5]. The reinforcement of polymeric materials is expressed by enhancement of certain processing and end-use properties. The past decades have witnessed a growing interest in the use of renewable resources as reinforcements in polymer composite systems. This is due to strong environmental regulations and increased interest in the proper utilization of renewable natural resources to develop eco-friendly components. Numerous studies have been carried out on the utilization of bamboo [6] and wood [7] or products like rice husk [8, 9], chitin [10], coir [11] and numerous natural fibers [12, 13] as reinforcement materials. Benefits of these natural fillers include abundance and low cost, light weight, biodegradability and so on [14, 15]. These advantages led to the use of natural fillers as potential replacement for traditional reinforcement materials such as glass fiber in composite systems [16]. However, the compatibility or miscibility of natural fillers in polymeric materials is often in doubt due to the non-polar and hydrophobic nature of most polymeric materials when compared with the polar and hydrophilic lignocellulosic filler material due to the presence of hydroxyl groups in cellulose [17]. To address this problem, studies have been conducted on surface modification of natural fibers for the purpose of making the hydrophilic surface more compatible with hydrophobic polymers by using coupling agents [18]. Excellent reports exist in the literature on chemical treatment of fiber surface and use of coupling agents to improve the compatibility between hydrophobic polymer matrices and hydrophilic fillers [18-20]. There are experimental results in the literature supporting polymeric systems as effective in-situ reactive compatibilizers for polymer blends [18, 21]. Onyeagoro [21] used maleic anhydride-grafted-polyisoprene and epoxy resin as reactive compatibilizers in natural rubber/carboxylated nitrile rubber blends and reported improvements in cure characteristics and mechanical properties in the blends. Ming-Yih Ju et al. [22] reported that a combination of styrene-maleic anhydride random copolymer (SMA – 8wt % MA) and tetra-glycidyl ether of diphenyl diamino methane (TGDDM) (epoxy resin) is able to compatibilize PET – Polystyrene (PS) blends. The authors revealed finer phase domain size of the dispersed phase in the compatibilized blends. Improvements in tensile and impact properties were also reported. It is well known that PET carboxyl terminal groups do not react with the anhydride of maleic anhydride-grafted-polypropylene (MAPP), while the reaction between hydroxyl groups of PET and dika nutshell powder (DNS) filler (a cellulosic filler) is insignificant without the presence of a catalyst. However, many researchers [22-24] have shown that epoxy is able to react with polyester terminal carboxyl group to compatibilize effectively many polyester-related blends. Epoxy is also well known to react with anhydride readily. Thus, the presence of epoxy in the PP/PET/MAPP blend is capable of producing PET-co-epoxy-co-MAPP copolymer at the interface, which is able to function as an effective compatibilizer. In the present study, the effect of epoxy resin on mechanical properties, water absorption, and sorption behavior of compatibilized biocomposites of PP/PET/MAPP/DNS is investigated. The use of DNS as filler for polymer systems has been reported in the literature. Thus, Onyeagoro [25] investigated the influence of carbonized dika (*Irivalgia Gabonensis*) nut shell powder on the vulcanizate properties of natural rubber/acrylonitrile-butadiene rubber blends. The author found that the synchronous use of carbon black and carbonized dika nutshell powder obtained at a carbonization temperature of 600°C brought significant improvements in the vulcanizate properties of the blends at filler loading of 10 phr, and suggested that carbonized dika nutshell powder could serve as potential substitute filler for carbon black in the rubber industry, especially in the production of low-cost/high volume rubber products where strength is not critical. Similarly, the sorption characteristics of dynamically vulcanized polypropylene/epoxidized natural rubber blends filled with carbonized dika nutshell (*Irivalgia Gabonensis*) were studied by Onyeagoro and Enyiegbulam [26]. The authors revealed that resistance to toluene sorption increased with dynamic vulcanization and also with increase in the filler carbonization temperature. Furthermore, studies on reactive compatibilization and dynamic vulcanization of polypropylene/epoxidized natural rubber blends filled with carbonized dika nutshell powder were carried out by Onyeagoro and Enyiegbulam [27]. The authors reported outstanding improvement in tensile and impact properties (higher values) and elongation at break (lower values) with increase in filler loading. Dika is a tropical nut grown in Nigeria and most tropical African countries [25]. Nigeria produces about 150,000 tonnes of dika annually [25-27]. The shell which is a by-product of dika nut processing is presently discarded as waste and could be found littering waste bins in our big cities and farm yards in most localities. Presently, it does not have any known domestic/industrial applications. The only existing practice of utilizing them as fuel by some oil processing mills in the country constitutes a great environmental hazard to the host communities and the practice has been discouraged. Therefore, the present study also seeks to harness the potentials of dika nutshells as filler in thermoplastic polymers.

II. EXPERIMENTAL

2.1. Materials

The recycled polymers used in this work were two thermoplastics (PP and PET). PP was obtained from industrial scraps. The PET used was obtained from a separate collection of post-consumer bottles (drinking and

soft drink bottles). The compatibilizers, maleic anhydride-grafted-polypropylene containing 10 wt% maleic anhydride (Samsung Chemical Co.) and epoxy resin (tetra-glycidylether of diphenyldiaminomethane, TGDMM) with the trade mark of NPEH-434 (Nan Yea Plastics Co. of Taiwan) were purchased from Rovet Chemicals Ltd, Benin City, Nigeria. Dika nutshells were sourced from different farm yards in Auchi, Edo State, Nigeria. The repeating units of the polymers used in this work are given in Table 1.

2.2. Preparation of Dika nutshell Powder

Dika nut shells were thoroughly washed to remove sand particles and other earthy materials. Dika nutshell powder (DNS) was produced by milling Dika nutshells to fine powder. The powder was sieved at a particle size of 150µm, dried at 110°C for 24 hours in a vacuum oven and then kept in a dessicator until required.

Table 1. Repeating units of each component

Component	Repeating unit
PP	$\text{---} \left[\begin{array}{c} \text{CH}_2 \text{---} \text{CH} \text{---} \\ \\ \text{CH}_3 \end{array} \right]_n \text{---}$
PET	$\text{HO---} \left[\begin{array}{c} \text{O} \qquad \qquad \text{O} \\ \qquad \qquad \quad \\ \text{C} \text{---} \text{C}_6\text{H}_4 \text{---} \text{C} \text{---} \text{O} \text{---} \text{CH}_2 \text{---} \text{CH}_2 \text{---} \text{O} \end{array} \right]_n \text{---H}$
MAPP	$\text{---} \left[\begin{array}{c} \text{HC} \text{---} \text{CH} \text{---} \text{CH}_2 \text{---} \text{CH} \text{---} \\ / \qquad \backslash \qquad \quad \\ \text{O} \text{=C} \qquad \quad \text{C} \text{=O} \qquad \quad \text{CH}_3 \end{array} \right] \text{---}$
EPR	$\begin{array}{c} \text{O} \qquad \qquad \qquad \text{O} \\ / \ \backslash \qquad \qquad \quad / \ \backslash \\ \text{H}_2\text{C} \text{---} \text{CH} \text{---} \text{CH}_2 \qquad \qquad \text{CH}_2 \text{---} \text{CH} \text{---} \text{CH}_2 \\ \qquad \qquad \qquad \quad \\ \text{H}_2\text{C} \text{---} \text{CH} \text{---} \text{CH}_2 \qquad \qquad \text{CH}_2 \text{---} \text{CH} \text{---} \text{CH}_2 \\ / \ \backslash \qquad \qquad \quad / \ \backslash \\ \text{O} \qquad \qquad \qquad \text{O} \end{array}$

2.3. Preparation of Composite Samples

Formulations of DNS powder filled recycled PP/PET bio-composites are given in Table 2. Blend composition of PP/PET was fixed at 30/70 parts per hundred parts of resin (phr) concentration, while varying filler (DNS) loadings of 0, 2, 4, 6, 8, 10 phr were used. Prior to the extrusion compounding technique employed, PET was dried at 120°C, and PP and MAPP were dried at 90°C for over 24 hours in separate vacuum ovens. The epoxy resin (EPR) was dried at 60°C for 2 hours before using. The compounding ingredients, excluding DNS powder were charged into the extruder. All composites were prepared by dry-mixing first, followed by melt-mixing in a 30mm co-rotating intermeshing twin-screw extruder with a 7:1 length-to-diameter screw operated at a rotational speed of 250rpm. The temperature of the melt ranged from 255 to 265°C. After 6 minutes of mixing, DNS powder was then added into the molten mixture and the composite mixture extruded as pellets. The extruded pellets were dried in a vacuum oven and compression molded using a hot press into standard ASTM specimens for mechanical property testing [9].

Table 2: Compounding recipe for recycled PP/PET/DNS bio-composites.

Ingredients (phr)	Uncompatibilized MAPP/EPR = 0/0	Compatibilized			
		MAPP = 2.0	MAPP/EPR = 2.0/0.1	MAPP/EPR = 2.0/0.3	MAPP/EPR = 2.0/0.5
PP	30	30	30	30	30
PET	70	70	70	70	70
MAPP	0	2.0	2.0	2.0	2.0
EPR	0	0	0.1	0.3	0.5
DNS	0, 2, 4, 6, 8, 10				

2.4. Measurement of Rheological Properties

Rheological properties of the composites were carried out on a rheometric dynamic spectrometer using a parallel-plate geometry ($R = 25 \text{ mm}$) at 230°C [30]. For strain sweep measurements, a strain range of 0.1 to 300% and an angular frequency of 7.5 rad/s were used. Measurements with frequency sweep were done at a constant strain of 2.5% and a frequency range of 0.1 to 100 rad/s.

2.5. Measurement of Mechanical Properties

Tensile tests were conducted at room temperature (27°C) using a Monsanto Tensile Tester (Model 1/m) using dumb bell test pieces measuring $45\text{mm} \times 5\text{mm} \times 2\text{mm}$ according to ASTM D412-87 method A. The crosshead speed was 500mm min^{-1} . Tensile strength, tensile modulus, and elongation at break of each composite sample were obtained from the average of five specimens with their corresponding standard deviations. Impact strengths were measured by carrying out Izod impact tests. All specimens for Izod impact test were stored in a desiccator until required for test to avoid moisture absorption. Izod bars of composite samples were notched and tested at room temperature (27°C) according to the ASTM D256 method. The value of impact strength of each specimen is the average of 5 runs.

2.6. Water Absorption Test

The water absorption test was carried out by immersing the composite samples in distilled water at room temperature (27°C). The samples were removed at specified time intervals and gently blotted with tissue paper to remove the excess water on the surface. The weight of each swollen sample was recorded. The sample was then dried at 40°C until a constant weight was achieved. The degree of water absorption (S_w), and degree of weight loss (L_w) were calculated using equations 1 and 2 [28].

$$S_w = \frac{W_2 - W_1}{W_1} \quad (1)$$

$$L_w = \frac{W_1 - W_3}{W_1} \times 100 \quad (2)$$

Where W_1 and W_2 are the weights of the sample before and after the water absorption, respectively, and W_3 is the dry weight of a sample after water absorption.

2.7. Sorption Test

Sorption test was conducted by immersing composite samples in ASTM No. 3 oil at room temperature (27°C) for 70 hours according to ASTM D 471-98. The samples were removed at specified time and gently wiped with tissue paper to remove the excess oil on the surface. The weight of each swollen composite sample was recorded. Swelling index was the swelling parameter used to assess the extent of swelling of the composite and was calculated by equation 3 [9].

$$S = \frac{W_s - W_0}{W_0} \times 100 \quad (3)$$

where W_0 and W_s are the initial dry weight and final (swollen) weights of the composite, respectively.

III. RESULTS AND DISCUSSION

3.1. Rheological Properties

Plot of complex viscosity, η , versus angular frequency, ω , for recycled PP/PET/DNS composites is presented in Fig. 1. It can be seen from the figure that the complex viscosity of compatibilized composite is always higher than that of uncompatibilized composite, at all the frequency levels investigated. The higher complex viscosity observed for compatibilized PP/PET/DNS composite in this study is attributed to the reactive compatibilization arising from chemical reaction between the acid groups of MAPP and PET, and the hydroxyl groups (-OH) of DNS during melt blending. Similar results were obtained in our previous report on reactive compatibilization and dynamic vulcanization of polypropylene (PP)/epoxidized natural rubber (ENR) blends filled with carbonized Dika nutshell [27]. The result of this finding is also consistent with some previous reports

on polymer blends which revealed general increases in complex viscosity when there is either a specific interaction between the phases [4, 29], or chemical bonding between the blend components [30]. Such a chemical bond will also induce a strong interaction between the phases. The net effect is that the matrix exhibits greater resistance to flow due to resultant increase in viscosity. On the other hand, in the absence of any such physical interaction or chemical bonding, low viscosity results because the domain can easily be elongated in the matrix. The use of MAPP alone as compatibilizer did not produce any significant increase in complex viscosity. This indicates that MAPP alone cannot effectively compatibilize recycled PP/PET/DNS composites.

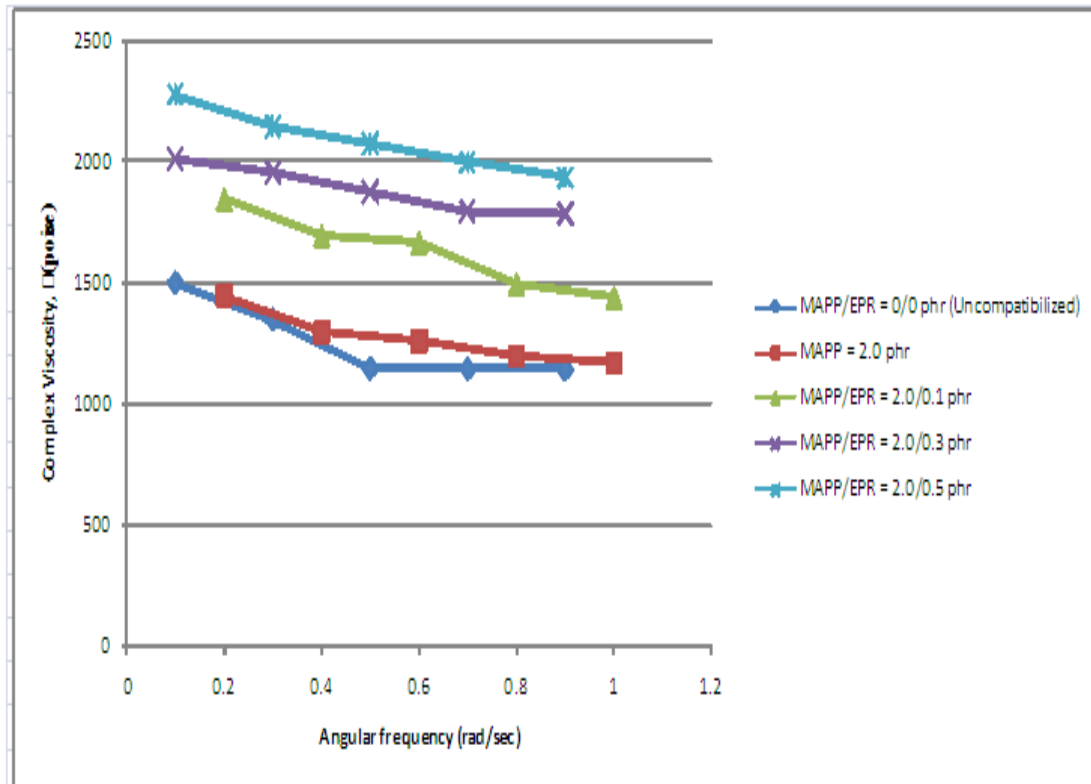


Figure 1: Plot of Complex Viscosity versus Angular frequency for recycled PP/PET/DNS Composites.

Figure 1 also shows that complex viscosity of the composites increased with increase in EPR loading due to the stiffening effect of EPR with increase in EPR loading. This result demonstrates that portion of EPR is able to act as an effective coupler to react with MAPP and PET simultaneously to produce the desired PET-co-EPR-co-MAPP copolymers. As a result of the chemical reaction, these in-situ-formed copolymers tend to anchor along the interface. Other portion of EPR may function as a chain extender to react with only one blend component (PET) to increase the molecular weight of PET. Increasing EPR content increases the concentration of the reactive functional groups of EPR. Thus, increase in EPR content causes light crosslinking of the composite which results to a corresponding increase in complex viscosity. Like the complex viscosity, the higher increase in storage modulus, G' , displayed by compatibilized recycled PP/PET/DNS composites over the uncompatibilized composites (Figure 2) is attributed to molecular build-up arising from the chemical reactions that occurred during the melt compounding process [29].

Figure 3 illustrates the effect of epoxy resin (EPR) on maximum torque value of PP/PET/DNS composites. The results show a low value (5.8 Nm) of maximum torque in the absence of MAPP/EPR compatibilizer, which indicates poor physical interaction between PP and PET phases in the absence of the compatibilizer. Again, like the complex viscosity and storage modulus the presence of MAPP alone as compatibilizer (MAPP/EPR = 2.0/0) did not produce any appreciable increase in maximum torque (only 3.0 Nm). This indicates that MAPP alone cannot effectively compatibilize polymer composites of PP/PET/DNS. However, the presence of only 0.1 phr EPR (MAPP/EPR = 2.0/0.1) is able to increase the maximum torque significantly. This result indicates that the coupling and chain extending reactions indeed occur during the melt blending process and produces various PET-co-EPR-co-MAPP copolymers and chain-extended PET in the compatibilized composites. The in-situ-formed copolymers tend to anchor along the interface and, therefore, raise the interfacial friction of the compatibilized composites under shear stress.

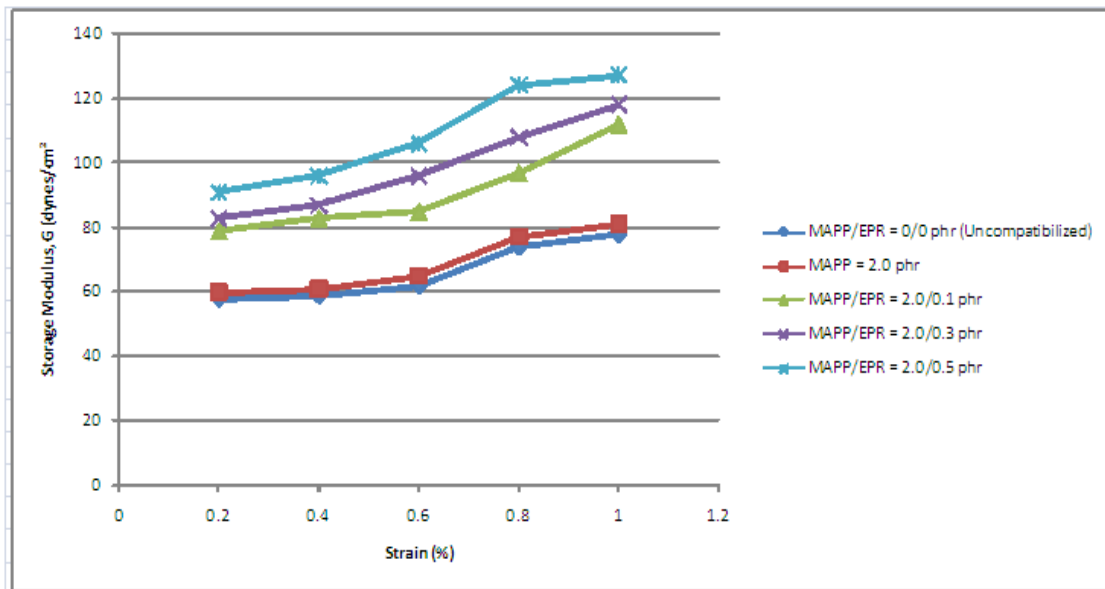


Figure 2: Plot of Storage Modulus versus Strain for recycled PP/PET/DNS Composites.

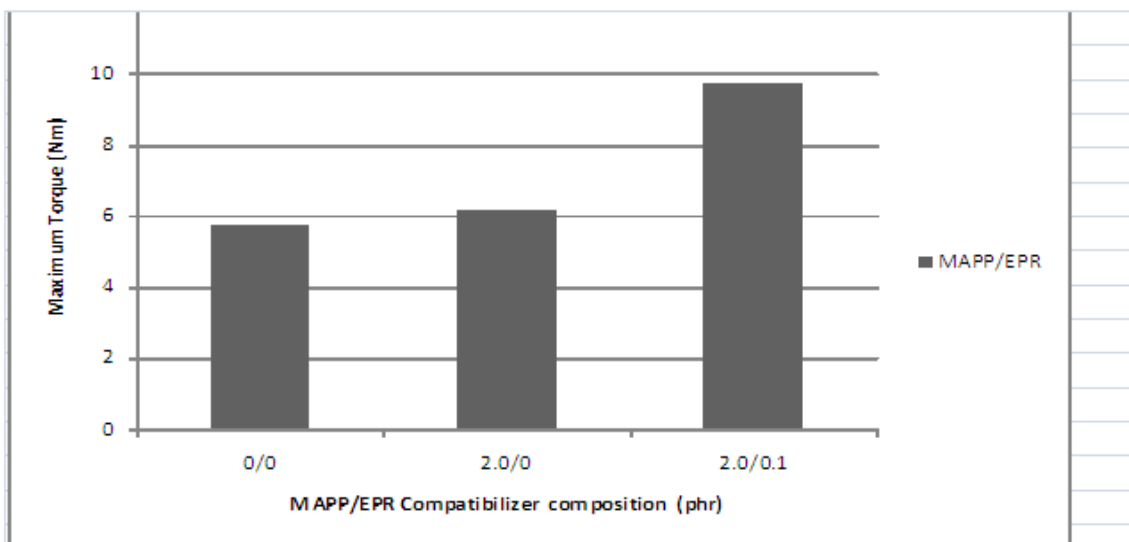
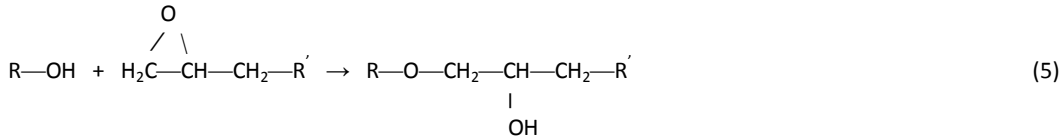
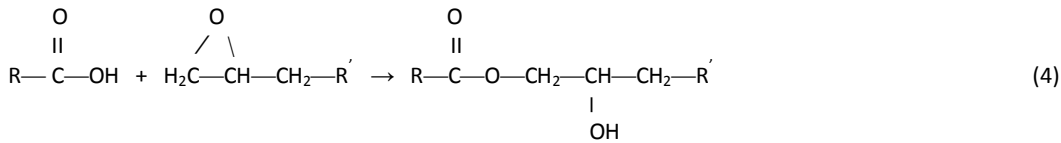


Figure 3. Effect of epoxy resin (EPR) on maximum torque value of Dika nutshell powder filled recycled PP/PET composites.

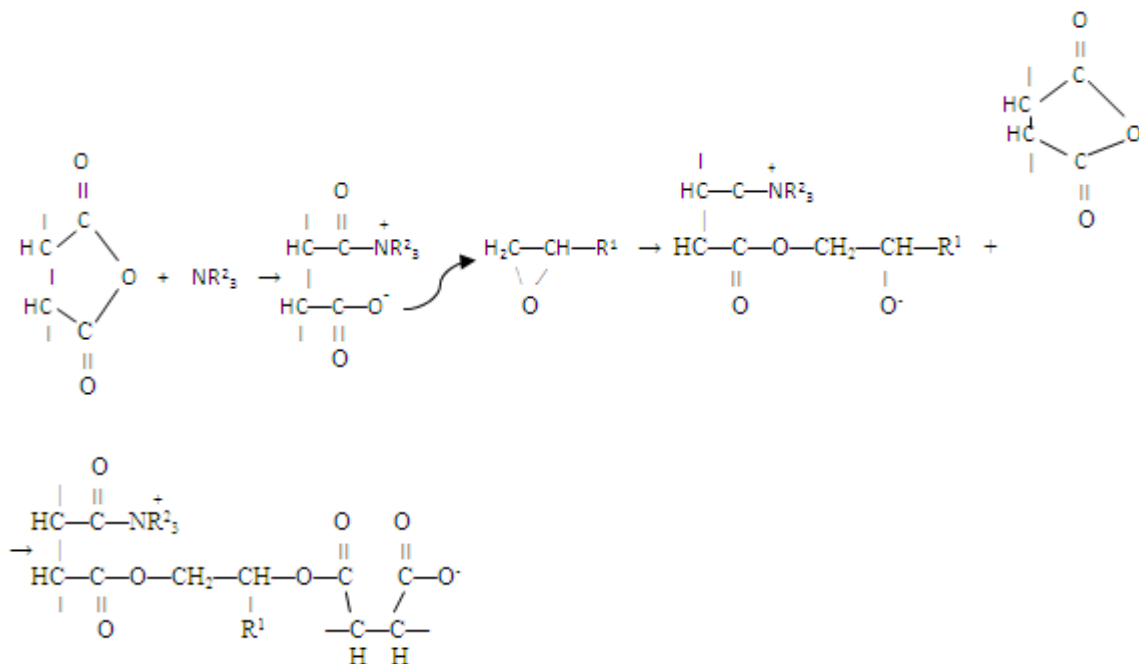
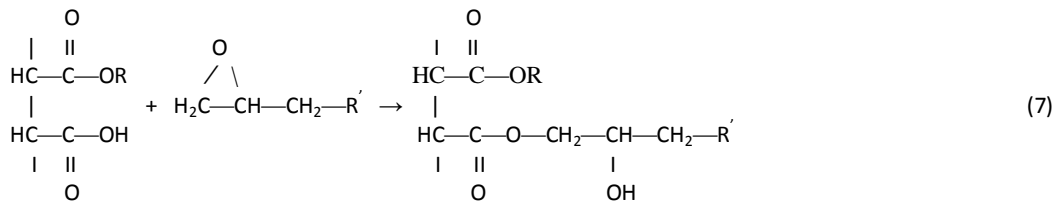
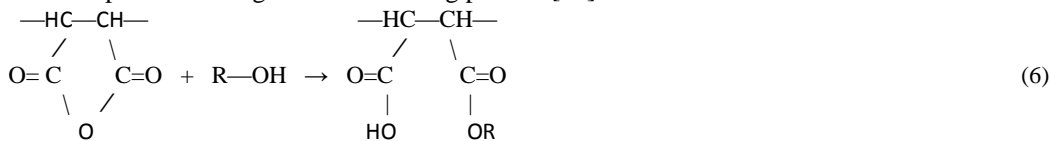
3.2. Mechanical properties

Figure 4 shows the effect of DNS loading and epoxy resin (EPR) on recycled PP/PET/DNS composites. The result shows that the tensile strength decreased with increase in DNS content. The decreasing trend in tensile strength with increase in DNS content may be due to poor adhesion between polar DNS and non polar PP matrices which makes the DNS incapable of supporting stress and transmitting it to polymer matrix. Figure 4 also shows that at a similar filler loading, the presence of MAPP alone as compatibilizer does not produce any appreciable increase in tensile strength of the composites. This result implies that the expected reaction between anhydride groups of MAPP and hydroxyl groups of PET does not occur or occurs insignificantly during extruder compounding. On the contrary, addition of EPR in the PP/PET/DNS composite leads to a significant increase in tensile strength, indicating improvement in interfacial adhesion which is attributed to the additional chemical reaction between EPR and PET terminal hydroxyl group, as well as the anhydride group of MAPP. The improved interfacial bonding provides better stress distribution which results in increase in tensile strength of the composites when compared with the composite with MAPP alone and the one without compatibilizer. Similar findings were reported by Ju and Chang. [22], whereby higher tensile strength in polymer blend of PET – Polystyrene (PS) was reported with progressive increase in tetra-glycidyl ether of

diphenyl diamino methane (TGDDM) (an epoxy resin) using styrene maleic anhydride (SMA) random copolymer and TGDDM as dual compatibilizers. The reaction mechanism between EPR and terminal groups of PET is well elucidated in the literature as the following simplified equations 4 and 5 [31].



Also, the reaction between epoxy resin and anhydride groups can be initiated by a hydroxyl-containing compound to proceed ring-opening reaction, as illustrated in equation 6 [22]. Furthermore, it has been reported that a hydroxyl-containing compound can be obtained from the reaction between TGDDM and PET or from the terminal group of PET and then, the ring-opened anhydride groups can react with epoxy group as the following equation 7 [22]: Scheme 1 illustrates the simplified reaction mechanism between EPR and anhydride groups catalyzed by a tertiary amine. The tertiary amine on the EPR can act as a catalyst, and the self-catalyzed reaction is able to proceed during the melt blending process [31].



Scheme 1: The simplified reaction mechanism between EPR and anhydride catalyzed by tertiary amine.

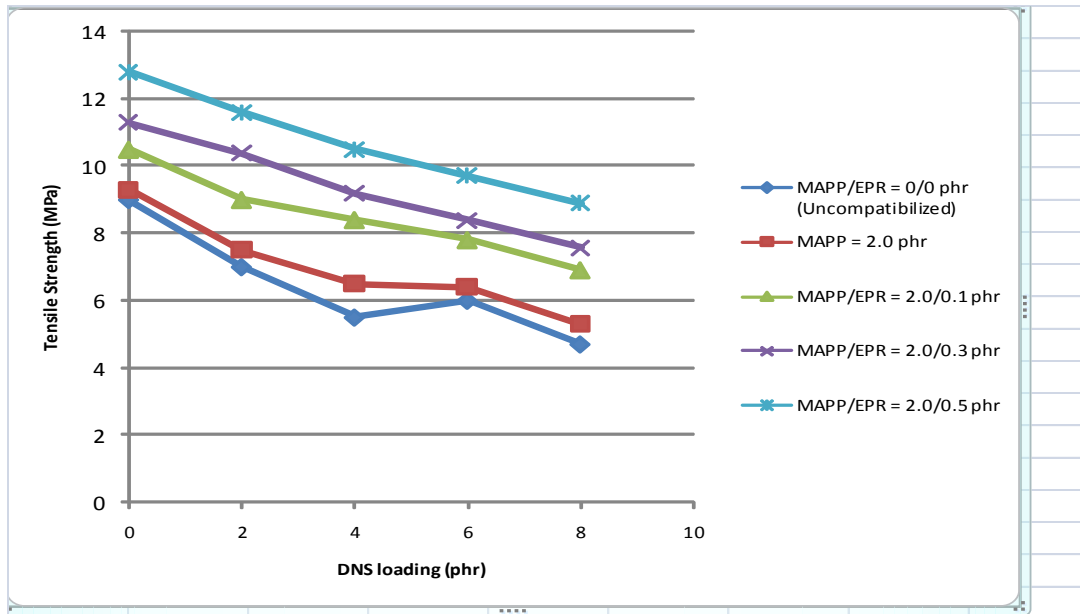


Figure 4: Effect of DNS loading and epoxy resin (EPR) on tensile strength of recycled PP/PET/DNS composites.

Figure 5 shows that increase in DNS loading produces increases in tensile modulus of composites with and without compatibilizer. The incorporation of DNS filler into the recycled PP/PET matrices increases the stiffness of the composites. This reduces the PP/chains mobility, consequently producing more rigid composites. At a similar filler loading, the composite obtained with MAPP compatibilizer alone did not produce significant increase in tensile modulus. However, the incorporation of only 0.1phr EPR compatibilizer exhibited appreciable increase in tensile modulus, which increased further with increasing amount of EPR compatibilizer. This is attributed to significant coupling and chain-extending reactions which occur on addition of EPR during the melt blending process, producing various PET-co-EPR-co-MAPP copolymers and chain-extended PET in the compatibilized composites. Similar findings were reported by Ismail et al. [35], whereby higher rigidity of rice husk powder filled polypropylene/recycled acrylonitrile butadiene (PP/NBRr/RHP) biocomposites produced higher tensile modulus due to better interaction between the matrix and filler in the presence of a silane coupling agent. Similarly, Liu et al. [32] who worked on mechanical properties of poly (butylenes Succinate) (PBS) bio-composites reinforced with surface modified jute fiber reported increases in tensile modulus, which the authors attributed to better interaction between the PBS matrix and silane coupling agent-modified jute fiber.

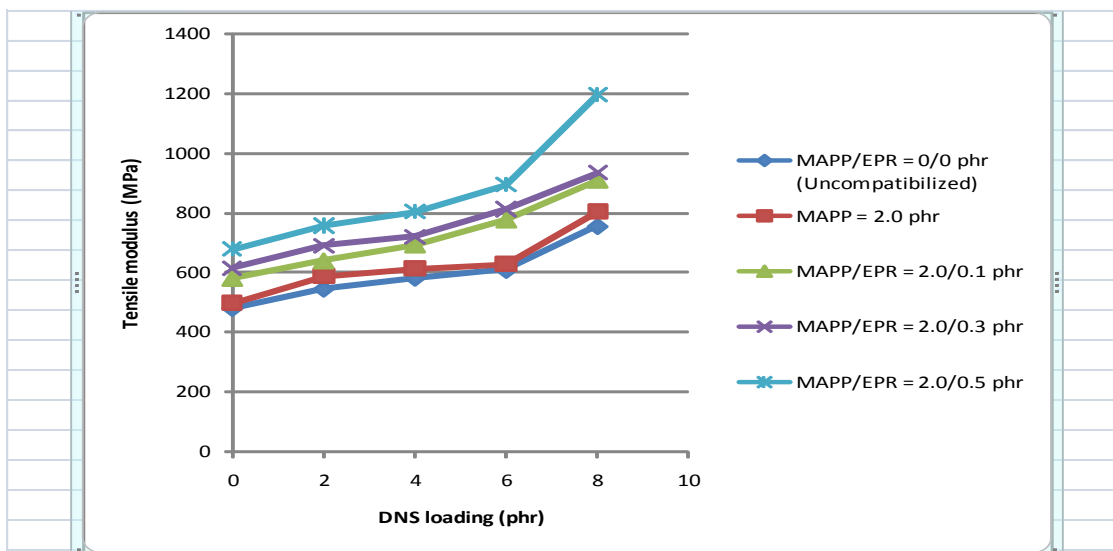


Figure 5: Effect of DNS loading and epoxy resin (EPR) on tensile modulus of recycled PP/PET/DNS composites.

The elongation at break of PP/PET/DNS composites with and without compatibilizer is shown in Figure 6. Clearly, the incorporation of DNS into the PP/PET matrices resulted in a reduction of elongation at break. The decreasing trend in elongation at break at higher DNS loading may be due to increase in stiffness and brittleness of the composites. The uncompatibilized composite produced the highest elongation at break. The decrease in elongation at break caused by MAPP compatibilizer alone is insignificant. However, addition of only small amount of EPR (0.1phr) compatibilizer in the composite is able to cause noticeable decrease in elongation at break, which decreased further with increasing amount of EPR in the composite. As explained earlier, this may be due to significant coupling and chain-extending reactions which occur on addition of EPR, which enhances the matrix-filler interaction resulting in lower elongation at break. This result is consistent with the findings of Hong et al. [33] who reported that silane-treated jute fibres yield a stronger interfacial adhesion, resulting in low elongation at break in silanized/polypropylene composites.

Figure 7 presents the effect of DNS loading and epoxy resin (EPR) on the impact strength of recycled PP/PET/DNS composites. The trend of impact strength for the composites with and without compatibilizer is consistent with corresponding tensile strength. EPR compatibilizer exhibits a significant effect on the enhancement of impact strength for PP/PET/DNS composites, which can be attributed to the in-situ-formed PET-co-EPR-co-MAPP copolymer molecules which anchor along the interface. A greater number of in-situ copolymer molecules are produced with increasing amount of EPR content as shown by progressive increase in impact strength.

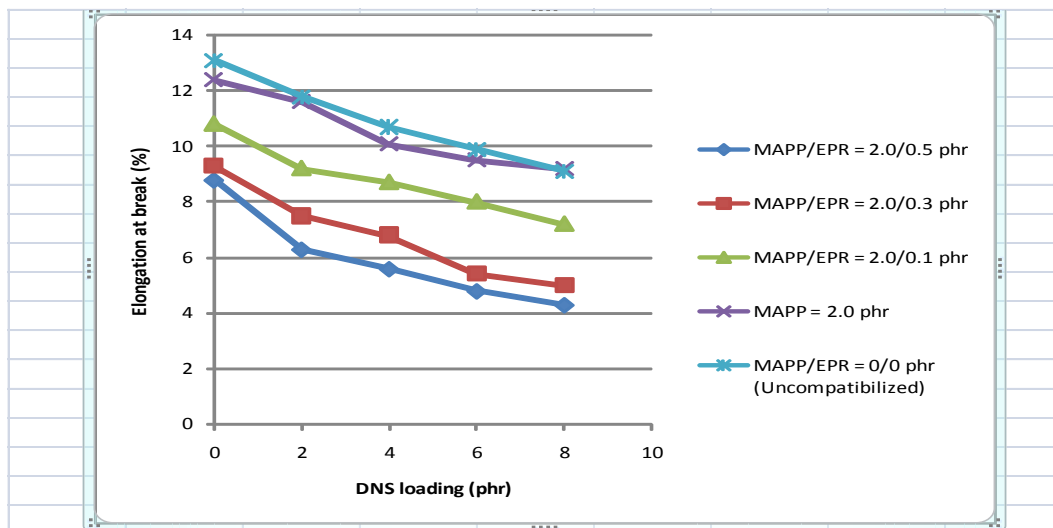


Figure 6. Effect of DNS loading and epoxy resin (EPR) on elongation at break of recycled PP/PET/DNS composites.

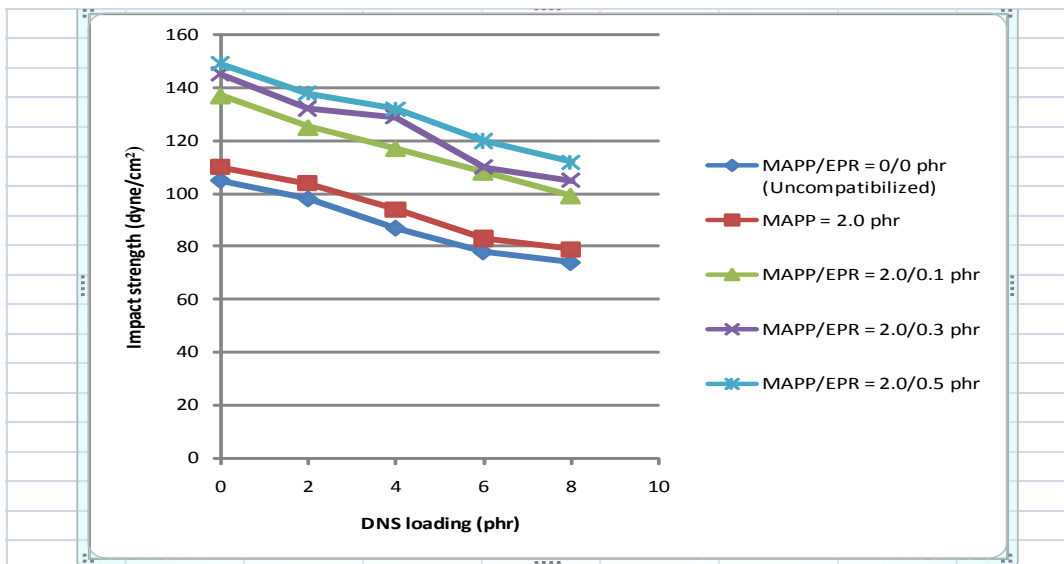


Figure 7. Effect of DNS loading and epoxy resin (EPR) on impact strength of PP/PET/DNS composites.

3.3. Water absorption Test

Figure 8 shows the effect of DNS loading and EPR compatibilizer on water uptake of recycled PP/PET/DNS composites. The results show that water uptake increased as DNS filler content increased. Natural fibers and fillers are highly hydrophilic due to hydroxyl (-OH) groups of polysaccharides found in cellulose, which are able to form hydrogen bonds between water and the DNS filler. As filler loading increases, the number of hydrogen bonds between organic components and water molecules also increases. This is due to the fact that as the filler loading in composite increases, the number of free OH groups on the lignocellulosic filler increases. Free OH groups come in contact with water through hydrogen bonding, which results in water uptake and gain in the composites. Similar findings have been reported by other researchers (Razavi et al. [34]; Ismail et al. [35]). At similar filler loading, it can be seen that the composite with MAPP compatibilizer alone showed a lower water uptake when compared to the composite with MAPP/EPR dual compatibilizers. Water uptake decreased further with increasing EPR content. This provides an indication that EPR enhances the filler-matrix interaction at the interface, thus decreasing the amount of equilibrium water uptake by the composites. This observation is consistent with the findings of Ismail and Mega. [18] in their study on the effect of a silane coupling agent on the properties of white rice ash-polypropylene/natural rubber (PP/NR/RHP) composites. The authors revealed lower water uptake by PP/NR/silane-treated RHP composites, and attributed this observation to the ability of silane coupling agent to form a protective layer at the interfacial zone and consequently prevent the direct diffusion of water molecules into the silane-treated filler composites.

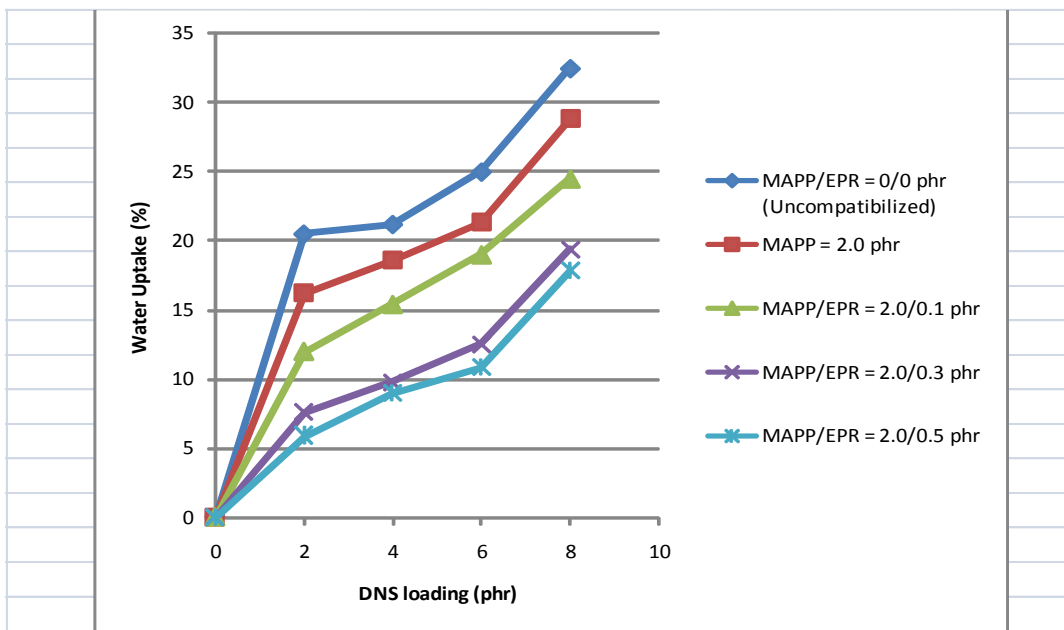


Figure 8. Effect of DNS loading and epoxy resin (EPR) on water uptake of recycled PP/PET/DNS composites.

3.4. Oil Sorption Test

Inhibition of oil uptake is primarily associated with the level of filler-matrix adhesion. Thus, oil sorption test was carried out to evaluate the degree of oil uptake in the composites. Figure 9 presents the variation of % swelling index of PP/PET/DNS composites with DNS loading and EPR content at room temperature (27°C) for 70 hours. The results show that the % swelling index decreased with increasing DNS loading. This is attributed to the hydrophilic character of DNS filler due to the OH groups found in the lignocellulosic DNS filler. Oil resistance (decrease in % swelling index) is expected to increase with increase in polarity [16]. Thus, the higher the DNS filler loading (increased polarity) the lower the % equilibrium oil absorption (lower % swelling index). The findings of this study are also in agreement with the work of Mathew et al. [36], who reported decreases in equilibrium solvent uptake of isora fiber filled natural rubber composites with increases in fiber loading. The authors attributed this observation to increased hindrance exerted by the polar fibers at higher fiber loading. It can also be seen that compatibilization by MAPP alone leads to insignificant degree of oil resistance by the composites. However, compatibilization by MAPP/EPR dual compatibilizers produced greater degree of oil resistance, which also indicates increases in oil resistance with increasing EPR content in the composite. This is probably due to adequate interfacial adhesion at phase boundaries by the compatibilizing effect of MAPP/EPR dual compatibilizers.

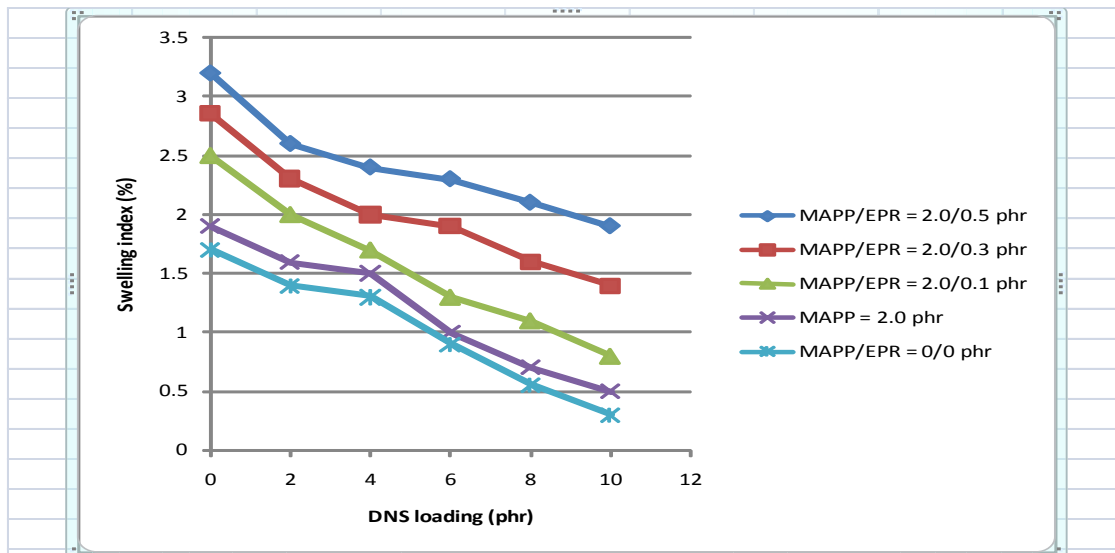


Figure 9. Variation of % Swelling index of PP/PET/DND composites with DNS loading and epoxy resin (EPR) at room temperature (27°C) in ASTM No. 3 oil.

IV. CONCLUSION

The following conclusion can be drawn from this study:

1 Dika nutshell powder (DNS) filled recycled polypropylene (PP)/polyethylene terephthalate (PET) biocomposites were prepared by reactive compatibilization using maleic anhydride-grafted-polypropylene (MAPP) and epoxy resin (EPR) as dual compatibilizers. The effects of DNS loading and EPR content on mechanical and rheological properties as well as water absorption and sorption behavior of the compatibilized bio-composites were investigated. Blends of PP and PET (and in general blends of polyolefins and polyesters) result in materials with inferior mechanical properties because of the incompatibility between the two phases. The problem is compounded when a third component, such as dika nutshell powder is added to produce composite material due to the high polarity of the lignocellulosic filler when compared with the non-polar PP. Thus, compatibilization is necessary in order to improve the mechanical performance of the resulting composite for commercial applications. Maleic anhydride-grafted-polypropylene (MAPP) alone is not an effective compatibilizer for PP/PET/DNS composites due to low reactivity between MAPP and PET without the presence of catalyst leading to the formation of insignificant quantity of PET-co-MAPP copolymer during the extrusion melt blending. Consequently, property improvement of the compatibilized composite is not substantial. However, upon addition of epoxy resin (EPR), the properties of the composite are strongly modified and the resulting materials show good mechanical performance. Thus, compatibilization improved with addition of EPR, which act as a coupling agent to produce PET-co-EPR-co-MAPP copolymers at the interface. These interfacially formed copolymers tend to anchor along the interface and act as effective emulsifiers. Consequently, the compatibilized composite gives greater interfacial adhesion with impressive improvement in the properties investigated.

2. Dika nutshell powder (DNS) used as particulate filler in this study is a biodegradable agricultural waste obtained from a cheap renewable resource. Thus, when used as filler in PP/PET blend, DNS confers biodegradability to the resulting composite. It also represents an environmentally friendly alternative to conventional non-biodegradable reinforcing fibres. This is in consonance with growing global environmental concerns as well as new environmental regulations which have forced the search for materials that are compatible with the environment.

3. PP and PET are frequently encountered in urban and industrial waste and are recycled after separating the polymers by flotation. Though, the separation may be quite easy and inexpensive, yet the heterogeneous recycling of these two thermoplastics can give rise to secondary materials, especially composites with good mechanical and permeation characteristics which can serve many application areas.

REFERENCES

- [1] Hemelrijck, E. V.; Puyvelde, P. V.; Velankar, S.; Macosko, C. W.; Moldenaers, P. Interfacial elasticity and coalescence suppression in compatibilized Polymer blends. *J. Rheol.* Vol. 48, no. 1, p. 143-158, 2004.
- [2] Puyvelde, V. P.; Velankar, S.; Moldenaers, P. Rheology and morphology of compatibilized polymer blends, *Curr. Opin. Colloid Interface Sci.*, 6, p. 457- 463, 2001.
- [3] Vranjes, N.; Lednicky, F.; Kotek, J.; Baldrian, J.; Rek, V.; Fortelny, I.; Horak, Z. Compatibilization efficiency of styrene-butadiene block copolymers as a function of their block number. *Journal of Applied Polymer Science*, vol. 108, p. 466-472, 2008.

- [4] Eastwood, E. A.; Dadmun, M. D. Compatibilization of poly(vinyl chloride) and polyolefin elastomer blends with multiblock/blocky chlorinated polyethylenes. *Polymer*, vol. 43, p. 6707-6717, 2002.
- [5] Yao, Z.; Yin, G. Morphology, thermal behavior, and mechanical properties of PA 6/UHMWPE blends with HDPE-g-MAH as a compatibilizing agent. *Journal of Applied Polymer Science*, vol. 75, no. 2, p. 232-238, 2000.
- [6] Onyeagoro, G. N. Cure characteristics and physico-mechanical properties of carbonized bamboo fiber filled natural rubber vulcanizates. *International Journal of Modern Engineering Research*, vol. 2, no. 6, p. 4683-4690, 2012.
- [7] Vladkova, T. G.; Dineff, P. D.; Gospodinova, D. N.; Avramova, I. Cure characteristics and the mechanical properties of natural rubber compounds filled by non-modified and corona treated wood flour. *Journal of Applied Polymer Science*, vol. 101, p. 651-658, 2006.
- [8] Costa H. M. D.; Visconte, L. L. Y.; Nunes, R. C. R.; Furtado, C. R. G. Mechanical and dynamic mechanical properties of rice husk ash-filled natural rubber compounds. *Journal of Applied Polymer Science*, vol. 83, p. 2331-2346, 2002.
- [9] Santiagoo, R.; Ismail, H.; Hussin, K. Mechanical properties, water absorption, and swelling behavior of rice husk powder filled polypropylene/recycled acrylonitrile butadiene rubber (PP/NBR/RHP) bio-composites using silane as a coupling agent. *BioResources*, vol. 6, no. 4, p. 3714-3726, 2011.
- [10] Yang, A.; Wu, R. Enhancement of the mechanical properties and interfacial interaction of a novel chitin-fiber-reinforced poly (ϵ -caprolactone) Composite by irradiation treatment. *Journal of Applied Polymer Science*, vol. 84, p. 486-492, 2002.
- [11] Rahman, M. M.; Khan, M. A. Surface treatment of coir (cocos nucifera) fiber and its influence on the fibers' physico-mechanical properties. *Composite Science Technology*, vol. 67, p. 2369-2376, 2007.
- [12] Sgriccia, N.; Hawley, M. C.; Misra, M. Characterization of natural rubber fiber surfaces and natural fiber composites Part A: *Applied Science and Manufacturing*, vol. 39, p. 1632-1637, 2008.
- [13] Satyanarayana, K. G.; Arizaga, G. G. C.; Wypych, F. Biodegradable composites based on lignocellulosic fibers: An Overview, *Progress in Polymer Science*, vol. 34, p. 982-1021, 2009.
- [14] Premalal, H. G. B.; Ismail, H.; Boharin, A. Comparison of the mechanical properties of rice husk powder filled polypropylene composites with talc filled Polypropylene composites. *Polymer Testing*, vol. 21, p. 833-839, 2002.
- [15] Abdelmouleh, M.; Boufi, S.; Belgacem, M. N.; Dufresne, A. Short natural fiber reinforced polyethylene and natural rubber composites: Effect of silane coupling agents and fiber loading. *Composite Science Technology*, vol. 67, p. 1627-1639, 2007.
- [16] Rozman, H. D.; Tay, G. S.; Kumar, R. N.; Abusamah, A.; Ismail, H. Polypropylene-oil palm empty fruit bunch-glass fiber hybrid composites: A preliminary study on the flexural and tensile properties. *European Polymer Journal*, vol. 37, p. 1283-1289, 2001.
- [17] Kim, K. P.; Yoon, T. H.; Rhee, J. M.; Lee, J. S. Wood-polyethylene composites using ethylene vinyl alcohol copolymer as adhesion promoter. *Bio-resources Technology*, vol. 97, p. 494-499, 2006.
- [18] Ismail, H.; Mega, L. The effect of a compatibilizer and a silane coupling agent on the mechanical properties of white rice husk filled polypropylene/ natural rubber blend. *Polymer Plastic Technology Engineering*, vol. 40, p. 463-478, 2001.
- [19] Onyeagoro, G. N. Dispersion characteristics of yellow poplar wood fiber in cellulose acetate butyrate/yellow poplar wood fiber compoite. *International Journal of Academic Research*, vol. 4, no. 1, p. 49-54, 2012.
- [20] Li, Q.; Matuana, L. M. Surface of cellulosic materials modified with functionalized polyethylene coupling agents. *Journal of Applied Polymer Science*, Vol. 88, p. 278-286, 2003.
- [21] Onyeagoro, G. N. Reactive compatibilization of natural rubber (NR)/caroxylated nitrile rubber (XNBR) blends by maleic anhydride-grafted- Polyisoprene (MApi) and epoxy resin dual compatibilizers. *International Refereed Journal of Engineering and Science*, vol. 2, Issue 3, p. 7-16, 2013.
- [22] Ju, M. Y.; Chang, F. C. Polymer blends of PET-PS compatibilized by SMA and epoxy dual compatibilizers. *Journal of Applied Polymer Science*, vol. 73, p. 2029-2040, 1999.
- [23] Lo, D. W.; Chiang, C. R.; Chang, F. C. *Journal of Applied Polymer Science*, vol. 65, p. 739, 1997.
- [24] Chin, H. C.; Chang, F. C. *Polymer*, vol. 38, p. 2947, 1997.
- [25] Onyeagoro G. N. Influence of carbonized dika (Irivalgia Gabonensis) nutshell powder on the vulcanizate properties of natural rubber/acrylonitrile- butadiene rubber blends. *Academic Research International*, vol. 2, no. 3, p. 218-229, 2012.
- [26] Onyeagoro G. N.; Enyiegbulam, M. E. Sorption characteristics of dynamically vulcanized polypropylene/epoxidized natural rubber blends filled with carbonized dika nutshell (Irivalgia Gabonensis). *Academic Research International*, vol. 3, no. 2, p. 117-127, 2012.
- [27] Onyeagoro, G. N.; Enyiegbulam, M. E. Studies on reactive compatibilization and dynamic vulcanization of polypropylene/epoxidized natural rubber blends filled with carbonized dika nutshell powder. *Academic Research International*, vol. 3, no. 2, p. 128-137, 2012.
- [28] Liu, C.; Ding, J.; Zhou, L.; Chen, S. Mechanical properties, water swelling behavior and morphology of water-swellaable rubber prepared using crosslinked sodium polyacrylate. *Journal of Applied Polymer Science*, vol. 102, p. 1489-1496, 2006.
- [29] Bagrodia, S.; Wilks, G. L.; Kennedy, J. P. *Polymer Engineering Science*, vol. 26, p. 662, 1986.
- [30] Ultracki, L. A. *Polymer Engineering Science*, vol. 28, p. 1401, 1988.
- [31] Ashcroft, W. R. *Chemistry and Technology of epoxy resins*, Ellis, B.; Blackie Academic & Professional, Glasgow, UK, chapter 2, 1993.
- [32] Liu, L.; YU, j.; Cheng, L.; Qu, W. Mechanical properties of poly (butylenes succinate) (PBS) bio-composites reinforced with surface modified jute fiber. *Composites Part A: Applied Science and Manufacturing*, vol. 40, p. 669-674, 2009.
- [33] Hong, C. K.; Hwang, I.; Kim, N.; Park, D. H.; Hwang, B. S.; Nah, C. Mechanical properties of silanized jute fiber/polypropylene composites. *Journal of Industrial and Engineering Chemistry*, vol. 14, p. 71-76, 2008.
- [34] Razavi, N. M.; Jafarzadeh, D. F.; Oromiehie, A.; Langroudi, A. E. Mechanical properties and water absorption behavior of chopped rice husk filled Polypropylene composites. *Iranian Polymer Journal*, vol. 15, p. 757-766, 2006.
- [35] Ismail, H.; Ragnathan, S.; Hussin, K. The effects of recycled acrylonitrile butadiene rubber content and maleic anhydride modified polypropylene (PPMAH) on the mixing, tensile properties, swelling percentage and morphology of polypropylene/recycled acrylonitrile butadiene rubber/rice husk Powder (PP/NBR/RHP) composites. *Polymer Plastic Technology Engineering*, vol. 49, p. 1323-1328, 2010.
- [36] Mathew, L.; Joseph, K. U.; Joseph, R. Swelling behavior of isora/natural rubber composites in oils used in automobiles. *Bull. Mater. Sci*, vol. 29, no. 1, p. 91-99, 2006.